

Cátia Joana Costa Magro

Mestre em Engenharia do Ambiente  
Ramo de Sistemas Ambientais



## Advances in applied electrokinetics: Treatment, by-products reuse and sensors' system

Dissertação para obtenção do Grau de Doutor em Ambiente e Sustentabilidade

Orientadores: Eduardo Manuel Hipólito Pires Mateus  
Investigador CENSE, Técnico Superior, Faculdade de  
Ciências e Tecnologia da Universidade Nova de Lisboa

Alexandra de Jesus Branco Ribeiro  
Professora Associada com Agregação, Faculdade de  
Ciências e Tecnologia da Universidade Nova de Lisboa

Juan Manuel Paz-Garcia  
Professor Assistente, Universidad de Málaga

Júri:  
Presidente: Virgílio António Cruz Machado  
Professor Catedrático, NOVA-FCT

Arguentes: Francesca Pagnanelli  
Professora Associada, Sapienza University of Rome  
Helena Isabel Caseiro Rego Gomes  
Anna McLaren Research Fellow, University of Nottingham

Vogais: Fernando José Pires Santana  
Professor Catedrático Jubilado, NOVA-FCT

Maria de Fátima Guerreiro da Silva Campos Raposo  
Professora Associada com Agregação, NOVA-FCT

Ana Cristina Moreira Simões  
Doutora Coordenadora da HiTech@Lisboa

Eduardo Manuel Hipólito Pires Mateus  
Investigador CENSE, Técnico Superior, NOVA-FCT

Outubro, 2019



Advances in applied electrokinetics: Treatment, by-products  
reuse and sensors' system

- *Cátia Joana Costa Magro* -



*Advances in applied electrokinetics: Treatment, by-products reuse and sensors' system*

Copyright © [Cátia Joana Costa Magro], NOVA School of Science and Technology, NOVA University Lisbon

A Faculdade de Ciências e Tecnologia e a Universidade Nova de Lisboa têm o direito, perpétuo e sem limites geográficos, de arquivar e publicar esta dissertação através de exemplares impressos reproduzidos em papel ou de forma digital, ou por qualquer outro meio conhecido ou que venha a ser inventado, e de a divulgar através de repositórios científicos e de admitir a sua cópia e distribuição com objectivos educacionais ou de investigação, não comerciais, desde que seja dado crédito ao autor e editor.



*"I have no special talent. I am only passionately curious."*

- Albert Einstein -

*To my parents,*

*"We've all got both light and dark inside us.  
What matters is the part we choose to act on.  
That's who we really are."*

- Sirius Black, Harry Potter and the Order of the Phoenix -





This dissertation is submitted in partial fulfilment of the requirements for the Doctoral Degree in Environment and Sustainability and includes the results of my PhD study carried out from October 2015 to September 2019 at the NOVA School of Science and Technology, NOVA University Lisbon. Most of the research work developed during the PhD project was undertaken at Resolution Lab, CENSE, Departamento de Engenharia e Ciências do Ambiente (DCEA), NOVA School of Science and Technology, NOVA University Lisbon, under the supervision of the Doctor Eduardo P. Mateus (Cense Researcher) and the co-supervision of the Associate Professor with Habilitation Alexandra B. Ribeiro and of the Assistance Professor Juan M. Paz-Garcia (University of Málaga, Spain). Additionally, the sensors' development and measurements were performed at the Centre of Physics and Technological Research, CEFITEC, hosted by the Associate Professor Maria Raposo. The Business Plan and market assessment were undertaken during the Hiseedtech training programme at the NOVA School of Business and Economics, NOVA University Lisbon.

During the period of my PhD scholarship, I worked abroad twice, hosted by prestigious international universities:

- March-July 2017. Department of Civil Engineering, Technical University of Denmark, BYG-DTU, Lyngby, Denmark. Hosted by the Associate Professor Lisbeth M. Ottosen
- July-October 2019. ECORECYCLING, at Sapienza Università di Roma, Italy. Hosted by the Associate Professor Francesca Pagnanelli

The present research is part of the projects entitled “Development of Nanostructures for Detection of Triclosan Traces on Aquatic Environments, PTDC/FIS-NAN/0909/2014”, sponsored by Fundação para a Ciência e a Tecnologia and e.THROUGH - Thinking rough towards sustainability, sponsored by Grant Agreement 778045, H2020-MSCA-RISE-2017 from the European Commission and Fundação para a Ciência e a Tecnologia for the research grand SFRH/BD/114674/2016.

Therefore, the dissertation is organized as follows:

*Part I* - The knowledge collected in the appended publications is compiled with the aim of organizing the information and explaining the methodology used. Part I contains a general introduction and a description of the PhD project, the statement of the research objectives and a summary of the main

achieved results from the papers published, submitted and planned (manuscripts) during the research period. Part I it is designed to organize the content and define the links between the peer-reviewed scientific publications submitted and published during the PhD project.

*Part II* - Collects the relevant peer-reviewed scientific publications submitted and published during the PhD project, including journal papers and conference contributions.

I hereby declare that, as the first author, I provided the major contribution to the research and experimental work developed, as well as to the interpretation of the results and the preparation of the publications submitted during the PhD project.

*Monte de Caparica, 23<sup>rd</sup> September 2019*

*Cátia Magro*

## Acknowledgments

---

*“Let us be grateful to the people who make us happy;  
They are the charming gardeners who make our souls blossom.”*

- Marcel Proust -

I would like to express my gratitude to my advisers, Eduardo Mateus, Alexandra Ribeiro and Juan Paz-Garcia, for always fight by my side for my ideas. Thank you so much! A special word of thanks is due to Eduardo Mateus for his continuous support and outstanding scientific discussions, no one has ever pushed me so far intellectually.

I had the opportunity to work with top research groups and I would like to thank:

- Maria Fátima Raposo, Susana Sérgio and Paulo Ribeiro: CEFITEC group, Department of Physics of NOVA-FCT
- Lisbeth Ottosen, Pernille Jensen, Gunvor Kirkelund, Ebba Schnell and Malene Møller: BYG-DTU group, Department of Civil Engineering, Technical University of Denmark
- Francesca Pagnanelli and António Rubino: ECORECYCLING, at the Department of Chemistry in Sapienza Università di Roma

Success is never individual. Therefore, I do thank my research group, *Resolution lab*. Thank you so much Flávia Freitas and Cátia Santos for all the help and emotional support. Thank you to Nazaré Couto, Marco Silva, Davide Mendes, Vanda Lopes, João Brinco and André Jorge, for all the assistance during my journey. A special thanks to Paula Guedes, for always being there to help, listen and support the craziness of a PhD student. As all help is important in times of need, thank you all the REQUIMTE's analysis team, Nuno Costa, Carla Rodrigues and Nuno Lapa, who always had his experience and laboratory available for me.

I am very grateful to Marta Cerejo, from Research and Innovation Accelerator – FCT, Cristina Simões and Pedro Vilarinho from HiseedTech and Paulo Amaral from Recipharm, for all the support, best efforts to put our scientific work into a real-life solution and, most of all, for believing in me: “if you try hard, you may change the world a bit”. Thanks to my colleagues in CENSE communication, Inês Cosme, Luis

Dias and Rita Domingues, you are the best guys! Thank you to Marta Martins for showing that it is possible to be a great scientist, professor and the coolest mother.

Thank you to my Danish family, for always make me feel that I am at home. To my Climate-KIC Journey sweeties' and their brilliant minds. Thank you to Bruno Moura who took care of my physical and mental health during these years.

To Paulo Zagalo, João Pereira-da-Silva and Filipa Fernandes my favourite nerds, who always help and have a smile for me, thank you for teaching me that sensors can be the trendiest subject and that strong friendship can happen any time.

To the sweetest and kindest, Joana Almeida, your support was a rock in my entire PhD journey. Thank you for your friendship, for the laughs and all the fun that we had in our complex laboratory experiments.

To my oldest and my always present friends, Daniela Sousa, Cláudia Silva, Rita Ferreira, Sílvia Dias, Vanessa Nunes, Joana Silva, Sofia Pereira, and José Santos, thank you as you are a gift in my life.

To João, thank you for the advice, the debates and the infinite encouragement. We indeed are the best team!

To my parents Jorge e Joana, my grandparents Cecília, Mariana, Francisco and António, my uncle Pedro and aunt Sandra, thank you for being the best family, thank you for being there for everything, unconditionally.

As principais barreiras encontradas para alterar o paradigma das soluções de reutilização de água estão relacionadas com o nível de maturação das tecnologias desenvolvidas, com a remoção de contaminantes orgânicos emergentes, com a carência de ferramentas de análise rápida, fiável e economicamente viáveis para monitorização ambiental. Neste sentido, a presente dissertação propõe a aplicação de tecnologias de base elétrica a efluente secundário com o objetivo de promover a sua reutilização através (i) da remoção de triclosan e de contaminantes inorgânicos, (ii) da concepção e estudo de línguas eletrónicas como potenciais ferramentas para monitorizar processos de degradação; (iii) da recuperação/reutilização de hidrogénio para fins energéticos e da produção de materiais de construção.

De acordo com os objetivos mencionados, os principais resultados do presente projeto de doutoramento são descritos de seguida:

(i)

- Os reatores eletroquímicos testados são eficazes para degradar triclosan e os seus produtos de degradação/metabolito. O tipo de eléctrodo utilizado no processo é uma variável importante, uma vez que afeta a eficiência e cinética de degradação, assim como os subprodutos gerados após o tratamento;
- A seletividade e sensibilidade de um GC/MS/MS permite, após otimização operacional, a deteção e quantificação de triclosan (em efluente na gama dos ng/L), sem a derivatização do analíto, demonstrando que os métodos-padrão devem ser ajustados consoante a matriz e os compostos em estudo.

(ii)

- Línguas eletrónicas revestidas com filmes finos de polieletrólitos orgânicos são capazes de distinguir com uma resolução de pico-molar, por meio de uma Análise de Componentes Principais, entre água mineral e efluente secundário, discriminando simultaneamente triclosan a diferentes concentrações;
- A estabilidade do revestimento nas línguas eletrónicas é afetada pelas características da matriz (p.e. pH e teor em elementos), em detrimento da molécula a ser detetada; tendo em conta esta dependência, filmes finos produzidos com a técnica de pulverização catódica, mais robustos e estáveis, foram adicionados à composição da língua eletrónica desenvolvida;

- A língua eletrónica desenvolvida tem potencial como ferramenta de monitorização ambiental e seguimento da degradação dos compostos em estudo, quando conectada a um reator eletroquímico dinâmico; observou-se a semi-quantificação de triclosan e metil-triclosan usando uma língua eletrónica composta por cinco sensores; observou-se a semi-quantificação de 2,4,6-triclorofenol e 2,4-diclorofenol usando um único sensor revestido com filmes de menor espessura.

(iii)

- O hidrogénio, um subproduto gerado durante o processo electrodiálítico, provou, conceitualmente, potencial para ser armazenado, reutilizado e/ou utilizado numa célula de combustível com membrana de troca de protões, para gerar energia;
- A utilização de efluente tratado com o processo electrodiálítico é uma solução com potencial para substituir a água potável utilizada na produção de materiais de construção. Esta substituição produz materiais com características indicadas para a indústria da construção, aumentando a sustentabilidade do processo e a valorização do reator desenvolvido, no mercado.

**Palavras-chave:** *água; processos eletroquímicos; contaminantes orgânicos emergentes; monitorização ambiental em tempo real; línguas eletrónicas; hidrogénio; reutilização de efluente secundário; materiais de construção.*

Some of the barriers for a paradigm change on water reuse solutions are related to their maturing technology level, to the removal of emerging organic contaminants and to the availability of rapid, reliable and cost-effective monitoring tools. Thus, in this dissertation, electro-based techniques were applied to secondary effluents aiming to promote water reuse through the (i) removal of triclosan and inorganic contaminants, (ii) development and test of electronic tongue sensors that may be used as complementary monitoring tools coupled with degradation processes, and (iii) enhancing of the technology maturity level with the recovery of self-produced hydrogen and freshwater replacement in the production of construction materials.

With these objectives, the main findings in this PhD project are described hereunder:

- (i)
  - Electrochemical reactors are effective for degrading triclosan and its by-products. The type of electrodes is an important variable that strongly impacts the degradation efficiency, the kinetics and the by-products generated after treatment;
  - GC/MS/MS selectivity and sensitivity allows, after operational optimization, the detection and quantification of triclosan, without the analyte derivatization, in the effluent at ng/L level, showing that standard methods should be adjusted “case-by-case”.
- (ii)
  - Electronic tongues coated with organic polyelectrolyte thin films are able to distinguish at pico-molar resolution, by means of principal component analysis, between mineral water and secondary effluent matrices and discriminating triclosan at different concentrations;
  - The coating’s stability is affected by characteristics of the water to be analysed (e.g. such as pH and elements content), rather than by the molecule to be detected; Due to this dependency, sputtering thin films, more robust and stable, should be added to the electronic tongue array;
  - A customized electronic tongue proved be a potential complementary monitoring tool to follow the degradation pathway of the target compounds across the treatment, when coupled to a dynamic electrochemical reactor; It was possible to semi-quantify methyl-triclosan and triclosan using the array, whereas for phenolic compounds (2,4-

dichlorophenol and 2,4,6-trichlorophenol) best results were obtained by using a single sensor and thinner film as coating.

(iii)

- The remediation process by-product, hydrogen, showed, on a proof of concept level, its potential to be stored, reused or used as fuel in a proton-exchange membrane fuel cell, to generate energy;
- The use of electro-treated effluent showed to be sustainable for replacing freshwater in construction materials production. This replacement can provide high quality materials with features that are valued by construction materials industry, increasing the market value of the reactor developed.

**Keywords:** *water; electrochemical processes; emerging organic contaminants; real time monitoring; electronic tongue's systems; hydrogen; secondary effluent reuse; construction materials.*



## Abbreviations

---

DCP	2,4-Dichlorophenol
E-tongue	Electronic Tongue
ED	Electrodialytic
EK	Electrokinetic
EOCs	Emerging organic contaminants
GC/MS/MS	Gas chromatography-triple quadrupole mass spectrometry
GO	Graphene Oxide
HPLC-DAD	High-Performance Liquid Chromatography with Diode-Array Detection
LbL	Layer-by-layer
MTCS	Methyl-Triclosan
Nb/BDD	Niobium/boron-doped diamond
PAH	Poly(allylamine hydrochloride)
PEI	Poly(ethyleneimine)
PSS	Poly(sodium 4-styrene sulfonate)
TCP	2,4,6-Trichlorophenol
TCS	Triclosan
Ti/MMO	Titanium/ Mixed Metal Oxide
TRL	Technology readiness level



Preface .....	iii
Acknowledgments .....	v
Resumo .....	vii
Abstract .....	ix
Abbreviations .....	xi
Contents .....	xiii

## **Part I**

1. Introduction.....	3
2. Objectives .....	7
3. Summary of the research .....	9
3.1 Electrochemical reactors for triclosan and its by-products degradation .....	11
3.2 Chromatography methods for triclosan detection in effluent .....	13
3.3 E-tongues to triclosan detection and quantification .....	15
3.4 Multi-analyte e-tongue coupled to an electrochemical reactor .....	17
3.5 Electrokinetic Hydrogen self-energy generation .....	19
3.6 Potential of replacing freshwater by electro-treated effluent in construction materials .....	21
3.7 Future work .....	23
References.....	25

## **Part II**

### Papers

<i>Emerging organic contaminants in wastewater: Understanding electrochemical reactors for triclosan and its by-products degradation</i> Published in: Chemosphere, 2019 <sup>a</sup> .....	31
<i>Analytical method for the monitoring of underivatized Triclosan by gas chromatography-triple quadrupole mass spectrometry in effluent</i> Under preparation, 2019 <sup>b</sup> .....	43
<i>Overview of electronic tongue sensing in environmental aqueous matrices: Potential for monitoring emerging organic contaminants</i> Published in: Environmental Reviews, 2019 <sup>c</sup> .....	55
<i>Polyelectrolyte based sensors as key to achieve quantitative electronic tongues: Detection of triclosan on aqueous environmental matrices</i> Submitted, 2019 <sup>d</sup> .....	71
<i>Electronic tongue coupled to an electrochemical flow reactor for emerging organic contaminants degradation monitoring</i>	

Published in: Sensors, 2019 <sup>e</sup> .....	95
<i>Exploring hydrogen production for self-energy generation in electroremediation: a proof of concept</i>	
Published in: Applied Energy, 2019 <sup>f</sup> .....	111
<i>Sustainability of construction materials: electrodialytic technology as a tool for mortars production</i>	
Published in: Journal of Hazardous Materials, 2019 <sup>g</sup> .....	121
<u>Provisional Patent Application</u>	
<i>Electrodialytic reactor and process for the treatment of contaminated aqueous matrices</i>	
Registration number: 115384, 2019.....	131
<u>Market Assessment</u>	
<i>Business plan for 2Resource potential solution</i>	
In: Hitech program, 2018.....	135
<u>Chapters</u>	
<i>Sensors potential to monitoring electroremediation systems: emerging organic contaminants in wastewater</i>	
Under preparation, 2019*.....	139
<i>Self-hydrogen recovery in electro-based technologies applied to environmental contaminated matrices</i>	
Under preparation, 2019**.....	143
<u>Conference Papers</u>	
<i>Detection and adsorption of Triclosan on sensors based on PAH/PVS thin-films</i>	
Published in: Proceedings IEEE, 2019.....	147
<i>Detection of Triclosan in tuned solutions by pH and ionic strength using PAH/PAZO thin films</i>	
Published in: Sensors Proceedings I3S, 2019.....	153
<i>Triclosan Detection in Aqueous Environmental Matrices by Thin-Films Sensors</i>	
Published in: Sensors Proceedings I3S, 2019 <sup>h</sup> .....	159
<u>Conference Contributions</u>	
<i>Triclosan detection in aqueous environmental matrices by thin-films sensors: impedantometric electronic tongue</i>	
Oral presented in: 7th International Symposium on Sensor Science, 2019.....	167
<i>Electrodialytic technology as effluent treatment for reuse in construction materials</i>	
Oral presented in: 5th International Conference on Sustainable Solid Waste Management, 2017.....	171
<i>Development of target methods for triclosan monitorization in effluents at trace levels using gas chromatography-triple quadrupole mass spectrometry and electronic tongues</i>	
Poster presented in: 11th Encontro Nacional de Cromatografia, 2019.....	175
<i>Innovating from Science: 2Resource - Recovering water, creating Resources to build</i>	
Poster presented in: HiTech Closing Session, 2018.....	179
<i>Prospective energy savings in electro-based technologies – PEM fuel cell</i>	
Poster presented in: 6th International Conference on Sustainable Solid Waste Management, 2018.....	183

*Optimization of an analytical method for the determination of underivatized triclosan and related compounds by gas chromatography-triple quadrupole mass spectrometry*  
Poster presented in: 10th Encontro Nacional de Cromatografia, 2017..... 187

*Assessment of emergent contaminants removal from wastewater by electrokinetics*  
Poster presented in: 15th International Symposium on Electrokinetic Remediation, 2017.....191



# *Part I*

*“Anyone who has never made a mistake has never tried anything new. “*

- Albert Einstein -





## 1. Introduction

---

Water scarcity can be defined as the shortage of the freshwater resources required to meet demand. Every continent is affected by water scarcity, and it was classified by the World Economic Forum (2015) [1] as the highest global risk regarding potential its effects over the next decade. Climate change, rapidly growing population and increased urbanization are the main reasons for this trend. Today, an estimated 3.6 billion people - nearly half the world's population - already live in areas that are potentially water-scarce at least one month per year. According to the United Nations, this number could increase to between 4.8 and 5.7 billion by 2050, as two out of every three people are likely to be living in cities or other urban centres. Logically, both the European Economic Area and the United Nations Environment Programme call for action to increase water-use efficiency in all sectors. Of the barriers to a wider uptake of water reuse solutions, technical and scientific uncertainties are considered to be among the top six main challenges: “the water reuse sector in Europe seems to be mature, technical solutions are well-known and available to cover a wide range of applications and environments. However, these solutions are not always cheap and there remain a few technical challenges, in particular, the removal of emerging organic contaminants (EOCs) and the need for rapid monitoring techniques that are reliable and cost-effective” (European Commission, 2015).

EOCs are defined as “chemical substances that have no regulation and are suspected to negatively affect the environment or whose effects are unknown” [3,4]. Among EOCs, triclosan (TCS, 2,4,4'-Trichloro-2'-hydroxydiphenyl ether) is an antimicrobial agent that has been used for more than 50 years as an antiseptic, disinfectant or preservative in clinical settings and in several consumer products. TCS has been detected in wastewater treatment plants [5–7] and in surface water [8,9]. Recent reviews of TCS recount numerous health effects, ranging from endocrine-disruption to uncoupling mitochondria [10,11]. Although, in 2016, the US Food and Drug Administration banned TCS from certain washing products, namely hand soap and body wash [12] and from hospital products by the end of 2018 [13], it is still permissible to have TCS in e.g. toothpastes, cosmetics, clothes or toys [14]. Furthermore, TCS derivatives, such as the metabolite methyl-triclosan (MTCS) [15], which is even more persistent [16] and TCS by-products formed by repeated exposure to chlorine in water, such as 2,4-Dichlorophenol (DCP) and 2,4,6-Trichlorophenol (TCP) are also a cause for concern, since they present a health risk to humans and are recognized as persistent priority pollutants in the United States, Europe and China [17].

The electrokinetic (EK) technique also referred to as “electroremediation” has been used to remove, separate, and promote contaminants degradation since the early nineteenth century, targeting soil remediation [18]. Favourable results have been observed for the removal of EOCs in soil [19,20], sludge [21] and effluent [22]. EK consists in the application of a low-level direct current, inducing physicochemical changes in the media, leading to species transports by (1) electromigration - the movement of ions in solution, (2) electrophoresis - the movement of charged, dissolved or suspended particles in pore fluid and (3) electroosmosis - the movement of fluids across a conduit. Additionally, the electrolysis of water occurs at the electrodes, generating  $H^+$  by water oxidation at the anode and  $OH^-$  by water reduction at the cathode. The “phenomenon” is a useful feature when remediation/degradation/removal/recovery processes are involved since the generated by-product, hydrogen, can be used as fuel in proton-exchange membrane fuel cells to produce electrical energy, to reduce the energy costs of electro-remediation, and to generate value. Moreover, as an energy carrier,  $H_2$  can be used to accumulate energy during electric power demand valleys, and to generate electric power during peak periods. Therefore, a reservoir can be integrated into the electro-dialytic (ED) system, from where the  $H_2$  produced can be recovered and used for different purposes.

Furthermore, not only cutting-edge technologies for contaminants removal are under the spotlight, but also sensors as monitoring tools. Electronic tongue (e-tongue) devices are gaining special attention for liquid matrices. One of the most interesting aspects that motivate the development of e-tongues is their potential for real time parallel monitoring of multi-analyte determination in a single sample analysis [23]. E-tongue is “a multi-sensory system, formed by an array of sensors with low-selective thin film layers or sensorial layers, combined with advanced mathematical procedures for signal processing based on pattern recognition and/or multi-variate data analysis” [24]. From a structural and manufacturing point of view the choice of the type of thin film or sensorial layer is a critical step for the accomplishment of a reliable qualitative and quantitative device. Compared to traditional sampling and analysis, sensors can provide a fast response on the output data in a continuous, safe, and cost-effective way. Notwithstanding the potential advantages of e-tongues, there are still many challenges related to the stability and monitoring reliability, including recognition and transduction elements, matrix effects, reversibility, and the need of *in situ* calibration. Finally, e-tongues are not intended to replace traditional methods, but they can be useful and complementary tools when speed and a lower-cost routine response are required.

The removal of EOCs using EK technologies in combination with fast monitoring tools has potential to ensure an effective, competitive and integrated solution for water reuse.

After water, concrete is the most widely consumed material in the world [25]. The concrete industry represents 9% of all industry withdrawals and 1.7% of all global water consumption [26]. In a concrete mix, the water-cement ratio is around 0.45 to 0.60. In other words, more than 17 billion m<sup>3</sup> of freshwater is used in the production of concrete each year. Today, freshwater is the only type of water that meets the industry standards for concrete production. Moreover, if inadequate water is used, the quality of the concrete can significantly decrease, leading to a structural failure that would represent between 5% and 9.4% of the total costs of concrete production [27]. However, tap water supply is highly limited, especially in dry regions such as the Middle East and Africa, where construction companies often have no other option than to rely on water that is at least partially polluted. The EK technology has the potential to reduce the need of freshwater by replacing it with electro-treated effluent in concrete production. The versatility of the EK reactor can provide full control of water characteristics (e.g. pH, salts content), allowing the production of high-quality construction materials, without jeopardizing reference parameters, e.g. compressive strength or setting times.

Different issues are discussed in Part I: electrochemical reactors for the degradation of TCS and its by-products (in Magro *et al.* submitted 2019<sup>a</sup>), GC/MS/MS as a monitoring technique for TCS detection and quantification in effluent (in Magro *et al.* under preparation 2019<sup>b</sup>), e-tongue build up with LbL thin films for detection and semi-quantification of TCS (in Magro *et al.* 2019<sup>c</sup>, Pereira-da-Silva *et al.* 2019, Zagalo *et al.* 2019, Magro *et al.* 2019<sup>h</sup>; Magro *et al.* submitted 2019<sup>d</sup>), customized e-tongue coupled to an electrochemical reactor to “follow” the analytes electro-degradation (in Magro *et al.* submitted 2019<sup>e</sup>; Magro *et al.* chapter under preparation 2020<sup>\*</sup>), EK hydrogen self-energy generation (in Magro *et al.* 2019<sup>f</sup>; Magro *et al.* chapter under preparation<sup>\*\*</sup>), potential of replacing freshwater with electro-treated effluent in construction materials production (in Magro *et al.* 2019<sup>g</sup>; Provisional patent application 2019; Market assessment 2018).



## 2. Objectives

---

The main objectives of this PhD project were: (i) to promote water reuse through the removal of contaminants by electro-based technologies, (ii) to develop and test sensors to be used as complementary, rapid and reliable monitoring tools, and (iii) to provide a market assessment of the potential of using electro-treated effluent in the construction sector.

The specific objectives and its achievements through this project are summarized as follows:

*Study electrokinetics as an effective and viable technology to remove and/or degrade emerging organic compounds and inorganic species in a wastewater matrix*

- Different batch, flow and customized EK reactors were evaluated to optimize the removal/degradation of TCS, its derivative by-products and inorganic elements
- Chromatographic techniques were developed and optimized for the analysis of TCS and its derivative by-products: DCP, TCP and MTCS

*Develop and test new monitoring tools for rapid, reliable and cost-effective detection of triclosan and its by-products during an electrochemical process, applied to a wastewater*

- Evaluation of Layer-by-layer polyelectrolytes and sputtering thin films as sensorial layers for e-tongue systems
- Evaluation of the combination of both layer-by-layer and sputtering thin films in a new e-tongue prototype coupled to a flow EK reactor - to detect and follow the degradation dynamics of target compounds

*Enhance the maturity level of electrokinetics technology*

- Self-produced hydrogen was evaluated as proof of concept concerning its purity, potential energy generation and remediation process savings
- Wastewater valorisation in the production of construction materials was studied and assessed at a market level



### 3. Summary of the research

---

As both the scarcity and price of clean drinking water continue to rise across the world, the value of wastewater, as a source of water recovery, has a tendency to increase. One of the opportunities for improvement is the establishment of legal regulations to define how to manage wastewater and to establish which treatment technologies should be used for different types of reuse purposes. Over the last three decades, many research projects have focused their attention on the different applications of electrochemical technology in environmental remediation. Thousands of publications (bibliometric evaluation through SCOPUS, with keywords “electrochemical process” or “electrokinetic process”) have sought to develop new technologies or improve existing processes. Now, at the end of this long period, very few are being applied at their full-scale and most of them remain at the stage of ‘promising’ technologies. Most have recognisable benefits, but important technological difficulties and cost handicaps can be identified, which are related to missing components in the value chain of the technology and the existence of only a few highly specialized stakeholders [28]. When competitive solutions are fully marketed, it is difficult to displace them, unless the advantages of the new technology would help to obtain the same or increased level of performance and payback. Lessons must be learned in order to achieve full applicability of electrochemical technologies and to allow returns on invested money to companies and society. Among electrochemical technologies, the EK processes are now in the position of improving their technology maturity level and, thus, to play a role in the practical solutions that may be implemented in the wastewater reuses value chain.

The methodology and results of the PhD research are summarized in the following subsections, 3.1 to 3.7.





### 3.1 Electrochemical reactors for triclosan and its by-products degradation

TCS and its derivative by-products reach water bodies due to the inefficient removal on wastewater treatment plants [29]. The electrochemical treatments, at bench scale, applied to EOCs, attains high performance in terms of TCS removal, mainly due to the stability and activity of the anode which significantly affects the generation of reactive species, such as  $\bullet\text{OH}$  [30]. Magro *et al.* (submitted 2019<sup>a</sup>) studied the degradation of TCS and its derivative by-products (MTCS, DCP and TCP) in effluent by two different electrochemical reactors. A batch and a flow reactor (mimicking a secondary settling tank in a wastewater treatment plant) were tested with two different working anodes: Titanium/mixed metal oxide (Ti/MMO) and niobium/boron-doped diamond (Nb/BDD). For both reactors, the best electrode combination was achieved with Ti/MMO as the anode. The batch reactor with 7 mA/cm<sup>2</sup> during 4h attained degradation rates below the detection limit for TCS and TCP, and 94% and 43% for DCP and MTCS, respectively. The flow reactor, in approximately 1h with the same current density as the batch reactor, achieved degradation efficiencies of between 41% and 87% for the four contaminants. The results suggest a possible alternative technology that may be implemented in a secondary settling tank, since the combination of a low current density with the flow and matrix induced disturbance increased and speeded up the elimination of compounds.

An upgraded “designed reactor” was developed and is the one included in the provisional patent application (2019). Being not in the patent application core, the reactor design also offers possibilities for the degradation of TCS and its by-products, as the design configuration includes the direct contact of electrodes into the matrix. In the “designed reactor”, the EOCs had two stages of degradation, in the cathode and the anode compartments, separately. EOCs suffer direct anodic oxidation when the contaminants come into contact with the anode surface and indirect oxidation in the liquid bulk, mediated by the oxidants that are formed electrochemically. From the point of view of removal rates, 92% to below the detection limit was achieved for TCS, DCP and TCP with direct oxidation as the main factor of degradation. For MTCS, the direct and indirect oxidation showed equal contributions to the compounds’ degradation. Differently from the batch and flow reactor presented in Magro *et al.* (submitted 2019<sup>a</sup>), the “designed reactor”, includes ion-exchange membranes. The movement of the EOCs through the membranes was not detected. The use of membranes in the degradation solutions can be a potential disadvantage as it may contribute to the membrane fouling. A voltage increase due to fouling was not observed. Only a slightly yellow colour was observed in the anion exchange membrane at the end of the experiments, suggesting the adsorption of organic matter. Comparing the adsorption of compounds between both membranes, the phenomenon is greater with anion exchange

membrane and may be explained by the electrostatic interactions between organics and the membrane (anion exchange membrane 17% vs cation exchange membrane 8% adsorption, for MTCS).

### 3.2 Chromatography methods for triclosan detection in effluent

When using High-Performance Liquid Chromatography with Diode-Array Detection (HPLC-DAD) it was not possible to detect TCS in the raw effluents used on the study. TCS is usually found in trace concentration in effluent matrices (2 ng/L - 40 µg/L) (Dhillon et al., 2015), a level below the LOD of the DAD method (around 0.5 mg/L). Therefore, it was necessary to develop a more sensitive and selective method using a gas chromatography-triple quadrupole mass spectrometry (GC/MS/MS) system. Magro *et al.* (2017) presented an optimized GC/MS/MS method for TCS detection, without analyte derivatization, using Multiple Reaction Monitoring (MRM) mode. To achieve the optimized conditions, the operational parameters tested are: splitless time, liner type, injector temperature, MS source and interface temperature, Q1 and Q3 resolution (peak shape and area offset), collision gas pressure, collision energy and dwell time. Results from injector temperature showed that too high temperatures (>270 °C) can lead to thermo-degradation. The most critical factor was the liner's type which can jeopardize the shape of the peak and its S/N on the chromatograph. Thus, if the liners are packed with quartz wool (normally used for "dirty" environmental matrices), TCS will react with the material even if it is deactivated and/or become adsorbed on it. Concerning the interface and source temperature, through a Design Expert programme and comparing TCS peak areas, the best results were obtained for the temperatures of 290 °C and 260 °C, respectively. The analyte peak area and shape are critical parameters for the quantitative analysis. Thus, Q1 and Q3 resolution, collision gas pressure (mtorr) and collision energy (eV) and dwell time (ms) were evaluated. The best results were achieved with Q1 resolution = 0.7 and Q3 resolution = 2, collision gas pressure at 2.4 mTorr, collision energy at 20eV and a dwell time of 100 ms.

The detection and optimized method conditions were reported preliminary in Magro *et al.* (2017) and comprehensively in Magro *et al.* (under preparation 2019<sup>b</sup>). For quantification purposes in effluent matrices, a calibration curve was built, using standard concentrations that were expected to be found in real samples: eight-points (20, 40, 80, 120, 240, 320, 400, 700) ng/L, with a correlation factor of  $R^2 = 0.9801$ . For TCS analysis in effluent, a solid phase extraction method was optimized (Magro *et al.* submitted 2019<sup>a</sup>). Thus, different pH values, spiking stirring time before extraction, volume elution with different solvents, cartridges and syringe filters were evaluated. The best operational results concerning the analyte recovery ( $95 \pm 3\%$ ) were achieved using (1) pH = 2 (no precipitation of organic matter; TCS in unionized form, less susceptible to photodegradation according to [31]); (2) 30 minutes of stirring time and a 30 minutes pause prior to extraction; (3) MeOH/ACE as the extraction solvent; (4) cartridges Oasis HLB; (5) PTFE syringe filters of (0.45 µm; 2% analyte loss). Six effluents (collected at two different

wastewater treatment plants at different times of the year) were analysed and TCS levels were found of between 106 and 624 ng/L.

### 3.3 E-tongues to triclosan detection and quantification

E-tongues have been gaining greater attention in liquid matrices since 1997. There has been an increase in the number of scientific articles, with several applications, although those whose focus is on the detection of EOCs are still few and are applied to simplified solutions. However, as it was investigated in Magro *et al.* (2019<sup>c</sup>), there is a high potential of e-tongues for qualitative and semi-quantitative multi-analyte analysis in complex matrices. If the e-tongues are well built and properly trained they can be used as tools for EOCs monitoring in aqueous environment matrices. The working electrodes in the e-tongues array can be covered with films (coatings), improving the sensitivity of the electrical measurements. The ability to tune the composition of nanostructured thin films allow for an improvement in the sensor's intrinsic (chemical or physical) properties for sensing applications. The layer-by-layer (LbL) nano-assembly technique is a flexible, easily-scalable, reproducible and versatile approach that allows the precise control of the coating thickness, composition and structure. This nano-assembly technique is a powerful tool for the incorporation of a wide variety of coating types, such as polyelectrolytes. Polyelectrolytes are polymers with ionizable functional groups that form charged polyions (with an overall positive or negative charge). A substance with positively charged functional groups, mostly quaternary ammonium or amino groups, is used as a polycation, for instance poly(allylamine hydrochloride) (PAH) and poly(ethyleneimine) (PEI); whereas a substance with negatively charged groups, mostly sulfonic acids or carboxylic acids, are the most common functional groups used in polyanions, such as, poly(sodium 4-styrene sulfonate) (PSS). In preliminary works about sensors for TCS detection, Pereira-da-Silva *et al.* (2019), Zagalo *et al.* (2019) and Magro *et al.* (2019<sup>h</sup>) proved that if the outer layer is a negatively charged polyelectrolyte, less adsorption into the sensing layers is observed. Additionally, the influence of the solution's pH and ionic strength in the electrical impedance measurements was demonstrated.

Magro *et al.* (submitted, 2019<sup>d</sup>) studied the e-tongue concept in an array of sensors based on uncoated and coated gold interdigitated electrodes with (PAH/Graphene Oxide (GO))<sub>5</sub> and (PEI/PSS)<sub>5</sub> layer-by-layer thin films. The main objective was to study the e-tongue performance (stability, detection and semi-quantification) for TCS analysis in mineral water and secondary effluent matrices by measuring the impedance spectra of the sensor device. The stability tests related with adsorption/desorption phenomena revealed that: (1) (PAH/GO)<sub>5</sub> LbL films should be used to analyse acid matrices with low ionic strength, since the salts in the solution tend to discharge the GO film; (2) (PEI/PSS)<sub>5</sub> LbL films combination reveals potential to be employed in alkaline aqueous matrices, such as secondary effluent, with high ionic strength; (3) uncoated gold sensors react with ions in the effluent and are damaged by S and Zn elements, and therefore should be avoided for these type of matrices. The data showed that

increasing the thickness (number of bi-layers to 10 or 20) did not directly increase the potential to TCS quantification. On the contrary, increasing the distance between the gold electrode and the outer layer of film that interacted with the TCS molecules, decreased the electrical signal. The choice of target sensing layers for each type of matrices is crucial to have a stable and robust device. Thus, if the highest performance sensors (uncoated gold sensors for mineral water and (PEI/PSS)<sub>5</sub> for effluent) are used for the array's composition, by means of Principal Component Analysis, it was possible to reach a device capable of distinguishing between aqueous matrices (mineral water vs effluent) and discriminate TCS according to its concentrations: (1) detection and semi-quantification of the target analyte in mineral and secondary effluent for a range of concentration from  $10^{-13}$  to  $10^{-7}$ M (0.3 ng/L- 30 µg/L); (2) device's sensitivity of  $0.19 \pm 0.02$  per decade ( $\sim$  limit of quantification); (3) device's resolution of 0.13 pM ( $\sim$  limit of detection).

### 3.4 Multi-analyte e-tongue coupled to an electrochemical reactor

According to Magro *et al.* (submitted 2019<sup>d</sup>), a combination of (PEI/PSS)<sub>5</sub> is suitable for TCS detection and semi-quantification in a secondary effluent matrix. However, when the matrix's pH is below 7, desorption of the thin film occurred when immersed in the solutions. In this regard and taking into account the fact that pH changes can occur in electrochemical remediation, stable thin films of TiO<sub>2</sub> and ZnO built up with the sputtering technique were considered to be part of the e-tongue's sensorial layers. Those films presented high mechanical stability under pH fluctuations. Magro *et al.* (submitted 2019<sup>e</sup>) reported a customized e-tongue, built up with an array of layer-by-layer and sputtering thin film sensors. The aim of the array set-up was to access real time degradation in a dynamic electrochemical flow reactor and provide a sensor that is capable of performing semi-quantification analysis for TCS and its derivative by-products: DCP, TCP and MTCS. The e-tongue's capability to "follow" the analytes electro-degradation kinetics in a secondary effluent was supported by the data obtained using HPLC-DAD. Monitoring and semi-quantitative analysis was accomplished using the sensor's array for TCS and MTCS. For DCP and TCP more accurate results were achieved using a single sensor device. These data observations lead to the discussion of the importance of characterizing the nanomaterial used to perform the impedance measurements. This characterization, using field emission scanning electron microscope, allowed total understanding of the "sensorial" impedance response. The observations supported that the "sensorial response" is related to the final morphology, structure and properties of the thin films and their consequent interactions with the different EOCs' physical-chemical behaviour on the effluent matrix. For DCP and TCP (with molecular weight of 163 and 197 g/mol), the better responses were achieved with the polyelectrolyte thin films (built with 5 bi-layers) or using a thin film, built by sputtering technique (TiO<sub>2</sub>), but with low thickness ( $\leq 160$  nm). For TCS and MTCS (with molecular weight of 290 and 303 g/mol) detection and semi-quantification, the sputtering technique with bilayers of semi conductive oxides (thickness = 713 nm) was the one giving better impedance response. According to the experimental data, the thin films with more "hydrophobic character" should be used for TCS and MTCS, the analytes with higher Log  $k_{ow}$ , whereas the more "hydrophilic" ones are best suited for DCP and TCP, the analytes with lower Log  $k_{ow}$ .

Although sensors' systems are becoming attractive to the market [32], as potential tools for environmental monitoring, there is still a lack of information when these sensor devices are targeting multi-analyte analysis. In Magro *et al.* (chapter under preparation 2019<sup>\*</sup>), the drawbacks, advantages and challenges of having electronic tongues coupled with electrochemical processes are discussed.





### 3.5 Electrokinetic Hydrogen self-energy generation

The hydrogen feedstock market has a total estimated value of €105 billion and is expected to grow in the coming years, reaching €142 billion by 2022 [33]. Hydrogen is gaining a more prominent role as an enabler of the clean energy transition. Technologies for H<sub>2</sub> production are taking advantage of the current market expansion, promoting their optimization and development to higher maturity levels. One of the most established technologies for hydrogen production from renewable energy sources is water electrolysis. Around 4 % of the global hydrogen supply is produced via electrolysis [33]. However, due to the high production costs, H<sub>2</sub> is still not economically competitive with other fuels [34].

Hydrogen is a by-product of EK technologies and thus they can be part of hydrogen market production. As in a symbiotic system, the remediation treatment can take the advantage of H<sub>2</sub> market technologies maturity trend, enhancing the technology readiness level (TRL) and minimizing, due to the potential of energy generation, one of its drawbacks for scaling-up. As a novel feature, the H<sub>2</sub> produced during the treatment in the cathode compartment may be used as fuel in a proton-exchange membrane fuel cell to produce electrical energy and reduce the energy costs of electroremediation processes. In this context, the design of the ED reactor may be reconfigured with the incorporation of a gas collection system that may avoid the H<sub>2</sub> dissipation during remediation of the environmental matrices. Thus, the H<sub>2</sub> produced in the process can be collected and recovered to be used for different purposes.

Magro *et al.* (2019<sup>f</sup>) addressed the feasibility (proof-of-concept) of using the H<sub>2</sub> produced by electrochemically-induced remediation of secondary effluent and mine tailings matrices. The results shown that the H<sub>2</sub> captured and reused is promising because: (1) The H<sub>2</sub> flow rate production is not dependent of the matrix under treatment. No statistically significant differences between the matrices were found when the highest current density was applied; (2) self-produced H<sub>2</sub> achieved average purities ranged between 73% and 98%; (3) for both matrices a stable open circuit voltage (~1V, cell maximum nominal voltage) was generated by a proton-exchange membrane fuel; (4) treatment energy savings of around 7% were reached (restriction due to fuel cell full capacity). This study supported that the H<sub>2</sub> purity, flow rate production and voltage generation are not directly affected by the matrices under treatment, when a three compartment ED reactor was used. Moreover, some improvements can be obtained. Thus, in the provisional patent application (2019), for its “designed reactor”, the H<sub>2</sub> flow rate was found to be 60% faster than in the conventional three compartments ED reactor. Also, for the “designed reactor”, when H<sub>2</sub> was directly collected from the matrix compartment, a similar level of gas purity was achieved.

Additionally, Magro *et al.* (chapter under preparation 2019\*\*), observed that for the conventional reactor, if the salty water is replaced by effluent in a mine tailings suspension, the proton-exchange membrane fuel voltage increases, as does its stability. A higher conductivity was measured, meaning more free ions in the system, which directly affects the fuel cell efficiency. Furthermore, the removal of hazardous contaminants and the recovery of critical raw materials can be enhanced (3% for Cu, 5% for As, 22% for Sn and 27% for W), increasing their further reuse.

### 3.6 Potential of replacing freshwater by electro-treated effluent in construction materials

The construction industry already recognizes the value of improving resources productivity and sustainability, namely in the replacement of cement and water sources [35]. However, the transition to a more circular economy requires changes throughout value chains, from product design to new business models, from new ways of turning waste into resources and by new modes of consumer behaviour [36]. Nowadays, the increased demand for construction materials, as a result of global growth, calls for an alternative way of developing construction materials from different sources. In this perspective of “changing times”, Magro *et al.* (2019<sup>g</sup>) reported the feasibility of replacing freshwater by electro-treated effluent in the production of mortars (construction materials). After the ED treatment applied to an effluent, the data showed removal rates of 50-100% for cations, 85-99.7% for anions and an acid final matrix pH, parameters that affect the quality and durability of materials. Using 50% and 100% of treated effluent in the materials mix showed higher setting times and workability, and similar flexural/compressive strengths compared to the reference mortars.

To overcome the parameters that were different to the reference values, such as setting times, workability and matrix final pH, a tuning reactor was developed: the provisional patent application (2019) “designed reactor”. In this application an optimal combination was disclosed: acid media - breaking complexes between elements; alkaline media - removing salts and electrodes in contact with the contaminated matrices - promoting electro-degradation (see section 3.1). The design modifications ensured that the alkaline pH does not change the setting time and workability values significantly. Design differences do not affect the overall removal efficiencies. The removal process, for the “designed reactor”, is slower compared to the three compartment reactors described in Magro *et al.* (2019<sup>g</sup>), but the process became more easier to control. 99% of the salts removal was achieved in the conventional reactor, but the “designed reactor” encompasses fewer hardness matrices in the end (approximately 70% of the elements removal) and offers a dynamic process which is easier to further work. It is important to point out that all the parameters studied are key-factors for the standards in the construction industry: EN 1015-3, EN-196 and EN 206-1 and NBR 15900. In addition, one of the positive features of the final materials, when the product is used as a pre-treatment is the change in the colour (grey to light brown – although not always, depending on the effluent source) or texture (rough to softer) of the materials, which may, for instance, avoid the use of artificial pigments.

As one of the main objectives of this PhD project was to enhance maturity level of EK process development, a market assessment was performed for provisional patent application (2019) “designed

reactor”. The TRL of the developed technology, on a scale of 1 to 7 is considered to be at level 3 (experimental proof of concept) to 4 (technology validated in laboratory), accordingly to the European Commission definition.

The primary market assessment was built for three potential markets segments: construction materials industry, municipal and industrial wastewater treatment plants. Following an 18 week study, the construction materials industry was found to be the priority market for the reuse of treated secondary effluent. There are several reasons for entering this market. First of all, the provisional patent application reactor performance is higher in this segment. More precisely, after the cleaning process, the treated effluent characteristics fulfil all the requirements stated by construction materials standards (e.g. salt content, conductivity) that allows its use in the production of materials while ensuring a high-quality concrete. Secondly, the analysis among the potential company’s stakeholders showed that entry barriers are lower in the concrete production segment, in comparison with the wastewater treatment segments. Thirdly, for the construction segment the novelty of the application is higher. Distributing effluents to concrete batch plants and/or reuse this “reclaimed water”, with the ultimate goal of producing high-quality concrete, is a practice which does not yet exist, accordingly to the conducted research. However, the potential control of the water characteristics used to materials production was seen as a feature that a client value significantly.

In a top-down approach, as the world’s demand for water will increase in the next few decades, making the total market of construction companies located in the United States, the Middle East and Africa, Europe and Asia more relevant. Therefore, in the market value simulations performed in the business plan and market assessment (2018), multiplying the number of companies located in these four regions (1 658 104) by the average reactor price (current water solutions product average price: €65 000) equals a total market value of €108 billion. The target market considers construction companies in which the need is already high. The water scarcity issue is higher in dry regions located in the Middle East and Africa as well as in Asia. Asia has the most polluted water [37] in the planet and the biggest concrete production accounting for 5 billion tons of concrete per year. Following the same logic, the target market will have the size of €440 million. The size of the target market shows the potential for starting the market entry strategy that will focus on scaling-up with an industrial partner in a *win-win* solution, with the purpose of testing the hypothesis that a full-scale product is viable.

### 3.7 Future work

Despite the conclusions in the appended papers regarding the three main core subjects on this PhD project, there are still gaps in the knowledge to be explored and some ideas to be developed, regarding the full application of electrokinetic process for the degradation of emerging organic contaminants, evaluation of new sensor systems for their monitoring and the viability of scaling-up electro-based technologies. Thus, some of the most important topics for future work are summarized as follows:

- The independent manufacture of mixed metal oxide electrodes, to be used in the ED process, should be evaluated. It is expected that at industrial level, significant additional costs may be incurred due to the outsourcing of this manufacture. The building of electrodes in-house would also be extremely important to have less dependency of electrodes production suppliers.
- The “sensorial” output impedance data are complex, demanding a time-consuming analysis. In order to compare sensor systems and therefore, their performance and drawbacks, it is important to develop of a standard analysis method. Additionally, it is needed a trained librarian, to gather all the information from previous sensors measurements. If standardized data treatment was employed in all research groups, the comparison between methods, sensors and their characteristics would be more accurate.
- The efficiency of e-tongue multi-analyte quantification may improve if: (1) biosensors build up with lipids are considered as sensing layers, since some EOCs are, e.g, TCS, lipophilic molecules; (2) hybrid layers are developed, such as  $\text{TiO}_2/\text{PSS}$ , that will provide a negative charge to the outcome layer, resulting in “sensorial” signal increase.
- The study of increasing the nominal voltage of the proton-exchange membrane fuel and understanding its full potential to feed a larger system.
- Regarding the provisional patent application “designed reactor”, the scaling-up is required to the next phase in order to conduct tests on industrial mortars production in a construction company, together with the reactor pilot implementation on the facility.
- One of the main obstacles in the EU wastewater reuse implementation is the price of wastewater. In this PhD project, initial values were achieved in an integrated solution that includes: wastewater as a raw material in a product reactor solution. However, we still do not fully understand its behaviour on a larger scale. It is believed that the scaling-up on an industrial level will improve the process, price and market knowledge. Additionally, a bottom-up approach regarding the market size is also recommended for further actions.



## References

---

- [1] United Nations World Water Assessment Programme, The United Nations World Water Development Report 2018: Nature-Based Solutions for Water, Paris, 2018.
- [2] EC, European Commission, Optimising water reuse in the EU - Final report, Part I, 2015. doi:10.2779/603205.
- [3] C.G. Daughton, Non-regulated water contaminants: Emerging research, *Environ. Impact Assess. Rev.* 24 (2004) 711–732. doi:10.1016/j.eiar.2004.06.003.
- [4] V. Geissen, H. Mol, E. Klumpp, G. Umlauf, M. Nadal, M. Van Der Ploeg, S.E.A.T.M. Van De Zee, C.J. Ritsema, Emerging pollutants in the environment: A challenge for water resource management, *Int. Soil Water Conserv. Res.* 3 (2015) 57–65. doi:10.1016/j.iswcr.2015.03.002.
- [5] R. Halden, The Great Sewage Census in *The Analytical Scientist*, 79 (2019) 22–30. <https://theanalyticalscientist.com/fields-applications/the-great-sewage-census>.
- [6] D.A. Brose, K. Kumar, A. Liao, L.S. Hundal, G. Tian, A. Cox, H. Zhang, E.W. Podczewinski, A reduction in triclosan and triclocarban in water resource recovery facilities' influent, effluent, and biosolids following the U.S. Food and Drug Administration's 2013 proposed rulemaking on antibacterial products, *Water Environ. Res.* 91 (2019) 715–721. doi:10.1002/wer.1101.
- [7] J. Chen, X. Meng, A. Bergman, R.U. Halden, Nationwide reconnaissance of five parabens, triclosan, triclocarban and its transformation products in sewage sludge from China, *J. Hazard. Mater.* 365 (2019) 502–510. doi:10.1016/j.jhazmat.2018.11.021.
- [8] W. Hua, E. Bennett, R. Letcher, Triclosan in waste and surface waters from the upper Detroit River by liquid chromatography-electrospray-tandem quadrupole mass spectrometry, *Environ. Int.* 31 (2005) 621–630. doi:10.1016/j.envint.2004.10.019.
- [9] D.C. McAvoy, B. Schatowitz, M. Jacob, A. Hauk, W.S. Eckhoff, Measurement of triclosan in wastewater treatment systems, *Environ. Toxicol. Chem.* 21 (2002) 1323–1329. doi:10.1002/etc.5620210701.
- [10] L.W.B. Olaniyan, N. Mkwetshana, A.I. Okoh, Triclosan in water, implications for human and environmental health, *Springerplus.* 5 (2016). doi:10.1186/s40064-016-3287-x.
- [11] L.M. Weatherly, J.A. Gosse, Triclosan exposure, transformation, and human health effects, *J. Toxicol. Environ. Heal. - Part B Crit. Rev.* (2017). doi:10.1080/10937404.2017.1399306.
- [12] Food and Drug Administration, FDA issues final rule on safety and effectiveness of antibacterial soaps, US, DHHS - Department Of Health And Human Services, 2016.
- [13] Food and Drug Administration, Safety and Effectiveness for Health Care Antiseptics; Topical Antimicrobial Drug Products for Over-the-Counter Human Use., US, DHHS - Department Of Health And Human Services, 2017.
- [14] C.S. Bever, A.A. Rand, M. Nording, D. Taft, K.M. Kalanetra, D.A. Mills, M.A. Breck, J.T. Smilowitz,

- J.B. German, B.D. Hammock, Effects of triclosan in breast milk on the infant fecal microbiome, *Chemosphere*. 203 (2018) 467–473. doi:10.1016/j.chemosphere.2018.03.186.
- [15] J.-H. Guo, X.-H. Li, X.-L. Cao, Y. Li, X.-Z. Wang, X.-B. Xu, Determination of triclosan, triclocarban and methyl-triclosan in aqueous samples by dispersive liquid–liquid microextraction combined with rapid liquid chromatography, *J. Chromatogr. A*. 1216 (2009) 3038–3043. doi:10.1016/j.chroma.2009.02.021.
- [16] M.E. Balmer, T. Poiger, C. Droz, K. Romanin, P.A. Bergqvist, M.D. Müller, H.R. Buser, Occurrence of Methyl Triclosan, a Transformation Product of the Bactericide Triclosan, in Fish from Various Lakes in Switzerland, *Environ. Sci. Technol.* 38 (2004) 390–395. doi:10.1021/es030068p.
- [17] L. Xing, J. Sun, H. Liu, H. Yu, Combined toxicity of three chlorophenols 2,4-dichlorophenol, 2,4,6-trichlorophenol and pentachlorophenol to *Daphnia magna*, *J. Environ. Monit.* 14 (2012) 1677–1683. doi:10.1039/c2em30185g.
- [18] Y.B. Acar, A.N. Alshwabkeh, Principles of Electrokinetic Remediation, *Environ. Sci. Technol.* 27 (1993) 2638–2647. doi:10.1021/es00049a002.
- [19] H.I. Gomes, C. Dias-Ferreira, A.B. Ribeiro, Overview of in situ and ex situ remediation technologies for PCB-contaminated soils and sediments and obstacles for full-scale application, *Sci. Total Environ.* 445–446 (2013) 237–260. doi:10.1016/j.scitotenv.2012.11.098.
- [20] P. Guedes, E.P. Mateus, N. Couto, Y. Rodríguez, A.B. Ribeiro, Electrokinetic remediation of six emerging organic contaminants from soil, *Chemosphere*. 117 (2014) 124–131. doi:10.1016/j.chemosphere.2014.06.017.
- [21] P. Guedes, C. Magro, N. Couto, A. Mosca, E.P. Mateus, A.B. Ribeiro, Potential of the electro-dialytic process for emerging organic contaminants remediation and phosphorus separation from sewage sludge, *Electrochim. Acta*. 181 (2015) 109–117. doi:10.1016/j.electacta.2015.03.167.
- [22] A.R. Ferreira, N. Couto, P. Guedes, J. Pinto, E.P. Mateus, A.B. Ribeiro, Electro-dialytic 2-compartment cells for emerging organic contaminants removal from effluent, *J. Hazard. Mater.* 358 (2018) 467–474. doi:10.1016/j.jhazmat.2018.04.066.
- [23] M.H.M. Facure, L.A. Mercante, L.H.C. Mattoso, D.S. Correa, Detection of trace levels of organophosphate pesticides using an electronic tongue based on graphene hybrid nanocomposites, *Talanta*. 167 (2017) 59–66. doi:10.1016/j.talanta.2017.02.005.
- [24] Y. Vlasov, A. Legin, A. Rudnitskaya, C. Di Natale, A. D’Amico, Nonspecific sensor arrays (“electronic tongue”) for chemical analysis of liquids (IUPAC Technical Report), *Pure Appl. Chem.* 77 (2005) 1965–1983. doi:10.1351/pac200577111965.
- [25] C.R. Gagg, Cement and concrete as an engineering material: An historic appraisal and case study analysis, *Eng. Fail. Anal.* (2014). doi:10.1016/j.engfailanal.2014.02.004.
- [26] S.A. Miller, A. Horvath, P.J.M. Monteiro, Impacts of booming concrete production on water resources worldwide, *Nat. Sustain.* 1 (2018) 69–76. doi:10.1038/s41893-017-0009-5.
- [27] P.E. Josephson, Y. Hammarlund, Causes and costs of defects in construction a study of seven building projects, *Autom. Constr.* 8 (1999) 681–687. doi:10.1016/S0926-5805(98)00114-9.



- [28] E. Lacasa, S. Cotillas, C. Saez, J. Lobato, P. Cañizares, M.A. Rodrigo, Environmental applications of electrochemical technology. What is needed to enable full-scale applications?, *Curr. Opin. Electrochem.* 16 (2019) 149–156. doi:<https://doi.org/10.1016/j.coelec.2019.07.002>.
- [29] J. Lyndall, T. Barber, W. Mahaney, M. Bock, M. Capdevielle, Evaluation of triclosan in Minnesota lakes and rivers: Part I – ecological risk assessment, *Ecotoxicol. Environ. Saf.* 142 (2017) 578–587. doi:<https://doi.org/10.1016/j.ecoenv.2017.04.049>.
- [30] J. Wang, D. Zhi, H. Zhou, X. He, D. Zhang, Evaluating tetracycline degradation pathway and intermediate toxicity during the electrochemical oxidation over a Ti/Ti4O7 anode, *Water Res.* 137 (2018) 324–334. doi:<https://doi.org/10.1016/j.watres.2018.03.030>.
- [31] A. Lindström, I.J. Buerge, T. Poiger, P.A. Bergqvist, M.D. Müller, H.R. Buser, Occurrence and environmental behavior of the bactericide triclosan and its methyl derivative in surface waters and in wastewater, *Environ. Sci. Technol.* 36 (2002) 2322–2329. doi:10.1021/es0114254.
- [32] K. Walia, *Global IoT Sensor Market Report 2018-2025*, 2019.
- [33] IRENA, *Hydrogen From Renewable Power: Technology outlook for the energy transition*, Abu Dhabi, 2018. [www.irena.org](http://www.irena.org).
- [34] P. Nikolaidis, A. Poullikkas, A comparative overview of hydrogen production processes, *Renew. Sustain. Energy Rev.* 67 (2017) 597–611. doi:10.1016/j.rser.2016.09.044.
- [35] European Commission, *Resource efficiency opportunities in the building sector*, 2014. <http://eur-lex.europa.eu/>.
- [36] A. Favier, C. De Wolf, K. Scrivener, G. Habert, *A sustainable future for the european cement and concrete industry - Technology assessment for full decarbonisation of the industry by 2050*, 2019. doi:10.3929/ethz-b-000301843.
- [37] World Health Organization, *National systems to support drinking-water, sanitation and hygiene: global status report 2019*. UN-Water global analysis and assessment of sanitation and drinking-water (GLAAS) 2019 report, 2019.



## *Part II*

*“Of course, it is happening inside your head, Harry, but why on earth should that mean that it is not real?”*

– Albus Dumbledore, Harry Potter and the Deathly Hallows -



## Paper

*“Emerging organic contaminants in wastewater: Understanding electrochemical reactors for triclosan and its by-products degradation”*

*C Magro, EP Mateus, JM Paz-Garcia & AB Ribeiro*

*Published in: Chemosphere, 2019*





## Emerging organic contaminants in wastewater: Understanding electrochemical reactors for triclosan and its by-products degradation



Cátia Magro <sup>a,\*</sup>, Eduardo P. Mateus <sup>a</sup>, Juan M. Paz-Garcia <sup>b</sup>, Alexandra B. Ribeiro <sup>a,\*\*</sup>

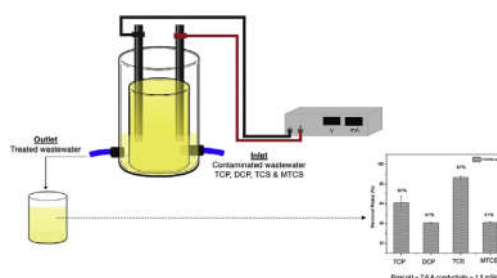
<sup>a</sup> CENSE, Department of Sciences and Environmental Engineering, NOVA School of Science and Technology, NOVA University Lisbon, Caparica Campus, 2829-516, Caparica, Portugal

<sup>b</sup> Department of Chemical Engineering, Faculty of Sciences, University of Malaga, Teatinos Campus, 29010, Málaga, Spain

### HIGHLIGHTS

- Electrochemical degradation reactors evaluation for triclosan and its by-products.
- Batch and flow reactors tested with two different anodes: Ti/MMO & Nb/BDD.
- Electro-batch reactor degradation efficiencies from 43% - < detection limit in 4 h.
- Electro-batch reactor kinetics higher with Ti/MMO used as anode.
- Electro-flow reactor degradation efficiencies from 41 to 87% in 1 h.

### GRAPHICAL ABSTRACT



### ARTICLE INFO

#### Article history:

Received 12 September 2019

Received in revised form

16 December 2019

Accepted 23 December 2019

Available online 30 December 2019

Handling Editor: Ignasi Sires

#### Keywords:

Emerging organic contaminants

Triclosan

By-products

Electrochemical process

Electrokinetics

Electro-degradation

### ABSTRACT

Degradation technologies applied to emerging organic contaminants from human activities are one of the major water challenges in the contamination legacy. Triclosan is an emerging contaminant, commonly used as antibacterial agent in personal care products. Triclosan is stable, lipophilic and it is proved to have ecotoxicologic effects in organics. This induces great concern since its elimination in wastewater treatment plants is not efficient and its by-products (e.g. methyl-triclosan, 2,4-dichlorophenol or 2,4,6-trichlorophenol) are even more hazardous to several environmental compartments. This work provides understanding of two different electrochemical reactors for the degradation of triclosan and its derivative by-products in effluent. A batch reactor and a flow reactor (mimicking a secondary settling tank in a wastewater treatment plant) were tested with two different working anodes: Ti/MMO and Nb/BDD. The degradation efficiency and kinetics were evaluated to find the best combination of current density, electrodes and set-up design. For both reactors the best electrode combination was achieved with Ti/MMO as anode. The batch reactor at 7 mA/cm<sup>2</sup> during 4 h attained degradation rates below the detection limit for triclosan and 2,4,6-trichlorophenol and, 94% and 43% for 2,4-dichlorophenol and methyl triclosan, respectively. The flow reactor obtained, in approximately 1 h, degradation efficiencies between 41% and 87% for the four contaminants. This study suggests an alternative technology for emerging organic contaminants degradation, since the combination of a low

**Abbreviations:** BDD, Boron-doped diamond; DCP, 2,4-dichlorophenol; EBR, Electrochemical Batch Reactor; EFR, Electrochemical Flow Reactor; EOCs, emerging organic contaminants; MTCS, methyl-triclosan; MMO, Mixed metal oxides; TCP, 2,4,6-trichlorophenol; TCS, triclosan.

\* Corresponding author.

\*\* Corresponding author.

E-mail addresses: [c.magro@campus.fct.unl.pt](mailto:c.magro@campus.fct.unl.pt) (C. Magro), [abr@fct.unl.pt](mailto:abr@fct.unl.pt) (A.B. Ribeiro).

current density with the flow and matrix induced disturbance increases and speeds up the compounds' elimination in a real environmental matrix.

© 2019 Elsevier Ltd. All rights reserved.

## 1. Introduction

The world's rapid population growth over the last century has been a major factor into the demand for water resources usage and reuse. To overcome these water challenges, water contamination must be taken into account. Recently, the environmental quality criteria of water resources have been linked to a new class of environmental pollutants, the emerging organic contaminants (EOCs), a reality that has increased the need for sustainable tools that guarantee their quality and safety standards, enable their monitoring and promote the prosperity of a healthy population and environment (Corcoran et al., 2010). EOCs are defined as "chemical substances that have no regulation and are suspected to negatively affect the environment or whose effects are unknown" (Daughton, 2004; Geissen et al., 2015). Among EOCs, triclosan (TCS, 2,4,4'-trichloro-2'-hydroxydiphenyl ether) is an antimicrobial agent that has been used for more than 50 years as an antiseptic, disinfectant or preservative in clinical settings and several consumer products. TCS has been detected in wastewater treatments plants (Brose et al., 2019; Chen et al., 2019; Halden, 2019) and in surface water (Hua et al., 2005; McAvoy et al., 2002). Recent reviews on TCS recount numerous health effects ranging from endocrine-disruption to uncoupling mitochondria (Olaniyan et al., 2016; Weatherly and Gosse, 2017). Although in 2016 the US Food and Drug Administration banned TCS from certain wash products, namely hand soap and body wash (Food and Drug Administration, 2016) and hospital products by the end of 2018 (Food and Drug Administration, 2017), it is permissible to have TCS in e.g. toothpastes, cosmetics, clothes or toys (Bever et al., 2018). Furthermore, TCS derivatives, such as the metabolite methyl-triclosan (MTCS) (Guo et al., 2009), which is even more persistent (Balmer et al., 2004) and TCS by-products, formed by repeated exposure to chlorine in water such as 2,4-dichlorophenol (DCP) and 2,4,6-trichlorophenol (TCP) are also under concern, since they present health risk to humans and are recognized as persistent priority pollutants in the United States, Europe and China (Xing et al., 2012).

Several clean-up technologies have been developed and used to improve the quality and safety of water reuses. Among these technologies, the electrochemically-induced advanced oxidation processes (e.g. Fenton's reaction and anodic oxidation) have been receiving special attention (Glaze et al., 1987; Oturan and Aaron, 2014; Panizza and Cerisola, 2009). Another alternative is the electrokinetic process which is based on the application of a low-level direct current between a pair of electrodes, that in addition to remove contaminants from the contaminated matrix by electric potential also promotes the generation of  $\cdot\text{OH}$  and therefore enhances the oxidation of EOCs. This technology proved to be efficient in the degradation of EOCs in soil (Guedes et al., 2014), sludge (Guedes et al., 2015) and effluent (Ferreira et al., 2018). The optimal combination between the electrode materials (e.g. titanium/mixed metal oxides (Ti/MMO), boron-doped diamond (BDD), platinum) and the reactor design are key factors, since the oxidation process is dependent on the materials nature and the reactor workability (Schranck and Doudrick, 2020; Walsh and Ponce de León, 2018). Regarding the reported works on different electrode materials and batch/flow reactors, Ren et al. (2016) presented a vertical-flow electro-Fenton reactor, composed of 10 cell compartments using

PbO<sub>2</sub> anode and modified graphite felt mesh cathode for the degradation of tartrazine, reaching with the optimal conditions, TOC removal efficiency of 100%. Pérez et al. (2017) studied a microfluidic flow-through electrochemical reactor for wastewater treatment that achieved, with diamond anodes, complete mineralization of clopyralid spiked in a low-conductive matrix. Wang et al. (2019) reported a continuous-flow reactor for electrochemical oxidation of various alcohols using a carbon anode, where 800 mA enabled effective oxidation up to 99% yield in 10 min. Moreover, comparative studies in electrodes combinations were described: Yoon et al. (2012) reported a flow reactor for the electrochemical degradation of phenol and 2-chlorophenol using Pt/Ti and BDD electrodes, as well as Ambauen et al. (2019) comprised an electrochemical oxidation batch reactor for salicylic acid degradation with BDD and Pt electrodes. In both studies similar removal rates in the different electrodes combinations were attained, showing that not only the electrodes type highly influence the compounds degradation efficiencies, but also the physicochemical characteristics of the contaminants to be degraded. BDD and MMO have been mainly and equally used as anodes (Moreira et al., 2017), both showing similar performances in the degradation efficiency (Brillas and Martínez-Huitle, 2015; Skoumal et al., 2008; Yoon et al., 2012). BDD was reported as electrochemical inactivator of phenolic compounds (Sirés et al., 2007; Wang and Farrell, 2004), and Ti/MMO was used to degrade organic contaminants in wastewater (Yuan et al., 2013).

The aim of this study was to carry out an experimental electrochemical treatment for the degradation of TCS and its by-products MTCS, DCP and TCP, in a real wastewater matrix: a secondary effluent. A batch reactor was the starting core, with experiments on (1) electrodes combination (Ti/MMO as anode and cathode; BDD/Nb as anode and Ti/MMO as cathode); (2) current densities; (3) degradation kinetics. Furthermore, a flow reactor, designed to mimic a secondary settling tank in a wastewater treatment plant, was introduced to find a system that has the potential for operational implementation.

## 2. Materials and methods

### 2.1. Chemical, standards and effluent characteristics

TCS (99%), MTCS (99%), DCP (98%) and TCP (98%) were purchased from Sigma–Aldrich (Steinheim, Germany), see Table S1, at supplementary data. Individual stock solutions for calibration purposes were prepared with 1000 mg/L in methanol and stored at  $-18\text{ }^{\circ}\text{C}$ . The methanol, acetonitrile, acetone and formic acid used were from Sigma–Aldrich (Steinheim, Germany) in gradient grade type. Water (Type I) was from a Millipore system (Bedford, MA, USA). The effluent used was the liquid fraction collected in the secondary settling tank at a wastewater treatment plant (Lisbon, Portugal). Effluent samples were collected in April and May and its initial characterization, for future works comparison, is presented in Table S2, at supplementary data.



## 2.2. Methods

### 2.2.1. Electrochemical degradation reactors

Two different set-ups are represented in Fig. 1. The experiments were carried out in an electrochemical batch reactor (EBR) and in an electrochemical flow reactor (EFR). The electrodes used were made of Ti/MMO Permaskand wire:  $\varnothing = 3$  mm,  $L = 80$  mm (Grønvold & Karnov A/S, Denmark) and Nb/BDD plate:  $H = 50$  mm,  $L = 80$  mm,  $T = 1$  mm (Neocoat, Switzerland), assembled in different configurations (as anode or as cathode). A power supply E3612A (Hewlett Packard, Palo Alto, USA) was used to maintain a constant current in the electrochemical reactors and the voltage was monitored. The volume of effluent treated was approximately 500 mL for each reactor. The effluent flow (9 mL/min) in the EFR was maintained by a peristaltic pump (Watson-Marlow 503 U/R, Watson-Marlow Pumps Group, Falmouth, Cornwall, UK).

All electrochemical experiments were carried out in duplicate, in dark conditions, and at a controlled room temperature of 22 °C, according to the conditions presented in Table 1. Control experiments, without applying current, were also carried out. During the experiments, the pH was measured with a Radiometer pH-electrode EDGE (HANNA, USA) and the conductivity with a Radiometer Analytic LAQUA twin (HORIBA Ltd., Japan). In both reactors (EBR and EFR) the matrix was spiked with the four compounds under study (TCS, MTCS, DCP and TCP), in order to monitor their degradation process (0.8 mg/L for each). To assess EOCs removal kinetics in the EBR, samples were collected every 15 min, during

4 h. For EOCs determination and quantification, initial and final samples were extracted following the procedures described in section 2.2.2.

### 2.2.2. Instruments and analytical procedures

The effluent initial characterization was performed for the following chemical parameters: Chemical Oxygen Demand, COD (determined by volumetric method after a previous oxidation with potassium dichromate in an open-reflux, at 160 °C, in an acidic environment, for 60 min); biological oxygen demand, BOD<sub>5</sub> (determined by using a specific probe: OxiTop IS6, GlobalW Gold River, CA, USA); Total P concentration was determined by Inductively Coupled Plasma with Optical Emission Spectrometry, ICP-OES (HORIBA Jobin-Yvon Ultima, Japan), equipped with generator RF (40.68 MHz), monochromator Czerny-Turner with 1.00 m (sequential), automatic sampler AS500 and dispersive CMA-Concomitant Metals Analyzer. Cl<sup>-</sup>, NO<sub>3</sub><sup>-</sup> and SO<sub>4</sub><sup>2-</sup> were analyzed by Ion Chromatography, IC (DIONEX ICS-3000, USA), equipped with conductivity detector.

The extraction of the analytes in the effluent was performed by solid-phase extraction using Oasis HLB (200 mg, 6 mL; Waters Corporation, Saint-Quentin-en-Yvelines Cedex, France). The solid-phase extraction cartridges were conditioned by washing with 3 × (6 mL) of methanol, followed by re-equilibrium with 3 × (6 mL) of Milli-Q water. For organic compounds enrichment, the samples were acidified to pH = 2 before extraction using nitric acid. The 200 mL aqueous samples were passed through the cartridge at a

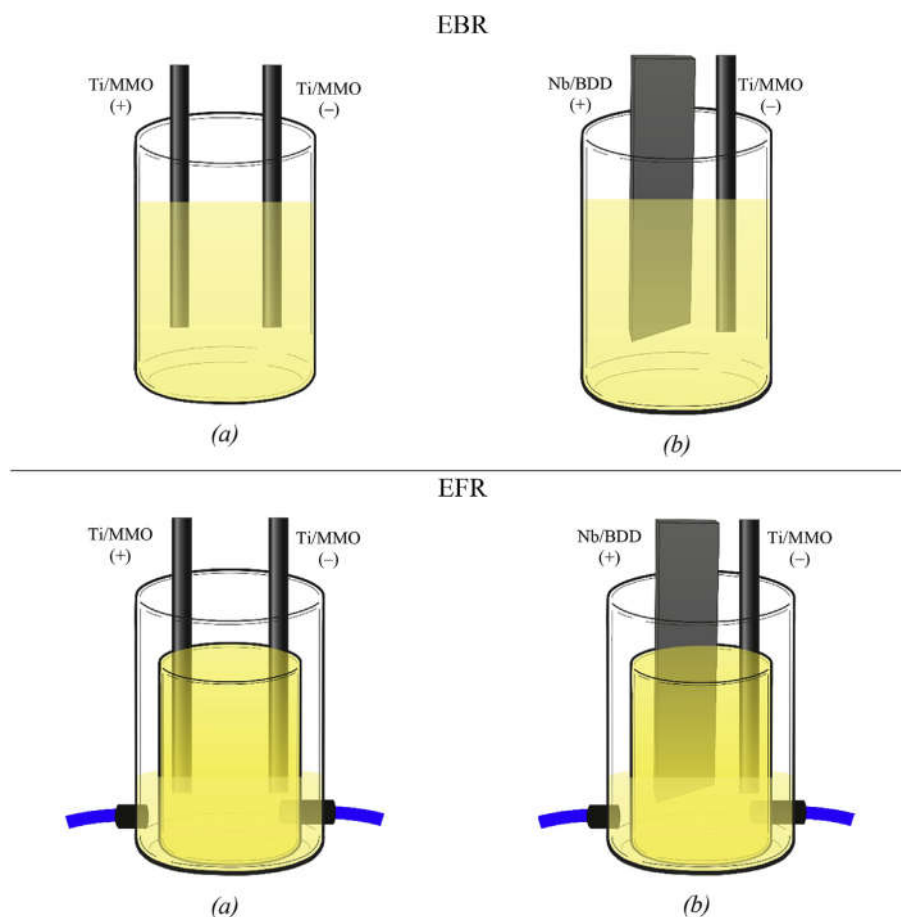


**Fig. 1.** Electrochemical reactors under study: (a) case 1 Ti/MMO as anode and cathode; (b) case 2 Nb/BDD as anode and Ti/MMO as cathode (EBR and EFR related to Electrochemical Batch Reactor and Electrochemical Flow Reactor, respectively).

**Table 1**  
Experimental scheme: evaluated parameters.

	Current density at anode (mA/cm <sup>2</sup> )	Kinetics study	Reactor type
Case 1: Ti/MMO as anode and cathode	2, 3, 7, 14	7 mA/cm <sup>2</sup>	EBR
Case 2: Nb/BDD as anode and Ti/MMO as cathode	2, 4, 8.5, 10	10 mA/cm <sup>2</sup>	EBR
Case 1: Ti/MMO as anode and cathode	7	–	EFR
Case 2: Nb/BDD as anode and Ti/MMO as cathode	10	–	EFR

flow rate of approximately 10 mL/min by applying a moderate vacuum, followed by a dried period of approximately 3 min by vacuum. The retained analytes were eluted sequentially with 2 × (4 mL) of methanol and 1 × (4 mL) of acetone, conferring a concentration factor of 16.7x to the analysis.

Determination of the target compounds was performed in an Agilent 1260 Infinity II high-performance liquid chromatography (HPLC) equipped with a quaternary pump and auto-sampler, and a diode array detector (DAD)/fluorescence detector 1100 Series (Agilent Technologies Inc., USA). An EC-C18 column (InfinityLab Poroshell 120 High Efficiency with 4.6 mm × 100 mm, 2.7 μm, Agilent Technologies Inc., USA) was used. All HPLC runs were performed at a constant flow (1.5 mL/min), in gradient mode, with the oven set to 36 °C. A mixture of acetonitrile/Milli-Q water/formic acid was used as eluents (A: 5/94.5/0.5% and B: 94.5/5/0.5%) with a gradient of 60% of B (0–2 min) followed by 97% of B (2–3.5 min) and 98% of B until 5 min. Calibration curve was performed in the range between 0.5 and 20.0 mg/L. The limits of detection and quantification in this work were, respectively, 0.7 and 2.0 mg/L for TCS, 1.3 and 3.9 mg/L for MTCS, 0.7 and 2.0 mg/L for DCP, 1.0 and 3.0 mg/L for TCP. Recovery tests were made with fortified effluent for 1 h of contact time (30 min of slow agitation). The recovery percentages were between 62 and 120% in all cases. The same HPLC system was used to monitor the EOCs' degradation rates and kinetics behavior. The percentage of degradation was calculated according to Equation (1):

$$\left(1 - \frac{\text{Final EOC mg/L}}{\text{Initial EOC mg/L}} \times 100\right) \quad (1)$$

The mineralization of EOCs was analyzed from the decay of their total organic carbon, TOC, which was determined on a Vario TOC select analyzer (Elementar, Langensfeld, Germany), after filtration using 0.70 μm membrane filters. The screen and diagnostic of new peaks related to compounds formed after the electrochemical treatments was performed by liquid chromatography/mass spectrometry (LC/MS)L, LC Agilent 1200 Series with Binary pump - MS Agilent 6130 B Single Quadrupole (Agilent Technologies Inc., USA).

All sample analysis was carried out in duplicate. The statistical data obtained was analyzed by the GraphPad Prism version 8.0e. Statistically significant differences among samples for 95% level of confidence were calculated through *t*-test on way and ANOVA.

### 3. Results and discussion

In the following section, electrochemical reactors for the degradation of EOCs in effluent were tested (cases according to Table 1 conditions), correspondingly:

- i. EBR was tested to find the best current for both electrodes' combination: Cases 1 and 2;
- ii. EBR degradation kinetics was studied for the most appropriated current, for both electrodes' combination: Cases 1 and 2; electro-byproducts were investigated as well.

- iii. EFR degradation was studied for both electrodes combination: Cases 1 and 2, in order to have a final decision on which one is the best option for a reactor operational implementation.

#### 3.1. Electrochemical treatment evaluation

##### 3.1.1. Electrochemical batch reactor (EBR): pH, conductivity and voltage

Table 2 presents the pH, conductivity and voltage measured at the beginning and after 4 h of the EBR treatment.

In the control experiments (data not shown) there were no significant pH and conductivity changes in the effluent. pH with the Ti/MMO as anode remained approximately constant, whereas for Nb/BDD as anode, acidification occurred, as the applied current increased (initial vs final at different pH: *p* value = 0.001–0.01 at 95% of confidence level). This indicates that Nb/BDD anode has a better tendency for water oxidation promoting, the acidification of the media (pH decreases from around 8 to 3.8).

The conductivity of the matrix increased in the experiment with the highest current density and only when using Nb/BDD as anode. The degradation process may cause the presence of more ions in solution, and consequently higher conductivity at the end of the experiments. The voltage drop behavior is in accordance with the changes observed in the conductivity. A slight variation of voltage between the working electrodes was observed in all cases, except in the control assay, related to the changes in conductivity due to electrolysis reactions. Concentration profiles within the reactor were observed, indicating that mixing could play an effect on energy requirements.

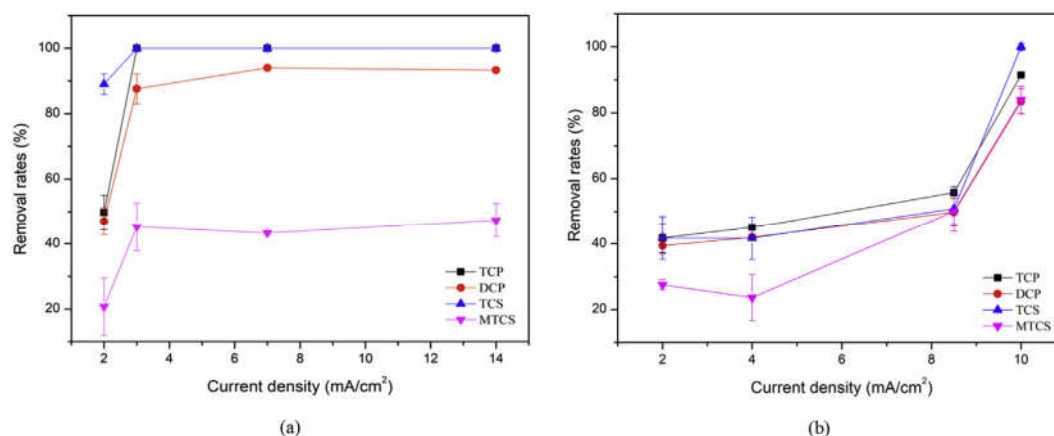
##### 3.1.2. Electrochemical batch reactor (EBR): current density

Fig. 2 shows the removal of the target EOCs, measured as the

**Table 2**  
pH, conductivity and voltage before and after the EBR treatment during 4 h, with Ti/MMO or Nb/BDD as anode.

	Current density at anode (mA/cm <sup>2</sup> )	pH	Conductivity (mS/cm)	Voltage (V)
Initial		8.3 ± 0.1	1.2 ± 0.2	13.7 ± 7.6
Ti/MMO	2	8.0 ± 0.1	0.7 ± 0.1	6.5 ± 0.6
	3	7.9 ± 0.1	1.0 ± 0.5	9.4 ± 3.5
	7	8.5 ± 0.5	1.1 ± 0.1	14.2 ± 0.8 <sup>C</sup>
	14	8.5 ± 0.6	1.0 ± 0.0	17.6 ± 5.6
Initial		8.4 ± 0.2 <sup>A</sup>	1.4 ± 0.9	15.4 ± 10.2
Nb/BDD	2	7.0 ± 0.0 <sup>B</sup>	1.1 ± 0.5	9.6 ± 1.9
	4	5.8 ± 1.3 <sup>A</sup>	1.0 ± 0.5	11.0 ± 0.1
	8.5	3.9 ± 0.0 <sup>A,b</sup>	1.2 ± 0.2	25.0 ± 5.4
	10	3.8 ± 0.1 <sup>A,b</sup>	2.4 ± 0.2	12.0 ± 1.4 <sup>C</sup>

Statistical analysis: Multiple comparisons were statistically performed at *p* < 0.05; data with lower case letters are statistically significantly different from the ones with the same capital letter.



**Fig. 2.** Emerging organic contaminants degradation with different currents intensities: (a) case 1: Ti/MMO as anode and cathode; (b) case 2: Nb/BDD as anode and Ti/MMO as cathode; during 4 h treatment (error bars related to the standard deviation:  $n = 2$ ; TCP - 2,4,6-trichlorophenol; DCP - 2,4-dichlorophenol; TCS - triclosan; MTCS - methyl-triclosan).

percentage of degradation. Control experiments showed no degradation. As the experiments were carried out in dark conditions, photodegradation was not taking place. Compound volatilization from effluent is not expected to be an important degradation process based on the estimated Henry's law constant of the studied compounds ( $k_H > 10^{-6}$ ) (Table S1 at supplementary data). Thus, the degradation rates are attributed namely to (1) biotic factors, (2) direct anodic oxidation, and (3) indirect oxidation in the liquid bulk. Direct anodic oxidation occurs as the contaminants get in contact with anode surface and are destroyed by the electron transfer reaction. Indirect oxidation in the liquid bulk is mediated by the oxidants that are formed electrochemically, such as chlorine, hypochlorite, hydroxyl radicals, ozone and hydrogen peroxide (Klavarioti et al., 2009). Also, if the pH during the experiments is greater than EOC's pKa (Ti/MMO 7 and 14 mA/cm<sup>2</sup>), the compounds were in their ionized form, more susceptible to degradation (Chianese et al., 2016).

In a simpler design as EBR (Fig. 1), the main removal mechanism is the electro-degradation that corresponds to compounds' oxidation and reduction. At the anode, the EOCs suffer both direct and indirect degradation whereas, in the cathode, only indirect degradation will occur. As mentioned before, in the case 2 experiments (4, 8.5, 10 mA/cm<sup>2</sup>, with Nb/BDD as anode) the pH turned acidic, thus, the hydroxyl radical had a standard reduction potential of 2.8 V ( $\cdot\text{OH} + e^- + \text{H}^+ = \text{H}_2\text{O}$ ). In the case 1 experiments the alkaline pH decreases the standard reduction potential to 1.8 V ( $\cdot\text{OH} + e^- = \text{OH}^-$ ). Moreover, chemical structures (Table S1 at supplementary data) and reactivity will play a role in the degradation process. For instance, the phenolic ring of TCS can be activated by the two O-containing groups and may be attacked by  $\cdot\text{OH}$  radicals, with production of hydroxylated TCS (Yuan et al., 2013). In both cases 1 and 2, TCS was degraded below its detection limit. Additionally, if an aromatic molecule carries an aliphatic side chain,  $\cdot\text{O}$  attacks there by H abstraction whilst  $\cdot\text{OH}$  adds preferentially to the aromatic ring (applied to TCS in its ionized: EBR experiments with 7 and 14 mA/cm<sup>2</sup>) (Buxton et al., 1988). Performing a statistical comparison with a one-way *t*-test, with 95% confidence, for the highest current densities, in case 1 (Ti/MMO as anode at 14 mA/cm<sup>2</sup>) and case 2 (Nb/BDD as anode at 10 mA/cm<sup>2</sup>) regarding the removal rates, Ti/MMO is slightly better at the degradation of TCP (<LOD and ~91%, with a *p* value = 0.0061). BDD is clearly more efficient at degrading MTCS (~47%–84% with a *p* value = 0.015).

According to the above data, the decision for the best current density in the following sections were based on: (1) Ti/MMO anode, 7 mA/cm<sup>2</sup> was chosen because either less intermediate peaks (by-

products formed after electro-degradation) were detected in the LC/MS analysis or also, in the case of the highest current tested, the ratio between the energy consumption and the degradation rates were similar and less costly; (2) Nb/BDD anode, 10 mA/cm<sup>2</sup> was chosen due to the higher degradation observed for MTCS compound.

### 3.1.3. Electrochemical batch reactor (EBR): degradation kinetics

Normalized decay of concentration as a function of time over 4 h, for the two electrodes combination at the best current density conditions, are present in Fig. S1 at supplementary data. Considering a pseudo first-order degradation for all contaminants, the corresponding law rate can be written as Equation (2):

$$\ln(C/C_0) = -kt \quad (2)$$

where  $k$  (min<sup>-1</sup>) is the apparent constant rate of the reaction.

According to experimental data, Table 3, the EOCs removal follow a pseudo first-order kinetics ( $R^2 \geq 0.9$ ).

From the kinetics obtained it is possible to estimate that the contaminants removal starts immediately after the application of the electric current (see Fig. S1 at supplementary data). The fastest rate was achieved with Ti/MMO for TCS and the slowest for MTCS in both electrodes combination (Table 3). Comparing both anodes, the degradation velocity is lower with Nb/BDD that also presents identical degradation rates for all the analytes under study, showing a more constant degradation velocity behavior. The higher adsorption's strength of  $\cdot\text{OH}$  radicals on each electrode surface (adsorption enthalpy) the lower oxidizing power (Kapařka and Comminellis, 2009). Even though, the BDD electrodes are well known by their high oxidizing power (Alfaro et al., 2006; Kapařka et al., 2008; Kapařka and Comminellis, 2009), the presence of chloride species can slow down the electrodes performance in the EOCs degradation, and therefore the indirect oxidation by active

**Table 3**  
Pseudo first-order kinetics ( $\ln(C/C_0) = -kt$ ) of EOCs removal through ( $k \times 10^{-2}$  h<sup>-1</sup>).

EOCs	Ti/MMO anode at 7 mA/cm <sup>2</sup>		Nb/BDD anode at 10 mA/cm <sup>2</sup>	
	k	R <sup>2</sup>	k	R <sup>2</sup>
TCP	1.67	0.94	0.61	0.96
DCP	1.97	0.92	0.60	0.99
TCS	7.61	0.97	0.60	0.90
MTCS	0.44	0.91	0.60	0.97

chlorine species may not occur (Anglada et al., 2009; Mascia et al., 2007; Pereira et al., 2015; Scialdone et al., 2009).

Following the kinetics, it is important to mention that EOCs degradation was considered as the elimination of parent organic compound. The parent compound loss indicates transformation at an unknown degree, and not necessarily mineralization (that showed in section 3.1.4), where sometimes the by-products can be more harmful than the parent compounds. In this sense, the experimental samples were screened by LC/MS. Comparing Ti/MMO and Nb/BDD as working anodes, the latter presents possible by-products from electro-EOCs degradation pathways, while the former produced no detectable by-products (results not shown). The degradation of TCS in chlorine matrices (effluent initial  $\text{Cl}^-$  concentration was  $192.6 \pm 83.9$  mg/L) led to the formation of two tetra- and one penta-chlorinated hydroxylated diphenyl ether, as well as 2,4-dichlorophenol. Chlorination of the phenolic ring and cleavage of the ether bond were identified as the main triclosan degradation pathways (Canosa et al., 2005). Free chlorine mediated oxidation of triclosan leads to the formation of chloroform and other chlorinated organics (Fiss et al., 2007; Rule et al., 2005). Therefore, TCS is assumed as the main contributor for the identified by-products, since the other three EOCs are TCS natural by-products or metabolite. Thus, the diagnostic of ions masses in case 2 ( $10 \text{ mA/cm}^2$ ) were screened and estimated from the profile isotopes of a mass spectrum: ion 128 with one hydroxyl and one chlorine in the phenolic ring, 161 and 196 ions (from TCS ring breaking or from spiking DCP and TCP), 177 ion with two hydroxyls and two chlorines that are not possible to conclude the position on the ring, and 272 ion corresponding to TCS losing the hydroxyls. Due to the obtained data, a more thorough study is needed to assess the exact mechanisms pathways for the four compounds under study, when an electrochemical treatment is applied.

### 3.1.4. Electrochemical flow reactor (EFR): emerging organic contaminants degradation at the best conditions

An EFR reactor, mimicking the secondary settling tank in a wastewater treatment plant was developed and tested. The EFR had a flow rate of 9 mL/min, meaning 55 min of retention time to every 500 mL of a batch of effluent spiked with EOCs. The path of the effluent goes through an internal chamber where the electrical current is being applied, followed by a second chamber, the reactor outlet (Fig. 1). Using a flow will have significant effect on the oxidation rates, since it can enhance the mass transport of organic species to the electrode surface where they undergo oxidation mainly by the hydroxyl radicals, and increase the turbulence in the system, that is, at that moment, hydrodynamic.

Table 4 presents the effluent pH, conductivity and voltage before and after the EFR treatment, where there were no statistically significant differences between these parameters, contrarily to EBR treatment (see Table 2). All the parameters remained approximately constant.

Fig. 3 shows the removal of the target EOCs. Similar to the EBR, the photodegradation and compound volatilization were not taking place in the degradation process, thus the degradation only occurs due to the direct anodic oxidation or indirect oxidation in the liquid

bulk.

Accordingly, in approx. 1 h of electrokinetic treatment, the setup achieved degradation rates for TCP 61% ( $\pm 7\%$ ), DCP 41% ( $\pm 1\%$ ), TCS 87% ( $\pm 1\%$ ) and, MTCS 41% ( $\pm 1\%$ ) when Ti/MMO was used as the working anode. The lower rates observed for DCP may be explained by the hypothesis that, due to the TCS degradation path, DCP will be formed when the  $\cdot\text{OH}$  radicals attached the phenolic ring (Yuan et al., 2013). Comparing the degradations rates in case 1 and 2, there are statistically significant differences at 95% confidence when different anodes are used: for TCP  $p$  value = 0.0196, for DCP  $p$  value = 0.0079 and for TCS  $p$  value = 0.0055. However, for MTCS degradation in both cases 1 and 2, no statistically significant differences were found. MTCS degradation data, points out for the compound's dependency in the matrix composition and treatment's retention time. Regarding the removal rates of TCS, DCP and TCP when Nb/BDD was used as anode in the EFR treatment, some clarifications can be pointed out: (1) processes such as polymerization of phenolic compounds on the electrode surface can occur, thus decreasing the performance of the electrode; (2) formation of organochloride molecules that are resistant to degradation (Korshin et al., 2006); (3) in alkaline conditions (end pH around 7.1) the Nb/BDD reacts with hydroxide ( $\text{OH}^-$ ), which can recombine with  $\cdot\text{OH}$  to form  $\text{H}_2\text{O}$ . At alkaline pH and lower current densities, the abundance of  $\text{OH}^-$  retarded the oxidation of compounds by  $\cdot\text{OH}$  (Hayashi et al., 2016); (4) additionally, though not observed in current work, at alkaline conditions the surface morphology of Nb/BDD may also change, producing inhibitory conditions for organic oxidation, and ultimately degrading the Nb/BDD surface (DeClements, 1997; González-González et al., 2010; Griesbach et al., 2005). Wachter et al. (2019) also observed a decrease in the removal efficiencies using Nb/BDD as anode, when lower applied current densities (5 and  $10 \text{ mA/cm}^2$ ) and pH 10 were combined.

In order to understand the dynamics of the degradation process between the two tested reactor designs, an estimation of the four EOCs was performed in the EBR using the pseudo first-order kinetics for 1 h treatment. Thus, the data suggested (estimations values obtained from Fig. S1, at supplementary data) that EFR leads to an improvement of degradation for TCP (EBR 45% vs EFR 61%), DCP (EBR 28% vs EFR 41%), and MTCS (EBR 12% vs EFR 41%), when Ti/MMO was used as working anode. In the case 2, Nb/BDD as anode, only MTCS (EBR 20% vs EFR 49%) increased its degradation using a dynamic system. For TCS, the degradation occurs in both anodes from the first 15 min on, however the degradation between the flow vs the batch reactors are not statistically different.

The Total Organic Carbon, TOC was analyzed for the different electrode combination (Ti/MMO anode,  $7 \text{ mA/cm}^2$  and Nb/BDD anode,  $10 \text{ mA/cm}^2$ ) in both EBR and EFR treatments. The potential to mineralization was given by comparison data from the TOC in the initial inlet (effluent spiked with EOCs) and the TOC data of the four experiments. Therefore, the TOC decay when Ti/MMO is used as working anode with  $7 \text{ mA/cm}^2$  in EBR and EFR was 36% and 27%, respectively, in effluent. If Nb/BDD is used as working anode with  $10 \text{ mA/cm}^2$  in EBR and EFR was 30% and 22%, respectively in effluent. Accordingly, the Ti/MMO as anode seems to present more efficiency to mineralization of the compounds under study.

**Table 4**

The pH, conductivity and voltage before and after EFR treatment during 1 h.

Anode	Current density at anode ( $\text{mA/cm}^2$ )		pH	Conductivity ( $\text{mS/cm}$ )	Voltage (V)
Ti/MMO	7	initial	$7.6 \pm 0.5$	$1.6 \pm 1.0$	$14.5 \pm 2.2$
		end	$7.6 \pm 0.6$	$1.2 \pm 0.5$	$13.4 \pm 2.8$
Nb/BDD	10	initial	$7.3 \pm 0.0$	$2.3 \pm 0.0$	$16.8 \pm 6.4$
		end	$7.1 \pm 0.0$	$1.5 \pm 0.4$	$13.8 \pm 3.3$

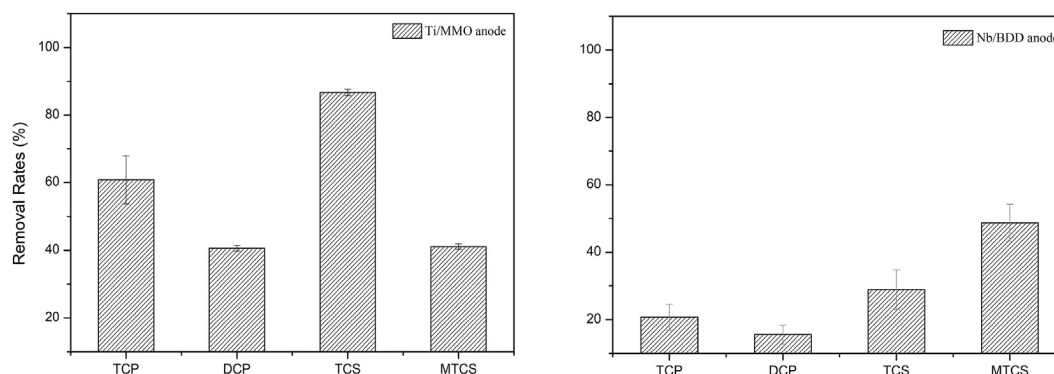


**Fig. 3.** Emerging organic contaminants degradation in electrochemical flow reactor with: Ti/MMO as anode with  $7 \text{ mA/cm}^2$  and Nb/BDD as anode with  $10 \text{ mA/cm}^2$  during 1 h treatment (error bars related to the standard deviation:  $n = 2$ ; TCP - 2,4,6-trichlorophenol; DCP - 2,4-dichlorophenol; TCS - triclosan; MTCS - methyl-triclosan).

Wachter et al. (2019) reported that, for a complete TOC removal many oxidation steps, higher current densities and longtime treatment should be applied. A non-dependence of the TOC removal rate on the electrodes characteristics may be expected for a system where the organic molecule and its oxidation intermediates are oxidized on the anode surface. The results obtained in the present work were in agreement with those reported by the Medeiros de Araújo et al., 2014 on the mineralization of the dye Rhodamine B and Souza et al. (2016) on the mineralization of the DCP.

In terms of reactor design, EFR using Ti/MMO anode could be a valid choice to a scale-up reactor for EOCs degradation, both by a financial point of view (Ti/MMO cheaper compared to Nb/BDD), an energy consumption perspective (lower current density, same degradation rates; energy consumption according to Portuguese energy price for householders (0.2154 €) and the kWh required for the EBR and EFR treatments: 0.0014 € for EBR using Ti/MMO anode and 0.0029 € using Nb/BDD anode or for EBR 0.0003 € for EFR using Ti/MMO anode and 0.0009 € using Nb/BDD anode, were calculated), but also due to the faster degradation kinetics (when  $t = 1, \ln(C/C_0) = -k \sim$ ). Furthermore, according to LC/MS analysis, no detectable by-products were observed with this set-up.

#### 4. Conclusion

Applied to a secondary effluent, two different electrochemical reactors were tested for the degradation of triclosan and its derivative by-products: methyl-triclosan, 2,4-dichlorophenol and 2,4,6-trichlorophenol. The compounds elimination promoted by two different anodes, Ti/MMO and Nb/BDD, in the electrochemical batch reactor and in the electrochemical flow reactor were evaluated. In both reactors the best electrode combination was accomplished with Ti/MMO, presenting faster kinetics degradation and less dependency on electrical current, achieving similar eliminations with a cheaper electrode. In the batch reactor at  $7 \text{ mA/cm}^2$ , during 4 h, the degradation rates were below the detection limit for triclosan and 2,4,6-trichlorophenol, and 94% and 43% for 2,4-dichlorophenol and methyl triclosan. In the flow reactor, in a 1 h treatment, the degradation efficiencies varied from 41% to 87% for the four contaminants under study. Electrochemical flow reactor implementation in wastewater treatment plants may be considered as viable option from an operational point of view. The combination of a low current density with the flow, and induced matrix disturbance, increased and speed up EOCs degradation.

#### Author contribution

**Cátia Magro:** Conceptualization; Methodology; Writing - Original Draft; Writing - Review & Editing; Software; Investigation, **Eduardo P. Mateus:** Validation; Supervision; Resources; Writing - Review & Editing, **Juan Manuel Paz-Garcia:** Validation; Supervision; Writing - Review & Editing; **Alexandra B. Ribeiro:** Validation; Supervision; Writing - Review & Editing; Funding acquisition; Resources.

#### Acknowledgements

This research was funded by Fundação para a Ciência e Tecnologia through projects UID/AMB/04085/2019, UID/FIS/00068/2019 and PTDC/FIS-NAN/0909/2014. This work has received funding from the European Union's Horizon 2020 research and innovation programme under the Marie Skłodowska-Curie grant agreement No. 778045. C Magro acknowledges Fundação para a Ciência e a Tecnologia for her PhD fellowship SFRH/BD/114674/2016. Paz-Garcia acknowledges the financial support from the Excellence Network E3TECH under project CTQ2017-90659-REDT (MCIUN, Spain), and from "Proyectos I + D + i en el marco del Programa Operativo FEDER Andalucía 2014–2020" – UMA18-FEDERJA-279. The authors thank Cátia de Almeida Santos and André Nunes Jorge for their help, valuable discussion and suggestions given in the LC/MS by-products diagnostic. The authors also thank Ricardo Faria for his help with the reactors drawing and Professor Nuno Lapa, Integrated Member of UBiA-NOVA-FCT, for providing the analytical equipment for effluent characterization. This research was anchored by the RESOLUTION LAB, an infrastructure at NOVA School of Science and Technology.

#### Appendix A. Supplementary data

Supplementary data to this article can be found online at <https://doi.org/10.1016/j.chemosphere.2019.125758>.

#### References

- Alfaro, M.A.Q., Ferro, S., Martínez-Huitle, C.A., Vong, Y.M., 2006. Boron doped diamond electrode for the wastewater treatment. *J. Braz. Chem. Soc.* 17, 227–236. <https://doi.org/10.1590/S0103-50532006000200003>.
- Ambauen, N., Muff, J., Mai, N.L., Hallé, C., Trinh, T.T., Meyn, T., 2019. Insights into the kinetics of intermediate formation during electrochemical oxidation of the organic model pollutant salicylic acid in chloride electrolyte. *Water (Switzerland)* 11, 1322. <https://doi.org/10.3390/w11071322>.
- Anglada, A., Urriaga, A., Ortiz, I., 2009. Pilot Scale performance of the electro-oxidation of landfill leachate at boron-doped diamond anodes. *Environ. Sci. Technol.* 43, 2035–2040. <https://doi.org/10.1021/es802748c>.
- Balmer, M.E., Poiger, T., Droz, C., Romanin, K., Bergqvist, P.A., Müller, M.D.,

- Buser, H.R., 2004. Occurrence of methyl triclosan, a transformation product of the bactericide triclosan, in fish from various lakes in Switzerland. *Environ. Sci. Technol.* 38, 390–395. <https://doi.org/10.1021/es030068p>.
- Bever, C.S., Rand, A.A., Nording, M., Taft, D., Kalanetra, K.M., Mills, D.A., Breck, M.A., Smilowitz, J.T., German, J.B., Hammock, B.D., 2018. Effects of triclosan in breast milk on the infant fecal microbiome. *Chemosphere* 203, 467–473. <https://doi.org/10.1016/j.chemosphere.2018.03.186>.
- Brillas, E., Martínez-Huitle, C.A., 2015. Decontamination of wastewaters containing synthetic organic dyes by electrochemical methods. An updated review. *Appl. Catal. B Environ.* 166–167, 603–643. <https://doi.org/10.1016/j.apcatb.2014.11.016>.
- Brose, D.A., Kumar, K., Liao, A., Hundal, L.S., Tian, G., Cox, A., Zhang, H., Podczewinski, E.W., 2019. A reduction in triclosan and triclocarban in water resource recovery facilities' influent, effluent, and biosolids following the U.S. Food and Drug Administration's 2013 proposed rulemaking on antibacterial products. *Water Environ. Res.* 91, 715–721. <https://doi.org/10.1002/wer.1101>.
- Buxton, G.V., Greenstock, C.L., Helman, W.P., Ross, A.B., 1988. Critical review of rate constants for reactions of hydrated electrons, hydrogen atoms and hydroxyl radicals ( $\cdot\text{OH}/\cdot\text{O}-$  in aqueous solution. *J. Phys. Chem. Ref. Data* 17, 513–886. <https://doi.org/10.1063/1.555805>.
- Canosa, P., Morales, S., Rodríguez, I., Rubí, E., Cela, R., Gómez, M., 2005. Aquatic degradation of triclosan and formation of toxic chlorophenols in presence of low concentrations of free chlorine. *Anal. Bioanal. Chem.* 383, 1119–1126. <https://doi.org/10.1007/s00216-005-0116-4>.
- Chen, J., Meng, X., Bergman, A., Halden, R.U., 2019. Nationwide reconnaissance of five parabens, triclosan, triclocarban and its transformation products in sewage sludge from China. *J. Hazard Mater.* 365, 502–510. <https://doi.org/10.1016/j.jhazmat.2018.11.021>.
- Chianese, S., Iovino, P., Canzano, S., Prisciandaro, M., Musmarra, D., 2016. Ibuprofen degradation in aqueous solution by using UV light. *Desalin. Water Treat.* 57, 22878–22886. <https://doi.org/10.1080/19443994.2016.1153908>.
- Corcoran, E., Nellemann, C., Baker, E., Bos, R., Osborn, D., 2010. Sick Water ? the Central Role of Wastewater Management in Sustainable Development. UNEP/Earthprint (eds), H.S.
- Daughton, C.G., 2004. Non-regulated water contaminants: emerging research. *Environ. Impact Assess. Rev.* 24, 711–732. <https://doi.org/10.1016/j.eiar.2004.06.003>.
- DeClements, R., 1997. The formation and electrochemical activity of microporous diamond thin film electrodes in concentrated KOH. *J. Electrochem. Soc.* 144, 856. <https://doi.org/10.1149/1.1837500>.
- Ferreira, A.R., Couto, N., Guedes, P., Pinto, J., Mateus, E.P., Ribeiro, A.B., 2018. Electro-dialytic 2-compartment cells for emerging organic contaminants removal from effluent. *J. Hazard. Mater.* 358 (15), 467–474. <https://doi.org/10.1016/j.jhazmat.2018.04.066>.
- Fiss, E.M., Rule, K.L., Vikesland, P.J., 2007. Formation of chloroform and other chlorinated byproducts by chlorination of triclosan-containing antibacterial products. *Environ. Sci. Technol.* 41, 2387–2394. <https://doi.org/10.1021/es062227l>.
- Food and Drug Administration, 2017. Safety and Effectiveness for Health Care Antiseptics; Topical Antimicrobial Drug Products for Over-the-counter Human Use. US, DHHS - Department of Health And Human Services.
- Food and Drug Administration, 2016. FDA Issues Final Rule on Safety and Effectiveness of Antibacterial Soaps. DHHS - Department of Health and Human Services, US.
- Geissen, V., Mol, H., Klumpp, E., Umlauf, G., Nadal, M., Ploeg, M., Van Der Zee, S.E., Ritsema, C.J., 2015. Emerging pollutants in the environment: a challenge for water resource management. *Int. Soil Water Conserv. Res.* 3, 57–65. <https://doi.org/10.1016/j.iswcr.2015.03.002>.
- Glaze, W.H., Kang, J.-W., Chapin, D.H., 1987. The chemistry of water treatment processes involving ozone, hydrogen peroxide and ultraviolet radiation. *Ozone Sci. Eng.* 9, 335–352. <https://doi.org/10.1080/01919518708552148>.
- González-González, I., Hernández-Lebrón, Y., Nicolau, E., Cabrera, C.R., 2010. Ammonia oxidation enhancement at square-wave treated platinum particle modified boron-doped diamond electrodes. *ECS Trans.* 33, 201–209. <https://doi.org/10.1149/1.3484517>.
- Griesbach, U., Zollinger, D., Pütter, H., Comninellis, C., 2005. Evaluation of boron doped diamond electrodes for organic electrosynthesis on a preparative scale. *J. Appl. Electrochem.* 35, 1265–1270. <https://doi.org/10.1007/s10800-005-9038-2>.
- Guedes, P., Magro, C., Couto, N., Mosca, A., Mateus, E.P., Ribeiro, A.B., 2015. Potential of the electro-dialytic process for emerging organic contaminants remediation and phosphorus separation from sewage sludge. *Electrochim. Acta* 181, 109–117. <https://doi.org/10.1016/j.electacta.2015.03.167>.
- Guedes, P., Mateus, E.P., Couto, N., Rodríguez, Y., Ribeiro, A.B., 2014. Electrokinetic remediation of six emerging organic contaminants from soil. *Chemosphere* 117 (1), 124–131. <https://doi.org/10.1016/j.chemosphere.2014.06.017>.
- Guo, J.-H., Li, X.-H., Cao, X.-L., Li, Y., Wang, X.-Z., Xu, X.-B., 2009. Determination of triclosan, triclocarban and methyl-triclosan in aqueous samples by dispersive liquid-liquid microextraction combined with rapid liquid chromatography. *J. Chromatogr. A* 1216, 3038–3043. <https://doi.org/10.1016/j.chroma.2009.02.021>.
- Halden, R., 2019. The great sewage census. *The Anal. Sci.* 79, 22–30.
- Hayashi, H., Akamine, S., Ichiki, R., Kanazawa, S., 2016. Comparison of OH radical concentration generated by under-water discharge using two methods. *Int. J. Plasma Environ. Sci. Technol.* 10, 24–28. [http://www.iesj.org/content/files/pdf/IJPEST\\_Vol10\\_No1\\_06\\_pp\\_024-028](http://www.iesj.org/content/files/pdf/IJPEST_Vol10_No1_06_pp_024-028).
- Hua, W., Bennett, E., Letcher, R., 2005. Triclosan in waste and surface waters from the upper Detroit River by liquid chromatography-electrospray-tandem quadrupole mass spectrometry. *Environ. Int.* 31, 621–630. <https://doi.org/10.1016/j.envint.2004.10.019>.
- Kapaika, A., Comninellis, C., 2009. The importance of electrode material in environmental electrochemistry: formation and reactivity of free hydroxyl radicals on boron-doped diamond electrodes. *Electrochim. Acta* 54, 2018–2023. <https://doi.org/10.1016/j.electacta.2008.06.045>.
- Kapaika, A., Comninellis, C., 2008. Kinetic modelling of the electrochemical mineralization of organic pollutants for wastewater treatment. *J. Appl. Electrochem.* 38, 7–16. <https://doi.org/10.1007/s10800-007-9365-6>.
- Klavarioti, M., Mantzavinos, D., Kassinos, D., 2009. Removal of residual pharmaceuticals from aqueous systems by advanced oxidation processes. *Environ. Int.* 35, 402–417. <https://doi.org/10.1016/j.envint.2008.07.009>.
- Korshin, G.V., Kim, J., Gan, L., 2006. Comparative study of reactions of endocrine disruptors bisphenol A and diethylstilbestrol in electrochemical treatment and chlorination. *Water Res.* 40, 1070–1078. <https://doi.org/10.1016/j.watres.2006.01.003>.
- Mascia, M., Vacca, A., Palmas, S., Polcaro, A.M., 2007. Kinetics of the electrochemical oxidation of organic compounds at BDD anodes: modelling of surface reactions. *J. Appl. Electrochem.* 37, 71–76. <https://doi.org/10.1007/s10800-006-9217-9>.
- McAvoy, D.C., Schatowitz, B., Jacob, M., Hauk, A., Eckhoff, W.S., 2002. Measurement of triclosan in wastewater treatment systems. *Environ. Toxicol. Chem.* 21, 1323–1329. <https://doi.org/10.1002/etc.5620210701>.
- Medeiros de Araújo, D., Cañizares, P., Martínez-Huitle, C.A., Rodrigo, M.A., 2014. Electrochemical conversion/combustion of a model organic pollutant on BDD anode: role of sp<sup>3</sup>/sp<sup>2</sup> ratio. *Electrochem. Commun.* 47, 37–40. <https://doi.org/10.1016/j.elecom.2014.07.017>.
- Moreira, F.C., Boaventura, R.A.R., Brillas, E., Vilar, V.J.P., 2017. Electrochemical advanced oxidation processes: a review on their application to synthetic and real wastewaters. *Appl. Catal. B Environ.* 202, 217–261. <https://doi.org/10.1016/j.apcatb.2016.08.037>.
- Olanikan, L.W.B., Mkwetshana, N., Okoh, A.I., 2016. Triclosan in water, implications for human and environmental health. *SpringerPlus* 5, 1639. <https://doi.org/10.1186/s40064-016-3287-x>.
- Oturan, M.A., Aaron, J.-J., 2014. Advanced oxidation processes in water/wastewater treatment: principles and applications: a review. *Crit. Rev. Environ. Sci. Technol.* 44, 2577–2641. <https://doi.org/10.1080/10643389.2013.829765>.
- Panizza, M., Cerisola, G., 2009. Direct and mediated anodic oxidation of organic pollutants. *Chem. Rev.* 109, 6541–6569. <https://doi.org/10.1021/cr9001319>.
- Pereira, G.F., Rocha-Filho, R.C., Bocchi, N., Biaggio, S.R., 2015. Electrochemical degradation of the herbicide picloram using a filter-press flow reactor with a boron-doped diamond or  $\beta$ -PbO<sub>2</sub> anode. *Electrochim. Acta* 179, 588–598. <https://doi.org/10.1016/j.electacta.2015.05.134>.
- Pérez, J.F., Llanos, J., Sáez, C., López, C., Cañizares, P., Rodrigo, M.A., 2017. A microfluidic flow-through electrochemical reactor for wastewater treatment: a proof-of-concept. *Electrochem. Commun.* 82, 85–88. <https://doi.org/10.1016/j.elecom.2017.07.026>.
- Ren, G., Zhou, M., Liu, M., Ma, L., Yang, H., 2016. A novel vertical-flow electro-Fenton reactor for organic wastewater treatment. *Chem. Eng. J.* 298, 55–67. <https://doi.org/10.1016/j.cej.2016.04.011>.
- Rule, K.L., Ebbett, V.R., Vikesland, P.J., 2005. Formation of chloroform and chlorinated organics by free-chlorine-mediated oxidation of triclosan. *Environ. Sci. Technol.* 39, 3176–3185. <https://doi.org/10.1021/es048943+>.
- Schranck, A., Doudrick, K., 2020. Effect of reactor configuration on the kinetics and nitrogen byproduct selectivity of urea electrolysis using a boron doped diamond electrode. *Water Res.* 168, 115130. <https://doi.org/10.1016/j.watres.2019.115130>.
- Scialdone, O., Randazzo, S., Galia, A., Silvestri, G., 2009. Electrochemical oxidation of organics in water: role of operative parameters in the absence and in the presence of NaCl. *Water Res.* 43, 2260–2272. <https://doi.org/10.1016/j.watres.2009.02.014>.
- Sirés, I., Oturan, N., Oturan, M.A., Rodríguez, R.M., Garrido, J.A., Brillas, E., 2007. Electro-Fenton degradation of antimicrobials triclosan and triclocarban. *Electrochim. Acta* 52, 5493–5503. <https://doi.org/10.1016/j.electacta.2007.03.011>.
- Skoumal, M., Arias, C., Cabot, P.L., Centellas, F., Garrido, J.A., Rodríguez, R.M., Brillas, E., 2008. Mineralization of the biocide chloroxylenol by electrochemical advanced oxidation processes. *Chemosphere* 71, 1718–1729. <https://doi.org/10.1016/j.chemosphere.2007.12.029>.
- Souza, F.L., Saéz, C., Lanza, M.R.V., Cañizares, P., Rodrigo, M.A., 2016. The effect of the sp<sup>3</sup>/sp<sup>2</sup> carbon ratio on the electrochemical oxidation of 2,4-D with p-Si BDD anodes. *Electrochim. Acta* 187, 119–124. <https://doi.org/10.1016/j.electacta.2015.11.031>.
- Wachter, N., Aquino, J.M., Denadai, M., Barreiro, J.C., Silva, A.J., Cass, Q.B., Bocchi, N., Rocha-Filho, R.C., 2019. Electrochemical degradation of the antibiotic ciprofloxacin in a flow reactor using distinct BDD anodes: Reaction kinetics, identification and toxicity of the degradation products. *Chemosphere* 234, 461–470. <https://doi.org/10.1016/j.chemosphere.2019.06.053>.
- Walsh, F.C., Ponce de León, C., 2018. Progress in electrochemical flow reactors for laboratory and pilot scale processing. *Electrochim. Acta* 280, 121–148. <https://doi.org/10.1016/j.electacta.2018.05.027>.
- Wang, D., Wang, P., Wang, S., Chen, Y.-H., Zhang, H., Lei, A., 2019. Direct electrochemical oxidation of alcohols with hydrogen evolution in continuous-flow reactor. *Nat. Commun.* 10, 2796. <https://doi.org/10.1038/s41467-019-10928-0>.

- Wang, J., Farrell, J., 2004. Electrochemical inactivation of triclosan with boron doped diamond film electrodes. *Environ. Sci. Technol.* 38, 5232–5237. <https://doi.org/10.1021/es035277o>.
- Weatherly, L.M., Gosse, J.A., 2017. Triclosan exposure, transformation, and human health effects. *J. Toxicol. Environ. Health Part B* 20, 447–469. <https://doi.org/10.1080/10937404.2017.1399306>.
- Xing, L., Sun, J., Liu, H., Yu, H., 2012. Combined toxicity of three chlorophenols 2,4-dichlorophenol, 2,4,6-trichlorophenol and pentachlorophenol to *Daphnia magna*. *J. Environ. Monit.* 14, 1677–1683. <https://doi.org/10.1039/c2em30185g>.
- Yoon, J.H., Shim, Y.B., Lee, B.S., Choi, S.Y., Won, M.S., 2012. Electrochemical degradation of phenol and 2-chlorophenol using Pt/Ti and boron-doped diamond electrodes. *Bull. Korean Chem. Soc.* 33, 2274–2278. <https://doi.org/10.5012/bkcs.2012.33.7.2274>.
- Yuan, S., Gou, N., Alshawabkeh, A.N., Gu, A.Z., 2013. Efficient degradation of contaminants of emerging concerns by a new electro-Fenton process with Ti/MMO cathode. *Chemosphere* 93, 2796–2804. <https://doi.org/10.1016/j.chemosphere.2013.09.051>.





## Paper

*“Analytical method for the monitoring of underivatized Triclosan by gas chromatography-triple quadrupole mass spectrometry in wastewater”*

*C Magro, D Mendes, F Freitas, EP Mateus, M Silva & AB Ribeiro*

*Under preparation, 2019*



# Analytical method for the monitoring of underivatized Triclosan by gas chromatography-triple quadrupole mass spectrometry in effluent

C. Magro<sup>a\*</sup>, D. Mendes<sup>b</sup>, F. Freitas<sup>b</sup>, M. Silva<sup>b</sup>, A.B. Ribeiro<sup>a</sup> and E.P. Mateus<sup>a\*</sup>

<sup>a</sup>CENSE, Departamento de Ciências e Engenharia do Ambiente, Faculdade de Ciências e Tecnologia, Universidade Nova de Lisboa, Caparica 2829-516, Portugal

<sup>b</sup>LAQV, REQUIMTE, Departamento de Química, Ciências e Engenharia do Ambiente, Faculdade de Ciências e Tecnologia, Universidade Nova de Lisboa, Caparica 2829-516, Portugal

\*Corresponding authors: c.magro@campus.fct.unl.pt, epm@fct.unl.pt

under preparation, 2019

Keywords: Gas chromatography-triple quadrupole mass spectrometry, MRM mode, triclosan, effluent

Abstract:

---

Triclosan (TCS) an antimicrobial agent is a personal care products widely used on a daily basis. TCS is being released to the environment by wastewater treatment plants processing at sub-ppb effluent concentrations, presenting toxic and endocrine disrupting activity. A method for detection and quantification of TCS in effluent was developed. The optimization of the method complies the different triple quadrupole gas chromatography mass spectrometer conditions: injector, transfer line and source temperature, collision gas pressure and energy, injection mode. This method will allow the fast and efficient environmental monitoring of TCS and related compounds in aqueous matrices.

---

## 1 INTRODUCTION

Emerging organic contaminants (EOC), among them the personal care products class, have gathered increasing interest in recent years [1]. This group of EOC encompasses a wide range of chemicals, including several phenolic compounds such as triclosan (TCS), see Table 1.

TCS is employed as antimicrobial and preservative agents in several consumer products, e.g. deodorants and toothpastes. The continuous detection of TCS has led to debate on its safety, effectiveness and usage regulation, that comply with the needs of environmentally friendly monitoring techniques [2]. Due to advances in analytical technology, a plethora of organic compounds, from pharmaceuticals to personal care products, are detectable and quantifiable in water if extremely sensitive techniques are applied. However, identification and quantification of environmental matrices is challenging due to the low sensitivity of available instrumentation, the vast physicochemical properties of target analytes, and the relatively low levels that occur in aqueous environmental

matrices (2 ng/L-1 - 40µg/L of TCS found ) [3–5]. Several detectors have been applied in tandem with GC and LC separations, yet, mass spectrometric detection has emerged as the most commonly employed due to its selectivity and sensitivity, where the triple quadrupole mass spectrometer is generally considered the most sensitive [6–8]. In this study an effective and non derivatization method for determination of TCS in effluent , by gas chromatography-triple quadrupole mass spectrometry in Multiple Reaction Monitoring mode (MRM), was developed. Solid phase extraction (SPE) was used to concentrate and purify the TCS in real effluent, prior to analysis. To the best of our knowledge, most studies do not challenge the standard conditions of the instrumentation, even though each case is different, and many analytes would benefit from this type of optimization.

## 2 EXPERIMENTAL

### 2.1 Chemicals and standards

TCS (99%) was purchased from Sigma–Aldrich (Steinheim, Germany). Individual stock solutions for calibration purposes were prepared at 200 mg/L in methanol/ACE (2:1) and stored at -18°C. The methanol and acetone used were from Sigma–Aldrich (Steinheim, Germany) in gradient grade type. Water (Type I) was from a Millipore system (Bedford, MA, USA). The effluent used was the liquid fraction collected in the secondary settling tank at a wastewater treatment plant (Lisbon, Portugal). The gas Hellium was 99.9% pure.

### 2.2 Standard solutions

A concentrated solution of TCS (200 mg/L) was prepared by dissolving in methanol/ACE (2:1). Eight-point calibration (20, 40, 80, 120, 240, 320, 400, 700) ng/L were performed in triplicate.

### 2.3 Samples and extraction

The extraction of TCS present in the effluent was performed by solid phase extraction (SPE), using Oasis HLB (200 mg, 6 mL) from Waters (Saint-Quentin En Yvelines Cedex, France). The SPE cartridges were conditioned by washing with 3 x 6 mL of methanol, followed by re-equilibrium with 3 x 6 mL of Milli-Q water. For TCS enrichment, the samples were acidified to pH 2 before extraction using nitric acid, with 30 min of slow stirring and 30 min pause time after the spiking. The 200 mL aqueous samples were passed through the cartridge at a flow-rate of approximately 10 mL/min by applying a moderate vacuum, flow by a dried period of approximately 3 min by vacuum. The retained analytes were eluted sequentially with 2 x 4 mL of methanol and 1 x 4 mL of acetone and filtrated by PTFE syringe filters before GC-MS/MS analysis.

### 2.4 Instrumentation

The GC-MS/MS method used for effluent detection and quantification is described in Tables 2.

To achieve the optimized conditions, it was tested in GC: splitless time, liner type, injector. In the MS: source and interface temperature, Q1 and Q3 resolution (peak shape and area offset), collision gas pressure, collision energy and dwell time. The tests were conducted in a standard solution of 1 mg/L of TCS to better understanding parameters changes.

## 3 RESULTS AND DISCUSSION

GC-MS/MS in MRM mode has become a popular analytical tool for the analysis of complex matrices due to its high specificity, and most of all selectivity. The identification of analytes is based on chromatographic retention time and specific transitions from the MS/MS analysis. The initial step for developing a GC-MS/MS method was establishing the chromatographic retention time in order to select an appropriate precursor ion for TCS. The GC-MS/MS analysis of triclosan standard in full-scan and SIM mode showed the molecular ion peaks of  $m/z$  288 for the native triclosan at time 21.1 min. The detection of triclosan and the established chromatographic retention time can be confirmed through the NIST EI-mass spectrum library search. The ion resulted from the loss of two chlorines was  $m/z$  218 for triclosan. Thus, the ions at  $m/z$  218 was chosen as the precursor ions for the second-stage mass spectrometric analysis, and after that ions at  $m/z$  155.

In the following section, the first phase was finding the best conditions in GC-MS, meaning the optimization of injection volume, split time and interface and injector temperature.

### 3.1 Optimization of GC-MS/MS conditions

The plots for the best splitless time and injector temperature are presented in Figure 1. These two parameters are crucial for success in the analysis, when the goal is to achieve a quantification method. Regarding Figure 1, the splitless at 1min is the one that presents less standard error, being the suitable choice. To injector temperature, the signal decrease beyond 260°C suggested possible degradation, therefore, for TCS analysis a temperature of 250°C was chosen, to guarantee the non-thermo-degradation. Additionally, not only the temperature or injector mode are critical factors, but also the type of liner's type which can jeopardize the shape of the peak and its S/N on the chromatograph (Figure 2). Thus, if the liners are packed with quartz wool (usually used for "dirty" environmental matrices), TCS will react with the material even if it is deactivated and/or become adsorbed on it.

The Design Expert program was used to find the maximum peak area, when temperatures of interface and source are combined, Figure 3. The curve obtained, implies the great dependency of TCS, mostly, on the interface's temperature. The higher area achieved for TCS was with a combination of 290 °C for the interface temperature and 260°C for the

source temperature.

### 3.2 MS/MS conditions

The optimization of the MS/MS parameters for triclosan analysis was reached by monitoring, not only the peak intensities, but also the shape of the selected quantification ions. In environmental samples, commonly present trace concentrations, where the peak shape is an imperative parameter for the analysis quantification. Thus, four parameters were studied and optimized: Q1 and Q3 resolution (peak shape and area offset), collision gas pressure, collision energy and dwell time.

Figure 4 present the Q1 and Q3 resolutions, where it can be observed for both combinations, peak shape and area offset, the best results were with Q1 at 0.7 and Q3 at 2.

Contrary to the typical energy used in organic compounds, to TCS, the highest area was achieved with 20eV of energy (Figure 5). Therefore, for the collision gas, it was found that both too high and too low pressures decreased the analyte signal. The ideal collision gas pressure, for the 20 eV of collision energy was 2.4 mTorr (Figure 5).

Moreover, the dwell time was evaluated. The lower (100 ms), in Figure 6, was the one with best peak shape and higher area.

The optimization of these parameters is crucial in trace analysis of environmental samples. The linearity and TCS peak shape were determined with standard solutions (section 2, standard solutions,  $n = 3$ ). Figure 7, show the calibration line through the different concentrations and the respective TCS chromatograms.

#### 3.2.1 Effluent samples

For effluent SPE extraction, different pH values (2,7 and 12), volume elution with different solvents (MeOH or MeOH/ACE), stirring time (1. spiked and stirred overnight; 2. spiked, 30 min stirred, 30 min of pause; 3. spiked immediately prior to extraction), cartridges (Oasis HLB, Strata-X, Strata C18-E, Strata C18-U) and syringe filters (RC, Nylon and PTFE) were evaluated. The experiments were performed by spiking TCS in effluent (0.8 mg/L) where all the experiments data were an average of duplicates. It was found that the recovery was higher at low and neutral pH values (2 and 7). The pH 2 was chosen as it will avoid precipitation of organic matter and elements that are in the matrix composition, and decrease the potential to photodegradation of TCS, as at pH 2 most molecules will be in their ionized form. At pH 12 the organic matter or fats/oil were not dissolved and promoted the saturation of SPE packings

after 50 mL in the loading sample step. For the stirring time the best option was a slow agitation (30 min), but not sufficient to promote the degradation, and a pause time where the TCS was diluted in the matrix (30 min). Methanol and a methanol/acetone solutions were examined as extraction solvent. The MeOH/ACE was found to be the most effective option, since ACE is a strong solvent for hydrophobic compounds, e.g. TCS. Additionally, the extraction volume of (4 x 4) mL MeOH + 4 mL ACE was found to be ideal, as 95% ( $\pm 3\%$ ) of TCS was recovered.

For effluent sample cleanup, the SPE cartridges were also studied. Recovery for TCS, when employing HLB showed a better result (95%) comparing to Strata-X (78%), Strata C18-E (114%), Strata C18-U (67%). The filtration with PTFE syringe filter obtained the lower losses (2% analyte loss).

Accordingly, a total of six effluent were analyzed for TCS using the present method and the results are shown in Table 3. Prior to the analysis, the SPE described above was applied. In the effluent samples, 106-624 ng/L of TCS was detected. The typical chromatogram is shown in Figure 8.

## 4 CONCLUSIONS

GC/MS/MS in MRM mode allowed the successful determination of trace amounts of TCS in effluent real samples, in a fast and efficient monitoring. TCS is an instable compound, with low volatility, found in trace concentration in aqueous environmental samples. Therefore, our proposed method has many practical advantages, including simplicity, higher selectivity and can be included in the green analytical monitoring techniques, since no derivative agent was used.

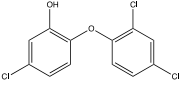
## ACKNOWLEDGEMENTS

This research was anchored by the *RESOLUTION LAB*, an infrastructure at NOVA School of Science and Technology. Project "Development of Nanostructures for Detection of Triclosan Traces on Aquatic Environments" (PTDC/FIS-NAN/0909/2014). CENSE which is financed by national funds from FCT/MEC (UID/AMB/04085/2013). C. Magro acknowledges Fundação para a Ciência e a Tecnologia for her PhD fellowship (SFRH/BD/114674/2016).

## REFERENCES

- [1] C.G. Daughton, Non-regulated water contaminants: Emerging research, 24 (2004) 711–732. doi:10.1016/j.eiar.2004.06.003.
- [2] E. Corcoran, C. Nellemann, E. Baker, R. Bos, D. Osborn, H.S. (eds), Sick water? The central role of wastewater management in sustainable development, UNEP/Earthprint., 2010.
- [3] W. Hua, E. Bennett, R. Letcher, Triclosan in waste and surface waters from the upper Detroit River by liquid chromatography-electrospray-tandem quadrupole mass spectrometry, *Environ. Int.* 31 (2005) 621–630. doi:10.1016/j.envint.2004.10.019.
- [4] A. Lindström, I.J. Buerge, T. Poiger, P.A. Bergqvist, M.D. Müller, H.R. Buser, Occurrence and environmental behavior of the bactericide triclosan and its methyl derivative in surface waters and in wastewater, *Environ. Sci. Technol.* 36 (2002) 2322–2329. doi:10.1021/es0114254.
- [5] P.E. Stackelberg, E.T. Furlong, M.T. Meyer, S.D. Zaugg, A.K. Henderson, D.B. Reisman, Persistence of pharmaceutical compounds and other organic wastewater contaminants in a conventional drinking-water-treatment plant, *Sci. Total Environ.* 329 (2004) 99–113. doi:10.1016/j.scitotenv.2004.03.015.
- [6] A. Togola, H. Budzinski, Analytical development for analysis of pharmaceuticals in water samples by SPE and GC-MS, *Anal. Bioanal. Chem.* 388 (2007) 627–635. doi:10.1007/s002160071251x.
- [7] F. Tohidi, Z. Cai, GC/MS analysis of triclosan and its degradation by-products in wastewater and sludge samples from different treatments, *Environ. Sci. Pollut. Res.* 22 (2015) 11387–11400. doi:10.1007/s113560154289x.
- [8] A. Klančar, M. Zakotnik, R. Roškar, J. Trontelj, Multi-residue analysis of selected pharmaceuticals in wastewater samples by stir-bar sorptive extraction followed by liquid desorption and liquid chromatography-mass spectrometry, *Anal. Methods*. 9 (2017) 5310–5321. doi:10.1039/c7ay01310h.

Table 1. Triclosan physical and chemical characteristics\*.

Chemical structure	Formula	Molar mass g mol <sup>-1</sup>	Log K <sub>ow</sub>	pKa	Solubility in water mg L <sup>-1</sup>	Polarizability Å <sup>3</sup>	Point <sup>o</sup>
 5-chloro-2-(2,4-dichlorophenoxy)phenol	C <sub>12</sub> H <sub>7</sub> Cl <sub>3</sub> O <sub>2</sub>	289.54	4.76	7.9	10 (20°C)	26.96	120°C

\* Pubchem, <https://pubchem.ncbi.nlm.nih.gov>.

Table 2. GC-MS/MS final method.

<i>Instrument</i>	Gas Chromatography - Triple Quadrupole MS Systems – EVOQ Bruker
<i>Column</i>	DB-5 30 m, 0.25 mm i.d., 0.25 µm film (d)
<i>Running</i>	Initial Temperature 40 °C for 1 min Heating Ramp 10 °C/min Final Temperature 300 °C for 3 min
<i>Carrier Gas</i>	helium
<i>Constant Flow</i>	1 mL/min
<i>Injector</i>	250 °C, 1 min splitless
<i>Interface</i>	290 °C
<i>Source</i>	260 °C
<i>MRM</i>	TCS (288>218, 288>155)
	Collision gas pressure 2.4
	Collision energy 20eV

Table 3. Concentrations of triclosan in SPE effluent extract samples.

	Effluent					
	<i>I</i>	<i>II</i>	<i>III</i>	<i>IV</i>	<i>V</i>	<i>VI</i>
TCS (ng/L)	127.80	106.58	472.41	623.61	519.92	458.37

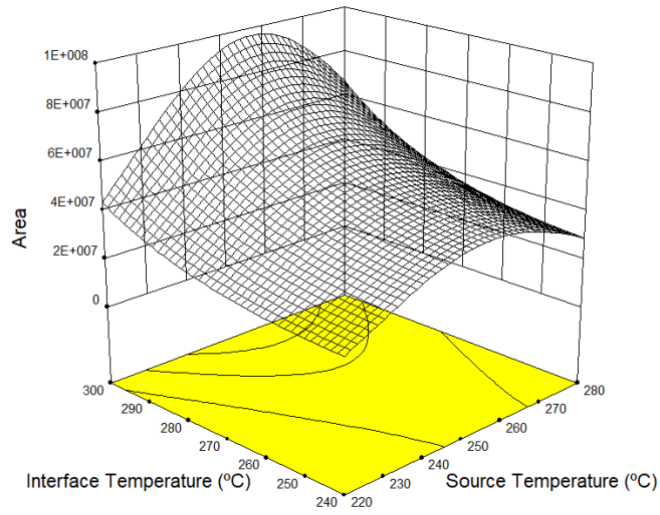


Figure 1. Interface and source temperature (injector at 250°C).

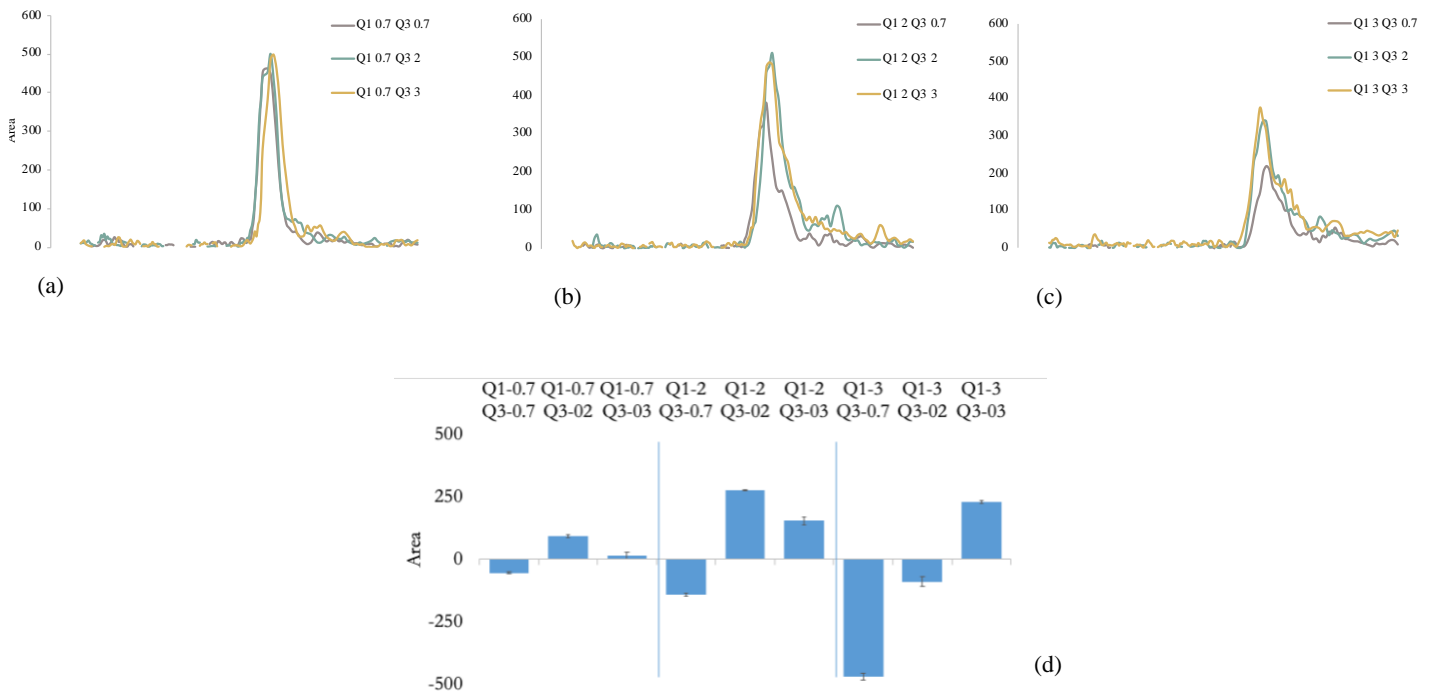


Figure 2. Q1 and Q3 resolution: peak shape (a-c) and area offset (d).



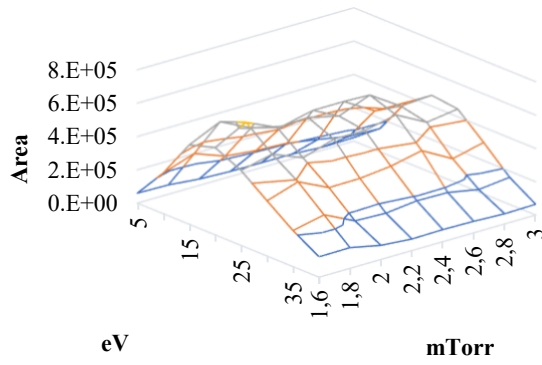
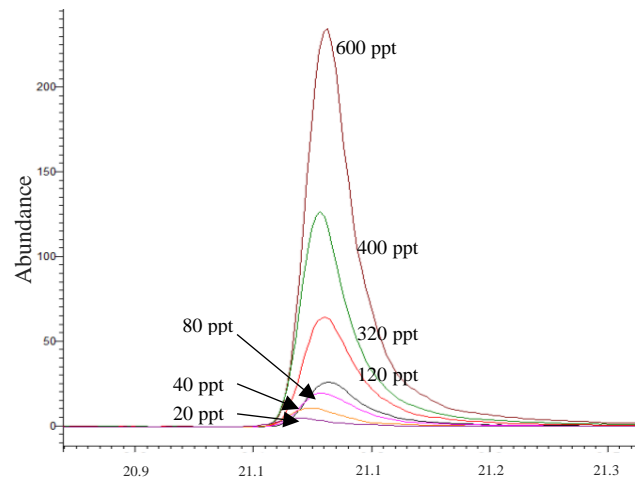
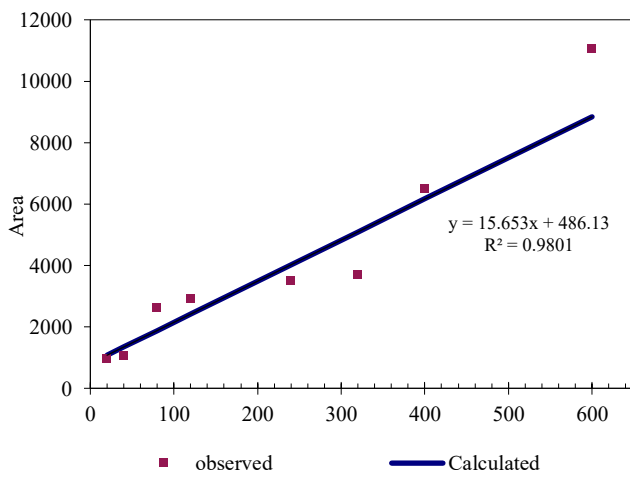


Figure 3. Relation between collision energy and collision gas pressure.



	20	40	80	120	240	320	400	600	<i>LOD</i>	<i>LOQ</i>
TCS (ng/L)	20	40	80	120	240	320	400	600		
RSD (%)	8	9	5	5	5	13	15	18	132	395

Figure 4. Calibration line and chromatograph for all the concentrations under study.

## Supplementary Material

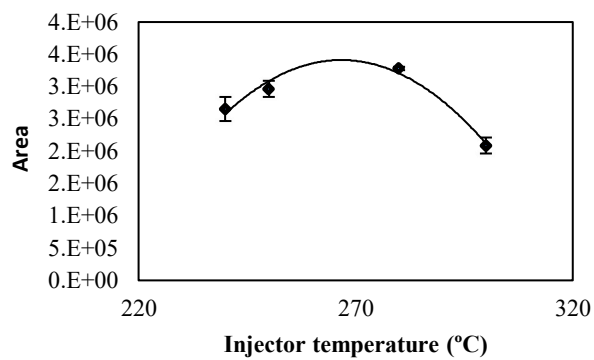
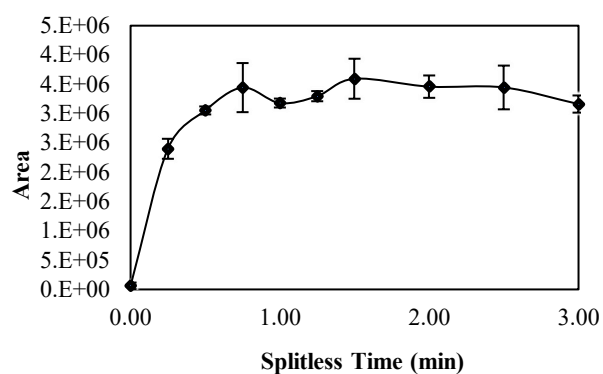


Figure S1. Splitless time and injector temperature.

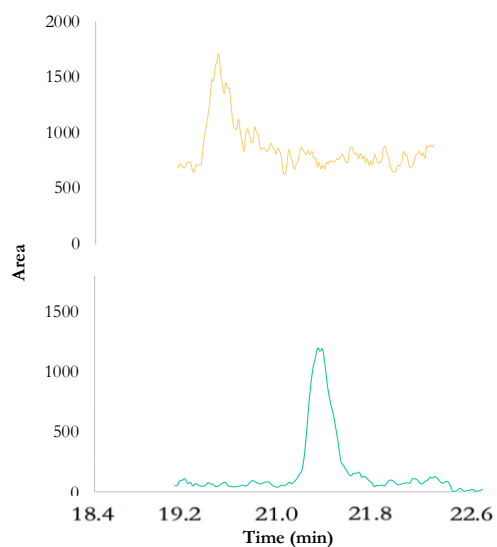


Figure S2. Liner type: (a) with glass fiber; (b) without glass fiber.

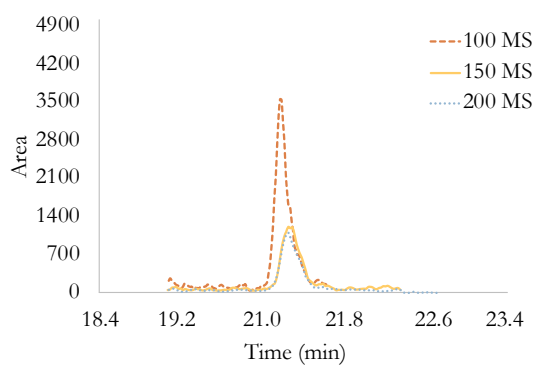


Figure S3. Dwell Time

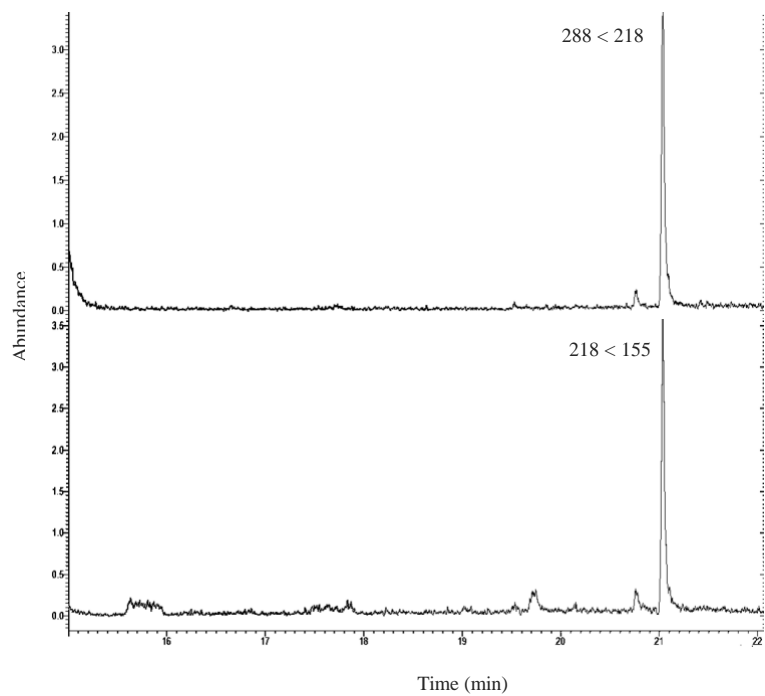


Figure S4. Typical MRM chromatogram of triclosan in effluent sample.



## Paper

*“Overview of electronic tongue sensing in environmental aqueous matrices: Potential for monitoring emerging organic contaminants”*

*C Magro, EP Mateus, M Raposo & AB Ribeiro*

*Published in: Environmental Reviews, 2019*



# Overview of electronic tongue sensing in environmental aqueous matrices: potential for monitoring emerging organic contaminants

Cátia Magro, Eduardo P. Mateus, Maria Raposo, and Alexandra B. Ribeiro

**Abstract:** Emerging organic contaminants (EOC) are synthetic or naturally occurring chemicals that have the potential to enter the environment and cause known or suspected adverse ecological and human health effects. Despite not being commonly monitored, EOC are often detected in effluents and water bodies because of their inefficient removal in conventional wastewater treatment plants. There is a growing concern about the presence and impact of EOC as well as the need for reliable and effective water monitoring using sensors capable of detecting the target molecules in complex media. Due to their specificities, such as fast response times, low cost, portability and user-friendly operation, electronic tongue (e-tongue) systems present some advantages over the traditional analytical techniques (e.g., chromatographic systems) used for environmental monitoring. We reviewed e-tongue sensors, focusing on their ability for real-time environmental monitoring. A bibliometric evaluation was carried out, along with a study of the status of the existing e-tongue systems, how they worked, and their applications in different fields. The potential of e-tongue sensors to detect organic contaminants in aqueous environmental matrices is discussed, with a particular focus on EOC.

**Key words:** electronic tongue, environmental monitoring sensing, emergent organic contaminants, pharmaceuticals and personal care products.

**Résumé :** Les contaminants organiques émergents (COE) sont des produits chimiques synthétiques ou d'origine naturelle qui pourraient s'immiscer dans l'environnement et causer des effets défavorables, connus ou soupçonnés, sur le plan écologique et sur la santé des humains. Malgré qu'ils ne soient pas généralement surveillés, les COE sont souvent détectés dans les effluents et les plans d'eau, à cause de la difficulté à les éliminer des stations d'épuration conventionnelles. Il y a une préoccupation croissante quant à la présence et à l'impact des COE, ainsi qu'un besoin de surveillance fiable et efficace de la pollution de l'eau en utilisant des capteurs capables de détecter les molécules cibles dans des milieux complexes. En raison de leurs spécificités, comme des temps de réponse rapides, leur prix avantageux, leur portabilité et fonctionnement simple, les systèmes de langue électronique (ou capteur organoleptique) présentent quelques avantages par rapport aux techniques analytiques traditionnelles (p. ex., systèmes chromatographiques) utilisées pour la surveillance de l'environnement. Dans le cadre de cet examen, les langues électroniques (capteurs organoleptiques) sont passés en revue, en se penchant sur leur capacité de surveiller l'environnement en temps réel. On a effectué une évaluation en utilisant la bibliométrie, de pair avec une étude de l'état des systèmes de langue électronique existants, de comment ils ont fonctionné et des applications de ceux-ci dans différents domaines. Le potentiel de ces capteurs organoleptiques à détecter des contaminants organiques dans des matrices environnementales aqueuses est discuté, avec un accent particulier sur les COE. [Traduit par la Rédaction]

**Mots-clés :** langue électronique, surveillance de l'environnement par capteurs, contaminants organiques émergents, produits pharmaceutiques et de soins personnels.

## 1. Introduction

Currently, the world faces a rising global demand for water due to an increasing population and climate change. Both water availability and quality are under stress (Pal et al. 2014). The global population is expected to exceed 9 billion by 2050, and 70% of people will be living in urban areas. This growing problem is usually coupled with poor wastewater management, old wastewater infrastructure plants, and limited disposal strategies with either minimal treatment practices or none at all (Corcoran et al. 2010). Consequently, wastewater treatment plants are releasing new classes of potential organic contaminants into water bodies,

known as emerging organic contaminants (EOC), as these are not completely removed by the existing technologies (Stülten et al. 2008; Matamoros et al. 2009).

EOC are defined as “chemical substances that have no regulation, are suspected of affecting the environment or whose effects are unknown” (Daughton 2004; Geissen et al. 2015). Some of the EOC are included in the priority pollutant lists developed by both the European Union and the United States Environmental Protection Agency. In 2000, an initial list of 33 priority substances was also identified under the European Union Water Framework Directive 2000/60/EC (European Commission) to be used as a control

Received 20 February 2018. Accepted 5 October 2018.

C. Magro, E.P. Mateus, and A.B. Ribeiro. CENSE, Departamento de Ciências e Engenharia do Ambiente, Faculdade de Ciências e Tecnologia, Universidade Nova de Lisboa, Caparica 2829-516, Portugal.

M. Raposo. CEFITEC, Functional Molecular Systems Group, Departamento de Física, Faculdade de Ciências e Tecnologia, Universidade Nova de Lisboa, Caparica 2829-516, Portugal.

**Corresponding authors:** Cátia Magro (email: [c.magro@campus.fct.unl.pt](mailto:c.magro@campus.fct.unl.pt)) and Eduardo Mateus (email: [epm@fct.unl.pt](mailto:epm@fct.unl.pt)).

Copyright remains with the author(s) or their institution(s). Permission for reuse (free in most cases) can be obtained from [RightsLink](https://rightslink.com).

measure for the next 20 years (Ellis 2008). In 2007, pharmaceuticals and personal care products (PPCP) such as diclofenac, iopamidol, musks, and carbamazepine were identified as future emerging priority candidates. Ibuprofen, clofibric acid, triclosan, phthalates, and bisphenol A are proposed additions to this list. Stuart and Lapworth (2013) have a clearer definition: "Emerging organic contaminants are compounds now being found in groundwater from agricultural and urban sources that were previously not detectable, or thought to be significant. EOC include pesticides and degradates, PPCP, industrial compounds, fragrances, water treatment byproducts, flame retardants, and surfactants, as well as 'life-style' compounds such as caffeine and nicotine".

It is necessary to find suitable sensors that allow for monitoring of EOC molecules. The development of reliable real-time sensors for environmental monitoring of EOC in wastewater treatment plants (WWTP) is challenging, as sensors must be selective for target compounds and sensitive enough to detect them at trace levels. One of the main challenges is to ensure analyte detection in environmental complex matrices that contain countless spurious molecules (potential interfering compounds) as well as microscopic life (Albareda-Sirvent et al. 2001). These matrix effects can jeopardize the analysis of a target molecule.

Sensors are an integral part of many engineered products, systems, and manufacturing processes as they provide feedback, monitoring, safety, and some other benefits (Stroble et al. 2009). The term sensor started to gain currency during the 1970s. The American National Standards Institute describes a sensor as "a device which provides a usable output in response to a specific measurand, where the output is defined as an electrical quantity, and a measurand is defined as a physical quantity, property, or condition which is measured" (American National Standards Institute (ANSI) 1982). Sensors should be in direct contact with the object under investigation, transform nonelectric information into electric signals, respond quickly, operate continuously or at least in repeated cycles, and be small in size (Gründler 2007).

Depending on the purpose, there are different types of sensors. Ranging from very simple to complex classifications (Fraden 2010), the sensor properties (materials and detection means used, specifications, conversion phenomena, field of applications, or stimuli) can be used to classify them. However, considering the purpose of monitoring target molecules in aqueous complex matrices, the optimal sensor would detect the presence of the target molecule, determine its concentration, and give general information about the complex matrix where the target molecules are inserted. Therefore, it seems that suitable sensors for providing that information are chemical sensors, taking into account the definitions given by Hulanicki et al. (1991).

Chemical sensors are complex devices optimized for a particular application. An ideal chemical sensor will respond instantaneously to a target compound (analyte) in a medium, producing a measurable signal output at a determined analyte concentration (Council 1995). However, despite significant advances in the last few decades, the way in which these devices respond to different stimuli in the sample is still relatively unknown. The complexity of a chemical sensor application is related to technical difficulties related with the measurements and specific nature (i.e., elemental or molecular) of the substance to be analyzed (Hulanicki et al. 1991). According to the International Union of Pure and Applied Chemistry, chemical sensors are defined "as devices or instruments that determine the detectable presence, concentration, or quantity of a given analyte."

Chemical sensors are based on two functional units: a receptor part and a transducer part. In the receptor, the chemical information is transformed into a form of energy, which may be measured by the transducer. The receptor may account for different principles: (i) physical, no chemical reaction takes place; (ii) chemical, where there is a chemical reaction with the analyte that gives rise to the analytical signal; and (iii) biochemical, in which a biochem-

ical process is the source of the analytical signal. In some cases, it is not possible to decide whether a sensor operates in a chemical or a physical mode, e.g., an absorption process. In the transducer section, the device transforms the energy-carrying chemical information on the sample into a useful analytical signal (Council 1995).

Regarding detection of EOC molecules in an environmental matrix, both physical and (bio)chemical principles are adequate. For physical detection, the electrical properties of a device constituted by a thin layer of film, for example, prepared from molecules with affinity to the target compound and deposited on the solid support with electrical electrodes, will change as the target molecules are being adsorbed. On the other hand, electrochemical sensors are based on the current measurement resulting from the oxidation–reduction reactions of the analyte at a suitable electrode. Electrochemical sensors achieve selectivity through molecular coatings, film coatings on electrodes, or chemically modified electrodes. The design of molecular selectivity for analytes involves an accurate choice of the sensing chemistry and associated materials (Ciosek and Wró 2007). Selectivity in sensing devices is related to a preferred response to a single sample substance, where the remaining substances can be considered formally as interfering substances. In a sensor's array, each sensor must have a specific capacity to distinguish between components of the mixture, i.e., it should distinguish between sample and interferent. The sensor can respond to both analyte and interferent with a different sensitivity (Gründler 2007). Chemical reactivity can involve a wide range of chemical phenomena, including: (i) recognition of size/shape/dipolar properties of molecular analytes by molecular films, phases, or sites; (ii) selective permeation of analyte in a thin-film sensor; and (iii) catalytic reaction cycle of the sensing materials, which results in analyte consumption (National Academy Press 1995).

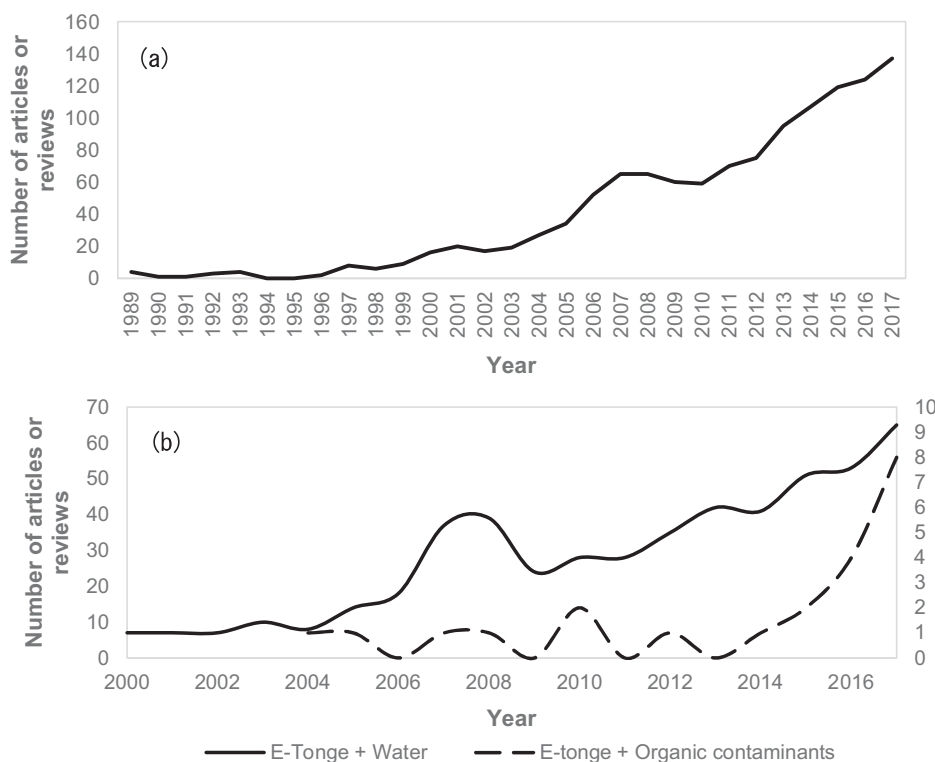
The concept of electronic tongue (e-tongue) emerged through the need for the detection, classification, and differentiation of complex substances. Since the first prototype in 1990 by Hayashi et al. (1990), e-tongue has become one of the most promising monitoring systems to develop a fast, cheap, and objective method for evaluating different matrices (Siliwiniska et al. 2014). Sensing tongue systems were inspired by the human tongue, which can detect five tastes: salty, sour, sweet, bitter, and umami (Winqvist 2008). The tasting senses in a human tongue are chemical senses, as they respond to a stimulus produced by food molecules on the tongue's taste cells, thus producing the sensation of taste. The taste receptor organs are located in the taste buds. In the process of flavor detecting, a series of electrical impulses are generated with different intensities and are transmitted to the brain–transducer, where they are compared to identify flavors (Smith and Margolskee 2001). In a similar way, the e-tongue with an array of sensors that measure electrical signals can be interpreted by mathematical methods, leading to information about the presence of the target molecule and its concentration in the complex matrix.

Given the importance of this new way of using sensors, the focus of this review is e-tongues, because of their scientific relevance for the detection of compounds in aqueous matrices and the growing number of scientific publications using this system. There are, however, other types of tongues or noses that may be considered for the detection of organic molecules, for example using optical sensors as in the work of the Suslick group (Rakow and Suslick 2000), and the Lundstrom and D'Amico groups (Filippini et al. 2006). The number of scientific publications on EOC detection is not yet strong enough.

To better recognize and assess the research status on e-tongues, we performed a bibliometric study (June 2018), making use of the online version of SCOPUS. With the search word "electronic tongue" (Fig. 1a), a total of 1297 scientific papers (articles and reviews) was obtained. In the 1297 papers with the subject of



**Fig. 1.** (a) Annual distribution of published scientific papers on e-tongues from 1989 to 2017 and (b) number of scientific papers published on e-tongues applied to water and organic contaminants (data adapted from SCOPUS, accessed in June 2018).



e-tongues, the dominant research areas are chemistry (36.3%), engineering (29.8%), and environmental sciences (6%), for which China, Spain, and USA are the top 3 countries, contributing 34% of the papers. The search word “electronic tongue” was refined with the sub-subject “water” (Fig. 1b) to link the subject to aqueous matrices. We also examined the connection between the search word “electronic tongue” and the sub-subject “organic contaminants” (e.g., EOC), obtaining an additional 22 papers from 2004 to 2017 (Fig. 1b).

Although the number of published papers on e-tongues that focused on the detection of organic components is still small, this detection method is considered a promising monitoring tool. Since its development, it has been used for a variety of purposes, e.g., water, wastewater and food analysis (Zhuiykov 2012; Panasiuk et al. 2015; Cetó et al. 2016; Díaz-gonzález et al. 2016; Gómez-Cravaca et al. 2016; Peris and Escuder-gilbert 2016; Wei et al. 2017; Son and Hyun 2018), while fulfilling environmental monitoring needs (Di Natale et al. 1997; Krantz-Rülcker et al. 2001; Gutiérrez et al. 2008; Winqvist 2008; Campos et al. 2012; Askim et al. 2013; Tahara and Toko 2013; Capelli et al. 2014; Justino et al. 2015).

Conventionally, chemical sensing of unknown substances is performed in an analytical laboratory with complex benchtop equipment, including mass spectrometry, chromatography, nuclear magnetic resonance, X-ray, and infrared technology. These methods are very accurate enabling the identification of most unidentified chemical classes with a high degree of confidence and precision (Banerjee et al. 2016), which can be used to calibrate sensors. Nonetheless, the e-tongue presents potential advantages: (i) sample pretreatment may not be mandatory, (ii) the source of errors due to sample transport or storage may be drastically reduced or eliminated, and (iii) a fast response may be achieved in environmental emergencies (Albaladejo et al. 2010). The possibility of environmental monitoring in real-time mode and operating on long-term scales can enable data collection that may be crucial

for understanding the full range of potential contamination in all its phases and environmental compartments. Moreover, real-time tools used for environmental monitoring represent a cutting-edge technology that, with the right approval and support from government agencies, along with an increase in the quality of the produced data, will undoubtedly become a part of modern environmental monitoring laboratories (Gałaszka et al. 2015).

This review aims to present how pollutants in aqueous media can be detected using the e-tongue, and to highlight the opportunities for the detection of EOC-PPCP in these matrices. In addition, the concept of the e-tongue and examples of its successful applications are analyzed.

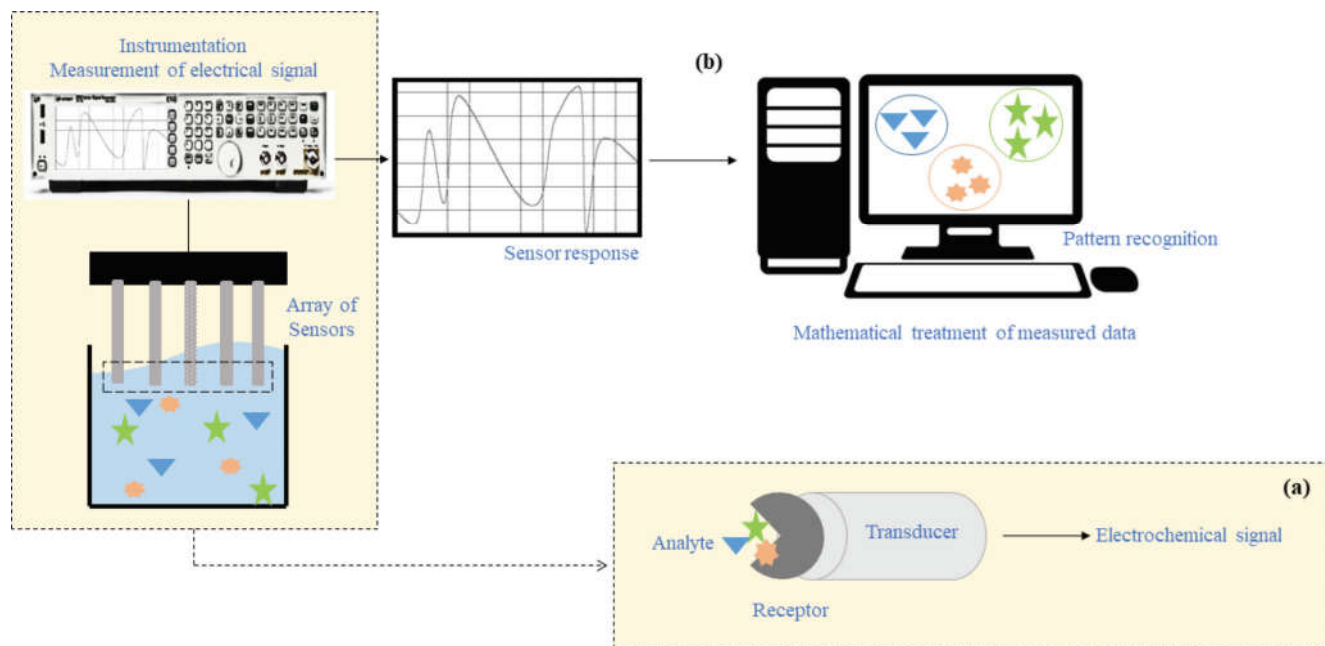
## 2. Electronic tongue—the concept

The e-tongue is based on chemical sensors with low selectivity, that display cross-sensitivity to multiple components in liquids (Ciosek and Wró 2007), and can be considered as “a multi-sensory system, formed by an array of low-selective sensors, combined with advanced mathematical procedures for signal processing, based on pattern recognition and (or) multi-variate data analysis” (Vlasov et al. 2005). The seminal work of Di Natale et al. (1997), one of the pioneers on the subject of the e-tongue, used a chalcogenide glass sensor array with an artificial neural network analysis for the detection of heavy metal cations and inorganic anions in a complex aqueous solution. Thus, if the e-tongue is configured and properly trained (e.g., the choice of materials), it can be used to characterize complex liquid samples and recognize the qualitative and quantitative composition of multi-species solutions (Escuder-gilbert and Peris 2010).

### 2.1. Components

The e-tongue system with its base components is schematized in Fig. 2. Typically, the electrical signals measured in an array of sensors immersed in, or covered with, liquid samples are recorded

Fig. 2. Schematic components of an electronic tongue.



and processed by mathematical procedures to achieve a pattern. This pattern allows for a comparison of the results obtained with the data of calibrated libraries already gathered from previous complex solutions in which its composition was also carefully analyzed in conventional laboratories. This means that a library should be attained for each sensor array. In most cases, the liquid sample must be placed in a controlled temperature or at a controlled flux, if the electrical properties are dependent on the temperature or atmosphere.

The e-tongue's components are explained in more detail as follows.

### 2.1.1. Methods for measuring the electrical signal

There are several types of sensors that can be applied in e-tongues. A wide variety of chemical sensors have been employed, but the ones most commonly used for detecting pollutants are electrochemical systems (e.g., potentiometric, voltammetric, and amperometric) and electrochemical-physical systems (e.g., impedance) (Krantz-Rülcker et al. 2001; del Valle 2010; Zou et al. 2015). The classification is related to the primary signal after an interaction with the analyte when a potential electrochemical current or resistivity-capacitance change is generated and measured.

Voltammetric and potentiometric sensors have several applications in environmental monitoring and the detection of pharmaceuticals in food (Gutiérrez et al. 2008; Mimendia et al. 2010; Wei and Wang 2011). In potentiometric sensors the current is monitored without current flow, whereas in voltammetry sensors a potential is applied, and the resulting current is measured (Winquist 2008). Voltammetric methods are more versatile and robust, as they are usually less influenced by electrical disturbances, and the potentiometric measurements are considered to be simpler (Holmin et al. 2001). From the point of view of detection, potentiometry operates in terms of the system's net charge being disadvantageous in nonelectrolyte media, whereas cyclic voltammetry operates in complex liquids requiring compounds that can be oxidized or reduced actively onto the working electrode (Legin et al. 1999; Holmin et al. 2001; Ivarsson et al. 2001).

Amperometry is preferred for monitoring a time-dependent change with a wide dynamic range (Wang et al. 2015). Amperometric systems are directly measured in electrochemical reaction

rates taking place at the electrodes, where the current derives from the oxidation or reduction of electroactive compounds at a working electrode while a constant potential is applied (Kirsanov et al. 2004).

In the impedance system, the full scan of different alternated current frequencies or a selected number of discrete values, may be used (conductivity or capacitance) in a simpler conceptual implementation (del Valle 2010). The impedance technique is based on the electrode perturbation caused by an external signal of small magnitude. Measurements can be performed in an equilibrium or stationary state, allowing for the characterization of aqueous environmental matrices by analyzing the electrical impedance as a function of frequency signals applied to nanostructures adsorbed onto solid substrates (Riul et al. 2002). E-tongue systems that measure the electric impedance using conducting polymers (alone or combined with lipids) can work as sensorial unities, as they recognize the taste below the biological limit (Ferreira et al. 2003), eliminating the need for human panels.

According to SCOPUS (accessed in June 2018), the number of publications referring to the term "electronic tongue" (broken down according to the different sensors: potentiometric, voltammetric, amperometric, and impedance) has been growing steadily since the research in 1997. On potentiometric, voltammetric and amperometric systems, the number of articles published appears to have stabilized over the last few years, whereas the number of articles published for impedance systems is increasing.

### 2.1.2. Array of sensors

The choice of sensors is dependent on the measuring method. In voltammetric measurements, for instance, a reference electrode (e.g., Ag/AgCl), a counter electrode (e.g., Platinum (Pt)), and a working electrode are typically required. Working electrodes are made of noble and non-noble metals, such as Copper (Cu), Gold (Au), Nickel (Ni), Palladium (Pd), Pt, and Silver (Ag), and other materials such as glassy carbon (GC). Working electrodes can also be covered with films, increasing the sensitivity of the sensor. The physical properties measured (e.g., capacitance and resistance) can be improved if the interdigitated electrodes (IE) are covered with thin films (Riul et al. 2002).

A thin film, deposited onto IE, based on insulator, semiconductor, or conductive materials with affinity for the target molecule, will have a different resistance and (or) capacity as the analyte molecules are being adsorbed onto it, allowing for the detection of a target compound or analyte in a solution. Taylor and Macdonald (1987) analyzed this situation and presented a simple equivalent circuit that describes the AC electrical behavior. Such impedance or conductance spectra will be dependent on both the number of molecules adsorbed onto the thin film surface and the other constituents of the solution matrix. The adsorption of target molecules could be due to both physical interactions (ionic, hydrogen bonds, van der Waals, dipolar) and chemical bonds, where the measured electrical signal will incorporate information from them in greater or lesser detail depending on the film used. Therefore, thin films should be prepared in view of their ability to adsorb the analyte or adsorb other constituents of the aqueous matrix. Hence, several thin films should be prepared to develop the e-tongue, based on both physical and chemical methods of detection. Different kinds of thin molecular films could be prepared, namely Langmuir–Blodgett or self-assembled or layer-by-layer films (Oliveira et al. 2014).

### 2.1.3. Mathematical treatment of measured data

Regardless of the system used (potentiometric, voltammetric, amperometric, or impedance systems) for monitoring aqueous environmental matrices, the complexity of the information extracted will involve an analysis of a large number of variables. Some of these variables are not significant in the interpretation of results, and only the relevant information is collected, thereby reducing the volume of data (Wilson and Baietto 2009). Thus, without losing any information, relevant data can be obtained using statistical methods that will reduce data volume. Some examples of the discussion on the processing methods of multivariate data in e-tongues and noses can be found in Richards et al. (2002), Scott et al. (2007), Palit et al. (2010), and Cetó et al. (2013).

Pattern recognition techniques (Fig. 2b) consist of the following sequential stages: signal preprocessing, dimensionality reduction, and prediction-validation (Rodríguez Méndez et al. 2016). The signal preprocessing prepares the feature vector for future processing. It includes compensation for sensor drift, scaling of the data, and extracting representative parameters (Raposo et al. 2016). The intrinsic complexity, richness, and cross-selectivity of the signals generated by sensor arrays provide certain advantages, as the resulting data set contains meaningful information about the sample. The choice of method depends on the type of available input data acquired from the sensors and the type of information that is sought. The digital outputs generated by e-tongue sensors need to be analyzed and interpreted to provide useful information to the operator (Wilson and Baietto 2009).

There are different advanced methods based on the statistical treatment of data that can be used for feature extraction and for finding the most important parameters (Rodríguez Méndez et al. 2016). Multi-variate data analysis comprises a set of techniques that can be used for the analysis of data sets with more than one variable by reducing high dimensionality in a multi-variate problem when variables are partly correlated (Wilson and Baietto 2009). The first approach for the classification of the sample typically involves graphical analysis and comparing samples or comparing the identification of unknown elements with those from known sources in libraries (Dymerski et al. 2011). This involves the development of calibrated libraries, which are required for each e-tongue. Multi-variate analysis can be divided into unsupervised or supervised techniques. Unsupervised methods are used to find or confirm patterns, making comparisons between different unknown samples to discriminate between them in cases where the database of known samples has not been previously constructed. Supervised methods use the response variable to discover patterns associated with the response.

Unsupervised methods include singular value decomposition and principal components analysis (PCA), which use only the matrix of features by samples, as well as clustering. Supervised methods include multiple regression and classification as well as more recently developed techniques, such as sliced inverse regression, requiring a variable response, which is usually a phenotype, in addition to the feature by sample matrix (Rodríguez Méndez et al. 2016). The training process for supervised methods, e.g., artificial neural networks, involves a discrete amount of known sample data to train the system and is very efficient in comparing unknown samples to known references (Hodgins 1997).

### 2.1.4. Conditioning of the liquid samples

When electrical signals are temperature dependent, a thermostat and (or) thermal bath enables continuous maintenance-monitoring of the sample temperature during analysis, providing reproducibility and repeatability of measurements (Siliwiniska et al. 2014).

In some instances, flow techniques are important for e-tongue systems, providing automation of the analytical methods. The main benefits of automation of the analytical procedures are the increase in sample frequency, minimization of sample contamination, improvement of analyst security, and lower reagent-sample consumption, which implies lower personal and consumable costs (Cerdà et al. 2014). In an e-tongue system, there are two main flow mechanisms that are commonly used for water analysis (Mesquita and Rangel 2009): flow injection analysis (FIA) operated exclusively by hand and sequential injection analysis (SIA) based on multi-commutation operation. Comparing the two techniques SIA presents advantages over FIA, as it uses fewer reagents and results in less waste production, being an environmentally friendly methodology that can perform the largest number of analyses. SIA systems have been successfully used with potentiometric e-tongues (Cortina et al. 2005). When these techniques are used, FIA and SIA have the potential to decrease analysis time and increase repeatability (Siliwiniska et al. 2014). Nonetheless, there is no solid argument in favor of using a particular flow technique separately, but the advantages increase if they are combined or developed specifically for the purpose, e.g., Richards et al. (2003).

## 2.2 Applications

Because of the ease with which the e-tongue can be operated, research efforts have been dedicated to the development and use of a wide range of applications, e.g., carcinogenic trihalomethanes in public water supply systems (Carvalho et al. 2007); detection of phenolic compounds (Olivati et al. 2009); detection and monitoring of ammonium, nitrite, and nitrate ions in waters (Nuñez et al. 2013); and quantification of ammonium and phosphate ions in wastewaters (Campos et al. 2014). Di Natale et al. (2000) combined e-nose and e-tongue sensors to classify urine, merging data obtained from each of the sensor arrays. Also, e-tongue coupled with e-nose was used for analyzing different types of Moroccan waters (Haddi et al. 2014). Table 1 presents a summary of some e-tongue and hybrid systems in different fields: aqueous environmental matrices and complex liquid matrices. Published manuscripts were chosen based on either their importance for improving the sensing field or the complexity of the matrices, which can actively contribute to the development of a new e-tongue system. The results from all these papers can serve to contribute to an upgraded e-tongue system for detecting EOC in aqueous environmental matrices.

Portable environmental sensing technology is particularly appealing for pollution monitoring, but it is more limiting than its nonportable counterparts. However, e-tongue systems have great potential and are highly relevant for continuous environmental pollutant monitoring (Kim et al. 2012). It is important to stress that environmental portable sensing technology meets the criteria of green analysis: automation, low power consumption, avoidance

**Table 1.** Applications of e-tongue and hybrid sensing systems.

Sensing type	Sensor specifications	Matrices	Measured parameters	Methods of data analysis	Concentrations	Detection limit	Main Conclusions	References
Environmental Matrices								
E-tongue	22 electrodes based on chalcogenide glasses variously spiked and conventional electrodes	Polluted water—river	Cu, Cd, Fe, Cr, Zn, Cl, SO <sub>4</sub> and H	MLR, PLS, NLLS and BP-NN	[Cu (6–8), Cd (6–7), Zn (3–5), Cr (4–7), Fe (4–7), Cl (3–5.3), SO <sub>4</sub> (3–3.9), H (2.6–8)] –log[C]	—	PLS, NLLS and BP-NN were similar in qualitative information.	Di Natale et al. 1997
E-tongue	Monolithically integrated array of chemical sensors, composed by six ISFETs, IDS and silicon diode	Mineral water	Na <sup>+</sup> , K <sup>+</sup> , Ca <sup>2+</sup> , Cl <sup>-</sup> ; conductivity and potential redox	HCA and PCA	—	—	The device responded with good reproducibility to different kinds of mineral water by using pattern recognition methods.	Moreno et al. 2006
E-tongue	PQC sensor array based on MIP coating	Tonic water	Quinine and saccharine	—	Quinine (10–1080) mg/L and saccharine (51–3420) mg/L	Quinine 2.04 mg/L and saccharine 32.8 mg/L	The sensor provided a satisfactory response detecting the change in bitter taste of drinks and beverages at practical concentrations, comparable to the taste assessment from a human taste panel.	Sun et al. 2008
E-tongue	Impedance response - NIIPPS compound on a carbon nanotube-coated glassy carbon electrode	Underground, tap water and lake water	Bisphenol A, nonylphenol, and ethynylestradiol	—	1 µmol/L	15–260 mmol/L	The results showed that the sensitivity, stability and detection limit of the composite electrode were significantly improved, compared with those obtained at electrodes coated with carbon nanotubes or other materials.	Liu et al. 2011
Others	Voltammetric response and electrochemical detection: polymer/CNT film coated electrode	Lake and river water	4-tert-Octylphenol	—	6.5–20 nM	0.5 nM	This method avoids a tedious extraction process, it is time saving and cost effective. This method therefore can be applied for the detection of 4-tert-octylphenol at low concentration levels and for in-site and on-line monitoring of 4-tert-octylphenol in water.	Wan et al. 2013
E-tongue	Potentiometric	Urban water reservoirs	<i>Daphnia magna</i> bioassay	PCA, CCA, PLSR and PRM	—	—	It was found that root mean square prediction errors, given by PRM and PLS, did not exceed 20%.	Kirsanov et al. 2014
Hybrid, e-nose coupled with e-tongue.	E-nose: MOS home-fabricated; e-tongue: potentiometric	Natural, sparkling, river and tap water and wastewater	E-nose: CH <sub>4</sub> and combustibles gases, alcohols, xylene, toluene, NH <sub>3</sub> , hydrogen, sulfide, methane; E-tongue: Ca <sup>2+</sup> , K <sup>+</sup> , Cd <sup>2+</sup> , F <sup>-</sup> , Na <sup>+</sup> , Cl <sup>-</sup> , NO <sub>3</sub> <sup>-</sup> and H <sup>+</sup>	PCA and LDA	—	—	The metal oxide sensors together with PCA, distinguishes the potable and nonpotable water samples with a total variance of 86.98 %. The potentiometric sensor showed an accuracy of 100% success rate in the recognition of the eight Moroccan water sources with LCA coupled with leave-one-out cross-validation method.	Haddi et al. 2014
Others	Allylmercaptane-modified gold surface plasmon resonance chip and printed p(HMAGA) nanofilm	Wastewater	Triclosan	—	0.10, 0.20, and 0.30 ng/ml	0.017 ng/ml	Recovery rates were 98%–102%; Compared with other complex analytic techniques, ICS-imprinted SPR nanosensor demonstrated comparable or better performance.	Atar et al. 2015
E-tongue	Potentiometric	Commercial mineral water, tap water and two types of surface water	Cyanobacterial microcystin toxins	PLS and PLS-DA	0.1 to 10 µg/L	10 <sup>-6</sup> mol/L	The experiments demonstrate the success of the e-tongue in the microcystin toxins concentration prediction comparing to standard chromatographic technique, UHPLC-DAD and colorimetric enzymatic analysis.	Livova et al. 2016

Table 1 (continued).

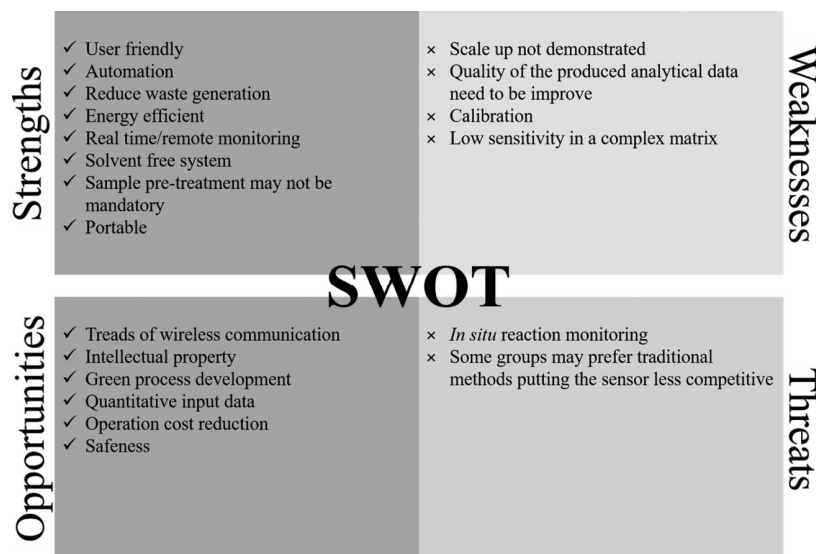
Sensing type	Sensor specifications	Matrices	Measured parameters	Methods of data analysis	Concentrations	Detection limit	Main Conclusions	References
E-tongue	Optical-colorimetric sensor array	Mineral water	Cyclohexanone, dimethylmethylphosphonate, piperazine, imidacloprid, 5-fluorouracil, and paraoxon.	PCA	1 10 <sup>-6</sup> mol/L to 3.9 10 <sup>-4</sup> mol/L	Below 3.9 10 <sup>-4</sup> mol/L	Results show that the sensors are sensitive, but with low selectivity, in the interval from 10 <sup>-7</sup> mol/L to 10 <sup>-4</sup> mol/L. The sensor signals show a linear correlation with the logarithm of the concentration. Although the limited selectivity of individual sensors, the different sensitivity patterns allow for a clear identification of the compounds, independent of their concentration.	Guarnais Gonçalves et al. 2016
E-tongue	Voltammetric-gold electrode	Spiked tap water	Brominated trihaloacetic acids	PCA and ANN	0–1200 µg/L	—	Satisfactory recovery values were obtained in the analysis of spiked water samples, as demonstrated from the lack of matrix effects.	Cetó et al. 2017
E-tongue	Impedance-reduction of graphene oxide in the presence of conducting polymers (PEDOT: PSS and polypyrrole) and AuNPs	Mineral and tap water	Organophosphate pesticides	PCA	0.1–5 mmol L <sup>-1</sup>	0.1 mmol L <sup>-1</sup>	The graphene oxide associated with conductive polymers and gold nanoparticles granted good stability, high reproducibility and high sensitivity to the developed e-tongue. With PCA analysis, the e-tongue was able to classify solutions of different pesticides at distinct nanomolar concentrations, and discriminate real samples from the samples prepared in buffer solutions, presenting a correlation with the concentration and the value of the PC component.	Facure et al. 2017
Complex Matrices E-tongue	Voltammetric	Bovine milk	Chloramphenicol, erythromycin, kanamycin sulfate, neomycin sulfate, streptomycin sulfate, tetracycline, and dimethyl sulfoxide	PCA, DFA, PCR, PLSR and IS-SVM	0.5, 1.0, 1.5, and 2.0 µg/kg	—	The six antibiotics at the maximum residual levels could not be separated from bovine milk completely by PCA; all the samples were demarcated clearly by DFA; PCR had the most stable results in regression models.	Wei and Wang 2011
Hybrid, e-tongue coupled with e-nose	E-tongue: potentiometric electrode sensors; e-nose: Porphyrint-based quartz microbalance gas sensor array	Urine and milk	Urine: protein, glucose, ketones, urobilinogen, bilirubin, blood, pH, specific weight. Milk: pasteurised and ultrahigh temperature distinction	PCA	—	—	High abstraction level (pre-analysis of each system and successive merging of the most prominent features) appears to be the most significant way to preserve the best knowledge content from each separate analysis.	Di Natale et al. 2000
E-tongue	Insent IS-5000Z and Astree2	Sodium saccharin, ibuprofen, acetaminophen, caffeine, citrate and quinine hydrochloride	Identification	PCA	Sodium saccharin (8 concentrations between 1 and 500 mmol/L), ibuprofen lysinate (10 concentrations between 0.01 and 30 mmol/L), Ibuprofen (10 concentrations between 0.03 and 0.13 mmol/L), acetaminophen (10 concentrations between 0.13 and 66 mmol/L), caffeine (10 concentrations between 0.05 and 90 mmol/L), caffeine citrate (10 concentrations between 0.03 and 45 mmol/L), quinine hydrochloride (9 concentrations between 0.02 and 5 mmol/L)	—	Ionic substances are easier to detect than neutral ones; quantification could only be performed for the IS-5000Z; Insent taste sensor provides more reliable (in vitro/in vivo correlation) and precise (reproducibility and repeatability).	Woertz et al. 2011

**Table 1** (continued).

Sensing type	Sensor specifications	Matrices	Measured parameters	Methods of data analysis	Concentrations	Detection limit	Main Conclusions	References
Others	Multi-walled carbon nanotubes modified glassy carbon electrode	Ethanol	4-n-octylphenol	—	$5 \times 10^{-8}$ to $1 \times 10^{-5}$ mol/L	$1.5 \times 10^{-8}$ mol/L	The modified electrode showed good selectivity, sensitivity, reproducibility, and high stability.	Zheng et al. 2012
E-tongue	15 potentiometric poly(vinyl chloride) membrane sensors sensitive to cations and anions	Milli-Q distilled water	$\text{NO}_3^-$ , $\text{NO}_2^-$ , $\text{Cl}^-$ , $\text{NH}_4^+$ , $\text{K}^+$ , and $\text{Na}^+$	ANN	$\text{NO}_3^-$ (0.01–1 mM), $\text{NO}_2^-$ (0.05–5 mM), $\text{Cl}^-$ (0.2–20 mM), $\text{NH}_4^+$ (0.01–1 mM), $\text{K}^+$ (0.01–1 mM) and $\text{Na}^+$ (0.2–20 mM)	$\text{NO}_3^-$ ( $4.6 \times 10^{-6}$ mol/L), $\text{NO}_2^-$ ( $3.4 \times 10^{-6}$ mol/L), $\text{Cl}^-$ ( $7.9 \times 10^{-5}$ mol/L), $\text{NH}_4^+$ ( $1.0 \times 10^{-7}$ mol/L) and $\text{Na}^+$ ( $6.4 \times 10^{-7}$ mol/L)	E-tongue system allowed the quantification of nitrate, nitrite, and ammonium in an aqueous medium in the presence of interfering species such as sodium, potassium and chloride ions. It was possible to distinguish between nitrate and nitrite species with some deviations for ammonium.	Núñez et al. 2013
Others	Electrical impedance of PAAH/PAZO nanofilm	Ethanol	Deltamethrin	—	$10^{-10}$ M to $10^{-6}$ M	Below 0.1 nM	Electrical resistance measurement at 100 Hz, revealed to be an adequate variable for deltamethrin concentration transduction.	Abegão et al. 2013
E-tongue	Potentiometric-8 miniaturized electrodes based on PVC membranes (plasticized using DOS or o-NPOE), containing an appropriate lipophilic salt, exhibiting generic anion (DMAc, TBHDPB, IL) or cation (KTFBB) response	Active Pharmaceutical Ingredients	Acetaminophen, ascorbic acid, acetylsalicylic acid, and caffeine as an interferent	PLS and ANN	Acetaminophen (1–20 mmol/L), ascorbic acid (0.3–7 mmol/L), acetylsalicylic acid (1.4–8 mmol/L), caffeine (0.13–1.3 mmol/L)	—	The extraction of dynamic components of the transient response employing the Wavelet transforms the removal of the less significant inputs by means of Causal Index pruning and training of an ANN with the selected coefficients allowed the simultaneous determination of the 3 APIs counterbalancing any interference caused by caffeine.	Wesoly et al. 2016
Others	Potentiometric	Pharmaceuticals	Dissolution identification: Naproxen Sodium and Diphenhydramine Hydrochloride	—	220 mg of naproxen sodium and 25 mg of diphenhydramine hydrochloride per tablet.	Naproxen Sodium: $8.28 \times 10^{-5}$ M Diphenhydramine Hydrochloride: $7.94 \times 10^{-6}$ M	In-line potentiometry in the simultaneous assay and dissolution monitoring of binary formulated oral solid dosage forms.	Shehata et al. 2017
E-tongue	Voltammetric: array of 4 sensors, reference Ag/AgCl and Pt counter electrode	Aqueous complex solution	2,4-dinitrophenol, 4-nitrophenol and picric acid	ANN	0–300 µg/L	—	The model successfully predicted the concentration of the three considered phenols with a normalized root mean square error of 0.030 and 0.076 for the training and test subsets, respectively, and $r \geq 0.95$ .	González-Calabug et al. 2018

**Note:** MLR, multiple linear regression; PLS, partial least squares; NLLS, nonlinear least squares; BP-NN, back-propagation-neural network; ISFET, ion-selective field-effect transistors; IDS, interdigitated platinum electrode; HCA, hierarchical clustering analysis; PCA, principal component analysis; CCA, canonical correlation analysis; PQC, piezoelectric quartz crystal; MIP, molecularly imprinted polymer; NiTiTPPS, Ni(II)tetraakis(4-sulfonatophenyl) porphyrin; CNT, carbon nanotubes; CCA, canonical correlation analysis; PLSR, partial least squares regression; PRM, partial robust M-regression; MOS, metal oxide semiconductor; LDA, linear discriminant analysis; p(HEMAGA), poly(2-hydroxyethylmethacrylate-methacryloylamidoglutamic acid); TCS, tricolosan; SPR, surface plasmon resonance; PLS-DA, partial least squares-discriminant analysis; UHP/PLC-DAD, Ultra High Performance Liquid Chromatography coupled to Diode Array Detection; ANN, artificial neural network; PEDOT:PSS, Poly(3,4-ethylenedioxythiophene)Polystyrene sulfonate; AuNPs, gold nanoparticles; DFA, discriminant function analysis; PCR, principal component regression; LS-SVM, least squares-support vector machines; PAH, poly(allylamine hydrochloride); PAZO, poly[1-(4-(3-carboxy-4-hydroxyphenylazo) benzene sulfonamido)-1,2-ethanediyl, sodium salt]; PVC, poly(vinyl chloride); DOS, bis(2-ethylhexyl) 120 sebacate; o-NPOE, plasticizers-o-nitro-phenyl octyl ether; TDMAc, tridodecylmethyl-ammonium chloride; TBHDPB, tributylhexadecylphosphoniumbromide; IL, ionic liquid; KTFBB, potassium tetrakis [3,5-bis(tri-fluoromethyl)phenyl] borate.

Fig. 3. Electronic tongue SWOT (strengths, weaknesses, opportunities, threats) analysis.



of reagent use, and no waste generation (Tobiszewski et al. 2010). Traditional analytical instruments can be less attractive, as they are not able to provide continuous monitoring or work as remote sensing, and have high operating costs.

### 3. Opportunities in sensing technology applied to aqueous matrices

Environmental samples can be extremely complex. Therefore the main obstacles when dealing with liquid samples are the low concentrations of EOC occurrence in water media (Bourgeois et al. 2003; Justino et al. 2015).

Either e-tongue systems or chromatography methods can be used to detect and determine such pollutants at low concentrations (ng/L or pg/L) levels. Consequently, to validate e-tongue data, chromatography methods are often used to confirm the concentration levels of the target compound. Tahri et al. (2018) showed that Headspace (HS) Gas Chromatography – Mass Spectrometry (MS) could contribute to the validation results obtained from a voltammetric e-tongue system. Here are some examples of studies that can be coupled with an e-tongue system. (i) Gas chromatography and liquid chromatography (LC), both coupled with tandem MS, were used to determine the contaminants of emerging concern (e.g., nonylphenol-PPCP) in municipal wastewater effluents and marine receiving water (Vidal-Dorsch et al. 2012). (ii) Ronan and Mchugh (2013) used LC coupled with tandem MS with electrospray ionization in negative mode to determine natural and synthetic steroid estrogens in seawater and marine biota. (iii) Li et al. (2016) also used the LC-MS-MS method to determine 45 commonly used PPCP in sludge. To achieve equal ranges of accuracy in detection and analysis when compared with chromatography methods, many electronic sensing investigations focused their efforts on the detection of contaminants in real environmental matrices.

A SWOT (strengths, weaknesses, opportunities, threats) analysis was carried out, Fig. 3 highlights some of advantages and limitations of e-tongue sensing; additionally, it emphasizes the positive external aspects that would enhance the benefits of this system and points out some of the negative aspects that can jeopardize the competitive advantages of e-tongue sensing. One of the main advantages of this technology is that it enables quick access to information in simple or complex liquid, which, combined with its relatively easy production, will soon allow the e-tongue to be used on a global scale. Moreover, e-tongue systems are embodied in the trend of Industry 4.0, allowing for the use of portable

instruments in environmental site assessments, automation, and online detection (the internet of things). Environmental samples represent a composite mixture of various compounds in gaseous, liquid, or solid states. This complexity can result in analytical problems, such as interferences, which usually pose a challenge for field analysts. From a global point of view, traditional environmental assessment techniques using off-site analysis provide better data quality, but the trade-off is a poorer understanding of the pollution distribution and a lower information value of the data set compared with on-site analysis.

The fast progress in e-tongue technology in recent years has increased the number of applications for environmental sample analysis. An example of a successful e-tongue system used in aqueous environment media is the work of Campos et al. (2013), who developed an e-tongue to monitor the presence of ammonium nitrate in water based on pulse voltammetry. It consisted of an array of eight working electrodes (Au, Pt, Rh, Ir, Cu, Co, Ag, and Ni) encapsulated in a stainless steel cylinder. The electrochemical response of these different electrodes was studied in the presence of ammonium nitrate in water to further improve the design of the wave form used in the voltammetric tongue. Afterwards, the response was tested with a set of 15 common inorganic salts ( $\text{NH}_4\text{NO}_3$ ,  $\text{MgSO}_4$ ,  $\text{NH}_4\text{Cl}$ ,  $\text{NaCl}$ ,  $\text{Na}_2\text{CO}_3$ ,  $(\text{NH}_4)_2\text{SO}_4$ ,  $\text{MgCl}_2$ ,  $\text{Na}_3\text{PO}_4$ ,  $\text{K}_2\text{SO}_4$ ,  $\text{K}_2\text{CO}_3$ ,  $\text{CaCl}_2$ ,  $\text{NaH}_2\text{PO}_4$ ,  $\text{KCl}$ ,  $\text{NaNO}_3$ ,  $\text{K}_2\text{HPO}_4$ ). PCA showed good discrimination between ammonium nitrate and the remaining studied salts. One year later, the same research team used a voltammetric e-tongue to evaluate the concentration of ammonia and orthophosphate in influent and effluent wastewater, since the quantification of these components in WWTP has further implications in the eutrophication process (Campos et al. 2014).

Regarding detection of EOC, e.g., PPCP, and excluding the cases of pharmaceutical applications, the publications mentioning e-tongues are practically nonexistent in the literature (Raposo et al. 2016 and the references therein). PPCP are of increasing concern because of their environmental persistence, accumulation in the environment at a global scale, and their steady detection in all environmental water compartments. Pharmaceutical products, for instance, are additionally designed to maintain their active forms and chemical properties long enough to perform their therapeutic purposes, and thus at least 50% of a dose may be potentially excreted unchanged into the environment, where these products will then remain (Bila and Dezotti 2003). Consequently, PPCP have been widely detected in the effluents of

WWTP due to their incomplete removal treatment rates and in their receiving water bodies (Matamoros et al. 2009; Zhang et al. 2014). PPCP and their metabolites (generated by metabolization and abiotic processes, such as hydrolysis or photolysis) are usually detected in trace concentrations, and many of them have raised considerable ecotoxicological concerns (Stülten et al. 2008).

To address detection of these micropollutants, attempts have been carried out to develop sensors that can work on the continuous monitoring in aqueous complex matrices. Arvand et al. (2012) developed a voltammetric sensor based on GC electrodes modified with carbon nanotubes for the detection of diclofenac (anti-inflammatory) in blood serum and seawater. Their aim was to develop a new technology that: (i) is simple, (ii) has a reduced-cost nanocomposition, (iii) has multi-functional properties benefitting from multi-walled carbon tubes (MWCNT) – Cu(OH)<sub>2</sub> nanoparticles and hydrophobic ionic liquid 1-ethyl-3-methylimidazolium hexafluorophosphate, and (iv) has good electrocatalytic activity for the electro-oxidation of diclofenac. The authors achieved a new voltammetric sensor sensitive in the range of 0.18–119 mM, with a detection limit of 0.04 mM (Arvand et al. 2012). Liu et al. (2011) developed an impedance Ni(II)tetrakis(4-sulfonatophenyl) porphyrin (NiTPPS) carbon nanotube composite electrode for the detection of three endocrine disrupting compounds—bisphenol A, nonylphenol, and ethynylestradiol—in underground, tap, and lake water. The authors optimized experimental parameters: hydrodynamic potential of 0.7 V for FIA and NiTPPS surface coverage of 2.2 nmol cm<sup>-2</sup>. The final results showed an improvement in the sensitivity, stability, and detection limit (from 15 nmol/L to 260 nmol/L).

To detect 4-n-octylphenol (OP) in solutions with a concentration range of  $5 \times 10^{-8}$  to  $1 \times 10^{-5}$  mol/L, Zheng et al. (2012) developed a MWCNT modified GC electrode (GCE). The oxidation peak of OP (oxidized directly on the MWCNT/GCE) showed an improvement with the use of MWCNT/GCE, compared with those using a bare GCE. The detection limit achieved was  $1.5 \times 10^{-8}$  mol/L. Wan et al. (2013) conducted studies in the detection of 4-tert-octylphenol in lake and river waters with a polymer-carbon nanotube film-coated electrode. The electrode was prepared by coating a polished and clean GCE with a carbon nanotube film and then covering it with a conducting film from L-lysine. The detection limit achieved was 0.5 nM, and the method could be applied for low concentration, in-site and online monitoring of 4-tert-octylphenol in water (Wan et al. 2013).

A sensing layer, based on layer-by-layer films prepared with the common polyelectrolyte poly (allylamine hydrochloride) and pazo-polyelectrolyte poly[1-[4-(3-carboxy-4-hydroxyphenyl-azo) benzenesulfonamido]-1,2-ethanediy], sodium salt) was used for the detection of deltamethrin, a pesticide, where the sensor response was obtained from impedance spectroscopy measurements (100 Hz) (Abegão et al. 2013). Sensor sensitivity was  $41.1 \pm 0.7$  kΩ per decade of concentration and had a reproducibility of approximately 2% in a binary solution of ethanol and deltamethrin. The sensor was able to detect concentrations below 0.1 nM. One year later, Pimentel (2014) also worked with an e-tongue system based on impedance spectroscopy, which attempted to detect a low concentration (nM and pM) of ibuprofen in an aqueous medium. The same working group developed a nano-sensor that can detect picomolar concentrations of triclosan in an aqueous medium (Marques et al. 2017). Also seeking to detect triclosan, Gao et al. (2010) synthesized molecularly imprinted core-shell carbon nanotubes and detected PPCP in aqueous matrices in concentration ranges from 0.01 to 40 μg/mL.

For sensitive and selective detection of the Carmine pigment in liquid samples, Zhao et al. (2018) developed a screen-printed carbon-based disposable electrochemical sensor: PEDOT (Polystyrene sulfonate – gold nanoparticles – carbon-Poly(3,4-ethylenedioxythiophene) and βMercaptoethylamine. The sensor response was obtained by cyclic voltammetry, differential pulse stripping voltammetry, and impedance spectroscopy in a range of concentrations between  $9.0 \times 10^{-9}$  to

$3.9 \times 10^{-6}$  mol/L, with a detection limit of  $6.05 \times 10^{-9}$  mol/L showing good stability and reproducibility.

The full implementation of the e-tongue system will require a high-sensitivity EOC concentration in the environment with long-term stability, together with amenability of being incorporated into automatic systems and then in the field. In contrast to the inorganic compound e-tongue applications (e.g., heavy metals that will potentially be deployable in the near future), e-tongue systems designed to detect organic molecules in complex aqueous matrices will require further development, especially regarding selectivity and stability (Díaz-gonzález et al. 2016).

#### 4. Conclusions

Since 1989, there has been an ever greater number of scientific publications regarding the applications of e-tongue systems for environmental monitoring. E-tongue prototypes can have different types of measuring methods (e.g., potentiometric, voltammetric, amperometric, or impedance), and several applications have been developed and studied over the years, resulting in a deeper understanding of these devices.

The choice of e-tongue methods is highly dependent on the composition and complexity of the solution to be examined. In real-time monitoring of EOC contaminants, such as PPCP, e-tongue sensing technologies are still under development. To the best of the authors' knowledge, there are a few works concerning both environmental aqueous matrices and EOC. Nevertheless, the efforts to properly train these devices to characterize complex liquid samples and detect contaminants in aqueous media have increased the possibility of constructing a device that is sensitive enough to be comparable with conventional techniques. However, despite the high sensitivity, low-cost, easy operation, and rapid response that will enhance its commercial value, there remains a lack of selectivity as far as e-tongue data are concerned.

E-tongue technology will undoubtedly find important applications in environmental monitoring. With continuing strides being made in scientific research, the e-tongue approach employed without sample preconditioning and using a simple analysis can address the problem of EOC in aqueous matrices. The hybrid systems that reap the advantages of different sensing devices, or the e-tongue system working with the impedance spectroscopy response and nanofilms produced (i.e., with the layer-by-layer technique) may present possible solutions that are of interest for the further development of real-time sensors.

#### Acknowledgements

Financial support was provided by project “Development of Nanostructures for Detection of Triclosan Traces on Aquatic Environments” (PTDC/FIS-NAN/0909/2014). CENSE-Center for Environmental and Sustainability Research, which is financed by national funds from FCT/MEC (UID/AMB/04085/2013). This paper is part of a project that has received funding from the European Union's Horizon 2020 research and innovation programme under the Marie Skłodowska-Curie grant agreement No 778045. C. Magro acknowledges to Fundação para a Ciência e a Tecnologia for her PhD fellowship (SFRH/BD/114674/2016).

#### References

- Abegão, L., Ribeiro, J., Ribeiro, P., and Raposo, M. 2013. Nano-molar deltamethrin sensor based on electrical impedance of PAH/PAZO layer-by-layer sensing films. *Sensors*, 13(8): 10167–10176. doi:10.3390/s130810167. PMID:23966185.
- Albaladejo, C., Sánchez, P., Iborra, A., Soto, F., López, J.A., and Torres, R. 2010. Wireless sensor networks for oceanographic monitoring: a systematic review. *Sensors*, 10(7): 6948–6968. doi:10.3390/s100706948. PMID:22163583.
- Albareda-Sirvent, M., Merkoçi, A., and Alegret, S. 2001. Pesticide determination in tap water and juice samples using disposable amperometric biosensors made using thick-film technology. *Anal. Chim. Acta*, 442(1): 35–44. doi:10.1016/S0003-2670(01)01017-0.
- American National Standards Institute (ANSI). 1982. Electrical transducer nomenclature and terminology. Instrument Society of America, Research Triangle Park, N. C.



- Arvand, M., Gholizadeh, T.M., and Zanjanchi, M.A. 2012. MWCNTs/Cu (OH) 2 nanoparticles/IL nanocomposite modified glassy carbon electrode as a voltammetric sensor for determination of the non-steroidal anti-inflammatory drug diclofenac. *Mater. Sci. Eng. C*, **32**(6): 1682–1689. doi:10.1016/j.msec.2012.04.066.
- Askim, J.R., Mahmoudi, M., and Suslick, K.S. 2013. Optical sensor arrays for chemical sensing: the optoelectronic nose. *Chem. Soc. Rev.* **42**(22): 8649. doi:10.1039/c3cs60179j. PMID:24091381.
- Atar, N., Eren, T., Yola, M.L., and Wang, S. 2015. A sensitive molecular imprinted surface plasmon resonance nanosensor for selective determination of trace triclosan in wastewater. *Sens. Actuators, B*, **216**: 638–644. doi:10.1016/j.snb.2015.04.076.
- Banerjee, R., Tudu, B., Bandyopadhyay, R., and Bhattacharyya, N. 2016. A review on combined odor and taste sensor systems. *J. Food Eng.* **190**: 10–21. doi:10.1016/j.jfoodeng.2016.06.001.
- Bila, D.M., and Dezotti, M. 2003. Fármacos no meio ambiente. *Quim. Nova*, **26**(4): 523–530. doi:10.1590/S0100-40422003000400015.
- Bourgeois, W., Romain, A.C., Nicolas, J., and Stuetz, R.M. 2003. The use of sensor arrays for environmental monitoring: interests and limitations. *J. Environ. Monit.* **5**: 852–860. doi:10.1039/b307905h. PMID:14710922.
- Campos, I., Alcañiz, M., Aguado, D., Barat, R., Ferrer, J., Gil, L., et al. 2012. A voltammetric electronic tongue as tool for water quality monitoring in wastewater treatment plants. *Water Res.* **46**(8): 2605–2614. doi:10.1016/j.watres.2012.02.029. PMID:22424964.
- Campos, I., Pascual, L., Soto, J., Gil-Sánchez, L., and Martínez-Mañez, R. 2013. An electronic tongue designed to detect ammonium nitrate in aqueous solutions. *Sensors*, **13**(10): 14064–14078. doi:10.3390/s131014064. PMID:24145916.
- Campos, I., Sangrador, A., Bataller, R., Aguado, D., Barat, R., Soto, J., and Martínez-Mañez, R. 2014. Ammonium and phosphate quantification in wastewater by using a voltammetric electronic tongue. *Electroanalysis*, **26**(3): 588–595. doi:10.1002/elan.201300538.
- Capelli, L., Sironi, S., and Del Rosso, R. 2014. Electronic noses for environmental monitoring applications. *Sensors*, **14**(11): 19979–20007. doi:10.3390/s141119979. PMID:25347583.
- Carvalho, E.R., Consolin Filho, N., Venancio, E.C., Jr., O, O.N., Mattoso, L.H.C., and Martin-neto, L. 2007. Detection of brominated by-products using a sensor array based on nanostructured thin films of conducting polymers. *Sensors*, **7**(12): 3258–3271. doi:10.3390/s7123258. PMID:28903292.
- Cerdà, V., Ferrer, L., Avivar, J., and Cerdà, A. 2014. Evolution and description of the principal flow techniques. *In* *Flow Analysis*. pp. 1–42. doi:10.1016/B978-0-444-59596-6.00001-2.
- Cetó, X., Céspedes, F., and del Valle, M. 2013. Comparison of methods for the processing of voltammetric electronic tongues data. *Microchim. Acta*, **180**: 319–330. doi:10.1007/s00604-012-0938-7.
- Cetó, X., Voelcker, N.H., and Prieto-Simón, B. 2016. Bioelectronic tongues: new trends and applications in water and food analysis. *Biosens. Bioelectron.* **79**: 608–626. doi:10.1016/j.bios.2015.12.075. PMID:26761617.
- Cetó, X., Saint, C., Chow, C.W.K., Voelcker, N.H., and Prieto-Simón, B. 2017. Electrochemical fingerprints of brominated trihaloacetic acids (HAA3) mixtures in water. *Sens. Actuators, B*, **247**: 70–77. doi:10.1016/j.snb.2017.02.179.
- Ciosek, P., and Wróblewski, W. 2007. Sensor arrays for liquid sensing – electronic tongue systems. *Analyst*, **132**(10): 963–978. doi:10.1039/b705107g. PMID:17893798.
- Corcoran, E., Nellemann, C., Baker, E., Bos, R., Osborn, D., and Savelli, H. (eds). 2010. Sick water? The central role of wastewater management in sustainable development. A rapid response assessment. UNEP/Earthprint.
- Cortina, M., Gutiérrez, A., Alegreta, S., and del Valle, M. 2005. Sequential injection system with higher dimensional electrochemical sensor signals Part 2. Potentiometric e-tongue for the determination of alkaline ions. *Talanta*, **66**: 1197–1206. doi:10.1016/j.talanta.2005.01.023. PMID:18970109.
- Daughton, C.G. 2004. Non-regulated water contaminants: emerging research. *Environ. Impact Assess. Rev.* **24**: 711–732. doi:10.1016/j.eiar.2004.06.003.
- del Valle, M. 2010. Electronic tongues employing electrochemical sensors. *Electroanalysis*, **22**(14): 1539–1555. doi:10.1002/elan.201000013.
- Di Natale, C., Macagnano, A., Davide, F., D'Amico, A., Legin, A., Vlasov, Y., et al. 1997. Multicomponent analysis on polluted waters by means of an electronic tongue. *Sens. Actuators, B*, **44**(1–3): 423–428. doi:10.1016/S0925-4005(97)00169-X.
- Di Natale, C., Paolesse, R., Macagnano, A., Mantini, A., D'Amico, A., Legin, A., et al. 2000. Electronic nose and electronic tongue integration for improved classification of clinical and food samples. *Sens. Actuators, B*, **64**(1–3): 15–21. doi:10.1016/S0925-4005(99)00477-3.
- Díaz-González, M., Gutiérrez-capitán, M., Niu, P., Baldi, A., Jiménez-Jorquera, C., and Fernández-Sánchez, C. 2016. Electrochemical devices for the detection of priority pollutants listed in the EU water framework directive. *TrAC, Trends Anal. Chem.* **77**: 186–202. doi:10.1016/j.trac.2015.11.023.
- Dymerski, T.M., Chmiel, T.M., and Wardencki, W. 2011. An odor-sensing system-powerful technique for foodstuff studies. *Rev. Sci. Instrum.* **82**(11). doi:10.1063/1.3660805.
- Ellis, J.B. 2008. Assessing sources and impacts of priority PPCP compounds in urban receiving waters. 11th Int. Conf. Urban Drainage, Edinburgh, Scotland, U.K. pp. 1–10.
- Escuder-Gilbert, L., and Peris, M. 2010. Review: highlights in recent applications of electronic tongues in food analysis. *Anal. Chim. Acta*, **665**(1): 15–25. doi:10.1016/j.aca.2010.03.017. PMID:20381685.
- Facure, M.H.M., Mercante, L.A., Mattoso, L.H.C., and Correa, D.S. 2017. Detection of trace levels of organophosphate pesticides using an electronic tongue based on graphene hybrid nanocomposites. *Talanta*, **167**: 59–66. doi:10.1016/j.talanta.2017.02.005.
- Ferreira, M., Riul, A., Wohnrath, K., Fonseca, F.J., Oliveira, O.N., and Mattoso, L.H.C. 2003. High-performance taste sensor made from Langmuir-Blodgett films of conducting polymers and a ruthenium complex. *Anal. Chem.* **75**(4): 953–955. doi:10.1021/ac026031p. PMID:12622390.
- Filippini, D., Alimelli, A., Di Natale, C., Paolesse, R., D'Amico, A., and Lundström, I. 2006. Chemical sensing with familiar devices. *Angew. Chem., Int. Ed.* **45**: 3800–3803. doi:10.1002/anie.200600050. PMID:16671131.
- Fraden, J. 2010. Handbook of modern sensors: physics, designs, and applications, Fourth Edition. Edited by J. Fraden. Springer Science+Business Media, New York, N.Y., USA. doi:10.1007/978-1-4419-6466-3.
- Gałuszka, A., Migaszewski, Z.M., and Namieśnik, J. 2015. Moving your laboratories to the field – advantages and limitations of the use of field portable instruments in environmental sample analysis. *Environ. Res.* **140**: 593–603. doi:10.1016/j.envres.2015.05.017. PMID:26051907.
- Gao, R., Kong, X., Su, F., He, X., Chen, L., and Zhang, Y. 2010. Synthesis and evaluation of molecularly imprinted core-shell carbon nanotubes for the determination of triclosan in environmental water samples. *J. Chromatogr. A*, **1217**(52): 8095–8102. doi:10.1016/j.chroma.2010.10.121. PMID:21093867.
- Geissen, V., Mol, H., Klumpp, E., Umlauf, G., Nadal, M., van der Ploeg, M., et al. 2015. Emerging pollutants in the environment: a challenge for water resource management. *International Soil and Water Conservation Research*, **3**(1): 57–65. doi:10.1016/j.iswcr.2015.03.002.
- Gómez-Caravaca, A.M., Maggio, R.M., and Cerretani, L. 2016. Chemometric applications to assess quality and critical parameters of virgin and extra-virgin olive oil, a review. *Anal. Chim. Acta*, **913**: 1–21. doi:10.1016/j.aca.2016.01.025. PMID:26944986.
- González-Calabuig, A., Cetó, X., and Del Valle, M. 2018. A voltammetric electronic tongue for the resolution of ternary nitrophenol mixtures. *Sensors*, **18**(1): 1–11. doi:10.3390/s18010216.
- Gründler, P. 2007. Chemical sensors - an introduction for scientists and engineers. Springer Berlin Heidelberg, Germany. doi:10.1007/978-3-540-45743-5.
- Guanais Gonçalves, C., Dini, F., Martinelli, E., Catini, A., Lundström, I., Paolesse, R., et al. 2016. Detection of diverse potential threats in water with an array of optical sensors. *Sens. Actuators, B*, **236**: 997–1004. doi:10.1016/j.snb.2016.04.080.
- Gutiérrez, M., Gutiérrez, J.M., Alegret, S., Leija, L., Hernández, P.R., Muñoz, R., et al. 2008. New sensor system for environmental monitoring: the potentiometric electronic tongue. *In* *International Congress on Environmental Modelling and Software*, Barcelona, Spain. pp. 54–60.
- Haddi, Z., Bougrini, M., Tahri, K., Braham, Y., Souiri, M., El Bari, N., et al. 2014. A hybrid system based on an electronic nose coupled with an electronic tongue for the characterization of Moroccan waters. *Sens. Transducers J.* **27**: 190–197.
- Hayashi, K., Yamanaoka, M., Toko, K., and Yamafuji, K. 1990. Multichannel taste sensor using lipid membranes. *Sens. Actuators, B*, **2**(3): 205–213. doi:10.1016/0925-4005(90)85006-K.
- Hodgins, D. 1997. The electronic nose: sensor array-based instruments that emulate the human nose. *In* *Techniques for analyzing food aroma*. Edited by R. Marsili. Marcel Dekker, New York, USA.
- Holmin, S., Spångéus, P., Krantz-Rülcker, C., and Winquist, F. 2001. Compression of electronic tongue data based on voltammetry – a comparative study. *Sens. Actuators, B*, **76**: 455–464. doi:10.1016/S0925-4005(01)00585-8.
- Hulanicki, A., Glab, S., and Ingman, F. 1991. Chemical sensors: definitions and classification. *Pure Appl. Chem.* **63**(9): 1247–1250. doi:10.1351/pac199163091247.
- Ivarsson, P., Holmin, S., Höjer, N.E., Krantz-Rülcker, C., and Winquist, F. 2001. Discrimination of tea by means of a voltammetric electronic tongue and different applied waveforms. *Sens. Actuators, B*, **76**(1–3): 449–454. doi:10.1016/S0925-4005(01)00583-4.
- Justino, C.L.L., Freitas, A.C., Duarte, A.C., and Santos, T.A.P.R. 2015. Sensors and biosensors for monitoring marine contaminants. *Trends Environ. Anal. Chem.* **6–7**: 21–30. doi:10.1016/j.teac.2015.02.001.
- Kim, H., Konnanath, B., Sattigeri, P., Wang, J., Mulchandani, A., Myung, N., et al. 2012. Electronic-nose for detecting environmental pollutants: signal processing and analog front-end design. *Analog Integr. Circ. Sig. Process.* **70**(1): 15–32. doi:10.1007/s10470-011-9638-1.
- Kirsanov, D., Legin, E., Zagrebina, A., Ignatieva, N., Rybakina, V., and Legin, A. 2014. Mimicking *Daphnia magna* bioassay performance by an electronic tongue for urban water quality control. *Anal. Chim. Acta*, **824**: 64–70. doi:10.1016/j.aca.2014.03.021. PMID:24759749.
- Krantz-Rülcker, C., Stenberg, M., Winquist, F., and Lundström, I. 2001. Electronic tongues for environmental monitoring based on sensor arrays and pattern recognition: a review. *Anal. Chim. Acta*, **426**(2): 217–226. doi:10.1016/S0003-2670(00)00873-4.
- Legin, A.V., Selenev, B.L., Rudnitskaya, A.M., Vlasov, Y.G., Tverdokhlebov, S.V., Mack, B., et al. 1999. Multisensor system for determination of iron (II), iron (III), uranium (VI) and uranium (IV) in complex solutions. *Czech. J. Phys.* **49**: 679–685. doi:10.1007/s10582-999-1049-5.
- Li, M., Sun, Q., Li, Y., Lv, M., Lin, L., Wu, Y., et al. 2016. Simultaneous analysis of

- 45 pharmaceuticals and personal care products in sludge by matrix solid-phase dispersion and liquid chromatography tandem mass spectrometry. *Anal. Bioanal. Chem.* **408**(18): 4953–4964. doi:10.1007/s00216-016-9590-0. PMID:27137519.
- Liu, X., Feng, H., Liu, X., and Wong, D.K.Y. 2011. Electrocatalytic detection of phenolic estrogenic compounds at NiTPPS/carbon nanotube composite electrodes. *Anal. Chim. Acta.* **689**(2): 212–218. doi:10.1016/j.aca.2011.01.037. PMID:21397076.
- Lvova, L., Guanais Gonçalves, C., Petropoulos, K., Micheli, L., Volpe, G., Kirsanov, D., et al. 2016. Electronic tongue for microcystin screening in waters. *Biosens. Bioelectron.* **80**: 154–160. doi:10.1016/j.bios.2016.01.050. PMID:26827145.
- Marques, I., Magalhães-Mota, G., Pires, F., Sério, S., Ribeiro, P.A., and Raposo, M. 2017. Detection of traces of triclosan in water. *Appl. Surf. Sci.* **421**: 142–147. doi:10.1016/j.apsusc.2016.12.170.
- Matamoros, V., Arias, C., Brix, H., and Bayona, J.M. 2009. Preliminary screening of small-scale domestic wastewater treatment systems for removal of pharmaceutical and personal care products. *Water Res.* **43**(1): 55–62. doi:10.1016/j.watres.2008.10.005. PMID:18986673.
- Mesquita, R.B.R., and Rangel, A.O.S.S. 2009. A review on sequential injection methods for water analysis. *Anal. Chim. Acta.* **648**: 7–22. doi:10.1016/j.aca.2009.06.030. PMID:19616686.
- Mimendia, A., Gutiérrez, J.M., Leija, L., Hernández, P.R., Favari, L., Muñoz, R., et al. 2010. A review of the use of the potentiometric electronic tongue in the monitoring of environmental systems. *Environ. Model. Softw.* **25**(9): 1023–1030. doi:10.1016/j.envsoft.2009.12.003.
- Moreno, L., Merlos, A., Abramova, N., Jiménez, C., and Bratov, A. 2006. Multi-sensor array used as an “electronic tongue” for mineral water analysis. *Sens. Actuators, B.* **116**: 130–134. doi:10.1016/j.snb.2005.12.063.
- National Academy Press. 1995. Expanding the vision of sensor materials. Washington, D.C. doi:10.17226/4782.
- National Research Council (NRC). 1995. Chemical sensors. In *Expanding the vision of sensor materials*. National Academies Press, Washington, D.C. pp. 73–88. doi:10.17226/4782.
- Núñez, L., Cetó, X., Pividori, M.I., Zaroni, M.V.B., and del Valle, M. 2013. Development and application of an electronic tongue for detection and monitoring of nitrate, nitrite and ammonium levels in waters. *Microchem. J.* **110**: 273–279. doi:10.1016/j.microc.2013.04.018.
- Olivati, C.A., Riul, A., Balogh, D.T., Oliveira, O.N., Jr., and Ferreira, M. 2009. Detection of phenolic compounds using impedance spectroscopy measurements. *Bioprocess Biosyst. Eng.* **32**(1): 41–46. doi:10.1007/s00449-008-0218-4. PMID:18408956.
- Oliveira, O.N., Jr., Iost, R.M., Siqueira, J.R., Jr., Crespilho, F.N., and Caseli, L. 2014. Nanomaterials for diagnosis: challenges and applications in smart devices based on molecular recognition. *ACS Appl. Mater. Interfaces*, **6**(17): 14745–14766. doi:10.1021/am5015056. PMID:24968359.
- Pal, A., He, Y., Jekel, M., Reinhard, M., and Gin, K.Y.H. 2014. Emerging contaminants of public health significance as water quality indicator compounds in the urban water cycle. *Environ. Int.* **71**: 46–62. doi:10.1016/j.envint.2014.05.025. PMID:24972248.
- Palit, M., Tudu, B., Bhattacharyya, N., Dutta, A., Dutta, P.K., Jana, A., et al. 2010. Comparison of multivariate preprocessing techniques as applied to electronic tongue based pattern classification for black tea. *Anal. Chim. Acta.* **675**(1): 8–15. doi:10.1016/j.aca.2010.06.036. PMID:20708109.
- Panasjuk, O., Hedström, A., Marsalek, J., Ashley, R.M., and Viklander, M. 2015. Contamination of stormwater by wastewater: A review of detection methods. *Journal of Environmental Management*, **152**: 241–250. doi:10.1016/j.jenvman.2015.01.050. PMID:25662485.
- Peris, M., and Escuder-Gilabert, L. 2016. Electronic noses and tongues to assess food authenticity and adulteration. *Trends Food Sci. Technol.* **58**: 40–54. doi:10.1016/j.tifs.2016.10.014.
- Pimentel, R. 2014. Desenvolvimento de um Sensor de Ibuprofeno em meio aquoso. Master thesis, Faculdade de Ciências e Tecnologia da Universidade Nova de Lisboa.
- Rakow, N.A., and Suslick, K.S. 2000. A colorimetric sensor array for odour visualization. *Nature*, **406**: 710–713. doi:10.1038/35021028. PMID:10963592.
- Raposo, M., Ribeiro, P.A., El Bari, N., and Bouchikhi, B. 2016. Sensing of component traces in complex systems. In *Electrokinetics across disciplines and continents*. Edited by B.A. Ribeiro, P.E. Mateus, and N. Couto. Springer International Publishing, Cham. pp. 401–426. doi:10.1007/978-3-319-20179-5\_20.
- Richards, E., Bessant, C., and Saini, S. 2002. Multivariate data analysis in electroanalytical chemistry. *Electroanalysis*, **14**(22): 1533–1542. doi:10.1002/1521-4109(200211)14:22<1533::AID-ELAN1533>3.0.CO;2-T.
- Richards, E., Bessant, C., and Saini, S. 2003. A liquid handling system for the automated acquisition of data for training, validating and testing calibration models. *Sens. Actuators, B.* **88**: 149–154.
- Riul, A., dos Santos, D.S., Wohnrath, K., Di Tommazo, R., Carvalho, A.C.P.L.F., Fonseca, F.J., et al. 2002. Artificial taste sensor: efficient combination of sensors made from Langmuir-Blodgett films of conducting polymers and a ruthenium complex and self-assembled films of an azobenzene-containing polymer. *Langmuir*, **18**(1): 239–245. doi:10.1021/la011017d.
- Rodríguez Méndez, M.L., De Saja, J.A., Medina-Plaza, C., and García-Hernández, C. 2016. Electronic tongues for the organoleptic characterization of wines. In *Electronic noses and tongues in food science*. Edited by M.L. Rodríguez Méndez. Academic Press, San Diego. pp. 265–273. doi:10.1016/B978-0-12-800243-8.00026-3.
- Ronan, J.M., and Mchugh, B. 2013. A sensitive liquid chromatography/tandem mass spectrometry method for the determination of natural and synthetic steroid estrogens in seawater and marine biota, with a focus on proposed Water Framework Directive Environmental Quality Standards. *Rapid Commun. Mass. Spectrom.* **27**(7): 738–746. doi:10.1002/rcm.6505. PMID:23495020.
- Scott, S.M., James, D., and Ali, Z. 2007. Review data analysis for electronic nose systems. *Microchim. Acta.* **207**: 183–207. doi:10.1007/s00604-006-0623-9.
- Shehata, M.A., Fawaz, E.M., El-Rahman, M.K.A., and Abdel-Moety, E.M. 2017. Double-track electrochemical green approach for simultaneous dissolution profiling of naproxen sodium and diphenhydramine hydrochloride. *J. Pharm. Biomed. Anal.* **146**: 179–187. doi:10.1016/j.jpba.2017.08.041. PMID:28881315.
- Siliwiniska, M., Wiśniewska, P., Dymerski, T., Namieśnik, J., and Wardencki, W. 2014. Food analysis using artificial senses. *J. Agric. Food Chem.* **62**: 1423–1448. doi:10.1021/jf403215y. PMID:24506450.
- Smith, D.V., and Margolskee, R.F. 2001. Making sense of taste. *Sci. Am. March* **284**(March): 32–39. doi:10.1038/scientificamerican0301-32.
- Son, M., and Park, T.H. 2018. The bioelectronic nose and tongue using olfactory and taste receptors: analytical tools for food quality and safety assessment. *Biotechnol. Adv.* **36**(2): 371–379. doi:10.1016/j.biotechadv.2017.12.017. PMID:29289691.
- Stroble, J.K., Stone, R.B., and Watkins, S.E. 2009. An overview of biomimetic sensor technology. *Sens. Rev.* **22**(2): 112–119. doi:10.1108/02602280910936219.
- Stuart, M., and Lapworth, D. 2013. Emerging organic contaminants in groundwater – smart sensors for real-time water quality monitoring. Edited by S.C. Mukhopadhyay and A. Mason. Springer Berlin Heidelberg, Berlin, Heidelberg. pp. 259–284. doi:10.1007/978-3-642-37006-9\_12.
- Stülten, D., Zühlke, S., Lamshöft, M., and Spittler, M. 2008. Occurrence of diclofenac and selected metabolites in sewage effluents. *Sci. Total Environ.* **405**: 310–316. doi:10.1016/j.scitotenv.2008.05.036. PMID:18640705.
- Sun, H., Mo, Z.H., Choy, J.T.S., Zhu, D.R., and Fung, Y.S. 2008. Piezoelectric quartz crystal sensor for sensing taste-causing compounds in food. *Sens. Actuators, B.* **131**: 148–158. doi:10.1016/j.snb.2007.12.014.
- Tahara, Y., and Toko, K. 2013. Electronic tongues-a review. *IEEE Sens. J.* **13**(8): 3001–3011. doi:10.1109/JSEN.2013.2263125.
- Tahri, K., Duarte, A.A., Carvalho, G., Ribeiro, P.A., da Silva, M.G., Mendes, D., et al. 2018. Distinguishment, identification and aroma compound quantification of Portuguese olive oils based on physicochemical attributes, HS-GC/MS analysis and voltammetric electronic tongue. *J. Sci. Food Agric.* **98**(2): 681–690. doi:10.1002/jsfa.8515. PMID:28671261.
- Taylor, D.M., and Macdonald, A.G. 1987. AC admittance of the metal/insulator/electrolyte interface. *J. Phys. D. Appl. Phys.* **20**(10): 1277. doi:10.1088/0022-3727/20/10/010.
- Tobiszewski, M., Mechlin, A., and Namiesnik, J. 2010. Green analytical chemistry — theory and practice. *Chem. Soc. Rev.* **8**: 2869–2878. doi:10.1039/b926439f.
- Vidal-Dorsch, D.E., Bay, S.M., Maruya, K., Snyder, S.A., Trenholm, R.A., and Vanderford, B.J. 2012. Contaminants of emerging concern in municipal wastewater effluents and marine receiving water. *Environ. Toxicol. Chem.* **31**(12): 2674–2682. doi:10.1002/etc.2004. PMID:22987561.
- Vlasov, Y., Legin, A., Rudnitskaya, A., Di Natale, C., and D’Amico, A. 2005. Non-specific sensor arrays (“electronic tongue”) for chemical analysis of liquids (IUPAC Technical Report). *Pure Appl. Chem.* **77**(11): 1965–1983. doi:10.1351/pac20057711965.
- Wan, Q., Yang, P., Cai, H., Song, H., and Yang, N. 2013. Voltammetry of nanomolar leveled environmental hazards on the polymer/CNT coated electrodes. *J. Electroanal. Chem.* **689**: 252–256. doi:10.1016/j.jelechem.2012.11.003.
- Wang, H., Ohnuki, H., Endo, H., and Izumi, M. 2015. Impedimetric and amperometric bifunctional glucose biosensor based on hybrid organic-inorganic thin films. *Bioelectrochemistry*, **101**: 1–7. doi:10.1016/j.bioelechem.2014.06.007.
- Wei, Z., and Wang, J. 2011. Detection of antibiotic residues in bovine milk by a voltammetric electronic tongue system. *Anal. Chim. Acta.* **694**(1–2): 46–56. doi:10.1016/j.aca.2011.02.053. PMID:21565301.
- Wei, Z., Yang, Y., Wang, J., Zhang, W., and Ren, Q. 2017. The measurement principles, working parameters and configurations of voltammetric electronic tongues and its applications for foodstuff analysis. *J. Food Eng.* doi:10.1016/j.jfoodeng.2017.08.005.
- Wesoły, M., Cetó, X., del Valle, M., Ciosek, P., and Wróblewski, W. 2016. Quantitative analysis of active pharmaceutical ingredients (APIs) using a potentiometric electronic tongue in a SIA flow system. *Electroanalysis*, **28**(3): 626–632. doi:10.1002/elan.201500407.
- Wilson, A.D., and Baietto, M. 2009. Applications and advances in electronic-nose technologies. *Sensors*, **9**(7): 5099–5148. doi:10.3390/s9075099. PMID:22346690.
- Winqvist, F. 2008. Voltammetric electronic tongues – basic principles and applications. *Microchim. Acta.* **163**(1–2): 3–10. doi:10.1007/s00604-007-0929-2.
- Woertz, K., Tissen, C., Kleinebudde, P., and Breikreutz, J. 2011. A comparative study on two electronic tongues for pharmaceutical formulation development. *J. Pharm. Biomed. Anal.* **55**(2): 272–281. doi:10.1016/j.jpba.2011.02.002. PMID:21353433.
- Zhang, D., Gersberg, R.M., Ng, W.J., and Tan, S.K. 2014. Removal of pharmaceu-

- tics and personal care products in aquatic plant-based systems: a review. *Environ. Pollut.* **184**: 620–639. doi:10.1016/j.envpol.2013.09.009. PMID:24080393.
- Zhao, X., Ding, J., Bai, W., Wang, Y., Yan, Y., Cheng, Y., and Zhang, J. 2018. PEDOT:PSS/AuNPs/CA modified screen-printed carbon based disposable electrochemical sensor for sensitive and selective determination of carmine. *J. Electroanal. Chem.* **824**: 14–21. doi:10.1016/j.jelechem.2018.07.030.
- Zheng, Q., Yang, P., Xu, H., Liu, J., and Jin, L. 2012. A simple and sensitive method for the determination of 4-n-octylphenol based on multi-walled carbon nanotubes modified glassy carbon electrode. *J. Environ. Sci.* **24**(9): 1717–1722. doi:10.1016/S1001-0742(11)60970-4.
- Zhuykov, S. 2012. Solid-state sensors monitoring parameters of water quality for the next generation of wireless sensor networks. *Sens. Actuators, B*, **161**(1): 1–20. doi:10.1016/j.snb.2011.10.078.
- Zou, Y., Wan, H., Zhang, X., Ha, D., and Wang, P. 2015. Electronic nose and electronic tongue. *In* *Bioinspired smell and taste sensors*. Edited by K.J. Wang, P. Liu, Q. Wu, and C. Hsia. Springer Netherlands. pp. 19–44. doi:10.1007/978-94-017-7333-1\_2.



## Paper

*“Polyelectrolyte based sensors as key to achieve quantitative electronic tongues: Detection of triclosan on aqueous environmental matrices”*

*C Magro, PM Zagalo, J Pereira-da-Silva, EP Mateus, AB Ribeiro, PA Ribeiro & M Raposo*

*Submitted, 2019*



# Polyelectrolyte based sensors as key to achieve quantitative electronic tongues: Detection of triclosan on aqueous environmental matrices

C. Magro<sup>a\*</sup>, P. Zagalo<sup>b</sup>, J. Pereira-da-Silva<sup>b</sup>, E.P. Mateus<sup>a</sup>, A.B. Ribeiro<sup>a</sup>, P. Ribeiro<sup>b</sup> and M. Raposo<sup>b\*</sup>

<sup>a</sup>CENSE, Departamento de Ciências e Engenharia do Ambiente, Faculdade de Ciências e Tecnologia, Universidade Nova de Lisboa, Caparica 2829-516, Portugal

<sup>b</sup>CEFITEC, Departamento de Física, Faculdade de Ciências e Tecnologia, Universidade Nova de Lisboa, Caparica 2829-516, Portugal

\*Corresponding authors: c.magro@campus.fct.unl.pt, mfr@fct.unl.pt

Submitted, 2019

**Keywords:** environmental monitoring; triclosan; layer-by-layer technique; interdigitated sensors; electronic tongue; impedance spectroscopy

**Abstract:**

Triclosan (TCS) is a bacteriostatic used in household items that has been raising health concerns, due to the promotion of antimicrobial resistance and endocrine disruption effects both to humans and biota, demanding therefore new devices for its continuous supervising in complex matrices. This work explores the potential of the electronic tongue concept to be used as an environmental monitoring tool. The sensor was based on polyelectrolyte layer-by-layer (LbL) films prepared onto gold interdigitated electrodes (IDE) and, the use of electrical impedance spectroscopy as a means of transduction, together with Principal Component Analysis (PCA). An electronic tongue, composed by sensors arrays with (polyethyleneimine (PEI)/ polysodium 4-styrenesulfonate (PSS))<sub>5</sub> and (poly(allylamine hydrochloride/graphene oxide))<sub>5</sub> LbL films together with gold IDE without coating were used to detect TCS concentrations from 10<sup>-15</sup> to 10<sup>-5</sup> M, in deionized water, mineral water and waste water. Results show the electronic tongue's ability to: 1) distinguish between TCS doped and non-doped solutions; 2) sort out the TCS range of concentrations. Regarding film stability, strong polyelectrolytes, as (PEI/PSS)<sub>n</sub>, presented more firmness as no significant desorption was observed when immersed in waste water, making them reliable sensor devices. Finally, the data of gold IDE sensors and (PEI/PSS)<sub>5</sub>, for the mineral water and waste water matrices, respectively, show the ability to distinguish the two matrices. A sensitivity value of 0.19±0.02 per decade to TCS concentration and a resolution of 0.13 pM were found from PCA second principal component, showing that the choice of stable sensing layers is the key to develop quantitative electronic tongues.

## Highlights:

- An e-tongue based on polyelectrolyte sensors to detect triclosan was developed;
- Traces of triclosan on waste water were monitored;
- Stable thin-films sensing layers are the key to develop quantitative e-tongues;
- PCA was used determine the sensitivity and resolution of the e-tongue;
- E-tongue achieved a resolution of 0.13 pM.

## Abbreviations:

DW, deionized water; E-tongue, electronic tongue; EF, waste water; GO, graphene oxide; IC, Ion Chromatography; ICP, Inductively Coupled Plasma with Optical Emission; IE, interdigitated electrodes; LbL, layer-by-layer; MW, mineral water; PAH, poly(allylamine hydrochloride); PCA, Principal Component Analysis; PEI, polyethyleneimine; PSS, poly(sodium 4-styrenesulfonate); TCS, triclosan.

# 1 INTRODUCTION

Triclosan (5-chloro-2-(2,4-dichlorophenoxy) phenol) (TCS) is widely used as an antimicrobial, antibacterial and preservative agent in different personal care and consumer products [1]. TCS main physical and chemical characteristics are presented in Table 1. Structurally, TCS molecule has functional groups for both phenol (5-chloro-2-(2,4-dichlorophenoxy) phenol) and ether (2,4,4-trichloro-2-hydroxydiphenyl ether) and its lipophilicity ( $\log K_{ow} = 4.8$ ) results in a potential for bioaccumulation. Several studies had proved its allergy risk, antimicrobial resistance, developmental toxicity, and endocrine disruption, both in humans and biota [2-8]. Due to its characteristics and inefficient removal in the waste water treatment plants, TCS and its bioactive metabolites and/or by-products, have been detected in waste waters and superficial waters, at  $10^{-8}$  M to  $10^{-12}$  M concentrations range ( $2 \text{ ng L}^{-1}$  -  $40 \text{ } \mu\text{g L}^{-1}$ ; Table A supplementary material) [9-11]. Consequently, TCS is continually being introduced in the aquatic environment via a number of routes, primarily by both untreated and treated waste water [12].

Hence, nowadays, the monitoring of TCS is a matter of concern and an important hot topic. Traditional analytical methods for TCS determination use gas or liquid chromatography and mass spectrometry [13-18]. However, chromatographic and mass spectrometric methods in spite of their high reliability are rather complex, time consuming and expensive [19]. Subsequently, there is a need for rapid, low-cost, and sensitive tools for real time monitoring of TCS in environmental matrices [20-23]. Due to their specificities, such as fast response times, and user-friendly operation the electronic tongue (e-tongue) systems present a great potential to compete, complement or replace traditional analytical techniques [24], used for environmental monitoring. Conceptually, an e-tongue is "a multi-sensory system, formed by an array of low-selective sensors, combined with advanced mathematical procedures for signal processing, based on pattern recognition and/or multivariate data analysis" [25]. TCS is one of the most studied pollutant in sensors development, as examples: a strand of carbon fibers has been designed and characterized for use in a voltammetric detector for high-performance liquid chromatography to detect triclosan in rabbit serum and urine [26]; an electropolymerizing o-phenylenediamine (o-PD) on a glassy carbon electrode was used to create an amperometric sensor over a linear range of  $2.0 \times 10^{-7}$  to  $3.0 \times 10^{-6}$  mol/L and a detection limit of  $8.0 \times 10^{-8}$  mol/L [21]; a multiwall carbon nanotube film was

developed for the rapid detection of TCS as electrochemical sensor with a linear range from  $50 \text{ } \mu\text{g L}^{-1}$  to  $1.75 \text{ mg L}^{-1}$ , and the limit of detection of  $16.5 \text{ } \mu\text{g L}^{-1}$  (about 57 nM) [27]. Accordingly, recent studies [28-32] have reported well succeeded applications with sensors composed of layer-by-layer (LbL) thin-films, that were produced with polyelectrolytes and used to detect organic compounds (in ultra-pure water matrices) using impedance measurements.

An impedance system, in a simpler conceptual implementation, is the full scan of different alternated current frequencies or a selected number of discrete frequency values, that can be used (conductivity or capacitance) [33]. The impedance technique approach is based on the electrode perturbation caused by an external signal of small magnitude [34]. Measurements can be performed in equilibrium or stationary. The characterization of aqueous environmental matrices is performed by analyzing the electrical impedance components (reactance, resistance, capacitance and loss tangent) as a function of frequency signals applied to nanostructures adsorbed onto solid substrates with interdigitated electrodes [31]. It has been reported that TCS adsorbed amount per unit of area on thin-films is reduced if the outer layers have negative charged polyelectrolyte [35]. The stability of the sensorial layers produced by the LbL technique is dependent of the solution's pH and the degree of ionization of the uppermost polyelectrolyte layer. Consequently, the TCS pKa (see Table 1) will play an essential role in its adsorption or non-absorption onto the used thin-films. The aim of the present study was to explore the potential of the e-tongue concept using impedantometric detection of TCS in environmental complex aqueous matrices. A deionized water, a Portuguese mineral water and a waste water effluent from a waste water treatment plant (considered the primary source of TCS into water bodies) were used as experimental matrices. TCS was spiked to the aqueous matrices and these "measured" using thin-films sensors based on polyethyleneimine (PEI), poly(sodium 4-styrenesulfonate) (PSS), poly(allylamine hydrochloride) (PAH) and graphene oxide (GO) (Figure 1), that have been prepared with the LbL technique onto solid supports with deposited gold electrodes.

To the best of our knowledge, regarding waste water real samples and these two combinations of thin-films sensors, this is the first study that explores: (1) an e-tongue based in a set of five sensor devices providing the possibility to distinguish different TCS concentrations; (2) the use of electrical impedance spectroscopy measurements for TCS detection in environmental aqueous matrices; (3) the stability of the thin-films layers, analysis of adsorption and desorp-



tion phenomena, submitted to different aqueous matrices and pH values.

## 2 MATERIALS AND METHODS

The experimental matrices were deionized water (DW), a Portuguese mineral water (MW) and a waste water (EF). DW was produced using a Millipore system (Bedford, MA, USA), MW was a commercial Portuguese mineral water and EF was the liquid fraction collected in the secondary clarifier at a waste water treatment plant (Lisbon, Portugal). Table 2 presents the characterization of the experimental matrices for conductivity, pH, and total ion concentration parameters. These features were measured because (1) pH of aqueous solutions can lead to desorption phenomena of thin-film layers, as well as, may change the TCS degree of ionization: from Table 2 one can observe that the studied matrices present pH values in the range of 6.1 - 8.4; and (2) ion species and respective concentration can interact with the outermost layer of the sensor's thin-films or with the gold in the gold IDE. All these measured parameters play a crucial role in the stability of the thin-film sensors and matrix-sensor interactions with the TCS molecule ( $pK_a$  7.9). pH was measured with a Radiometer pH-electrode EDGE (HANNA, USA). The conductivity values were measured in a Radiometer Analytic LAQUA twin (HORIBA Ltd., Japan). Ca, Cu, K, Mg, Na, P, S and Zn were determined by Inductively Coupled Plasma with Optical Emission Spectrometry (ICP-OES) (HORIBA Jobin-Yvon Ultima, Japan).  $Cl^-$  and  $SO_4^{2-}$  were analyzed by Ion Chromatography (IC) (DIONEX ICS-3000, USA), equipped with a conductivity detector. Triclosan (TCS  $\geq 97\%$ ) and methanol (MeOH; gradient grade) used were from Sigma-Aldrich (Steinheim, Germany). Experimental TCS dilutions range,  $10^{-5}$  to  $10^{-15}$  M were made sequentially from a mother solution with a concentration of  $10^{-4}$  M and analyzed immediately after preparation. All dilutions were prepared using experimental matrices/MeOH (9:1) solutions. A solution of each experimental matrix/MeOH, without TCS, was used as the blank standard (0 M).

The sensor devices used in this work were purchased from DropSens (Llanera Asturias, Spain) and are constituted by glass BK7 solid support with deposited gold interdigitate electrodes (IDE) comprising 250 "fingers" each. The supports' dimensions were 22.8 x 7.6 x 0.7 mm and each "finger" has 5  $\mu$ m of width which is the same spacing between the "fingers". An array of sensor devices without and with different polyelectrolyte thin films deposited

onto IDE surface were used to detect the TCS in aqueous solutions. The deposited thin films were prepared with polyethyleneimine (PEI), poly(sodium 4-styrenesulfonate) (PSS), poly(allylamine hydrochloride) (PAH) and graphene oxide (GO) polyelectrolytes, all from Sigma-Aldrich (St Louis, MO, USA), by the LbL technique [36]. Accordingly, thin films of PAH/GO and of PEI/PSS deposited on BK7 solid support with gold IDE were obtained by adsorbing alternate layers of electrically charged polyelectrolytes at solid/liquid interface, washing away with water the already adsorbed layers after being immersed in the polyelectrolyte solution in order to remove any polyelectrolyte molecules that were not completely adsorbed. The polyelectrolytes were made with a monomeric concentration of  $10^{-2}$  M diluted in water Type I, produced with a Millipore system (Bedford, MA, USA). The adsorption time period of each layer (i.e. immersion time in each polyelectrolyte solution), was 30 seconds and, after the adsorption of each layer, the thin-film was dried using nitrogen gas. Films of PAH/GO were prepared with 5 bilayers, (PAH/GO)<sub>5</sub>, while films of PEI/PSS were prepared with 5, 10 and 20 bilayers, designated by (PEI/PSS)<sub>5</sub>, (PEI/PSS)<sub>10</sub> and (PEI/PSS)<sub>20</sub>, respectively. Table 3 lists the thin-films used to characterize the aqueous solutions matrices under study.

The electrical analysis of aqueous matrices was performed by measuring the impedance spectra of these sensor devices when immersed in the aqueous matrices with different TCS concentrations with a Solartron 1260 Impedance Analyzer in the frequency range of 1 Hz to 1 MHz, applying an AC voltage of 25 mV. To avoid contamination of the sensor devices, the impedance spectra of thin-films sensors and gold IDE were recorded for the TCS experimental matrices in a sequence of increasing concentrations from 0 to  $10^{-5}$  M. All measurements were performed at room temperature 25°C. The stability of thin-films on the different experimental matrices was also studied by measuring the ultraviolet-visible spectra of the LbL thin-films before and after being immersed in the experimental matrices/MeOH solutions spiked with  $10^{-9}$  M of TCS. The absorbance spectra were attained using a double beam spectrophotometer UV-2101PC (Shimadzu) with a sampling interval between 800 nm to 200 nm, with a resolution of 0.5 nm. For each thin-film combination, three absorbance spectra were obtained: (1) before being immersed in the TCS solution ( $t = 0$  min) to establish a baseline; (2) after five minutes of immersion ( $t = 5$  min); (3) after a cumulative immersion time of ten minutes ( $t = 10$  min). Characterization of LbL thin-films stability, in EF at pH values of 3, 6, and 8, were also performed.

Principal component analysis (PCA) was carried out, regarding the normalized (Z normalization) impedance spectroscopy data, to reduce the size of data and to obtain a new space of orthogonal components, in which different concentration patterns can be observed and explained. Additionally, an array of sensors, composed by all the thin-films and gold IDE sensors, was analyzed as an e-tongue for TCS detection in EF experimental matrix. The ANOVA t-test was performed at 95% of confidence ( $p < 0.05$ ), concerning the Table 2 data, to prove that they are statistically different.

### 3 RESULTS AND DISCUSSION

#### 3.1 Impedance spectroscopy measurements: Sensor response

To evaluate the prepared sensors' ability to detect TCS in DW, MW and EF, impedance spectra, of sensor devices without and with thin-films adsorbed on the IDE surface were measured. Figure 2 shows the imaginary impedance spectra, also designated as electrical reactance, measured by the different sensor devices when immersed in the different aqueous matrices doped with TCS concentrations from 0 to  $10^{-5}$  M. The data points are related to the average of three impedimetric measurements (reproducibility in supplementary material Figure B for the lowest TCS concentration).

Different footprints were observed according to the experimental aqueous matrices and sensor devices. Similar behaviour is observed for DW for all sensors. The gold IDE sensor presents a similar footprint for the MW and EF matrices. The (PAH/GO)<sub>5</sub> sensor shows a similar behaviour, but different from the gold IDE, for the same matrices. The (PEI/PSS)<sub>5</sub> sensor shows different behaviour for MW and EF matrices, however similar to the gold IDE and (PAH/GO)<sub>5</sub> sensor, for MW and EF matrices, respectively. Sensor physical properties (PP), such as reactance, loss tangent and resistance at constant frequency, may present increasing or decreasing monotone functions as a function of TCS concentration. In order to allow operational TCS measurements (sensor sensitivity), a trend function of its concentration must be found, for example at a given frequency, expressed as normalized reactance, loss tangent or resistance spectra. A normalized response can be achieved using the following relation:

$$\frac{PP(C) - PP(M)}{(PP(0M))} \quad (1)$$

where  $PP(C)$  is the physical property measured at a given concentration, and  $PP(0M)$  is the physical property measured at a reference solution for the different type of matrices (TCS 0M in DW, MW or EF). Plots I, II and III of Figure 3 present examples of the normalized PP spectra to fixed frequencies, for the different films and type of environmental aqueous matrices.

The accomplished detailed analysis of obtained spectra in TCS solutions prepared with all the experimental matrices, Figure 2, shown that, the imaginary impedance or reactance can be used as a transducing variable. Regarding DW matrix (Figure 2 I a, b, c), the gold IDE sensor does not show a clear trend, compared to the thin-films sensors that present a more pronounced sensitivity to discriminate different concentrations in the frequency ranges of 1 to 10 kHz, and of 100 to 1000 kHz. Thus, in order to better analyze the response of these sensors, the reactance values measured in the gold IDE, (PAH/GO)<sub>5</sub> and (PEI/PSS)<sub>5</sub> sensors, at frequencies of 6.3, 25119 and 25119 Hz, respectively, were normalized and plotted as a function of TCS concentrations in Figure 3 I. This figure reveals that the reactance at these frequencies tends to increase or decrease, depending on the type of sensor for the TCS concentration ranges under study. The gold IDE sensor appears to be insensitive (no visible trend) to TCS presence in the studied concentrations, while (PEI/PSS)<sub>5</sub> sensor displays only significant sensitivity in the  $10^{-5}$  to  $10^{-7}$  M concentration range. Regarding DW matrix, the (PAH/GO)<sub>5</sub> sensor (Figure 3 I) presents almost constant values of reactance at 25119 Hz, was concerning data discrimination (discussed in section 3.2), the most "efficient" sensor.

Concerning the TCS detection in MW solutions, the reactance spectra, represented in Figures 2 II a and c, revealed analogous behavior for both gold IDE and (PEI/PSS)<sub>5</sub> sensors. In the present case (Figure 3 II), the loss tangent at fixed frequencies, was used as the transducing variable. The frequency values chosen were 63, 100, and 16 kHz, respectively, for the gold IDE, (PEI/PSS)<sub>5</sub> and (PAH/GO)<sub>5</sub> sensors. It should be remarked that all sensors tend to follow a decrease in loss tangent with decreasing TCS concentrations.

Overall, for the EF, the (PEI/PSS)<sub>5</sub> sensor show to be the most sensitive in the studied TCS concentration range. At frequencies between 1 and 10 kHz, the reactance spectra present a good response discrimination (Figure 2, III(c)). The normalized responses at 4 kHz as exhibited in Figure 3 III, clearly shows an electrical resistance trend with increasing TCS concentrations. It is important to remark, concerning the sensitivity of the sensor, that TCS is being detected/measured in a range of concentrations in accordance with real

samples. For instance, the results showed that for the EF matrix, as the TCS concentrations increase, the measured electrical resistance also increases in the range of  $10^{-8}$  to  $10^{-12}$  M, in accordance with the reported for waste water samples [9–11], supporting its potential field applicability. Should also be referred that EF matrix has a high amount of anions, Table 2, which directly contribute to the increase of electrical charge that can flow between electrodes, EF conductivity takes a value of  $1400 \mu\text{S}/\text{cm}$  [2]. Concerning the gold IDE sensors, the electrical response was operationally difficult to obtain, due to the high conductivity of the medium, and only lower measurable values of resistance were obtained, as can be observed in Figure 3 III. The EF matrix is composed by a high concentration of ions, such as Zn and S (Table 2), that interact with the gold electrodes, thus promoting an overload of electrical resistance and contributing to sensor damage during the electrical measurements (optical microscopy images, in supplementary material Figure D).

### 3.2 Principal Component Analysis: Sensor capabilities

In this section three questions will be addressed: (1) *Are the tested sensors able to detect concentrations of TCS equal and higher than zero?*; (2) *Are the tested sensors able of distinguish different TCS concentrations?*; (3) *Do the tested sensors produce PCA plots with observable patterns and trends according to TCS concentrations?* To look for sensor “discrimination” from different concentrations of TCS, on different matrices, the principal component analysis (PCA), a multivariate analysis technique, was performed after data normalization (Z type). The PCA was used to explore the sensors sensory attributes to produce different patterns for the range of TCS concentrations. The PCA was applied for the most sensitive sensor, regarding impedance normalized data (average of 3 loops impedance measurements). The PCA with the best score plots obtained for the sensors when immersed in DW, EF and MW matrices, respectively, are presented in Figure 4 I, II, III. The characterization associated to the best sensor is the one where the variations in the plot among TCS concentrations are more significant [37]. The first component F1, explains the greatest data variation and is considered the most important, explaining more than 79.69% of the variance. With the exception of the measurements on DW (Figure 4, I), PCA plots produced clearly distinguish the sample matrices without TCS from the samples with TCS (Figure 4, II and III).

Regarding the DW experimental matrices (Figure

4 I), although the PCA plot distinguishes the different concentrations, one can observe that a trend of TCS concentration per principal components according to concentrations was not achieved. In the case of the (PAH/GO)<sub>5</sub> sensor, the non-doped solution is in the same quadrant of the higher TCS concentration. A concentration pattern and trend, related to TCS concentrations, is visible for the data plot obtained by the gold IDE sensor (Figure 4, II), where eigenvectors points tend to increase over the range of concentrations. The first two principal components, F1 and F2, explain 98.63% of the total variance. Even more, this distinction is better when compared to the one obtained by the thin-films sensors. For the EF matrix, the best discrimination among concentrations was achieved by the (PEI/PSS)<sub>5</sub> sensor (Figure 4 III). It can be observed that TCS concentrations produce a clear trend between  $10^{-5}$  and  $10^{-13}$  M. The first two principal components F1 and F2 account 99.65% of the total variance. This sensor is capable of detection and semi quantification, having a clear trend and pattern within the PCA plot. Considering MW and EF experimental matrices, there is an evident pattern, where the concentration of the non-doped solutions (TCS = 0) may be regarded as an outlier point, being the nearest concentration, in both cases  $10^{-15}$  M. Additionally, for EF the effect of the number of bilayers was tested for the most sensitive sensor obtained, (PEI/PSS)<sub>5</sub>. The PCA plots, showed that 5 bilayers revealed better response (PCA separation to TCS concentrations) and signal intensity for impedance, when compared to the ones with 10 or 20 bi-layers of (PEI/PSS)<sub>5</sub> (PCA plots in supplementary material Figures E and F). This could be due to the thickness increase with the number of bilayers which leads to the increase of the distance between the gold electrode and the outer layer of film that interacted with the TCS molecules. As the film thickness increases, the capacitance decreases, reducing the electrical signals intensity measured in TCS solutions with different concentrations, i.e, for two distinct concentrations the difference of any measured electric property is smaller. The decrease in double-layer capacitance is associated with a higher resistance imposed to electron spillover, where this phenomenon reduces the metal capacitance according to jellium model[38].

The combination of sensor arrays is expected to improve the capability of TCS concentration discrimination. The array of sensors composed by the sensor devices without any film deposited (gold IDE) and with (PAH/GO)<sub>5</sub>, (PEI/PSS)<sub>5</sub>, (PEI/PSS)<sub>10</sub> and (PEI/PSS)<sub>20</sub> thin-films deposited, was used to test the e-tongue concept and to analyses its ability to produce discrimination among TCS concentrations in the EF

matrix. The respective PCA plot, Figure 5, clearly distinguish the sample matrices without TCS from the samples with TCS. A concentration pattern and trend, related to TCS concentrations, can be seen on the PCA plot along the main axis. The first two principal components F1 and F2 accounts for 81.71% of the total variance. As it was observed in Figure 4 II and III, the data followed the same direction, from region A (TCS) = 0 to region B where (TCS) > 0, proving that the electronic based in those sensor devices is able to distinguish between non-doped waste water and doped TCS waste water, producing an observable pattern and trend regarding the different concentration values.

### 3.3 Sensorial layers' evaluation - sensor stability

Notwithstanding the positive response behavior of the thin-films sensors in the presence of the TCS molecules in different aqueous matrices, both individually and in array tell us that we are on the right track for TCS detection, there is a need to evaluate the stability of the thin-films in order to confirm that the positive results are due to the presence of TCS in the aqueous matrix and not to the loss of polyelectrolyte molecules from the films by desorption. It is known that the LbL film stability is related with the electrostatic interactions, in the range of one hundred of kJ/mol, between the opposite ionized groups of cationic and polyelectrolyte molecules [39,40]. Therefore electrostatic interactions play a vital role in the adsorption of these molecular bilayers but are also strongly pH dependent since the degree of ionization of each polyelectrolyte is a function of pH [39,40]. Having in mind the goal of develop a sensor dedicated to detect a specific molecule in complex media that can present different pH, the electrostatic interactions must be taken into account. Moreover, the salts and/or other elements present in the environmental matrices, change the degree of ionization of LbL films and of molecules involved [41] and therefore affecting the electrical properties (e.g. impedance) of the sensor. Additionally, the ionic elements present in the matrices, can be adsorbed onto the polyelectrolyte's layers, changing the electrical properties of the sensor. Thus, in order to ascertain which sensor holds the best features for the detection of TCS with no loss/desorption of thin-film layers and no irreversible adsorption of TCS onto thin-film, the adsorbed amount on the different thin-films was analyzed before and after the thin-films to be immersed on the different TCS aqueous matrices. The adsorbed amount per unit of area can be easily es-

timated by measuring the UV-visible spectra of the films since they absorb in this wavelength region and TCS presents two main absorbance bands at 230 and at 280 nm. In figures 6 are shown the UV-vis absorbance spectra of the LbL films, before and after their immersion ( $t = 0, 5$  and  $10$  minutes) into  $10^{-9}$  M TCS aqueous solutions, prepared with DW, MW and EF (see Materials and Methods section). These obtained spectra were plotted together by type of film and aqueous matrix, thus allowing for an insight on the effects of adsorption and/or desorption occurring on each LbL thin-film. Accordingly, if the absorbance is seen to increase compared to the  $t = 0$  is likely that TCS molecules are being adsorbed on the thin-film outermost surface. Contrarily, if the absorbance is seen to decrease when compared to the spectrum measured before immersion of the film on the aqueous matrix,  $t = 0$ , it is likely that polyelectrolyte molecules are being desorbed from the thin-film. This desorption is related with losses in the electrostatic interactions with consequence in changes in the electrical impedance measured during the sensing procedure. By analysing the spectra of (PAH/GO)<sub>5</sub> thin-film displayed in Figures 6 I a), b) and c) it is possible to observe that in both DW (a) and MW (b) there was adsorption of TCS molecules on the films being more significant in the case of DW. Also, in the DW, results show that a slight desorption took place when the film was immersed from five to ten minutes. This could be due to the more surface-located layers not being properly adsorbed during the film preparation, and when immersed for a second time suffer a washing process, resulting in a loss of previous adsorbed matter. The adsorption phenomenon in these cases holds an additional relevance aside from the detection factor, as it can be used for removing TCS from solutions.

According to spectra of Figure 6 I(a) and I(b), the GO outer layer does not seem to be deeply influenced by pH, given that both waters have different pH values (5.7 for MW and 7.2 for DW, Table 1), and there was adsorption, nonetheless. Moreover, given the chemical structures of the TCS molecule and the polyelectrolyte (GO), the adsorption observed could be a result of either the formation of hydrogen bonds or from the interactions of  $\pi$ - $\pi$  stacking [42]. In the case of EF, Figure 6 I(c), desorption takes place since the absorbance decrease as the immersion time in the EF matrix increased. This behaviour can be attributed to the abundant presence of ions such as  $Mg^{2+}$ ,  $Na^+$ ,  $SO_4^{2-}$  (Table 1), which strongly interacting with the GO outer layer of, facilitating the change of charge within GO layer, from negatively charged to a predominantly neutral one. By turning neutral, the strong electrostatic interactions between the GO outer layer

and the remaining layers were weakened, which in turn leads to polyelectrolyte molecules detachment as shown in Figure 6(c) [43]. The effect of pH on the degree of ionization of PAH and GO has been already discussed in literature [39,44,45]. In fact, it was shown that although at higher pH GO is electrically charged, the PAH film molecules lost a large amount of charge, leading to both PAH and GO desorption. Due to this fact, this type of film (PAH/GO)<sub>5</sub> should not be considered as sensing film for future works containing EF.

From the characterization of UV-vis spectra of (PEI/PSS)<sub>5</sub> thin-films, Figure 6II, there was a clear effect of film desorption in the cases of DW (a) and MW (b). While for the DW the observed desorption increased with the immersion time, for the MW, although desorption to be significant after five minutes, remained seemingly constant after the second immersion, suggesting that a desorption plateau was reached. As desorption was observed in both DW and MW, (PEI/PSS)<sub>5</sub> thin-films should not be elected as sensing films for these aqueous matrices.

Regarding the thin-films in EF, spectra of Figure 6 II(c) show that the absorbance between immersion times from  $t = 0$  to  $t = 10$  minutes slightly varied. This indicate that there was no significant adsorption either desorption, i.e., TCS adsorption or film losses. It is also possible to infer that pH plays a fundamental role in the adsorption and desorption phenomena regarding (PEI/PSS)<sub>5</sub> LbL films. According to [46], the PEI degree of ionization is strongly pH dependent but the PSS is a strong polyelectrolyte, with a pKa near 1 [41,47], it can be influenced by solution pH due to the presence of a sulfonate group in its chemical structure and furthermore, reaching a more stable state at  $\text{pH} > 7$  [48]. Therefore, not only due to this last referred reason but also due to the mineral waters (both have  $\text{pH} < 7$ ), while for EF ( $\text{pH}$  above 8, see Table 1) the (PEI/PSS)<sub>5</sub> LbL films are highly stable. To better understand the involved phenomena, a subsequent study about the stability of (PEI/PSS)<sub>5</sub> thin-films was conducted by measuring the absorbance spectra of (PEI/PSS)<sub>5</sub> thin-films before and after to be immersed during different periods in EF matrices with different pH, namely, 3, 6 and 8, see Figures 7 a), b) and c), respectively. Clear desorption occurred after immersion in Figures 7 (a) and (b) while in (c) a seemingly constant pattern happens among the three spectra. Furthermore, as pH increases in the TCS solutions from pH 3 to pH 8, the phenomenon of desorption decreases, suggesting that pH has a direct effect on the interaction between the thin-film and TCS. The behaviours displayed in Figures 7 further show that the absorbance of TCS onto

the outer layer of PSS is deeply influenced by pH, confirming what was observed in Figure 6 II(c). At pH 8, the film exhibits a stable behaviour, due to PSS being fully charged and PEI maintaining about 40% of its electrical charge which is sufficient to maintain the polyelectrolyte layers adsorbed in the LbL film and, therefore, no desorption occurs. As the outermost layer of the (PEI/PSS)<sub>5</sub> thin-film is negative and, at high pH, the TCS is negatively charged, the TCS molecules are repelled by the films and are not adsorbed on its surface. Thus, neither desorption nor adsorption phenomena are observed.

### 3.4 Electronic Tongue - Sensor sensitivity and resolution

The results of the previous sections indicate that (PAH/GO)<sub>5</sub> LbL sensor should be applied to acid aqueous matrices with lower ionic strengths, while the (PEI/PSS)<sub>5</sub> LbL sensor should be used with alkaline aqueous matrices with higher ionic strengths. Additionally, the gold IDE sensor should be applied to medium ionic strength in neutral solutions. Thus, to the environmental aqueous matrices under study, an array of sensors, composed by the gold IDE and (PEI/PSS)<sub>5</sub> sensors was set in order to understand if the e-tongue concept were capable of “tasting”, through the impedance data, MW and EF, doped with TCS.

The PCA plot corresponding to the use of the adequate sensor devices to the matrix is presented in Figure 8(a). This plot clearly distinguishes the MW from EF matrix. Inside each matrix PCA region it was also possible to discriminate the TCS concentrations across the principal component F2. In Figure 8(b) the values of F2 were plotted as a function of TCS concentrations for both type of matrices, and a linear relation and working range of the e-tongue was attained. The principal component F2 linear tendency suggests that F2 data can be used to determine the sensitivity, the slope of a linear function, of the sensor. Analyzing F2 curves, in detail, one can infer a linear range between  $10^{-13}$  and  $10^{-7}$  M range of TCS concentrations. Considering the data within this concentration range, the F2 feature plot vs. the logarithm of concentration, allows fitting the plotted data points to a straight line with a slope,  $(\Delta F2)/\Delta \log C = 0.19 \pm 0.02$ , which corresponds to the sensor sensitivity or limit of quantification. Additionally, the sensor resolution (smallest concentration that can be detected) can be found near the smallest concentration (Cs). The Cs 0.1 pM, the minimum value which can be measured is 0.02, therefore,  $\Delta \log C = (0.02)/(0.19)$  meaning,  $\Delta \log C = \log C - \log C_s$  and, thus,  $C - C_s \sim$

0.13pM, which corresponds to the sensor resolution, or limit of detection, of 0.13pM ( 0.3pg/L).

## 4 CONCLUSIONS

An electronic tongue, consisting of an array of sensors based on uncoated IDE and coated with different LbL films was shown to be able to detect and quantify triclosan trace concentrations, within the range of  $10^{-15}$  to  $10^{-5}$  M, in a MW and in EF matrices, by measuring the impedance spectra of the sensor device. Sensor devices stability tests related with adsorption/desorption phenomena revealed that some of the films are not appropriate as TCS monitoring tools as they are highly influenced by both matrices' ion composition and pH. The experimental data suggests that: 1) (PAH/GO)<sub>5</sub> LbL films may be used to analyze acid matrices with low ionic strength, since the salts in the solution tend to discharge the GO film; 2) (PEI/PSS)<sub>5</sub> LbL films combination reveals potential and capacity to be employed in alkaline aqueous matrices, such as waste water, with high ionic strength; 3) gold IDE (uncoated) sensors react with ions in the solutions and are damaged by S and Zn elements and, may be considered to analyze neutral solutions with low ionic strengths.

Regarding the aim of this proof-of-concept study, an e-tongue, which can be used as an "analytical" sensor for the detection and quantification of TCS in the monitoring of environmental aqueous matrices (EF and MW), was achieved. The experimental data, analyzed through a PCA, supported and demonstrated the sensor's ability and potential to distinguish between aqueous matrices and to discriminate TCS concentrations using the principal component F2. For an experimental/environmental range of triclosan concentrations of  $10^{-13}$  to  $10^{-7}$  M (0.3 ng/L - 30  $\mu$ g/L), the e-tongue presents a sensitivity value of  $0.19 \pm 0.02$  and a resolution of 0.13 pM. Finally, these results show that the choice of more stable sensing layers is the key to develop quantitative e-tongues and, in the case of LbL films that stability is only achieved when strong polyelectrolytes are employed in its preparation.

## ACKNOWLEDGEMENTS

This work was supported by the Project "Development of Nanostructures for Detection of Triclosan Traces on Aquatic Environments" (PTDC/FIS-NAN/0909/2014). The Center for Environmental and Sustainability Research CENSE, which is financed by national funds from FCT/MEC

(UID/AMB/04085/2019). J. Pereira-da-Silva and P.M. Zagalo acknowledge their fellowships PD/BD/142768/2018, PD/BD/142767/2018 from RaBBiT Doctoral Programme, respectively. C. Magro acknowledges to Fundação para a Ciência e a Tecnologia for her PhD fellowship (SFRH/BD/114674/2016).

## REFERENCES

- [1] L. Sanchez-prado, C. Garcia-jares, M. Llompert, Microwave-assisted extraction: Application to the determination of emerging pollutants in solid samples, *J. Chromatogr. A.* 1217 (2010) 2390–2414. doi:10.1016/j.chroma.2009.11.080.
- [2] J. Fang, R.L. Stingley, F.A. Beland, W. Harrouk, D.L. Lumpkins, P. Howard, Occurrence, Efficacy, Metabolism, and Toxicity of Triclosan, *J. Environ. Sci. Heal. Part C.* 28 (2010) 147–171. doi:10.1080/10590501.2010.504978.
- [3] D. Sabaliunas, S.F. Webb, A. Hauk, M. Jacob, W.S. Eckhoff, Environmental fate of Triclosan in the River Aire Basin, UK, *Water Res.* 37 (2003) 3145–3154. doi:10.1016/S0043-1354(03)00164-7.
- [4] J. Skarha, L. Mínguez-alarcón, P.L. Williams, T.I.M. Korevaar, R.A. De Poortere, M.A.C. Broeren, J.B. Ford, M. Eliot, R. Hauser, J.M. Braun, Cross-sectional associations between urinary triclosan and serum thyroid function biomarker concentrations in women, *Environ. Int.* 122 (2019) 256–262. doi:10.1016/j.envint.2018.11.015.
- [5] X. Ma, Y. Wan, M. Wu, Y. Xu, Q. Xu, Z. He, W. Xia, Occurrence of benzophenones, parabens and triclosan in the Yangtze River of China, and the implications for human exposure, *Chemosphere.* 213 (2018) 517–525. doi:10.1016/j.chemosphere.2018.09.084.
- [6] A. Juric, K. Singh, X.F. Hu, H.M. Chan, Exposure to triclosan among the Canadian population: Results of the Canadian Health Measures Survey ( 2009 – 2013 ), *Environ. Int.* 123 (2019) 29–38. doi:10.1016/j.envint.2018.11.029.
- [7] R.F. Lehutso, A.P. Daso, J.O. Okonkwo, Occurrence and environmental levels of triclosan and triclocarban in selected wastewater treatment plants in Gauteng Province, South

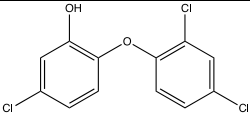
- Africa, *Emerg. Contam.* 3 (2017) 107–114. doi:10.1016/j.emcon.2017.07.001.
- [8] R. Freitas, F. Coppola, S. Costa, C. Pretti, L. Intorre, V. Meucci, A.M.V.M. Soares, M. Solé, The influence of temperature on the effects induced by Triclosan and Diclofenac in mussels, *Sci. Total Environ.* 663 (2019) 992–999. doi:10.1016/j.scitotenv.2019.01.189.
- [9] W. Hua, E.R. Bennett, R.J. Letcher, Triclosan in waste and surface waters from the upper Detroit River by liquid chromatography-electrospray-tandem quadrupole mass spectrometry, *Environ. Int.* 31 (2005) 621–630. doi:10.1016/j.envint.2004.10.019.
- [10] A. Lindström, I.J. Buerge, T. Poiger, P.A. Bergqvist, M.D. Müller, H.R. Buser, Occurrence and environmental behavior of the bactericide triclosan and its methyl derivative in surface waters and in wastewater, *Environ. Sci. Technol.* 36 (2002) 2322–2329. doi:10.1021/es0114254.
- [11] P.E. Stackelberg, E.T. Furlong, M.T. Meyer, S.D. Zaugg, A.K. Henderson, D.B. Reisman, Persistence of pharmaceutical compounds and other organic wastewater contaminants in a conventional drinking-water-treatment plant, *Sci. Total Environ.* 329 (2004) 99–113. doi:10.1016/j.scitotenv.2004.03.015.
- [12] C.G. Daughton, T. a. Ternes, Pharmaceuticals and personal care products in the environment: Agents of subtle change?, *Environ. Health Perspect.* 107 (1999) 907–938. doi:10.1289/ehp.99107s6907.
- [13] F. Tohidi, Z. Cai, GC/MS analysis of triclosan and its degradation by-products in wastewater and sludge samples from different treatments, *Environ. Sci. Pollut. Res.* 22 (2015) 11387–11400. doi:10.1007/s11356-015-4289-x.
- [14] S.C.N. Queiroz, K. Lazou, P. Sandra, I.C.S.F. Jardim, Determination of pesticides in water by liquid chromatography-(electrospray ionization)-mass spectrometry (LC-ESI-MS), *Pestic. Rev. Ecotoxicologia e Meio Ambient.* 14 (2004) 53–60. doi:10.5380/pes.v14i0.3123.
- [15] J. Sun, C.L. Yi, R.S. Zhao, X. Wang, W.Q. Jiang, X.K. Wang, Determination of trace triclosan in environmental water by microporous bamboo-activated charcoal solid-phase extraction combined with HPLC-ESI-MS, *J. Sep. Sci.* 35 (2012) 2781–2786. doi:10.1002/jssc.201200328.
- [16] J. Regueiro, E. Becerril, C. Garcia-Jares, M. Llompарт, Trace analysis of parabens, triclosan and related chlorophenols in water by headspace solid-phase microextraction with in situ derivatization and gas chromatography–tandem mass spectrometry, *J. Chromatogr. A.* 1216 (2009) 4693–4702. doi:10.1016/j.chroma.2009.04.025.
- [17] J.-H. Guo, X.-H. Li, X.-L. Cao, Y. Li, X.-Z. Wang, X.-B. Xu, Determination of triclosan, triclocarban and methyltriclosan in aqueous samples by dispersive liquid–liquid microextraction combined with rapid liquid chromatography, *J. Chromatogr. A.* 1216 (2009) 3038–3043. doi:10.1016/j.chroma.2009.02.021.
- [18] L. Sanchez-Prado, M. Llompарт, M. Lores, C. García-Jares, J.M. Bayona, R. Cela, Monitoring the photochemical degradation of triclosan in wastewater by UV light and sunlight using solid-phase microextraction, *Chemosphere.* 65 (2006) 1338–1347. doi:10.1016/j.chemosphere.2006.04.025.
- [19] W. Bourgeois, R.M. Stuetz, Use of a chemical sensor array for detecting pollutants in domestic wastewater, *Water Res.* 36 (2002) 4505–4512. doi:10.1016/S0043-1354(02)00183-5.
- [20] T. Wu, T. Li, Z. Liu, Y. Guo, C. Dong, Talanta Electrochemical sensor for sensitive detection of triclosan based on graphene / palladium nanoparticles hybrids, *Talanta.* 164 (2017) 556–562. doi:10.1016/j.talanta.2016.12.027.
- [21] Y. Liu, Q.J. Song, L. Wang, Development and characterization of an amperometric sensor for triclosan detection based on electropolymerized molecularly imprinted polymer, *Microchem. J.* 91 (2009) 222–226. doi:10.1016/j.microc.2008.11.007.
- [22] J. Zheng, M. Zhang, Y. Ling, J. Xu, S. Hu, T. Hayat, N.S. Alharbi, F. Yang, Fabrication of one dimensional CNTs / Fe<sub>3</sub>O<sub>4</sub> @ PPy / Pd magnetic composites for the accumulation and electrochemical detection of triclosan, *J. Electroanal. Chem.* 818 (2018) 97–105. doi:10.1016/j.jelechem.2018.04.026.
- [23] B. Petrie, R. Barden, B. Kasprzyk-Hordern, A review on emerging contaminants in wastewaters and the environment: Current knowledge, understudied areas and recommendations for future monitoring, *Water Res.* 72 (2015) 3–27. doi:10.1016/j.watres.2014.08.053.

- [24] C. Magro, E. Mateus, M. Raposo, A.B. Ribeiro, Overview of electronic tongue sensing in environmental aqueous matrices: Potential for monitoring emerging organic contaminants, *Environ. Rev.* (2019) 1–13. doi:10.1139/er-2018-0019.
- [25] Y. Vlasov, A. Legin, A. Rudnitskaya, C. Di Natale, D’Amico, Nonspecific sensor arrays (“electronic tongue”) for chemical analysis of liquids ( IUPAC Technical Report ), *Pure Appl. Chem.* 77 (2005) 1965–1983. doi:10.1351/pac200577111965.
- [26] L.-H. Wang, S.-C. Chu, Voltammetric Detector for Liquid Chromatography: Determination of Triclosan in Rabbit Urine and Serum, *Chromatographia.* 60 (2004) 385–390. doi:10.1365/s10337-004-0414-6.
- [27] J. Yang, P. Wang, X. Zhang, K. Wu, Electrochemical sensor for rapid detection of triclosan using a multiwall carbon nanotube film, *J. Agric. Food Chem.* 57 (2009) 9403–9407. doi:10.1021/jf902721r.
- [28] E.R. Carvalho, N.C. Filho, E.C. Venancio, O.N.O. Jr, L.H.C. Mattoso, L. Martin-neto, Detection of Brominated By-Products Using a Sensor Array Based on Nanostructured Thin Films of Conducting Polymers, (2007) 3258–3271. doi:10.3390/s7123258
- [29] H. Wang, H. Ohnuki, H. Endo, M. Izumi, Impedimetric and amperometric bifunctional glucose biosensor based on hybrid organic – inorganic thin films, *Bioelectrochemistry.* 101 (2015) 1–7. doi:10.1016/j.bioelechem.2014.06.007.
- [30] L. Abegão, J. Ribeiro, P. Ribeiro, M. Raposo, Nano-Molar Deltamethrin Sensor Based on Electrical Impedance of PAH/PAZO Layer-by-Layer Sensing Films, *Sensors.* 13 (2013) 10167–10176. doi:10.3390/s130810167.
- [31] A. Riul, D.S. Dos Santos, K. Wohnrath, R. Di Tommazo, A.C.P.L.F. Carvalho, F.J. Fonseca, O.N. Oliveira, D.M. Taylor, L.H.C. Mattoso, Artificial taste sensor: Efficient combination of sensors made from Langmuir-Blodgett films of conducting polymers and a ruthenium complex and self-assembled films of an azobenzene-containing polymer, *Langmuir.* 18 (2002) 239–245. doi:10.1021/la011017d.
- [32] I. Marques, G. Magalhães-Mota, F. Pires, S. Sérgio, P.A. Ribeiro, M. Raposo, Detection of traces of triclosan in water, *Appl. Surf. Sci.* 421 (2017) 142–147. doi:10.1016/j.apsusc.2016.12.170.
- [33] M. del Valle, Electronic tongues employing electrochemical sensors, *Electroanalysis.* 22 (2010) 1539–1555. doi:10.1002/elan.201000013.
- [34] Y. Elamine, P.M.C. Inácio, B. Lyoussi, O. Anjos, L.M. Estevinho, M. da Graça Miguel, H.L. Gomes, Insight into the sensing mechanism of an impedance based electronic tongue for honey botanic origin discrimination, *Sensors Actuators B Chem.* 285 (2019) 24–33. doi:10.1016/j.snb.2019.01.023.
- [35] J.P. da Silva, P.M. Zagalo, Paulo A. Ribeiro, Maria Raposo, Adsorption of Triclosan on sensors based on PAH/PAZO thin-films: the effect of pH, in: 15th Int. Conf. Comput. Intell. Methods Bioinforma. Biostat., Caparica, Portugal (6-8 September), 2018: pp. 1–48. doi:10.1109/ENBENG.2019.8692527
- [36] O.N. Oliveira, M. Raposo, A. Dhanabalan, Langmuir-Blodgett (LB) and Self-assembled (SA) polymeric films, in: H.S.B.T.-H. of S. and I. of M. Nalwa (Ed.), *Handb. Surfaces Interfaces Mater.*, Academic Press, Burlington, 2001: pp. 1–63. doi:10.1016/B978-012513910-6/50047-5.
- [37] V. Parra, Á.A. Arrieta, J.A. Fernández-Escudero, M.L. Rodríguez-Méndez, J.A. De Saja, Electronic tongue based on chemically modified electrodes and voltammetry for the detection of adulterations in wines, *Sensors Actuators, B Chem.* 118 (2006) 448–453. doi:10.1016/j.snb.2006.04.043.
- [38] J.O. Bockris, A.K.N. Reddy, The Electrified Interface, in: *Mod. Electrochem. Vol. 2*, 1970. doi:10.1007/97894011069172.
- [39] Q. Ferreira, P.J. Gomes, P.A. Ribeiro, N.C. Jones, S. V. Hoffmann, N.J. Mason, O.N. Oliveira, M. Raposo, Determination of degree of ionization of poly(allylamine hydrochloride) (PAH) and poly[1-[4-(3-carboxy-4 hydroxyphenylazo)benzene sulfonamido]-1,2- ethanediyl, sodium salt] (PAZO) in layer-by-layer films using vacuum photoabsorption spectroscopy, *Langmuir.* 29 (2013) 448–455. doi:10.1021/la304036h.
- [40] M. Raposo, O.N. Oliveira, Energies of adsorption of poly(o-methoxyaniline) layer-by-layer films, *Langmuir.* 16 (2000) 2839–2844. doi:10.1021/la990945y.



- [41] M. Raposo, J.M.C. Lourenço, A.M. Botelho do Rego, A.M. Ferraria, P.A. Ribeiro, Counterions - A new approach to control the degree of ionization of polyelectrolytes in layer-by-layer films, *Colloids Surfaces A Physicochem. Eng. Asp.* 412 (2012) 1–10. doi:10.1016/j.colsurfa.2012.05.005.
- [42] M. Raposo, O.N. Oliveira Jr, Adsorption mechanisms in layer-by-layer films, *Brazilian J. Phys.* 28 (1998). doi:10.1590/s0103-97331998000400014.
- [43] C.-W. Chang, S.R. Kumar, C.-B. Wong, S.J. Lue, F. Baskoro, C.-H. Chen, D.W. Chen, Graphene oxide-cation interaction: Inter-layer spacing and zeta potential changes in response to various salt solutions, *J. Memb. Sci.* 554 (2018) 253–263. doi:10.1016/j.memsci.2018.03.006.
- [44] J. Choi, M.F. Rubner, Influence of the degree of ionization on weak polyelectrolyte multilayer assembly, *Macromolecules.* 38 (2005) 116–124. doi:10.1021/ma048596o.
- [45] B. Konkena, S. Vasudevan, Understanding aqueous dispersibility of graphene oxide and reduced graphene oxide through pK<sub>a</sub> measurements, *J. Phys. Chem. Lett.* 3 (2012) 867–872. doi:10.1021/jz300236w.
- [46] X. Zhu, F. Tang, T.S. Suzuki, Y. Sakka, Role of the initial degree of ionization of polyethylenimine in the dispersion of silicon carbide nanoparticles, *J. Am. Ceram. Soc.* (2003). doi:10.1111/j.1151-2916.2003.tb03302.x.
- [47] J.M.C. Lourenço, P.A. Ribeiro, A.M.B. Do Rego, F.M.B. Fernandes, A.M.C. Moutinho, M. Raposo, Counterions in poly(allylamine hydrochloride) and poly(styrene sulfonate) layer-by-layer films, *Langmuir.* (2004). doi:10.1021/la049872v.
- [48] R.N. Smith, M. McCormick, C.J. Barrett, L. Reven, H.W. Spiess, NMR studies of PAH/PSS polyelectrolyte multilayers adsorbed onto silica, *Macromolecules.* 37 (2004) 4830–4838. doi:10.1021/ma049797v.

Table 1. Triclosan physical and chemical characteristics

Chemical structure	Formula	Molar mass g mol <sup>-1</sup>	Log K <sub>ow</sub>	pKa	Solubility in water mg L <sup>-1</sup>	Polarizability Å <sup>3</sup>	CAS-No
 5-chloro-2-(2,4-dichlorophenoxy)phenol	C <sub>12</sub> H <sub>7</sub> Cl <sub>3</sub> O <sub>2</sub>	289.54	4.76	7.9	10 (20°C)	26.96	3380-34-5

References: <http://pubchem.ncbi.nlm.nih.gov/>; <https://chemicalize.com/>

Table 2. Characterization of the environmental matrices under study.

	DW	MW	EF*
pH	7.2 ± 0.1	5.7 ± 0.3	8.4 ± 0.1
Conductivity (µS/cm)	46.5 ± 0.7	113 ± 37	1400 ± 500
ICP analysis (mg/L)			
Ca	-	0.75 ± 0.1	39.1 ± 2.8
Cu	-	-	0.02 ± 0.01
K	-	-	22.9 ± 0.4
Mg	-	7.3 ± 0.6	18.2 ± 5.1
Na	-	1.7 ± 0.1	161 ± 58
P	-	-	2.2 ± 0.2
S	-	-	32.9 ± 8.6
Zn	-	-	0.07 ± 0.02
IC analysis (mg/L)			
Cl <sup>-</sup>	-	9.3 ± 0.4	488.7 ± 593.2
SO <sub>4</sub> <sup>2-</sup>	-	1.3 ± 0.3	84.1 ± 92.4

DW - deionized water; MW - mineral water; EF - waste water

\*collected between September and December 2018

Table 3. Characteristics of the thin-films deposited on BK7 solid support with gold IDE to characterize the aqueous solutions matrices.

<b>Aqueous matrices</b>	<b>Thin-film combinations</b>	<b>Number of bilayers</b>
DW	PAH/GO and PEI/PSS	5
MW	PAH/GO and PEI/PSS	5
EF	PAH/GO	5
	PEI/PSS	5, 10 and 20

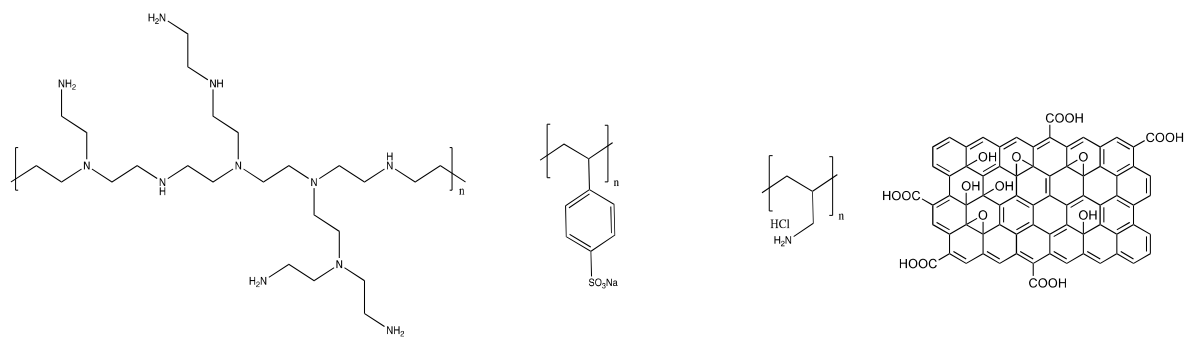


Figure 1. Chemical structure of polyethyleneimine (PEI), poly (sodium 4-styrenesulfonate) (PSS), poly(allylamine hydrochloride) (PAH) and graphene oxide (GO).

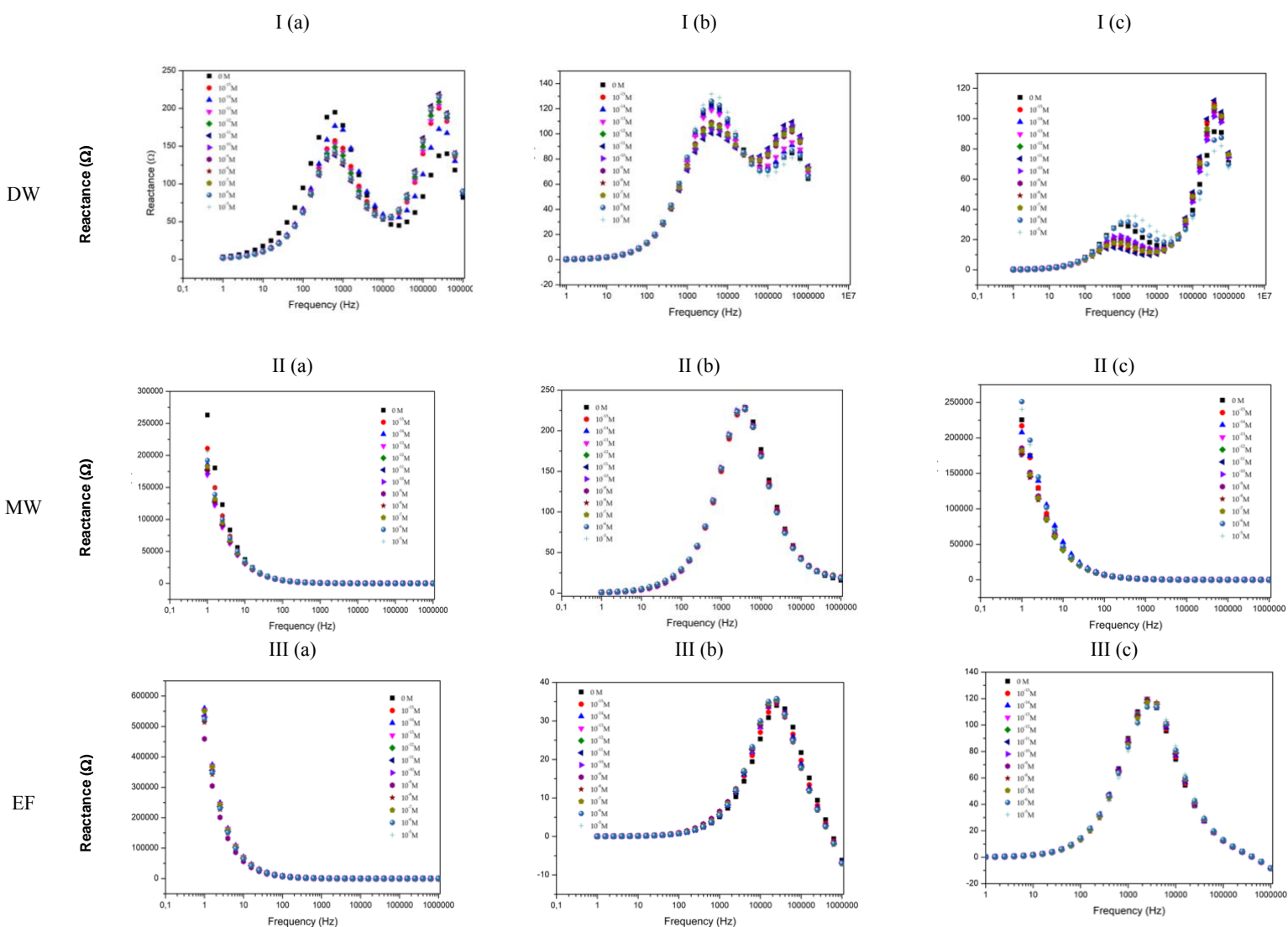


Figure 2. Reactance (imaginary) impedance spectra of sensor device (a) of gold IDE sensor, (b) (PAH/GO)5 sensor and (c) of (PEI/PSS)5 sensor, immersed in TCS DW (I) MW (II) and EF (III) at different TCS concentrations.

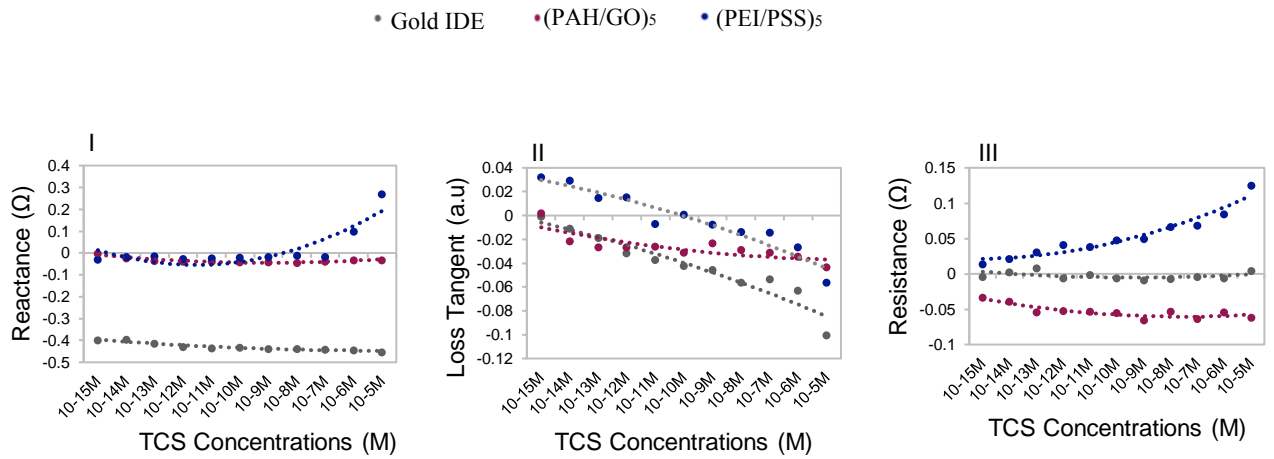
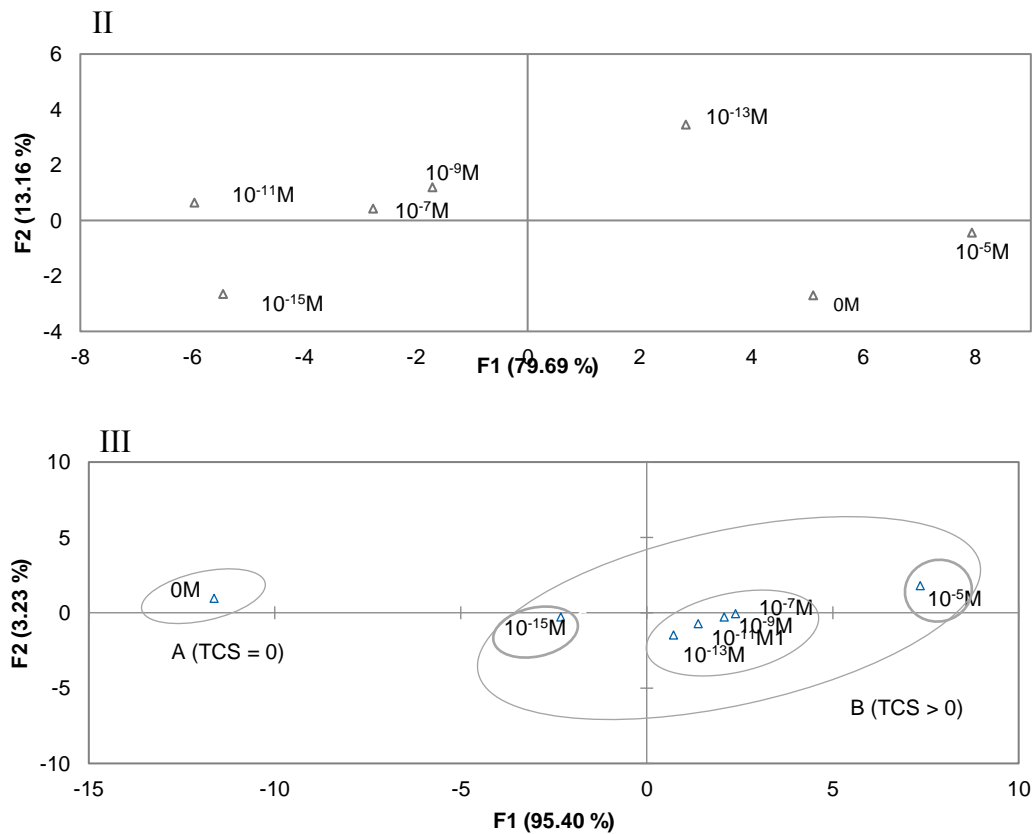


Figure 3. Transducing variables normalization as function of TCS concentrations at fixed frequencies: I) DW - Reactance spectra at 6.3, 25119, 25119 Hz; II) MW - Loss tangent spectra at 63095, 16000, 100000 Hz and III) EF - Resistance spectra at 100000, 16000, 3981 Hz; to Gold IDE, (PAH/GO)<sub>5</sub> and (PEI/PSS)<sub>5</sub> sensors, respectively (n=3, average and standard deviations of the respective impedance data used for the normalization, in supplementary material C 1-3)



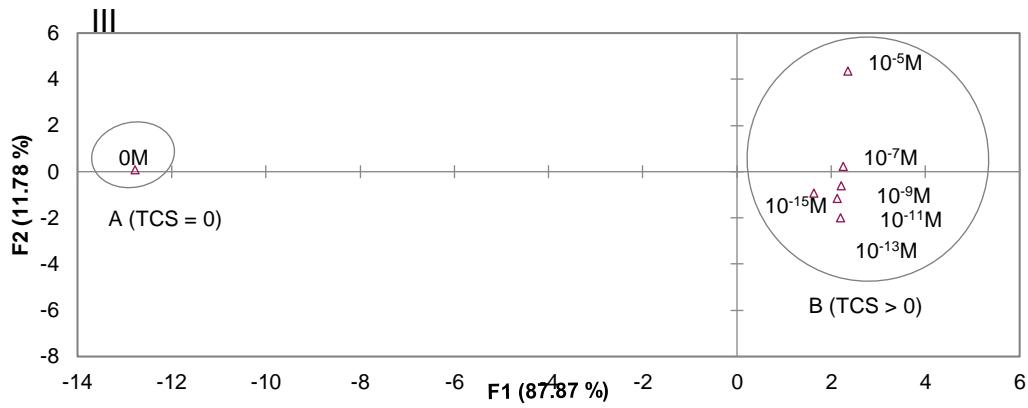


Figure 4. PCA plots of TCS concentrations ( $10^{-5}$  to  $10^{-15}$  M) distinguished with: I) (PAH/GO)<sub>s</sub> sensor for DW, II) gold IDE sensor for MW; III) (PEI/PSS)<sub>s</sub> sensor for EF.

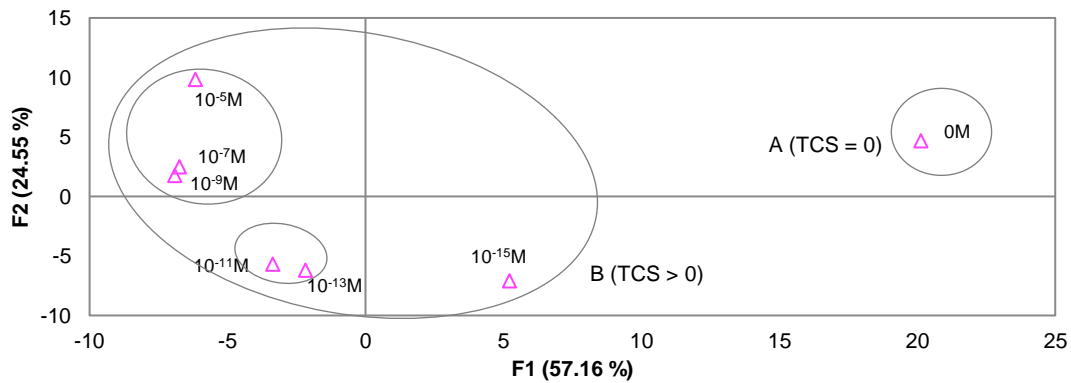


Figure 5. PCA plot of TCS concentrations ( $10^{-5}$  to  $10^{-15}$  M) distinguished with an electronic tongue sensor for EF.

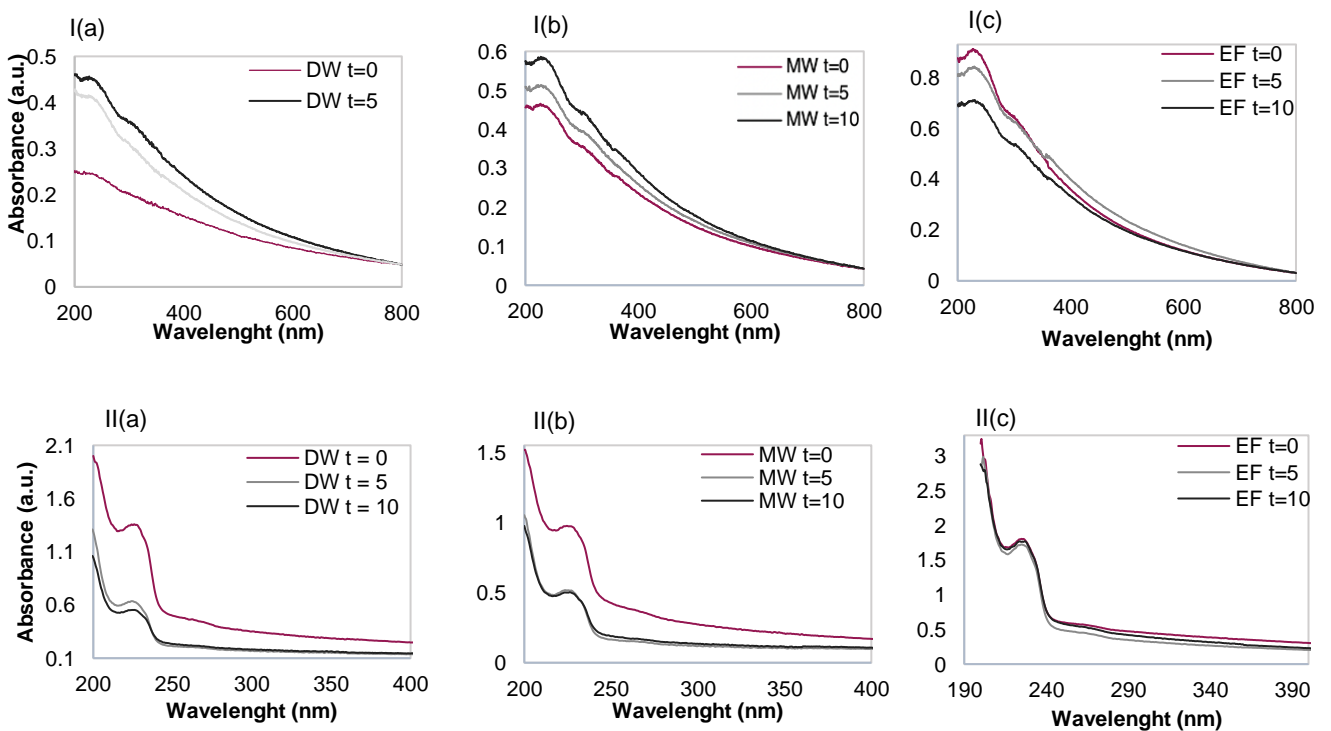


Figure 6. UV-Vis spectra of I) (PAH/GO)<sub>s</sub> films and II) (PEI/PSS)<sub>s</sub> before and after immersions times in  $10^{-9}$  M TCS solutions of: (a) DW; (b) MW and (c) EF.

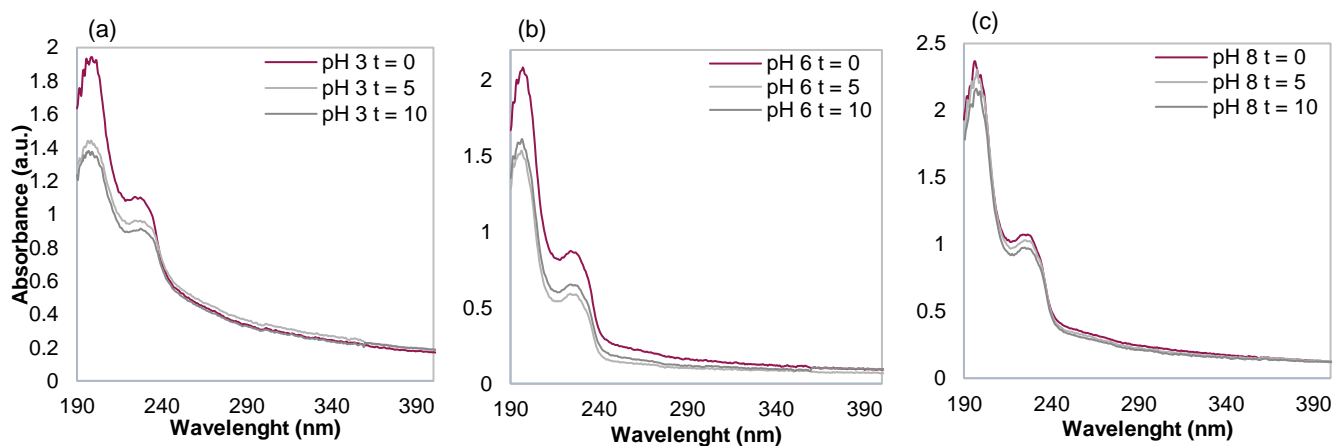


Figure 7. UV-Vis spectra of (PEI/PSS)<sub>5</sub> films before and after immersions in  $10^{-9}$  M TCS solutions in EF with pH of: (a) 3; (b) 6 and (c) 8.

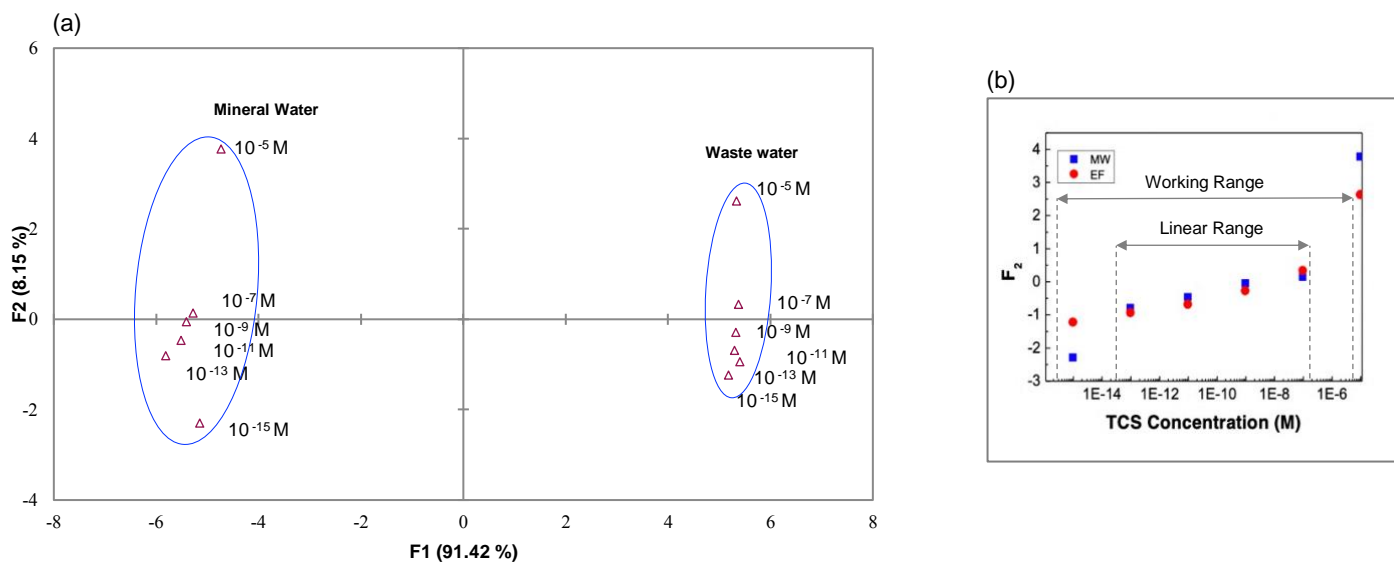


Figure 8. (a) PCA plot of TCS concentrations ( $10^{-5}$  to  $10^{-15}$  M) distinguished gold IDE sensor for MW and (PEI/PSS)<sub>5</sub> sensor for EF; (b) ((a) PCA data) principal components F2 factor scores as function of TCS concentrations for gold IDE sensor in MW and (PEI/PSS)<sub>5</sub> sensor in EF.

# Supplementary Material

Table A. Concentration guidance: molar,  $\mu\text{g/L}$ ,  $\text{ng/L}$  and  $\text{pg/L}$

$M$	$\mu\text{g/L}$	$\text{ng/L}$	$\text{pg/L}$
$10^{-5}$	3000		
$10^{-6}$	300		
$10^{-7}$	30		
$10^{-8}$	3		
$10^{-9}$	0.3		
$10^{-10}$		30	
$10^{-11}$		3	
$10^{-12}$		0.3	300
$10^{-13}$			30
$10^{-14}$			3
$10^{-15}$			0.3

Figure B. Reactance (imaginary) impedance spectra of sensor device of gold IDE sensor, (PAH/GO)<sub>5</sub> sensor and of (PEI/PSS)<sub>5</sub> sensor, immersed in deionized water, mineral water and waste water with  $10^{-15}\text{M}$  of TCS (Related to the measurements in Figure 2)

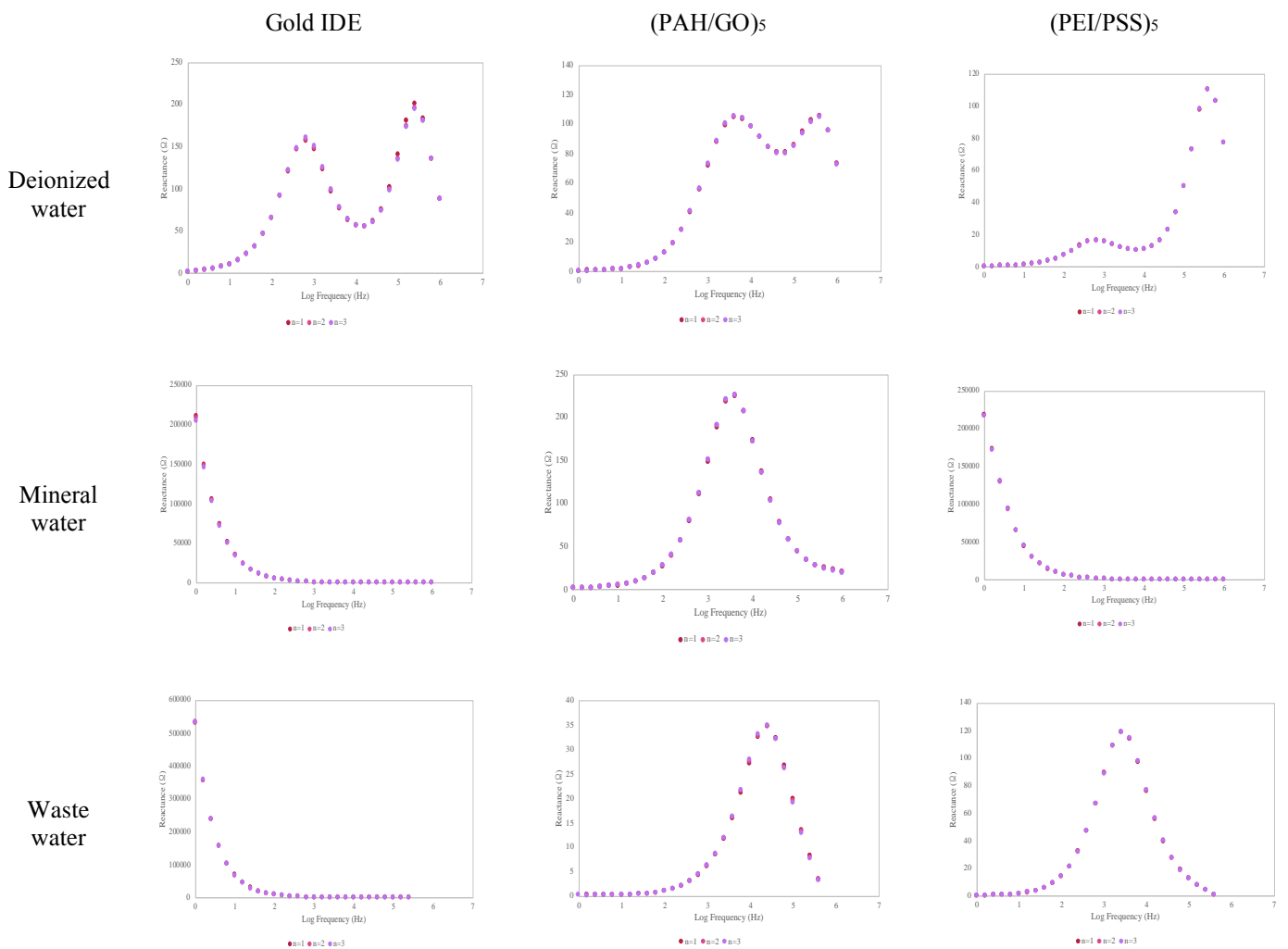




Table C.1 Impedance data measurements, reactance (imaginary), used for the normalization of Plots I in Figure 3

		Fixed Frequency (Hz)						
		6.3		25119		25119		
		TCS (M)	Gold IDE	(PAH/GO) <sub>5</sub>	(PEI/PSS) <sub>5</sub>			
Reactance (imaginary) ( $\Omega$ ) for deionized water			<i>Average</i>	<i>SD</i>	<i>Average</i>	<i>SD</i>	<i>Average</i>	<i>SD</i>
		0	13.035	0.654	87.201	0.112	16.837	0.021
		10 <sup>-15</sup>	7.466	0.041	84.483	0.030	16.338	0.004
		10 <sup>-14</sup>	7.508	0.028	84.460	0.048	16.576	0.004
		10 <sup>-13</sup>	7.270	0.032	83.752	0.092	16.616	0.005
		10 <sup>-12</sup>	7.085	0.027	83.488	0.053	16.379	0.012
		10 <sup>-11</sup>	7.035	0.030	83.668	0.017	16.461	0.003
		10 <sup>-10</sup>	7.051	0.041	83.694	0.029	16.508	0.008
		10 <sup>-9</sup>	6.976	0.019	83.889	0.017	16.541	0.003
		10 <sup>-8</sup>	7.015	0.029	83.834	0.023	16.638	0.002
		10 <sup>-7</sup>	6.939	0.023	84.166	0.015	16.538	0.011
		10 <sup>-6</sup>	6.939	0.014	85.315	0.136	18.439	0.100
		10 <sup>-5</sup>	6.795	0.020	87.068	0.086	21.371	0.044

*SD* – standard deviation

Table C.2 Impedance data measurements, loss tangent, used for the normalization of Plots II in Figure 3

		Fixed Frequency (Hz)						
		63095		16000		100000		
		TCS (M)	Gold IDE	(PAH/GO) <sub>5</sub>	(PEI/PSS) <sub>5</sub>			
Loss Tangent (a.u) for mineral water			<i>Average</i>	<i>SD</i>	<i>Average</i>	<i>SD</i>	<i>Average</i>	<i>SD</i>
		0	6.586	0.038	2.956	0.000	4.454	0.001
		10 <sup>-15</sup>	6.613	0.009	2.961	0.005	4.600	0.008
		10 <sup>-14</sup>	6.547	0.009	2.892	0.003	4.578	0.006
		10 <sup>-13</sup>	6.492	0.010	2.877	0.003	4.517	0.002
		10 <sup>-12</sup>	6.413	0.005	2.876	0.005	4.522	0.002
		10 <sup>-11</sup>	6.382	0.001	2.877	0.006	4.423	0.003
		10 <sup>-10</sup>	6.347	0.001	2.863	0.003	4.457	0.001
		10 <sup>-9</sup>	6.327	0.002	2.887	0.002	4.419	0.001
		10 <sup>-8</sup>	6.256	0.001	2.870	0.003	4.386	0.004
		10 <sup>-7</sup>	6.272	0.003	2.863	0.004	4.388	0.002
		10 <sup>-6</sup>	6.210	0.003	2.854	0.004	4.329	0.004
		10 <sup>-5</sup>	5.942	0.036	2.826	0.002	4.206	0.009

*SD* – standard deviation

Table C.3 Impedance data measurements, resistance, used for the normalization of Plots III in Figure 3

Resistance ( $\Omega$ ) for waste water	Fixed Frequency (Hz)						
	100000		16000		3981		
	TCS (M)	Gold IDE	(PAH/GO) <sub>5</sub>	(PEI/PSS) <sub>5</sub>	Average	SD	
0		40.920	0.057	98.217	0.338	149.621	1.055
10 <sup>-15</sup>		40.781	0.041	94.688	0.561	150.891	0.286
10 <sup>-14</sup>		41.064	0.027	94.458	0.289	151.813	0.168
10 <sup>-13</sup>		41.241	0.066	93.091	0.145	153.332	0.217
10 <sup>-12</sup>		40.712	0.011	93.272	0.095	154.904	0.241
10 <sup>-11</sup>		40.906	0.032	93.219	0.076	154.231	0.124
10 <sup>-10</sup>		40.716	0.029	93.034	0.068	155.732	0.124
10 <sup>-9</sup>		40.596	0.030	92.116	0.047	156.077	0.153
10 <sup>-8</sup>		40.645	0.043	93.234	0.066	158.578	0.192
10 <sup>-7</sup>		40.794	0.023	92.224	0.039	158.783	0.142
10 <sup>-6</sup>		40.718	0.009	93.262	0.004	161.490	0.401
10 <sup>-5</sup>		41.151	0.021	92.677	0.218	167.916	0.771

SD – standard deviation

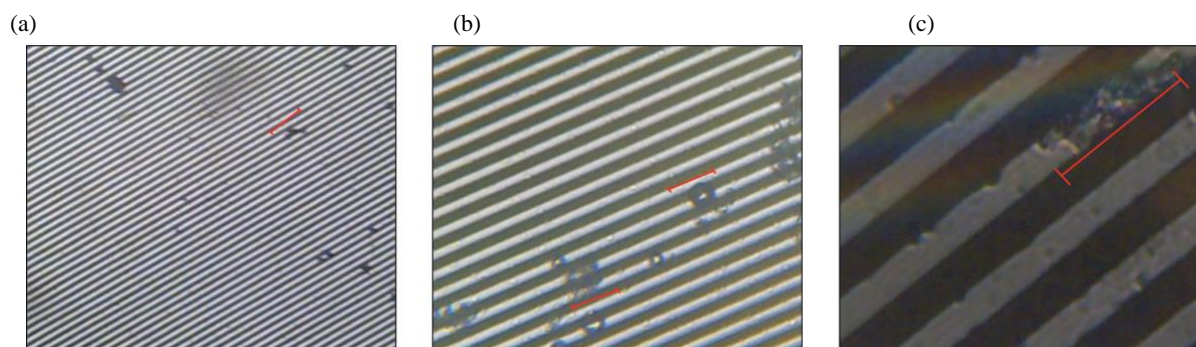


Figure D. Optical Microscopy Images of gold interdigitated electrodes without coating, gold IDE; Magnitude: (a) 4x, (b) 10x and (c) 40x, analysed in waste water

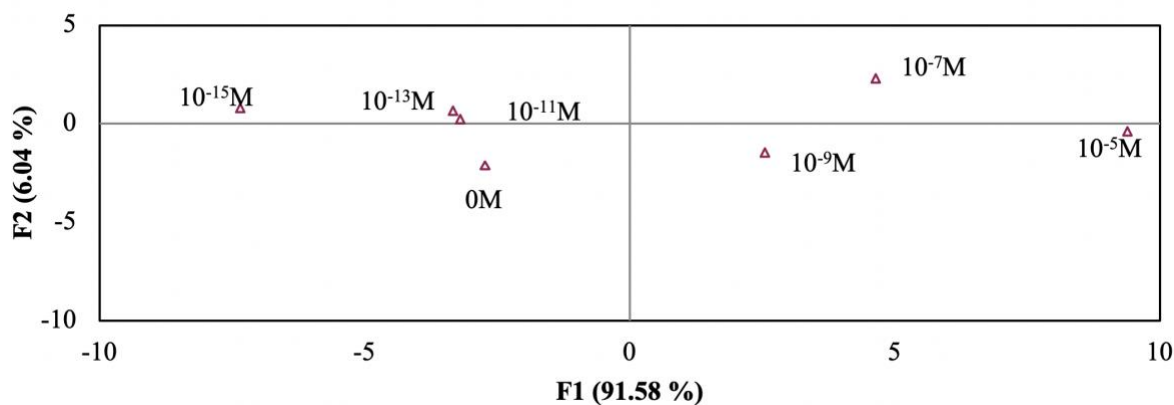


Figure E. PCA plot of TCS concentrations (10<sup>-5</sup>M to 10<sup>-15</sup>M) distinguished with (PEI/PSS)<sub>10</sub> sensor for waste water

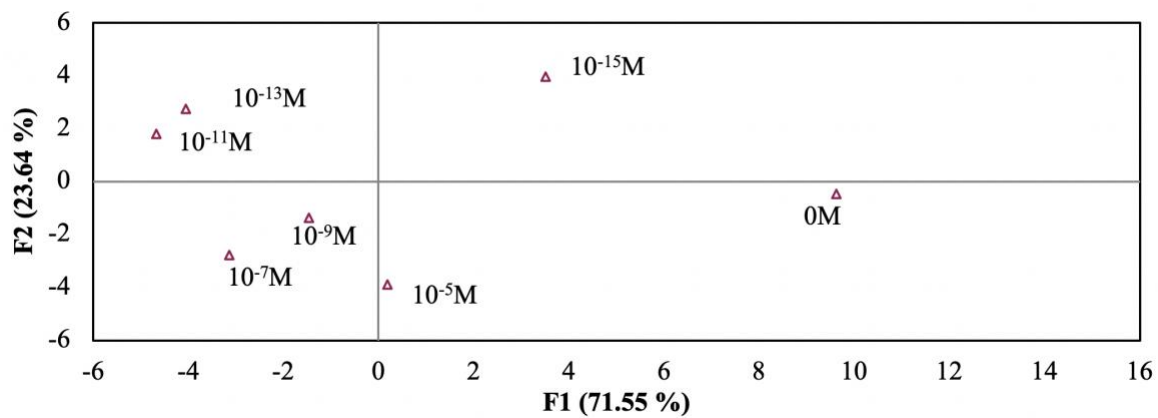


Figure F. PCA plot of TCS concentrations ( $10^{-5}\text{M}$  to  $10^{-15}\text{M}$ ) distinguished with (PEI/PSS)<sub>20</sub> sensor for waste water



## Paper

*“Electronic Tongue Coupled to an Electrochemical Flow Reactor for Emerging Organic Contaminants Real Time Monitoring”*






*C Magro, EP Mateus, JM Paz-Garcia, S Sério, M Raposo & AB Ribeiro*

*Published in: Sensors, 2019*



Article

# Electronic Tongue Coupled to an Electrochemical Flow Reactor for Emerging Organic Contaminants Real Time Monitoring

Cátia Magro <sup>1,\*</sup> , Eduardo P. Mateus <sup>1</sup>, Juan M. Paz-Garcia <sup>2</sup> , Susana Sérgio <sup>3</sup> ,  
Maria Raposo <sup>3</sup>  and Alexandra B. Ribeiro <sup>1,\*</sup> 

<sup>1</sup> CENSE, Department of Sciences and Environmental Engineering, NOVA School of Science and Technology, NOVA University Lisbon, Caparica Campus, 2829-516 Caparica, Portugal; epm@fct.unl.pt

<sup>2</sup> Department of Chemical Engineering, Faculty of Sciences, University of Malaga, Teatinos Campus, 29010 Malaga, Spain; juanma.paz@uma.es

<sup>3</sup> CEFITEC, Department of Physics, NOVA School of Science and Technology, NOVA University Lisbon, Caparica Campus, 2829-516 Caparica, Portugal; susana.serio@fct.unl.pt (S.S.); mfr@fct.unl.pt (M.R.)

\* Correspondence: c.magro@campus.fct.unl.pt (C.M.); abr@fct.unl.pt (A.B.R.)

Received: 31 October 2019; Accepted: 2 December 2019; Published: 4 December 2019



**Abstract:** Triclosan, which is a bacteriostatic used in household items, has raised health concerns, because it might lead to antimicrobial resistance and endocrine disorders in organisms. The detection, identification, and monitoring of triclosan and its by-products (methyl triclosan, 2,4-Dichlorophenol and 2,4,6-Trichlorophenol) are a growing need in order to update current water treatments and enable the continuous supervision of the contamination plume. This work presents a customized electronic tongue prototype coupled to an electrochemical flow reactor, which aims to access the monitoring of triclosan and its derivative by-products in a real secondary effluent. An electronic tongue device, based on impedance measurements and polyethylenimine/poly(sodium 4-styrenesulfonate) layer-by-layer and TiO<sub>2</sub>, ZnO and TiO<sub>2</sub>/ZnO sputtering thin films, was developed and tested to track analyte degradation and allow for analyte detection and semi-quantification. A degradation pathway trend was observable by means of principal component analysis, being the sample separation, according to sampling time, explained by 77% the total variance in the first two components. A semi-quantitative electronic tongue was attained for triclosan and methyl-triclosan. For 2,4-Dichlorophenol and 2,4,6-Trichlorophenol, the best results were achieved with only a single sensor. Finally, working as multi-analyte quantification devices, the electronic tongues could provide information regarding the degradation kinetic and concentrations ranges in a dynamic removal treatment.

**Keywords:** triclosan; electrochemical treatment; real time monitoring; layer-by-layer technique; sputtering technique; electronic tongue; sensors

## 1. Introduction

Nowadays, both water quality and availability are under stress. The global population is expected to exceed nine-billion by 2050, where 70% will be, living in urban areas [1]. This rising demand for water, together with poor or inefficient wastewater management and limited disposal strategies with minimal treatment practices, increases the need of sustainable tools to assure the quality, monitoring, and prosperity of a healthy population and environment [2]. Emerging organic contaminants (EOCs) are defined as “chemical substances that have no regulation and are suspected to negatively affect the environment or whose effects are unknown” [3,4]. Among EOCs, antibiotics, disinfectants, and antiseptics are especially relevant, as thousands of tons are yearly consumed worldwide in medicine, agricultural, and as daily consumer products [5]. Furthermore, the reported

data show that conventional wastewater treatment plants are inefficient in their elimination [6–12]. Triclosan (TCS or 2,4,4'-Trichloro-2'-hydroxydiphenyl ether) is a broad antimicrobial agent, with low water-solubility (more susceptible to bio-accumulation) and that has been used for more than 50 years as an antiseptic, disinfectant, or preservative in clinical settings and several consumer products, i.e., toothpastes, cosmetics, and plastics. On the basis of the available studies, it is now accepted that it has extensive environmental and health effects, also being toxic to water living organisms due to its photodegradation to chlorodioxins [13,14]. TCS has been detected in wastewater treatments plants and surface waters [15,16]. Moreover, TCS derivatives have also been found, such as the metabolite methyl-triclosan (M-TCS) [17], which is considered to be more persistent [18] and TCS by-products, such as 2,4-Dichlorophenol (DCP) and 2,4,6-Trichlorophenol (TCP), which pose a health risk to humans and are recognized as persistent priority pollutants in the United States, Europe, and China [19].

Innovative green tools for monitoring the degradation processes are currently in the spotlight. Sensors, as compared to traditional sampling and analysis procedures, can provide fast response on the output data in a continuous, safe, and cost-effective way, and therefore may play a role in monitoring contaminants' dynamics [20]. Among sensors, the electronic tongue (e-tongue) is gaining special attention for liquid matrices. An e-tongue is a multi-sensory system, which formed by an array of sensors with low-selective thin film layers or sensorial layers, and combined with advanced mathematical procedures for signal processing based on pattern recognition and/or multi-variate data analysis [21]. E-tongues have proved to be suitable devices for monitoring aqueous environmental matrices contaminated with EOCs [22,23]. Some examples are Campos et al. (2012) [24], who developed a voltammetric e-tongue [set of noble (Au, Pt, Rh, Ir, and Ag) and non-noble (Ni, Co, and Cu) electrodes to the prediction of concentration levels of soluble chemical oxygen demand, soluble biological oxygen demand, ammonia, orthophosphate, sulphate, acetic acid, and alkalinity from influent and effluent wastewater. Years later, Cetó et al. (2015) [25] used a voltammetric bio e-tongue for simultaneous monitoring of catechol, m-cresol, and guaiacol mixtures in wastewater. Thus, one of the most interesting aspects that motivate the development of e-tongues is their potential for real-time parallel monitoring of multiple species and multi-analyte determination in a single sample analysis [26,27]. The working electrodes in the e-tongues array can be covered with films (coatings), which improves the sensitivity of the electrical measurements. The ability to tune the composition of nanostructured thin films allow for an improvement in the sensor's intrinsic (chemical or physical) properties for sensing applications. The layer-by-layer (LbL) nano-assembly technique, where the Brazilian group was the pioneer in the subject [28–31], is a flexible, easily-scalable, reproducible, and versatile approach that allows for the precise control of the coating thickness, composition, and structure. This nano-assembly technique is a powerful tool for the incorporation of a wide variety of coating types, such as polyelectrolytes. The type of thin film or sensorial layer chosen is a critical step for the accomplishment of a reliable qualitative and quantitative device. In a preliminary study, Magro et al (2019) [32] found that the LbL films prepared with polyethylenimine (PEI) and poly (sodium 4-styrenesulfonate) (PSS) build up with five bilayers were suitable for TCS detection in wastewater. However, the polyelectrolyte layers of these thin films may desorb when they are immersed in solutions below  $\text{pH} = 7$ . According to Zhu et al. (2003) [33], even if the PEI degree of ionization is strongly pH dependent and the PSS is a strong polyelectrolyte, with a  $\text{pK}_a$  near 1, it can be influenced by solution pH due to the presence of a sulfonate group in its chemical structure and furthermore. Studies on layer-by-layer films that were prepared from aqueous solution with pH below 7 revealed that the PSS is completely ionized [34,35]. In this regard, thin films of  $\text{TiO}_2$  and ZnO build-up with the sputtering technique can also be considered as sensorial layers. These films proved to be efficient for the detection of molecules with phenolic rings and they presented high mechanical stability under pH fluctuations [36–38]. This study aimed to achieve a customized e-tongue device to follow real-time degradation and quantification of TCS and its derivative by-products in an electrochemical flow reactor (EFR) treatment. The EFR, which mimics the secondary clarifier in a wastewater treatment plant, was considered to be the most appropriate choice



to couple with a monitoring real time tool device, due to its potential to operational implementation and final matrix conditions (non-aggressive for thin film layers, e.g., pH effluent around 7.6).

To attain this proof-of-concept goal: (1) an array of thin films were prepared by LbL and sputtering techniques and were characterized by a field emission scanning electron microscope, in order to understand the device response for each EOCs; (2) the impedance electrical properties of these films when immersed in effluent spiked with EOCs' were acquired; (3) "calibration curves", to individually distinguish each EOCs were the base to train the customized e-tongue; and, (4) PCA results from the e-tongue attached to a dynamic EFR were analysed to apprehend the potential for working as a monitoring real time tool for EOCs' degradation detection and semi-quantification.

## 2. Materials and Methods

### 2.1. Chemical and Standards

TCS (99%), M-TCS (99%), DCP (98%), and TCP (98%) were purchased from Sigma-Aldrich (Steinheim, Germany, Table S1). Individual stock solutions for calibration purposes were prepared with 1000 mg/L in methanol and stored at  $-18\text{ }^{\circ}\text{C}$ . The methanol, acetonitrile, acetone, and formic acid used were from Sigma-Aldrich (Steinheim, Germany) in gradient grade type. Water (Type I) was from a Millipore system (Aqua Solutions, Bedford, MA, USA).

The sensor devices were purchased from DropSens (Llanera Asturias, Spain) and they were formed by either a BK7 glass solid substrate with deposited interdigitated electrodes comprising 125 "fingers" each or by a ceramic solid substrate with deposited gold interdigitated electrodes comprising eight "fingers" each. The supports' dimensions were  $22.8 \times 7.6 \times 0.7\text{ mm}$  and each "finger" had 10 or 200  $\mu\text{m}$  of width, which was the same spacing between them. PEI and PSS from Sigma-Aldrich (St Louis, MO, USA) were the chemicals used to prepare the sensing layers on the interdigitated electrodes. The used gases argon, oxygen, and nitrogen had  $\geq 99.9\%$  of purity. The used effluent, pH ( $7.6 \pm 0.5$ ) and conductivity ( $1.6 \pm 1.0$ ), was the liquid fraction that was collected in the secondary settling tank at a wastewater treatment plant (Lisbon, Portugal).

### 2.2. Methods

#### 2.2.1. Emerging Organic Contaminants Extraction and Quantification: Chromatography Approach

The extraction of EOCs in the effluent was performed by solid-phase extraction (SPE) while using Oasis HLB (200 mg, 6 mL) from Waters (Saint-Quentin-En-Yvelines Cedex, France). The SPE cartridges were conditioned by washing with  $3 \times (6\text{ mL})$  of methanol, followed by re-equilibrium with  $3 \times (6\text{ mL})$  of Milli-Q water. For EOCs enrichment, the samples were acidified to pH = 2 before extraction using nitric acid. The 200 mL aqueous samples passed through the cartridge at a flow rate of approx. 10 mL/min by applying a moderate vacuum, followed by a dried period of approx. 3 min by vacuum. The retained EOCs were eluted sequentially with  $2 \times (4\text{ mL})$  of methanol and  $1 \times (4\text{ mL})$  of acetone.

The EOCs determination was performed in an Agilent 1260 Infinity II high-performance liquid chromatography (HPLC) that was equipped with a quaternary pump and auto-sampler and a diode array detector (DAD)/fluorescence detector 1100 Series. An EC-C18 column (InfinityLab Poroshell 120 High Efficiency,  $100\text{ mm} \times 4.6\text{ mm}$ ;  $2.7\text{ }\mu\text{m}$  with Column ID, Agilent, Santa Clara, CA, USA) was used. All of the HPLC runs were performed at a constant flow of 1.5 mL/min in gradient mode, with the oven set to  $36\text{ }^{\circ}\text{C}$ . A mixture of acetonitrile, Milli-Q water and formic acid was used as eluents (A: 5/94.5/0.5% and B: 94.5/5/0.5%) with a gradient of 60% of B (0–2 min), followed by 97% of B (2–3.5 min) and 98% of B until 5 min "Calibration curves" were performed in the range between 0.5 and 20.0 mg/L. The limits of detection and quantification were, respectively, 0.7 and 2.0 mg/L for TCS, 1.3 and 3.9 mg/L for M-TCS, 0.7 and 2.0 mg/L for DCP, and 1.0 and 3.0 mg/L for TCP. The recovery tests were made with fortified effluent for 1 h of contact time (30 min of slow agitation). The recovery percentages were between 62% and 120% in all cases.

### 2.2.2. Emerging Organic Contaminants Quantification: Customized Electronic Tongue Concept

An array of sensor devices with different thin films that were prepared by LbL and sputtering techniques deposited onto solid substrates with gold interdigitated electrodes were coupled to an EFR (Figure 1). The e-tongue (Figure S1 for the information of the five sensors that composed the e-tongue) was used to detect the TCS, M-TCS, DCP, and TCP degradation in the effluent.

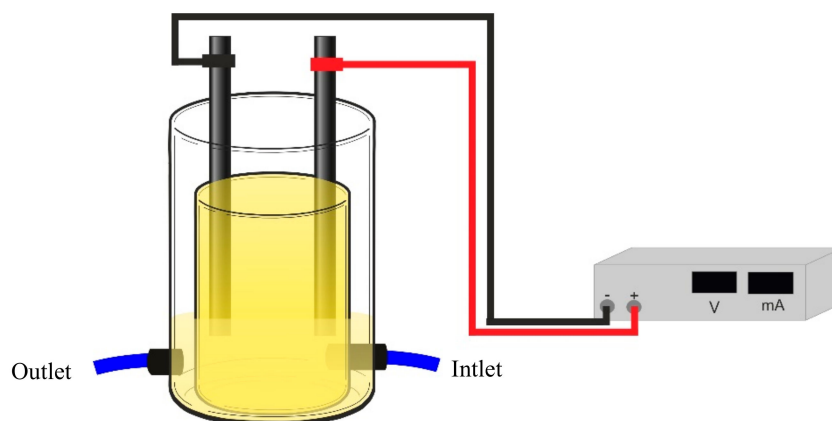


**Figure 1.** Electrochemical flow reactor used to attach the e-tongue.

The LbL thin films were prepared with PEI and PSS polyelectrolytes by the LbL technique [28]. Accordingly, thin films of PEI/PSS that were deposited onto solid support with gold interdigitated electrodes were obtained by adsorbing alternate layers of electrically charged polyelectrolytes at solid/liquid interface, carefully washing with water (Type I) the already adsorbed layers after immersion in the polyelectrolyte solution to remove the polyelectrolyte molecules that were not completely adsorbed. The polyelectrolytes solutions were prepared with a polymeric concentration of  $10^{-2}$  M diluted in water Type I, produced with a Millipore system (Bedford, MA, USA). The adsorption time period of each layer (immersion time in each polyelectrolyte solution) was 30 s and the thin film was dried [39] while using a nitrogen flow after the adsorption of each layer. The aforementioned sequence was repeated five times in order to obtain a film with five bilayers, denoted as (PEI/PSS)<sub>5</sub>.

Monolayered films: TiO<sub>2</sub>, ZnO and bilayered film: TiO<sub>2</sub>/ZnO (being ZnO the upper layer) were deposited at room temperature onto gold interdigitated electrodes glass substrates ( $22.8 \times 7.6 \times 0.7$  mm), by DC (voltage source, Huttinger PFG 10000) reactive magnetron sputtering in a custom-made system. Titanium and zinc discs (Goodfellow, 99.99% purity) with 64.5 mm of diameter and 4 mm of thickness each were used as the sputtering targets. A turbomolecular pump (Pfeiffer TMH 1001) was used to achieve a base pressure of  $10^{-4}$ – $10^{-5}$  Pa (before introducing the sputtering gas). Before the sputter-deposition step of the films, a movable shutter was interposed between the target and the substrates. The target was pre-sputtered in the Ar atmosphere for 2 min to clean the target surface. The target-to-substrate distance was kept constant at 100 mm. Gases in the system were pure Ar and O<sub>2</sub> and needle valves separately controlled their pressures. TiO<sub>2</sub> and ZnO depositions were both carried out in 100% O<sub>2</sub> atmosphere. For the TiO<sub>2</sub> film the total pressure was kept constant at 2 Pa, the sputtering power was 530 W, and the deposition time was 25 min. In the case of ZnO film, the total pressure was fixed at 4.8 Pa, the sputtering power was 300 W, and the deposition time was 30 min. TiO<sub>2</sub>/ZnO bilayered films were prepared while using the aforementioned deposition conditions for TiO<sub>2</sub> and ZnO. No external substrate heating was used during the deposition. The substrate temperature was measured by a thermocouple passing through a small hole in a copper piece that was in contact with the substrate. During the deposition process, the sample temperature increased up to 60 °C due to the plasma particle bombardment of the substrate. The characterization of the thin films thickness and morphology was performed by a field emission scanning electron microscope (FEG-SEM JEOL 7001F) operating at 15 keV. A gold thin film was coated on the films surface before SEM analysis to charge

build-up prevention. The images of the cross section allowed for the estimation of the films' thickness. Therefore, the measured thickness is given by the trigonometric equation since the positioning of the sample has a slope relative to the axis of incidence of the electron beam which can be deduced through the geometry involved. The indicated correction was calculated while using Equation (1).

$$d_{SEM} = \frac{d_{obs}}{\cos \alpha} \quad (1)$$

where the  $d_{SEM}$  is the real thickness,  $d_{obs}$  is an average of the measured thickness values estimated from the cross-section images and  $\alpha$  is the beam incident angle ( $20^\circ$ ).

The electrical analysis of the aqueous matrices was performed by measuring sequentially the impedance spectra of each sensor device when immersed (about 3 min each) in effluent with different EOCs concentrations, while using a Solartron 1260 Impedance Analyzer (Solartron Analytical, AMETEK scientific instruments, Berwyn, PA, USA) in the frequency range of 1 Hz to 1 MHz, while applying an AC voltage of 25 mV. The impedance data was collected from the SMaRT Impedance Measurement Software (AMETEK scientific instruments, Berwyn, PA, USA). Calibration solutions were performed at  $25^\circ\text{C}$  and then prepared while using effluent spiked with EOCs concentrations in the degradation range that were expected in the electrochemical flow reactor (0 to 0.8 mg/L). For all measurements a blank standard (0 mg/L) was used. For the electro-degradation monitoring, every 15 min (total time of treatment 120 min) was assembled an aliquot to be measured for each sensor, in the impedance conditions that are described above.

### 2.2.3. Data Analysis

Principal component analysis (PCA) was carried out regarding the normalized Z-score normalization,  $z = \frac{x-\mu}{\sigma}$  impedance spectroscopy data (capacitance, impedance, imaginary, and real and loss tangent measurements), where  $x$  is the mean of three impedance measurements at a fixed frequency,  $\mu$  the average of all the frequency ranges, and  $\sigma$  the standard deviation of all the frequency ranges. PCA was the choice of data proceeding to reduce the size of data and obtain a new space of orthogonal components, in which different concentration patterns can be observed and explained with Excel XLSTAT Programme. All of the sample analyses were carried out in duplicate or triplicate.

## 3. Results and Discussion

### 3.1. Sensors Characterization: Morphology and Thickness

As described in the Materials and Methods section, (PEI/PSS)<sub>5</sub> LbL films and TiO<sub>2</sub>, ZnO, and TiO<sub>2</sub>/ZnO sputtered films (see sensors composition in Figure S1 in Supplementary Materials) were prepared and characterized. Figure 2a,b presents the SEM images and the respective thickness of those thin films. The characterization of the sensors layers is important to explain the sensors performance, since the homogeneity, particle size, and thickness will affect the electrical measurements: resistance, molecules' adsorption, capacitance, and further capability of detection.

In agreement with Figure 2a, glass conducting substrates are covered by homogeneous films. However, the surface morphology of these films changes according to the deposition technique. Thus, the LbL films exhibited a smooth surface with evidence of very small agglomerates or grains. On the contrary, sputtering films presented a rougher surface and much larger agglomerates with different shapes, depending on the oxide used. In particular, for TiO<sub>2</sub> films, the agglomerates of grains with an average lateral size of 30 nm are distributed over the substrate surface with a 'blooming flower-like' appearance. In the case of ZnO films, the surface presents a pronounced cone-like morphology and lateral average size of approximately 100–120 nm. The outermost ZnO layer of the TiO<sub>2</sub>/ZnO bilayered films show globular shape agglomerates, with the lateral average size approximately 100–150 nm. The formation of agglomerates or particulates are a product of individual nano-phase grains that exhibit different dimensions (ZnO > TiO<sub>2</sub>), which result in an increase of the active surface area and

also promotes the formation of porous films. These characteristics are critical in the response device to EOCs detection. The films thickness was evaluated from FEG-SEM cross-section images and Figure 2b summarizes the obtained values. It can be observed that the thickness of the (PEI/PSS)<sub>5</sub>, TiO<sub>2</sub>, ZnO, and TiO<sub>2</sub>/ZnO increases from 133 to 713 nm, in the mentioned order.

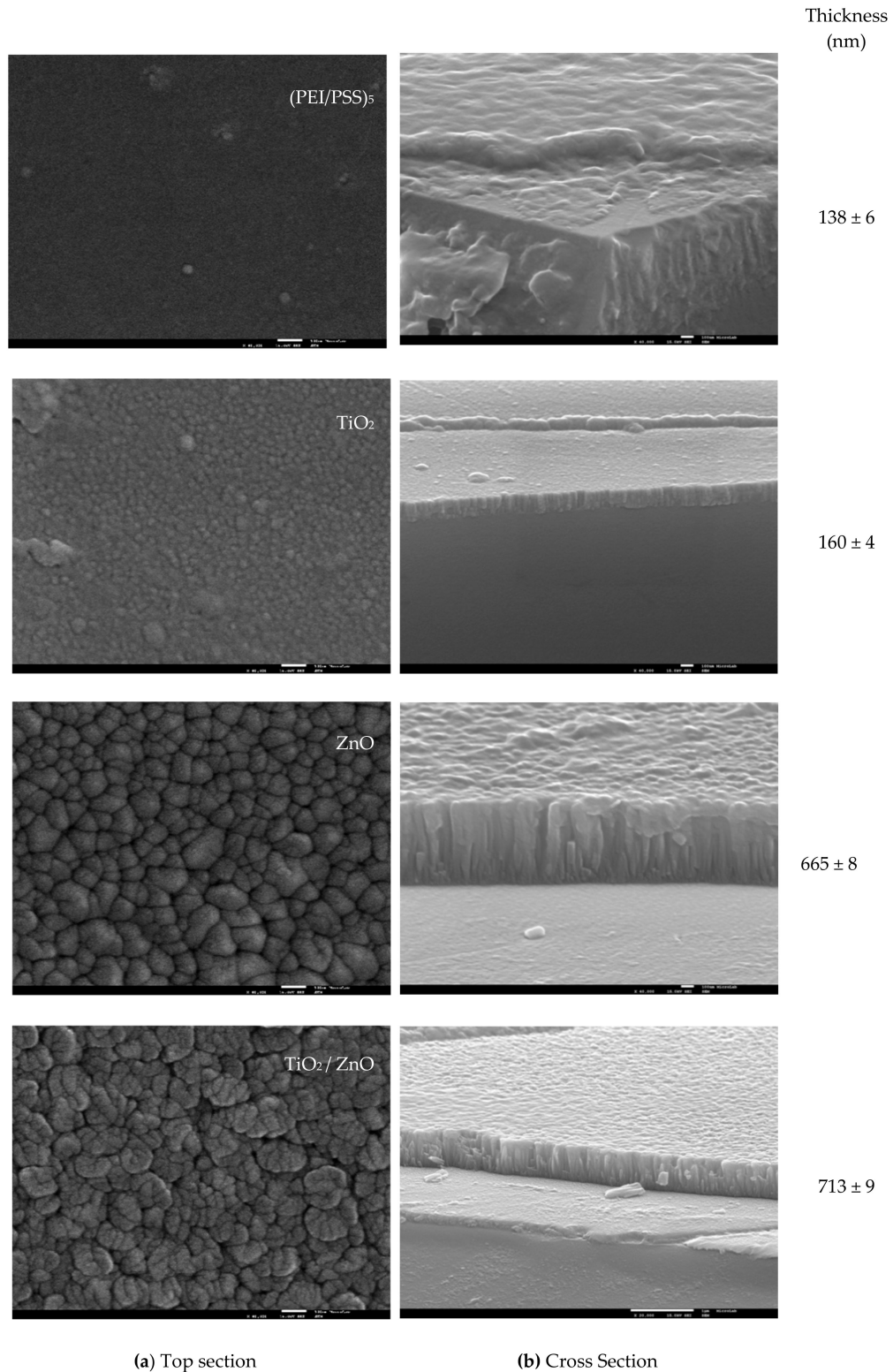


**Figure 2.** Scanning electron microscope (SEM) image of (PEI/PSS)<sub>5</sub>, TiO<sub>2</sub>, ZnO and TiO<sub>2</sub>/ZnO thin films combinations: (a) Top and (b) cross section.

### 3.2. E-Tongue Training for Emerging Organic Contaminants Recognition

To train the e-tongue device, it is first necessary to find the “calibration curves” for the individual compounds. For that, i.e. to analyze their degradation pathway, impedance spectra of the sensors when immersed in effluent spiked with the EOCs, at different concentrations, were acquired.

The PCA method was applied to carry out an exploratory analysis of the obtained impedance data, though the reduction of the size of data and the creation of a new space of orthogonal components, in which different concentration patterns can be observed. Figure 3 presents the PCA score plot of the measured impedance data (see spectra in Figure S2 in the Supplementary Materials), obtained when the five sensors (composition on Figure S1 in Supplementary Materials; (PEI/PSS)<sub>5</sub> onto 10 μm interdigitated electrode, (PEI/PSS)<sub>5</sub> onto 200 μm interdigitated electrode, TiO<sub>2</sub> onto 10 μm interdigitated electrode, ZnO onto 10 μm interdigitated electrode, and TiO<sub>2</sub>/ZnO onto 10 μm interdigitated electrode) were immersed in effluent that was spiked with the four EOCs at different concentrations. Correspondingly, the reproducibility of the measurements for the lowest concentrations (0.1 mg/L, more susceptible to error), for each sensor for each compound can be observed in Figure S3 (in Supplementary Materials).

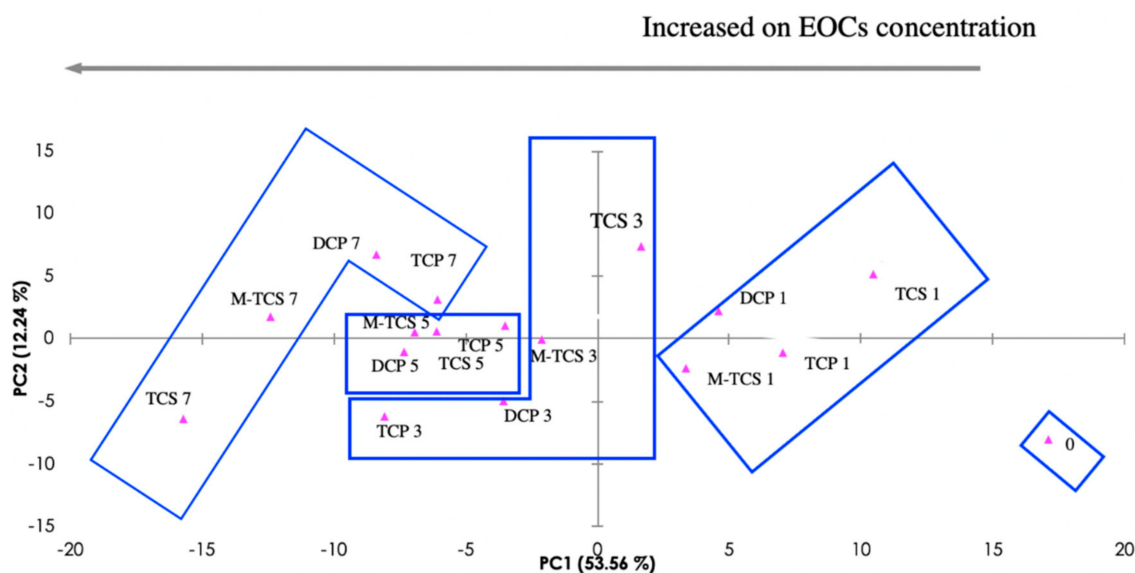


**Figure 3.** Principal component analysis (PCA) Score plot for the electronic tongue (five types of sensors) for 2,4,6-Trichlorophenol (TCP), 2,4-Dichlorophenol (DCP), triclosan (TCS), and metabolite methyl-triclosan (M-TCS)) individual measurements in the range of concentration 0, 1, 3, 5, 7, that correspond to the effluent as sampled, and effluent spiked with 0.1, 0.3, 0.5 and 0.7 mg emerging organic contaminants/L (EOCs/L).

On the PCA plot, as shown in Figure 3, the resulting analyte clustering by concentration are represented. The first two components of the PCA explain 65.80% of the observed variation. The plot observation supports the ability of the e-tongue device to “recognize” between individual EOCs-spiked effluents and raw effluent (non-spiked) matrices. A trend along the first component (PC1), according to the analyte concentrations might be observed on the plot, where the concentration increases from right to left across PC1 axis, moving away from concentration zero, and thus supporting the potential of the e-tongue device to discriminate quantitatively individual EOCs.

It was possible to determine individual “calibration curves” through the first two principal components data (Figure S4 in Supplementary Materials). These estimated curves are useful tools for a semi-quantitative extrapolation of the EOCs’ during EFR monitoring, where the effluent has a mix contamination. It was observed that the best fitting is not linear, as it is usually demanded and seen in chromatography methods [28], but polynomial, where the measure of goodness-of-fit observed ranged from  $R^2 = 0.86$  (TCP) to  $R^2 = 0.99$  (TCS).

### 3.3. E-tongue Performance for Emerging Organic Contaminants Semi-Quantification

Figure 4 shows the PCA plot from the normalized impedance data that were obtained by the customized e-tongue for the EFR treatment dataset. The dataset is composed by the analysed aliquots that were collected every 15 min in the course of the EFR treatment (120 min;  $t_0$ – $t_{120}$ ). A pattern in the plot, through the two first principal components, related to the time of EFR treatment is identifiable. The first two components of the PCA explain 77.27% of the observed variation. This observable trend supports the device responsiveness towards the EOCs decreasing concentration (observation that is supported by HPLC data) across time. The trend follows a similar behaviour from that observed for the individual EOCs measurements, as on the mixed EOCs measurements are the highest concentrations that drift away from concentration zero (see Figure S5 in Supplementary Materials). As noted for the individual EOCs calibration plot (Figure 3), the e-tongue, when monitoring the mixed EOCs in the effluent (Figure 4), is also able to “recognize” between EOCs-spiked effluent and raw effluent (non-spiked) matrices.

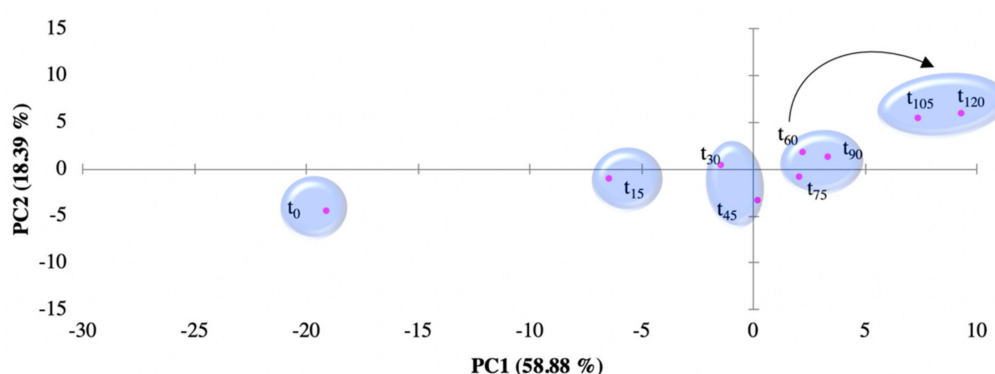


**Figure 4.** PCA Score plot for electrochemical flow reactor (EFR) degradation path measured by the electronic tongue in the effluent spiked with the four EOCs:  $t_0$  to  $t_{120}$  correspond to sampling every 15 min.

A three-dimensional (3D) plot was developed (Figure 5), by adding to the PC1 and PC2 data axis, a Z axis with the EOCs concentration values  $t_0$  cross-check the individual EOCs e-tongue semi-quantitative “sensorial signal” (Figure 3) with the mixed EOCs “sensorial signal” at the end of EFR treatment (Figure 4). The purpose of adding the z axis was to allow for a visual evaluation of the concentration range dimension obtained for the EOCs at the end of EFR treatment. Three parameters compose the plot data: (1) the EOCs estimated concentrations by HPLC at  $t_{120}$  (TCP = 0.3 mg/L; DCP = 0.45 mg/L; TCS = 0.03 mg/L; and, M-TCS = 0.29 mg/L) and (2) the PC1 and PC2 data attained from Figure 4 at  $t_{120}$  (pink dots); (3) the interpolated PC1 and PC2 values from the data in Figure 3 that are close to the HPLC estimated concentrations (TCP = 0.3 mg/L; DCP = 0.5 mg/L; TCS = 0.0 mg/L; and, M-TCS = 0.3 mg/L) for each of the EOCs at  $t_{120}$  (blue dots)

It is observed on Figure 5 that, for TCS and M-TCS, the distance between the interpolation points and the calibration points was lower, when compared with DCP and TCP. It is important to refer that TCP and DCP are the most common by-products for the TCS and M-TCS degradation pathway, and thus they are created at the same time that they are degraded, which might explain the experimental results for these compounds.

Additionally, it was also important to understand which individual sensor, of the multi sensor e-tongue, had the higher influence in the impedance “sensorial signal” for each EOCs. Thus, for TCS and M-TCS, the best response was obtained with  $\text{TiO}_2/\text{ZnO}$ , with the first two components of the PCA explaining 96.65% and 96.92% (see PCA data on Supplementary Materials, Figure S6a,b) of the total variance, respectively. For TCP, the best semi-qualitative analysis was achieved while using the  $\text{TiO}_2$  sensor, with the first two components of the PCA explaining 99.96% (see PCA data on Supplementary Materials, Figure S6c) of the total variance. Finally, for DCP, and apart from the

others three EOCs, the (PEI/PSS)<sub>5</sub> sensor with 10 µm interdigitated gold electrode had the highest semi-qualitative response with the first two components of the PCA, explaining 98.68% (see PCA data on Supplementary Materials, Figure S6d) of the total variance.

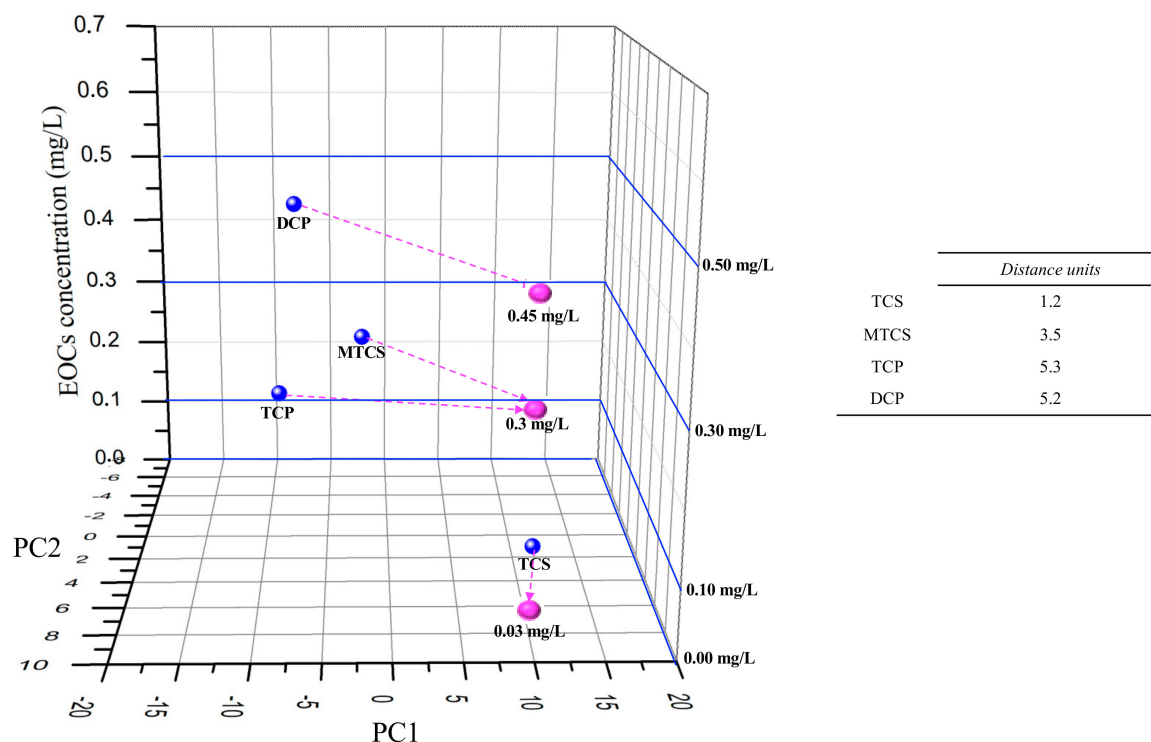


**Figure 5.** Visual evaluation of individual EOCs e-tongue semi-quantitative “sensory signal” (individual vs mix measurements). Blue dots: EOCs Individual PC1 and PC2 data from Figure 3; Pink dots: high-performance liquid chromatography (HPLC) EOCs estimated concentrations for PC1 and PC2 data attained from Figure 4 at  $t_{120}$ .

Figure 6 presents the same methodology for TCP and DCP, but only with TiO<sub>2</sub> or (PEI/PSS)<sub>5</sub> sensor impedance data for the semi-quantitative analysis of TCP and DCP.

Hence, analysing Figure 6, the distance between the interpolation points and the calibration points was lower (distance units decreased 3.2 to DCP and 1.8 to TCP), while comparing to Figure 5 e-tongue multisensory analyses for DCP and TCP.

The experimental data points to the importance of the nanomaterial used to build the e-tongue that will influence the impedance response as the thin film final morphology, structure, and properties of the thin films, and their consequent interactions with the different EOCs’ physical-chemical behaviour on the effluent matrix [29].

According to [30] reported data, the thickness of the film is related to the hydrophobic or hydrophilic final character. Thus, the film presents a more hydrophobic character when the thickness is higher. The thin film morphology of the tested sensors, as presented at Figure 2a, suggests a hydrophilic character for all the films tested, although, as the thickness increases, the hydrophobic characters also increase (Figure 2a, (PEI/PSS)<sub>5</sub> < rough surface < TiO<sub>2</sub>/ZnO). According to the experimental data, the thin films with more “hydrophobic character”, due to film thickness, such as the TiO<sub>2</sub>/ZnO and ZnO thin films presented better impedance responses in the semi-quantitative analysis of TCS and M-TCS, the analytes with higher Log  $k_{ow}$  (Table S1 in Supplementary Materials).

For the sensors that were considered to be “more hydrophilic”, the TiO<sub>2</sub> and (PEI/PSS)<sub>5</sub> films presented the best responses for DCP and TCP, the less lipophilic analytes. To DCP, for instance, the higher porous size in the films with higher thickness, endorsed the molecule “semi-permeability” through the thin film net, “giving” to the molecules a fluid character, which may be masking their

detection. Thus, in the  $\text{TiO}_2/\text{ZnO}$  and  $\text{ZnO}$  thin films (“hydrophobic character”), the phenolic molecules movement will be faster than the detection, not allowing for the complete analysis understanding. In the polyelectrolytes thin film,  $(\text{PEI}/\text{PSS})_5$ , this behaviour does not occur, since the film layers are organic and without hole structures, only providing an impedance response to the electronegativity of the DCP and TCP, as the film combination is itself negatively charged.

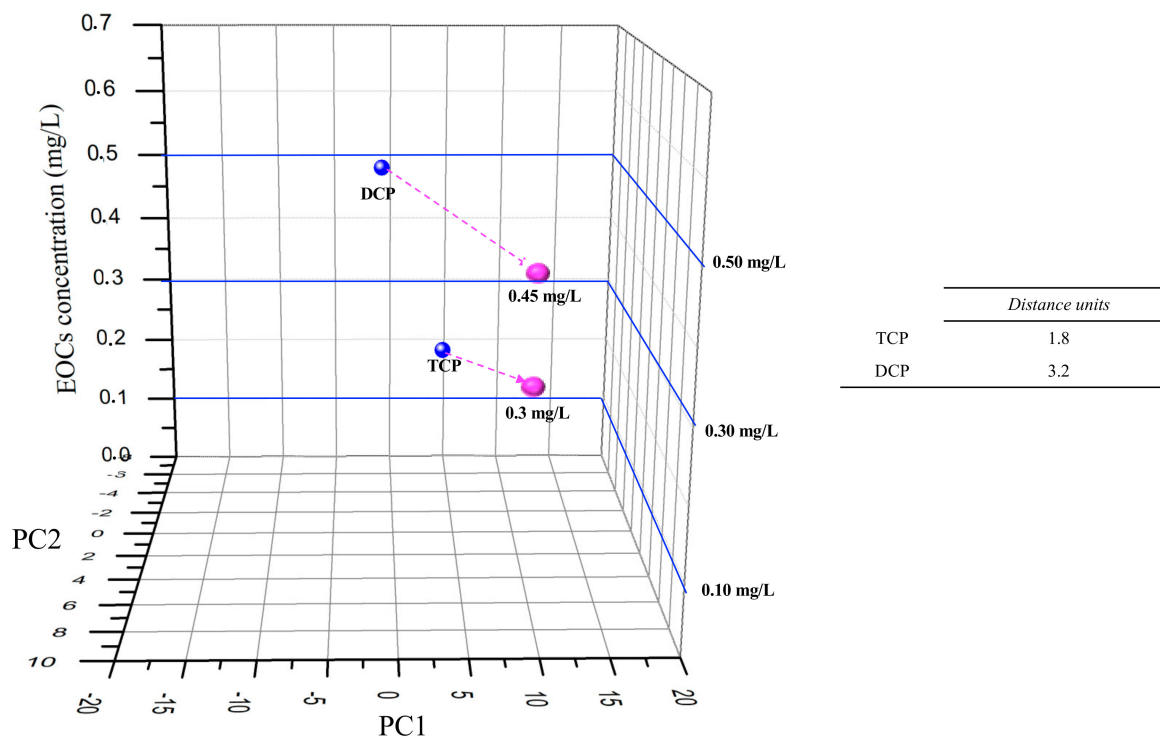


**Figure 6.** Visual evaluation of individual semi-quantitative “sensorial signal” (individual vs mix measurements) for TCP with  $\text{TiO}_2$  sensor and for DCP with  $(\text{PEI}/\text{PSS})_5$  sensor. Blue dots: EOCs individual PC1 and PC2 data for TCP with  $\text{TiO}_2$  sensor and for DCP with  $(\text{PEI}/\text{PSS})_5$  sensor; Pink dots: HPLC EOCs estimated concentrations for PC1 and PC2 data attained from Figure 4 at  $t_{120}$ .

#### 4. Conclusions

At an electrochemical reactor’s outlet a customized e-tongue was attached, which was composed of five sensors, built up with layer-by-layer and sputtering thin-films, to access the degradation monitoring of TCS, M-TCS, DCP, and TCP. Three main issues were evaluated to analyse this hypothesis: (1) characterization of the thin-films; (2) e-tongue training for the recognition of the different EOCs; and, (3) e-tongue array performance in the detection and semi-quantification of the EOCs in a mix contaminated effluent. Therefore, performing impedance measurements into the e-tongue array, was observed analytes clustering by concentration in the calibration curves, where the first two components of the PCA explained 65.80% of the total variance. The e-tongue array showed responsiveness towards the EOCs decreasing concentrations during the electrochemical treatment, showing a pattern trend through the first two principal components, being explained by 77.27% of the total variance. The e-tongue recognized between individual EOCs-spiked effluents and raw effluent (non-spiked) matrices. At the end of the treatment,  $t_{120}$ , the cross-check of the analytes individual semi-quantification was achieved for TCS and M-TCS with the e-tongue array. For DCP and TCP, better results were accomplished with a single sensor,  $(\text{PEI}/\text{PSS})_5$  with  $10\ \mu\text{m}$  interdigitated gold electrode and  $\text{TiO}_2$ , respectively. The characterization of thin films, while using field emission scanning electron microscope, allowed for a total understanding of the “sensorial” impedance response. The present study suggests innovative alternatives for complementing the traditional analysis with sensors devices,



since the customized e-tongue was capable of semi-qualitative analyses through electro-dynamic degradation's kinetics.

**Supplementary Materials:** The following are available online at <http://www.mdpi.com/1424-8220/19/24/5349/s1>, Figure S1. Scheme of the thin films used in the electronic tongue array; Figure S2. Resistance impedance spectra of each sensor device under study to TCP; DCP, TCS and M-TCS; Figure S3. Resistance impedance spectra of each sensor device under study to the effluent spiked with 0.1 mg/L of TCP; DCP, TCS and M-TCS (Reproducibility of  $n = 3$  impedance measurements); Figure S4. Electronic tongue calibration curves for each EOCs under study: TCP, DCP, TCS and M-TCS, in the range of concentration: 0–0.8 ppm (x axis): data from Figure 3, first component PC1 (y axis); Figure S5. EFR degradation path measured by an electronic tongue in the effluent with the 4 EOCs: 0 mg/L (non-spiked);  $t_0$  to  $t_{120}$  (spiked with the 4 EOCs) sampled every 15 min; Figure S6. PCA Score plot for the best sensors, concerning effluent spiked (0–0.7 mg/L) with the 4 EOCs. Table S1. Chemical properties of the EOCs under study; Table S2. Average and standard deviation error to the electronic tongue presented at Figure 4.

**Author Contributions:** Conceptualization, C.M. and S.S.; Data curation, C.M.; Formal analysis, E.P.M., J.M.P.-G., S.S., M.R. and A.B.R.; Funding acquisition, M.R. and A.B.R.; Methodology, C.M.; Project administration, M.R. and A.B.R.; Resources, E.P.M., M.R. and A.B.R.; Supervision, E.P.M., J.M.P.-G. and A.B.R.; Validation, E.P.M., J.M.P.-G., M.R. and A.B.R.; Writing—original draft, C.M.; Writing—review & editing, C.M., E.P.M., J.M.P.-G., S.S. and A.B.R.

**Funding:** This study was partially funded by Fundação para a Ciência e a Tecnologia through projects UID/AMB/04085/2019, UID/FIS/00068/2019 and PTDC/FIS-NAN/0909/2014. This work has received funding from the European Union's Horizon 2020 research and innovation programme under the Marie Skłodowska-Curie grant agreement No. 778045. C. Magro acknowledges Fundação para a Ciência e a Tecnologia for her PhD fellowship SFRH/BD/114674/2016.

**Acknowledgments:** This research was anchored by the RESOLUTION LAB, an infrastructure at NOVA School of Science and Technology. C. Magro acknowledges Fundação para a Ciência e a Tecnologia for her PhD fellowship SFRH/BD/114674/2016. The authors thank Ricardo Faria for his help with the reactors drawing.

**Conflicts of Interest:** The authors declare no conflict of interest.

## References

1. United Nations. *World Population Prospects 2019 (ST/ESA/SER.A/423)*; United Nations Department of Economic and Social Affairs: New York, NY, USA, 2019.
2. Corcoran, E.; Nellemann, C.; Baker, E.; Bos, R.; Osborn, D.; Savelli, H. *Sick Water? The Central Role of Wastewater Management in Sustainable Development*; UNEP/Earthprint: Nairobi, Kenya, 2010; ISBN 9788277010755.
3. Daughton, C.G. Non-regulated water contaminants: Emerging research. *Environ. Impact Assess. Rev.* **2004**, *24*, 711–732. [[CrossRef](#)]
4. Geissen, V.; Mol, H.; Klumpp, E.; Umlauf, G.; Nadal, M.; Van Der Ploeg, M.; Van De Zee, S.E.A.T.M.; Ritsema, C.J. Emerging pollutants in the environment: A challenge for water resource management. *Int. Soil Water Conserv. Res.* **2015**, *3*, 57–65. [[CrossRef](#)]
5. Sirés, I.; Oturan, N.; Oturan, M.A.; Rodríguez, R.M.; Garrido, J.A.; Brillas, E. Electro-Fenton degradation of antimicrobials triclosan and triclocarban. *Electrochim. Acta* **2007**, *52*, 5493–5503. [[CrossRef](#)]
6. Daughton, C.G.; Ternes, T.A. Pharmaceuticals and personal care products in the environment: Agents of subtle change? *Environ. Health Perspect.* **1999**, *107*, 907–938. [[CrossRef](#)]
7. Rivera-Utrilla, J.; Sánchez-Polo, M.; Ferro-García, M.Á.; Prados-Joya, G.; Ocampo-Pérez, R. Pharmaceuticals as emerging contaminants and their removal from water. A review. *Chemosphere* **2013**, *93*, 1268–1287. [[CrossRef](#)]
8. López-Serna, R.; Petrović, M.; Barceló, D. Occurrence and distribution of multi-class pharmaceuticals and their active metabolites and transformation products in the Ebro River basin (NE Spain). *Sci. Total Environ.* **2012**, *440*, 280–289. [[CrossRef](#)]
9. Jurado, A.; López-Serna, R.; Vázquez-Suné, E.; Carrera, J.; Pujades, E.; Petrovic, M.; Barceló, D. Occurrence of carbamazepine and five metabolites in an urban aquifer. *Chemosphere* **2014**, *115*, 47–53. [[CrossRef](#)]
10. Paíga, P.; Santos, L.H.M.L.M.; Ramos, S.; Jorge, S.; Silva, J.G.; Delerue-Matos, C. Presence of pharmaceuticals in the Lis river (Portugal): Sources, fate and seasonal variation. *Sci. Total Environ.* **2016**, *573*, 164–177. [[CrossRef](#)]
11. Roberts, J.; Kumar, A.; Du, J.; Hepplewhite, C.; Ellis, D.J.; Christy, A.G.; Beavis, S.G. Pharmaceuticals and personal care products (PPCPs) in Australia's largest inland sewage treatment plant, and its contribution to a major Australian river during high and low flow. *Sci. Total Environ.* **2016**, *541*, 1625–1637. [[CrossRef](#)]

12. Wu, Y.; Yu, C.P.; Yue, M.; Liu, S.P.; Yang, X.Y. Occurrence of selected PPCPs and sulfonamide resistance genes associated with heavy metals pollution in surface sediments from Chao Lake, China. *Environ. Earth Sci.* **2016**, *75*, 1–8. [[CrossRef](#)]
13. Aranami, K.; Readman, J.W. Photolytic degradation of triclosan in freshwater and seawater. *Chemosphere* **2007**, *66*, 1052–1056. [[CrossRef](#)] [[PubMed](#)]
14. Constantin, L.A.; Nitoi, I.; Cristea, N.I.; Constantin, M.A. Possible degradation pathways of triclosan from aqueous systems via TiO<sub>2</sub> assisted photocatalysis. *J. Ind. Eng. Chem.* **2018**, *58*, 155–162. [[CrossRef](#)]
15. Hua, W.; Bennett, E.; Letcher, R. Triclosan in waste and surface waters from the upper Detroit River by liquid chromatography-electrospray-tandem quadrupole mass spectrometry. *Environ. Int.* **2005**, *31*, 621–630. [[CrossRef](#)] [[PubMed](#)]
16. McAvoy, D.C.; Schatowitz, B.; Jacob, M.; Hauk, A.; Eckhoff, W.S. Measurement of triclosan in wastewater treatment systems. *Environ. Toxicol. Chem.* **2002**, *21*, 1323–1329. [[CrossRef](#)]
17. Guo, J.-H.; Li, X.-H.; Cao, X.-L.; Li, Y.; Wang, X.-Z.; Xu, X.-B. Determination of triclosan, triclocarban and methyl-triclosan in aqueous samples by dispersive liquid–liquid microextraction combined with rapid liquid chromatography. *J. Chromatogr. A* **2009**, *1216*, 3038–3043. [[CrossRef](#)]
18. Balmer, M.E.; Poiger, T.; Droz, C.; Romanin, K.; Bergqvist, P.A.; Müller, M.D.; Buser, H.R. Occurrence of methyl triclosan, a transformation product of the bactericide triclosan, in fish from various lakes in Switzerland. *Environ. Sci. Technol.* **2004**, *38*, 390–395. [[CrossRef](#)]
19. Xing, L.; Sun, J.; Liu, H.; Yu, H. Combined toxicity of three chlorophenols 2,4-dichlorophenol, 2,4,6-trichlorophenol and pentachlorophenol to *Daphnia magna*. *J. Environ. Monit.* **2012**, *14*, 1677–1683. [[CrossRef](#)]
20. Zhao, N.; Li, X.; Jin, X.; Angelidaki, I.; Zhang, Y. Integrated electrochemical-biological process as an alternative mean for ammonia monitoring during anaerobic digestion of organic wastes. *Chemosphere* **2018**, *195*, 735–741. [[CrossRef](#)]
21. Vlasov, Y.; Legin, A.; Rudnitskaya, A.; Di Natale, C.; D’Amico, A. Nonspecific sensor arrays (“electronic tongue”) for chemical analysis of liquids ( IUPAC Technical Report ). *Pure Appl. Chem.* **2005**, *77*, 1965–1983. [[CrossRef](#)]
22. Magro, C.; Mateus, E.P.; Raposo, M.; Ribeiro, A.B. Overview of electronic tongue sensing in environmental aqueous matrices: Potential for monitoring emerging organic contaminants. *Environ. Rev.* **2019**, *27*, 202–214. [[CrossRef](#)]
23. Mimendia, A.; Gutiérrez, J.M.; Leija, L.; Hernández, P.R.; Favari, L.; Muñoz, R.; del Valle, M. A review of the use of the potentiometric electronic tongue in the monitoring of environmental systems. *Environ. Model. Softw.* **2010**, *25*, 1023–1030. [[CrossRef](#)]
24. Campos, I.; Alcañiz, M.; Aguado, D.; Barat, R.; Ferrer, J.; Gil, L.; Marrakchi, M.; Martínez-Mañez, R.; Soto, J.; Vivancos, J.-L. A voltammetric electronic tongue as tool for water quality monitoring in wastewater treatment plants. *Water Res.* **2012**, *46*, 2605–2614. [[CrossRef](#)] [[PubMed](#)]
25. Cetó, X.; González-Calabuig, A.; del Valle, M. Use of a bioelectronic tongue for the monitoring of the photodegradation of phenolic compounds. *Electroanalysis* **2015**, *27*, 225–233. [[CrossRef](#)]
26. Facure, M.H.M.; Mercante, L.A.; Mattoso, L.H.C.; Correa, D.S. Detection of trace levels of organophosphate pesticides using an electronic tongue based on graphene hybrid nanocomposites. *Talanta* **2017**, *167*, 59–66. [[CrossRef](#)]
27. Liu, X.; Feng, H.; Liu, X.; Wong, D.K.Y. Electrocatalytic detection of phenolic estrogenic compounds at NiTPPS/carbon nanotube composite electrodes. *Anal. Chim. Acta* **2011**, *689*, 212–218. [[CrossRef](#)]
28. Oliveira, O.N.; Raposo, M.; Dhanabalan, A. Langmuir-blodgett and self-assembled polymeric films. In *Handbook of Surfaces and Interfaces of Materials*; Nalwa, H.S., Ed.; Elsevier: Burlington, NJ, USA, 2001; pp. 1–63. ISBN 978-0-12-513910-6.
29. Riul, A.; Dos Santos, D.S.; Wohnrath, K.; Di Tommazo, R.; Carvalho, A.C.P.L.F.; Fonseca, F.J.; Oliveira, O.N.; Taylor, D.M.; Mattoso, L.H.C. Artificial taste sensor: Efficient combination of sensors made from Langmuir-Blodgett films of conducting polymers and a ruthenium complex and self-assembled films of an azobenzene-containing polymer. *Langmuir* **2002**, *18*, 239–245. [[CrossRef](#)]
30. Paulovich, F.V.; De Oliveira, M.C.F.; Oliveira, O.N. A future with ubiquitous sensing and intelligent systems. *ACS Sens.* **2018**, *3*, 1433–1438. [[CrossRef](#)]

31. Riul, A.; Dantas, C.A.R.; Miyazaki, C.M.; Oliveira, O.N. Recent advances in electronic tongues. *Analyst* **2010**, *135*, 2481–2495. [[CrossRef](#)]
32. Magro, C.; Zagalo, P.M.; Mateus, E.P.; Ribeiro, A.B.; Ribeiro, P.A.; Raposo, M. Triclosan Detection in Aqueous Environmental Matrices by Thin-films Sensors: Impedantometric Electronic Tongue. In Proceedings of the 7th International Symposium on Sensor Science, Napoli, Italy, 9–11 May 2019; MDPI: Basel, Switzerland, 2019; pp. 1–4.
33. Zhu, X.; Tang, F.; Suzuki, T.S.; Sakka, Y. Role of the initial degree of ionization of polyethylenimine in the dispersion of silicon carbide nanoparticles. *J. Am. Ceram. Soc.* **2003**, *86*, 189–191. [[CrossRef](#)]
34. Raposo, M.; Lourenço, J.M.C.; Botelho do Rego, A.M.; Ferraria, A.M.; Ribeiro, P.A. Counterions - A new approach to control the degree of ionization of polyelectrolytes in layer-by-layer films. *Colloids Surf. A Physicochem. Eng. Asp.* **2012**, *412*, 1–10. [[CrossRef](#)]
35. Lourenço, J.M.C.; Ribeiro, P.A.; Do Rego, A.M.B.; Fernandes, F.M.B.; Moutinho, A.M.C.; Raposo, M. Counterions in poly(allylamine hydrochloride) and poly(styrene sulfonate) layer-by-layer films. *Langmuir* **2004**, *20*, 8103–8109. [[CrossRef](#)] [[PubMed](#)]
36. Zhu, B.L.; Xie, C.S.; Wang, W.Y.; Huang, K.J.; Hu, J.H. Improvement in gas sensitivity of ZnO thick film to volatile organic compounds (VOCs) by adding TiO<sub>2</sub>. *Mater. Lett.* **2004**, *58*, 624–629. [[CrossRef](#)]
37. Chaudhary, S.; Umar, A.; Bhasin, K.K.; Baskoutas, S. Chemical sensing applications of ZnO nanomaterials. *Materials* **2018**, *11*, 1–38. [[CrossRef](#)] [[PubMed](#)]
38. Siopa, D.; Sérgio, S.; Jorge, M.E.M.; Viana, A.S.; Gomes, A. ZnO seed layers prepared by DC reactive magnetron sputtering to be applied as electrodeposition substrates. *J. Electrochem. Soc.* **2016**, *163*, H697–H704. [[CrossRef](#)]
39. De Souza, N.C.; Silva, J.R.; Pereira-da-Silva, M.A.; Raposo, M.; Faria, R.M.; Giacometti, J.A.; Oliveira, O.N. Dynamic scale theory for characterizing surface morphology of layer-by-layer films of poly(o-methoxyaniline). *J. Nanosci. Nanotechnol.* **2004**, *4*, 548–552. [[CrossRef](#)]



© 2019 by the authors. Licensee MDPI, Basel, Switzerland. This article is an open access article distributed under the terms and conditions of the Creative Commons Attribution (CC BY) license (<http://creativecommons.org/licenses/by/4.0/>).



## Paper

*“Exploring hydrogen production for self-energy generation in electroremediation: a proof of concept”*

*C Magro, J Almeida, JM Paz-Garcia, EP Mateus & AB Ribeiro*

*Published in: Applied Energy, 2019*





# Exploring hydrogen production for self-energy generation in electroremediation: A proof of concept

C. Magro<sup>a,\*</sup>, J. Almeida<sup>a,1</sup>, J.M. Paz-Garcia<sup>b</sup>, E.P. Mateus<sup>a</sup>, A.B. Ribeiro<sup>a,\*</sup>

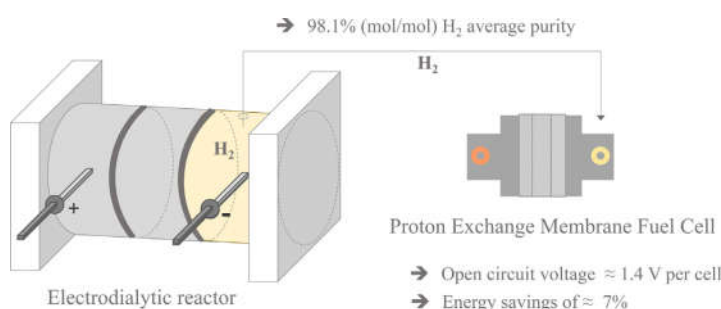
<sup>a</sup> CENSE, Department of Sciences and Environmental Engineering, NOVA School of Science and Technology, NOVA University Lisbon, Caparica Campus, 2829-516 Caparica, Portugal

<sup>b</sup> Department of Chemical Engineering, Faculty of Sciences, University of Malaga, Teatinos Campus, 29010 Málaga, Spain

## HIGHLIGHTS

- Self-produced H<sub>2</sub> from electrodialytic treatment of environmental matrices collected.
- Collected H<sub>2</sub> average purity (% mol/mol) of ≈ 98%.
- A fuel cell used to produce electricity from the self-produced H<sub>2</sub> (~1 V).
- Experimental self-generated energy promotes savings on electroremediation (≈ 7%).

## GRAPHICAL ABSTRACT



## ARTICLE INFO

### Keywords:

Electrodialytic treatment  
Hydrogen production  
Proton-exchange membrane fuel cell  
Energy savings

## ABSTRACT

Electrodialytic technologies are clean-up processes based on the application of a low-level electrical current to produce electrolysis reactions and the consequent electrochemically-induced transport of contaminants. These treatments inherently produce electrolytic hydrogen, an energy carrier, at the cathode compartment, in addition to other cathode reactions. However, exploring this by-product for self-energy generation in electroremediation has never been researched. In this work we present the study of hydrogen production during the electrodialytic treatment of three different environmental matrices (briny water, effluent and mine tailings), at two current intensities (50 and 100 mA). In all cases, hydrogen gas was produced with purities between 73% and 98%, decreasing the electrical costs of the electrodialytic treatment up to ≈ 7%. A proton-exchange membrane fuel cell was used to evaluate the possibility to generate electrical energy from the hydrogen production at the cathode, showing a stable output (~1 V) and demonstrating the proof of concept of the process.

## 1. Introduction

Global energy demands from an increasing human population is a major concern for the planet sustainability. Extensive research and technology development have been focused on renewable energy sources and other strategies to reduce CO<sub>2</sub> emissions [1]. Fuel cell

technology, which can efficiently generate electricity using hydrogen as fuel, has attracted widespread attention in recent years [2]. The proton-exchange membrane fuel cells success depends on their ability to obtain optimal fuel to electricity conversion with a high current density, as well as the sustainable and economical production of the fuel [3]. Pure hydrogen gas is scarce in Earth's atmosphere. However, it can be

\* Corresponding authors.

E-mail addresses: [c.magro@campus.fct.unl.pt](mailto:c.magro@campus.fct.unl.pt) (C. Magro), [abr@fct.unl.pt](mailto:abr@fct.unl.pt) (A.B. Ribeiro).

<sup>1</sup> The authors had an equal contribution.

produced from different primary-energy sources. For instance, it can be generated from fossil fuels through steam reforming, partial oxidation or gasification and from renewable sources through biomass gasification and water electrolysis [4,5]. Generation of H<sub>2</sub> via water electrolysis is still limited by the high cost, namely  $\approx 3.8$  times more expensive than gasification, and  $\approx 5$  times more expensive than from methane steam reforming [6]. Hence, steam reforming, which combines high-temperature steam with natural gas, currently accounts for the majority of the H<sub>2</sub> produced. Hydrogen production via water electrolysis is currently only applied in combination with renewable energy sources, like solar or wind, and used as an energy storage system.

Electro-based technologies, such as electrokinetic and electro-dialytic processes, have been the focus of vast environmental remediation research over the last three decades [7,8], both *in-situ* [9,10], and *ex-situ* [11–13]). Despite such research efforts, the technology readiness level (TRL) for many of those technologies remains very low; although most are considered promising, many are far from being introduced as efficient processes into the market. Important barriers need to be overcome to reach high TRLs [14]. Operational energy costs have to be considered and, are related not only to the electrolysis reactions but mainly with the stirring, the ohmic losses and the energy required for the transport of charge through the porous matrix. In fact, the distance between electrodes (cell size) plays a crucial role in the energy costs of the specific-energy required for the target contaminants removal [7,15]. To the best of our knowledge, there has been minimal research conducted related to the reuse of the elemental gases produced in the electrolysis reactions during electrochemically-induced treatments. The drawbacks found in the current literature are associated to the reactors' design. Most electrokinetic and electro-dialytic (ED) setups are designed to allow for the produced gases to flow freely into the atmosphere, while aiming to reduce pressure-related transport mechanisms. Thus, a gas collection strategy during the treatment is not included in the system, causing gas losses to the atmosphere. As a novel feature, the H<sub>2</sub> produced during the treatment at the cathode compartment may be used as fuel in a proton-exchange membrane fuel cells to produce electrical energy and reduce the energy costs of electro-remediation. Additionally, as an energy carrier, H<sub>2</sub> can be used to accumulate energy during the electric power demand valleys, and to generate electric power during the peaks. Therefore, a reservoir can be integrated into the ED system where it can recover and use the H<sub>2</sub> produced for different purposes.

This work evidences the possibility of using the H<sub>2</sub> produced during electrochemically-induced remediation of three different environmental matrices: (1) moderately-salted water – briny water, (2) secondary effluent from a wastewater treatment plant, and (3) mine tailings. Our proof of concept demonstrates that the H<sub>2</sub> captured and reused from these ED treatments is feasible. Herein, a three-compartment ED set-up was used to minimize the interactions of the sample and the contaminants with the electrolysis reactions (Fig. 1).

## 2. Theory

### 2.1. Proton-exchange fuel cell

A fuel cell is an electrochemical device that converts the chemical energy from a fuel into electricity through the reaction of the fuel with oxygen or another oxidizing agent. For example, a proton-exchange membrane fuel cell (PEMFC) combines H<sub>2</sub> and O<sub>2</sub> to produce electricity and heat without emitting other products which are different from the water formed in the reaction Eq. (1) [16]:

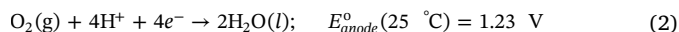


A fuel cell, unlike a battery, produces electricity as long as fuel is supplied, never losing its charge. The pollution-free production of energy and high power density makes the fuel cell technology a viable

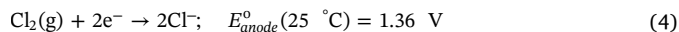
approach for future energy industries [2]. Fuel cells show high energy conversion efficiency, up to 60%, higher than traditional internal combustion engines [17]. This efficiency can increase up to 80% with heat-recovery systems [18].

### 2.2. Electro-based technologies

Electrokinetic and ED strategies are commonly applied to remove organic [19] and/or inorganic contaminants from soils or other porous matrices, such as sewage sludge, fly ash or construction materials [20–22]. The electrochemically-induced transport is based on the application of a low level direct current which promotes electrolysis reactions at the electrodes [20,23,24], involving in most cases water oxidation at the anode, Eq. (2), and water reduction at the cathode, Eq. (3):



Competing redox reactions may occur as, for example, the production of chlorine at the anode in systems with high chloride contents [25], Eq. (4):



or the deposition of metals (Me) at the cathode, Eq. (5):



The electrochemical-induced transport of chemical species takes place by three main transport mechanisms: electromigration, electro-osmosis, and electrophoresis. Diffusion and advection may also play an important role [20]. In the case of the ED process, electro-dialysis also occurs, as ion-exchange membranes are used to separate the matrix from the electrolyte compartments (aiming to control the pH conditions of the electrolytes and the treated matrix while improving the selectivity on the contaminant removal [20]). Over the years, different electro-based remediation set-ups have been proposed, where the configuration of the sample and the electrode compartments have been modified depending on the nature of the contaminant and matrix [26,27].

## 3. Materials and methods

### 3.1. Materials

The briny water solution was prepared with NaCl (PA grade, Merck, Germany) and tap water (Almada, Portugal). Effluent, the liquid fraction that results from wastewater treatments, was collected in the secondary clarifier at a wastewater treatment plant (Lisbon, Portugal). Mine tailings were collected at Panasqueira mine (Covilhã, Portugal, 40°10'11.0604"N, 7°45'23.8752"W). Panasqueira mine produces around 900 t WO<sub>3</sub>/year [28] and the pond where the residues are deposited is an open air impoundment that contains rejected ore concentrates with high metal levels [29]. The matrix used for this study is a rejected fraction from the sludge circuit, that is directly pumped to the Panasqueira dam.

### 3.2. Experimental set-up

The ED cell set-up was a 3 compartment acryl XT cell [30] (RIAS A/S, Roskilde, Denmark), as represented in Fig. 1. The internal diameter was 8 cm and the central and electrolyte compartments length were 5 cm. The two electrode compartments were separated from the central section by an anion exchange membrane, AR204SZRA, MKIII, Blank (Ionics, USA) and a cation exchange membrane, CR67, MKIII, Blank (Ionics, USA). The electrodes were made of Ti/MMO Permaskand wire:  $\varnothing = 3\text{ mm}$ ,  $L = 50\text{ mm}$  (Grønvold & Karnov A/S, Denmark). Ti/MMO



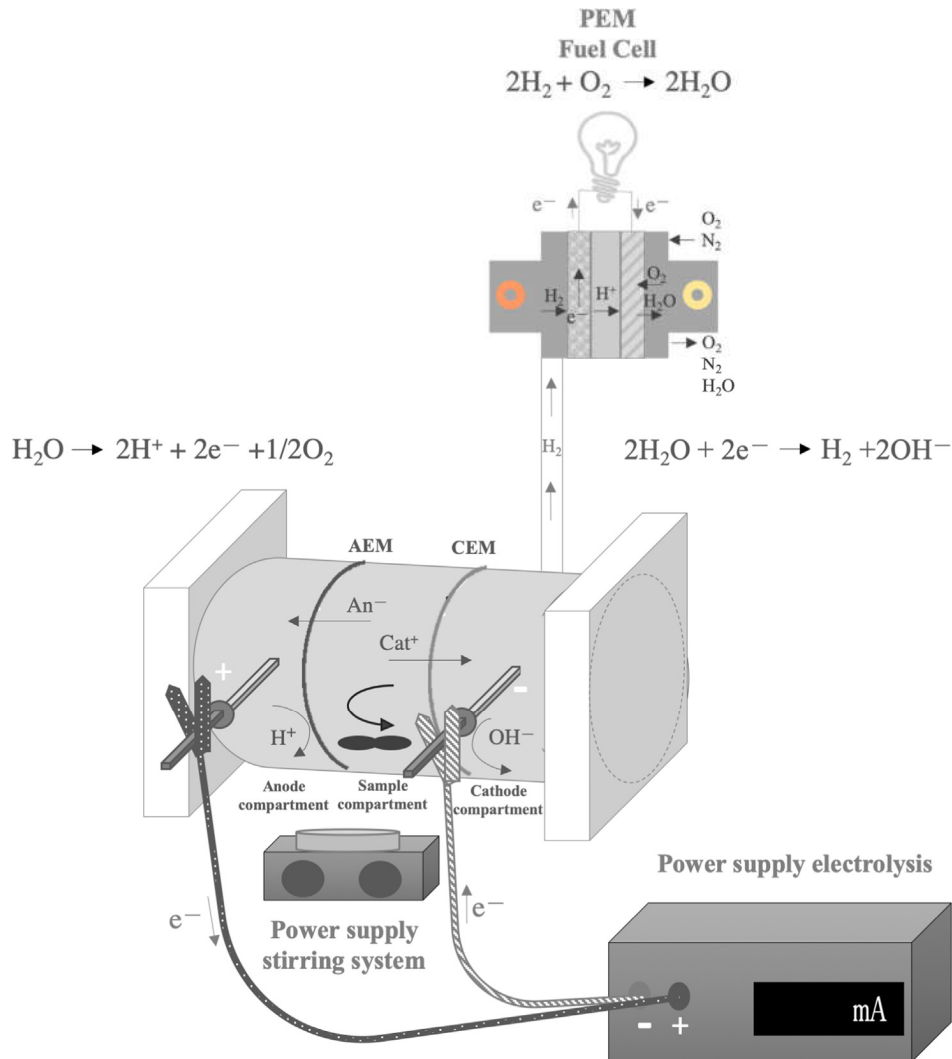


Fig. 1. Electrolytic cell with 3 compartments [ $\phi = 8$  cm, central and electrolyte compartments with  $L = 5$  cm, CEM – cation exchange membrane; AEM – anion exchange membrane,  $An^-$  – anions,  $Cat^+$  – cations], stirrer (only used for mine tailings suspension) connected to a proton-exchange membrane fuel cell.

anodes are used to degrade organic contaminants in wastewaters, and Ti/MMO is also applied as cathode to reduce chlorinated and nitro compounds in groundwater [31]. A power supply E3612A (Hewlett Packard, Palo Alto, USA) was used to maintain a constant current in the ED cell.

For briny water and effluent experiments, 250 mL of liquid sample was added to the central cell compartment. For the mine tailings experiments, suspensions were prepared at a liquid/solid (L/S) ratio of 9, by mixing 22.2 g of solid mine tailings within 200 mL of briny water. The anolyte and catholyte compartments were set with 250 mL of 0.01 M  $NaNO_3$ .

Twelve ED experiments were carried out in duplicate according to the conditions presented in Table 1. In experiments 1–6 the gas produced at the cathode, rich in  $H_2$ , was collected in a 30 mL storage cylinder (Horizon Fuel Cell Technologies, USA) (experimental scheme at supplementary data B.1), where the volume was verified every 10 min. In experiments 7–9, the cathode compartment exhaust was directly connected to the tedlar sample bag, single polypropylene fitting with 500 mL of capacity (SKC, USA), for purity analysis. In experiments 10–12, the cathode compartment exhaust was directly connected to the PEMFC. In all cases, the ED cell voltage and the fuel cell open circuit voltage were registered every 10 min. The fuel cell open circuit voltage was measured in order to validate the  $H_2$  catchment and conversion into power needs.

Table 1

Electrolytic experimental conditions.

Experiment ED	Code	Duration (h)	Current intensity (mA)
ED tests with gas capture at the cell cathode compartment (n = 2)			
1	BW 50	2	50
2	EF 50	2	50
3	BW 100	1	100
4	EF 100	1	100
5	MTBW 50	2	50
6	MTBW 100	1	100
ED tests to $H_2$ purity (n = 2)			
7	BW	6	100
8	EF	6	100
9	MTBW	6	100
ED tests with direct connection to PEMFC (n = 2)			
10	BW	1	100
11	EF	1	100
12	MTBW	1	100

BW-Briny Water; EF-Effluent; MT-Mine Tailings; PEMFC – Proton-Exchange Membrane Fuel Cell.

The single PEMFC (Horizon Fuel Cell Technologies, USA) was used ( $32 \times 32 \times 10$  mm), with a nominal voltage of  $\approx 1$  V. The PEMFC has a cathodic plate, designed as a part of the cell's membrane electrode

assembly that collects O<sub>2</sub> directly from the air by natural convection. PEMFC voltage and resistance were measured and monitored by a multimeter KT1000H (KIOTTO, Portugal).

### 3.3. Methods

pH and conductivity were measured at the beginning and at the end of all ED experiments, both in central and electrode compartments. Briny water, effluent and mine tailings pH were measured with a Radiometer pH-electrode EDGE (HANNA, USA), and conductivity was measured in a Radiometer Analytic LAQUA twin (HORIBA Ltd., Japan). The mine tailings pH and conductivity measurements are referred to the liquid phase resulting from the suspension from a liquid component (either deionized H<sub>2</sub>O or briny water), with a L/S ratio of 9.

Total concentrations of As, Ca, Cu, K, Mg, Na, P, S, Sn, W, and Zn were determined by Inductively Coupled Plasma with Optical Emission Spectrometry (ICP-OES) (HORIBA Jobin-Yvon Ultima, Japan), equipped with generator RF (40.68 MHz), monochromator Czerny-Turner with 1.00 m (sequential), automatic sampler AS500 and dispersive CMA-Concomitant Metals Analyser. Cl<sup>-</sup> and SO<sub>4</sub><sup>2-</sup> were analyzed by Ion Chromatography (IC) (DIONEX ICS-3000, USA), equipped with conductivity detector. To quantify the elements in the solid matrix, an acid extraction was carried out mixing 0.5 g of mine tailings, 3 mL of HCl (37%) and 9 mL of HNO<sub>3</sub> (65%) and, placed on a shaking table for 48 h at 125 rpm. For the IC analysis of the mine tailings (Cl<sup>-</sup> and SO<sub>4</sub><sup>2-</sup> content), microwave assisted acid extraction was carried out according to EPA method 3051 A: 0.5 g of mine tailings were placed in a vessel with 3 mL of HCl (37%), and 9 mL of HNO<sub>3</sub> (65%) and placed in a microwave Ethos (Milestone S.r.l, Bergamo, Italy). At the end, all the samples were diluted in deionized water (1:25), filtered by vacuum using 0.45 μm MFV3 glass microfibre filters (Filter lab, Barcelona, Spain) and analyzed by ICP-OES and IC.

The H<sub>2</sub> purity percentage was determined by Gas Chromatography Thermal Conductivity Detector (GC-TCD) using a Trace GC Ultra (Thermo Electron Corporation, USA), with a Carboxen 1010 plot column (length: 30 m, diameter: 0,32 mm). The analytical run was performed in an isothermal mode at 35 °C for 50 min. A gastight syringe (vici precision sampling, Baton Rouge, Louisiana, USA) was used to inject a volume of 250 μL (injector at 200 °C), detector/transfer line at 120 °C. To calculate the H<sub>2</sub> purity two methods were used: (1) internal linear calibration and response factor (H<sub>2</sub> peak area/response factor), where the standard deviation is related to error of these methods, by comparing with the injection of 100% H<sub>2</sub>; (2) molar proportions (mol/mol), were determined assuming air as impurity in the H<sub>2</sub>. Thus, the H<sub>2</sub> was calculated considering the number of H<sub>2</sub> mol in 100 mol of air (H<sub>2</sub> + air gases).

All sample analysis was carried out in duplicate. The data from the experiments were analyzed by the software Origin Pro 8.5 and the statistical data obtained by the GraphPad Prism version 7.0e. Statistically significant differences among samples for 95% level of significance were calculated through ANOVA tests.

## 4. Results and discussion

### 4.1. Matrix characterization

Matrices selection is an important step as the matrices' characteristics will affect H<sub>2</sub> purity and further energy generation. PEMFC, despite the robustness and stability, may be sensitive to contaminants in the fuel [32]. The briny water was chosen as a working system blank, where NaCl was added to emulate the effluent without interferences. Briny water, with sufficient ionic conductivity to maintain the current applied for the remediation period chosen (1 and 2 h), is typically used in systems for the electrolytic production of H<sub>2</sub>. The effluent and mine tailings are, individually, matrices with high potential to be reused as raw materials in several sectors. For example, ED treated effluent has

**Table 2**

Initial characterization of briny water, effluent and mine tailings.

	Matrix		
	BW*	EF**	MT*
pH	6.89 ± 0.08	7.67 ± 0.16	4.57 ± 1.74
Conductivity (mS/cm)	1.81 ± 0.11	2.41 ± 2.12	0.84 ± 0.52
ICP-OES analysis	(mg/L)	(mg/L)	(mg/kg)
Ca	29.06 ± 0.02	51.74 ± 18.34	91.11 ± 27.08
K	5.33 ± 0.01	47.80 ± 29.10	–
Mg	10.30 ± 0.38	118.00 ± 137.17	–
Na	602.5 ± 17.68	524.55 ± 532.55	–
P	0.07 ± 0.10	3.21 ± 0.04	36.57 ± 18.74
S	49.04 ± 26.07 <sup>a</sup>	84.89 ± 65.27	789.59 ± 214.13 <sup>A</sup>
As	<i>n.d.</i>	<i>n.d.</i>	218.57 ± 132.31
Cu	0.09 ± 0.01	0.04 ± 0.00	76.82 ± 39.30
Sn	<i>n.d.</i> <sup>b</sup>	<i>n.d.</i> <sup>b</sup>	1.95 ± 0.53 <sup>B</sup>
W	<i>n.d.</i> <sup>c</sup>	<i>n.d.</i> <sup>c</sup>	5.34 ± 1.42 <sup>C</sup>
Zn	1.07 ± 0.88	0.07 ± 0.06	–
IC analysis	(mg/L)	(mg/L)	(mg/kg)
Cl <sup>-</sup>	499.3 ± 8.1	908.1 ± 1013.7	5.6 ± 2.3
SO <sub>4</sub> <sup>2-</sup>	66.8 ± 1.5 <sup>de</sup>	149.45 ± 127.07 <sup>de</sup>	240.9 ± 4.6 <sup>D</sup>

BW-Briny Water; EF-Effluent; MT-Mine Tailings.

\*collected at 2-09-2018; \*\* collected at 5-09-2018 and 12-09-2018; nd- not detected.

Statistical analysis: Multiple comparisons were statistically performed at  $p < 0.05$  (95% confidence interval); data with lower case letters is statistically significantly different to the ones with the same capital letter.

recently been tested for cement based construction materials [33]. Mine tailings are an example of solid matrix that can be successfully treated via ED as stirred suspensions mixtures [34]. In these cases, H<sub>2</sub> production and exploitation is highly attractive, since it can allow the decrease of energy costs in an industrial scale application.

Table 2 presents the initial characterization of the three studied matrices. The matrices had enough initial conductivity to allow current passage and facilitate the electrolysis reactions to occur at the imposed rate. The initial pH of the studied matrices was in the range 4.6–7.7. Mine tailings were slightly acidic (pH ≈ 4.57), presenting a high concentration of arsenic (218.57 ± 132.31 mg As/kg), and significant amounts of other metals (76.82 ± 39.30 mg Cu/kg, 1.95 ± 0.53 mg Sn/kg and 5.34 ± 1.42 mg W/kg), as well as a high sulfur content (240.9 ± 4.6 mg/kg).

The ED process was applied to briny water, effluent and mine tailings suspension in briny water. In all cases, the pH at the anode compartment decreased to ~2 and the pH at the cathode compartment increased until ~12. The pH at the central compartment also decreased in all cases. This phenomenon was expected as anion exchange membranes are known to have limited perm-selectivity, which means that only protons (H<sup>+</sup>) are able to cross this membrane. The acidification of the central compartment was more noticeable in the experiments at 100 mA (Fig. 2). The acidification phenomena proved to be influenced by the current intensity. The smallest variation in the potential applied in the ED cell will increase the H<sup>+</sup> production in the media. Thus, not only the current intensity should be considered to analyze the results, but also the error associated to the power supplier (± 3 mA).

Final concentrations of the major concerned elements in the liquid matrices (Cl<sup>-</sup> and SO<sub>4</sub><sup>2-</sup>) and in the mine tailings suspension (As, Cu, Sn and W) are presented in Tables 3 and 4, respectively.

In general, the target contaminants removal from the matrices was higher in the experiments operated at 100 mA, for the same amount of circulated charge. When ED treatment is performed at higher current intensities, the electromigration transport is predominant over diffusion or other transportation phenomena. The amount of salts amount is extremely heterogeneous in the effluent. The season periods of the sampling procedure affected chemical and physical properties of the

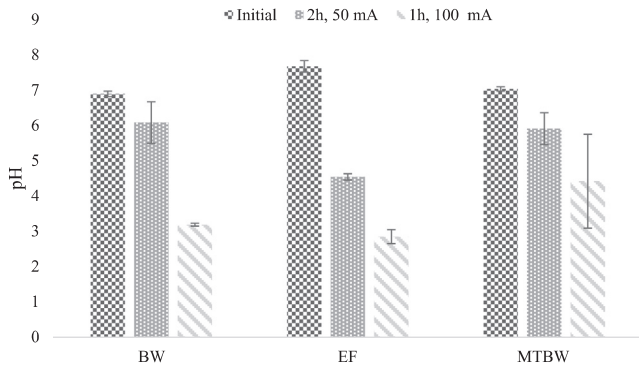


Fig. 2. pH of the liquid phase at the central cell compartment before and after the electrodiolytic experiments at 50 mA and 100 mA (error bars related to the standard deviation:  $n = 2$ ). BW-Briny Water; EF-Effluent; MT-Mine Tailings.

Table 3

Concentration of anions in briny water and effluent, before and after the electrodiolytic experiments at 50 mA (2 h) and 100 mA (1 h).

		Initial (mg/L)	50 mA Final (mg/L)	100 mA Final (mg/L)
Cl <sup>-</sup>	BW	499.3 ± 8.1	285.5 ± 40.3	15.7 ± 22.2
	EF1	1624.9	490.5	129.1
	EF2	191.3	83.0	20.5
SO <sub>4</sub> <sup>2-</sup>	BW	66.8 ± 1.5	16.8 ± 2.3	14.1 ± 5.0
	EF1	239.3	114.4	36.1
	EF2	59.6	30.0	27.9

BW – Briny Water; EF-Effluent.

EF1 – collected at 5-09-2018.

EF2 – collected at 12-09-2018.

Table 4

Concentration of elements in mine tailings before and after the electrodiolytic experiments at 50 mA (2 h) and 100 mA (1 h).

	Initial solid phase (mg/kg)	50 mA Final solid phase (mg/kg)	100 mA Final solid phase (mg/kg)
As	218.6 ± 132.3	196.2 ± 50.73	113.9 ± 19.7
Cu	76.8 ± 39.3	38.3 ± 13.9	26.4 ± 3.5
Sn	2.0 ± 0.5	2.2 ± 0.2	1.7 ± 0.4
W	5.3 ± 1.4	5.7 ± 0.4	4.9 ± 1.6

samples collected due to the fluctuations in weather conditions and also the wastewater treatment plant process efficiency.

The slightly extraction of Sn and W from mine tailings may be related to specific chemical limitations, such as desorption or dissolution mechanisms. For example, W complexes are quickly decomposed and stabilized by high concentrations of chloride ions (MT:  $5.6 \pm 2.3$  mg/kg; BW:  $499.3 \pm 8.1$  mg/kg), where the most common product of the decomposition is  $[W_2Cl_9]^{3-}$ . Alternatively, the adsorption of sulfate ions on metallic W surface results in the electronic structure modification. The O<sub>2</sub> reduction reaction is blocked during the ED process, which is already low in cationic dissolution in electrochemical processes [35].

#### 4.2. Hydrogen generation and use

Fig. 3 shows the volume of collected gas produced at the cathode compartment during experiments 1–6. As the volume of the gas deposit was 30 mL, it was filled before the ED process ended. Experiments at 50 mA showed matrix related differences in the gas flow rate, reaching the 30 mL of H<sub>2</sub> production at different rates. There are no statistically significant differences for the flow rates obtained at 100 mA (Table E at

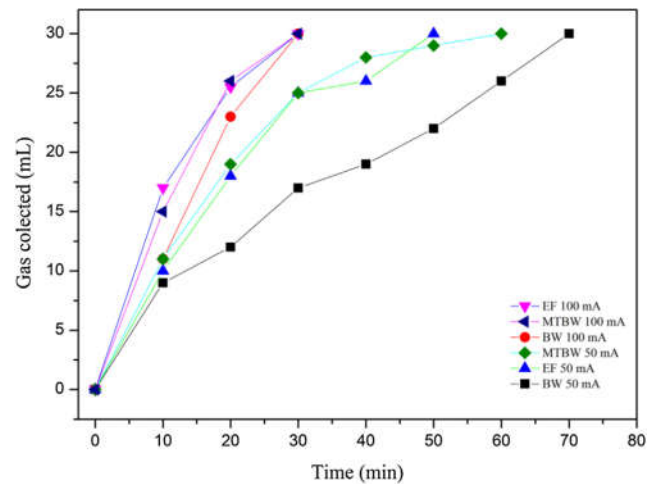


Fig. 3. Gas flow rate generation (mL/min) during the electrodiolytic experiments with BW, EF and MTBW, at 50 mA and 100 mA (collected maximum volume 30 mL). BW-Briny Water; EF-Effluent; MT-Mine Tailings.

supplementary data). However, the flow rates of H<sub>2</sub> are significantly different ( $p < 0.001$ ) in the experiments at 50 mA.

The gas generated at the cathode compartment, in the experimental setup 3, 4 and 6 during 6 h, was captured and analyzed via GC-TCD, in a tedlar sample bag. Table 5 presents the purity of the captured gas for these experiments carried out at 100 mA.

The average H<sub>2</sub> purity (% w/w) of the produced gas was  $\approx 73\%$  (w/w), where the highest value observed was in the ED experiment applied to the effluent, that produced a gas with  $90.4 \pm 0.3\%$  of H<sub>2</sub>. Thus, only the H<sub>2</sub> purity in the effluent experiment has a statistically significant difference ( $p < 0.05$ ) compared to briny water and mine tailings suspension, while briny water and mine tailings suspension does not have a statistically significant difference between each other (Table 5). In order to validate and make a comparison with the purity results obtained in % w/w, another approach to determine the H<sub>2</sub> purity was carried out. Thus, the calculation of the gas was also performed considering the molar fraction of the H<sub>2</sub> in the air gases. Comparing the two methods, the % mol/mol of H<sub>2</sub> of the produced gas was 19% higher, in average, comparing to the % w/w (Table 5). In the % mol/mol analysis, the purity of the H<sub>2</sub> was higher than 97% in all samples, whereas in the % w/w the H<sub>2</sub> purity oscillated between 72% and 90%. The mass and the molar compositions are different, and it is expected a higher molar purity, as long as the other components in the gaseous phase are heavier (e.g. N<sub>2</sub>, O<sub>2</sub>).

As mentioned before, the flow rate production for H<sub>2</sub> in the ED treatments can be directly related to the current intensity and the matrix. Assuming the H<sub>2</sub> captured at 1 atm and 25 °C, a total of  $\approx 45.6$  mL of pure dry H<sub>2</sub> would be theoretically obtained, at a rate of 0.76 mL/min in the experiments at 100 mA. The volume of collected gas at the cathode, shown in Fig. 3 (Table B.2 at supplementary data), was clearly higher than the expected during the first few minutes of treatment, with

Table 5

H<sub>2</sub> purity analysis by GC-TCD.

Matrix	H <sub>2</sub> (% w/w)	H <sub>2</sub> (% mol/mol)*
BW	74.19 ± 0.63 <sup>A</sup>	97.63 ± 0.08 <sup>B</sup>
EF	90.43 ± 0.25 <sup>A</sup>	99.26 ± 0.02 <sup>B</sup>
MTBW	72.39 ± 0.68 <sup>A</sup>	97.41 ± 0.09 <sup>B</sup>

\*Calculated assuming air as impurity in the H<sub>2</sub>; Statistical analysis: Multiple comparisons were statistically performed at  $p < 0.05$  (95% confidence interval); data with lower case letters is statistically significantly different to the ones with the same capital letter; BW-Briny Water; EF-Effluent; MT-Mine Tailings.

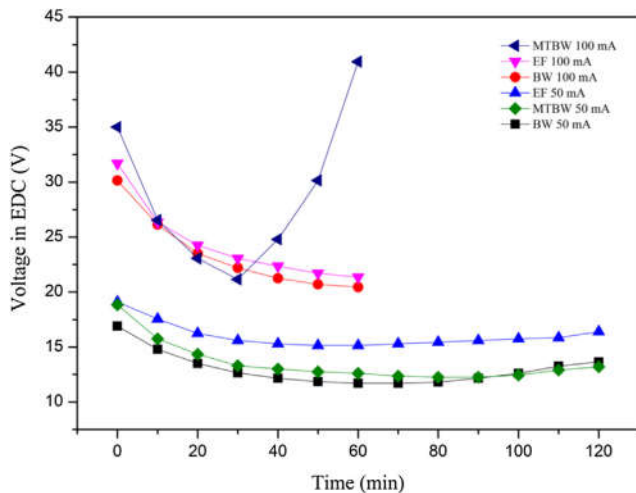
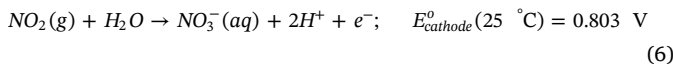


Fig. 4. Cell voltage during the electrodiolytic experiments with BW, EF and MTBW, at 50 mA and 100 mA. BW-Briny Water; EF-Effluent; MT-Mine Tailings.

a change in the production rate after the first 10 to 20 min. This may indicate that competing cathode reactions took place. For example, a possible electrode reaction that could have taken place is the formation of  $\text{NO}_2$  (g) from the reduction of the nitrates ( $E_0 = 0.803$  V), shown in Eq. (6).



This reaction produces 1 mol of  $\text{NO}_2$  (g) per circulated electron, twice as much as the  $\text{H}_2$  reaction and would increase the pH of the cathode compartment twice as fast. However, the pH changes at the cathode and the decrease of nitrate concentration in time will promote that the water reduction electrolysis reaction become predominant after the first several minutes of the reaction.  $\text{NO}_2$  (g) might be in a solution in the form of  $\text{N}_2\text{O}_4$  below  $21^{\circ}\text{C}$ .

#### 4.3. Electrical energy requirements in the ED experiments

Among the ED experiments with  $\text{H}_2$  capture (experiments 1–6 in Table 1), the ED cell voltage decreased overtime. The rapid decrease of the cell voltage was more evident in the experiments at 100 mA (Fig. 4).

According to the Ohm's law, if the current intensity ( $I$ ) is constant, the voltage ( $V$ ) and the resistivity ( $R$ , or conductivity) are strongly related, Eq. (7):

$$V = RI(V) \quad (7)$$

where  $I$  is the current intensity,  $V$  the voltage and,  $R$  is the resistance.

The decrease of the ED cell voltage is related to a conductivity increase in the electrode compartments. The initial conductivity of the electrolyte was moderately low,  $0.90 \pm 0.06$  mS/cm, and it increased to values between 3 and 4 mS/cm at the anode, and 2–3 mS/cm at the cathode, at the end of all experiments, which is consistent with the pH changes observed. In the central compartment, the conductivity changed depending on the matrix (Fig. 5). Due to the highly heterogeneous environmental samples under study, high standard deviations in the ED experiments' behavior were observed. Nevertheless, in general, it stayed with values that assure conductivity. However, the experiment MTBW at 100 mA had a voltage increase after half an hour and a decrease on the conductivity at the end of the experiment (Fig. 5). The treatment at 100 mA produced the reduction of ions (related to the  $\text{H}^+$  migration through the anion exchange membrane) in the central compartment, and an energy efficiency decrease of the process due to an increase of the ohmic losses. In the experiments at 50 mA, the longer

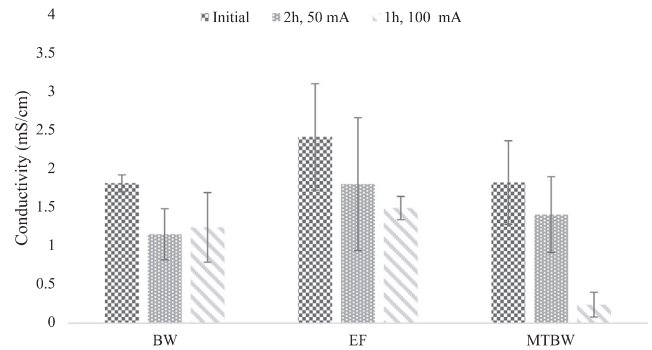


Fig. 5. Conductivity of the liquid phase at the central cell compartment before and after the electrodiolytic experiments (error bars related to the standard deviation:  $n = 2$ ). BW-Briny Water; EF-Effluent; MT-Mine Tailings.

running times allowed diffusion and dissolution/desorption kinetics to replenish the ion content in the central cell compartment. Effluent and mine tailings are matrices with high dependency on the sampling and weather conditions (effluent high standard deviations in the salts content, in line with the conductivity values). Mine tailings are a heterogeneous matrix implying different amounts of metals and salts content, with different variations in the charged species during the sampling.

As the ED experiments are carried out at a constant current, the electrical energy required during the process, accounting only for the energy applied by the DC power source, can be calculated from Eq. (8):

$$E = I \int_{t_0}^t V_{\text{cell}}(t) dt \quad (8)$$

Using a numerical chained-trapezoidal integration, the estimated electrical energy is presented in Fig. 6. As expected, the electrical energy required increases as the electrical current increases, for the same amount of circulated charge. These results are consistent with the conductivity of those matrices. According to the results presented in the Fig. 6, the experiments carried out at 100 mA required  $\sim 8.7 \pm 0.8$  kJ of electrical energy, while the experiments carried out at 50 mA required an average of  $\sim 4.8 \pm 0.7$  kJ.

#### 4.4. Energy savings

Considering a faradaic efficiency of 100% and no competition to the water reduction as the cathode electrolysis reaction,  $\sim 1.86$  mmol of  $\text{H}_2$  would be produced in experiments 1–6 at the end of the ED experiment, either at 50 mA in 2 h or at 100 mA in 1 h. Using a fuel cell at low

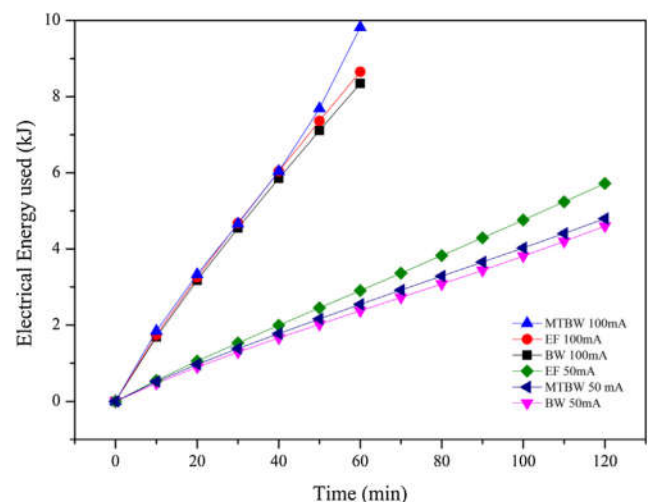


Fig. 6. Estimation of the cumulative electrical energy consumed during the electrodiolytic experiments. BW-Briny Water; EF-Effluent; MT-Mine Tailings.

temperatures and considering the higher heat of combustion of  $H_2$  as  $141.8 \text{ MJ kg}^{-1}$ , a total of  $0.53 \text{ kJ}$  may have been recovered from the process. The efficiency of the chemical energy conversion to electrical energy at the fuel cell depends on the quality of the  $H_2$  gas produced, where a maximum of 98% (mol/mol) hydrogen average purity was achieved during the ED treatments. Considering that current fuel cell has energy conversion efficiencies of around 60%, a total of  $0.32 \text{ kJ}$  could have been transformed into electrical energy. This translates to  $\sim 3.1\%$  of the electrical energy required in experiment 4 (EF 100 mA, the worst case), and  $\sim 6.9\%$  of the electrical energy required in experiment 5 (MTBW 50 mA, the best case). Reducing the electrical energy dependency, mainly due to stirring needs (for solid fine matrices), transport of charge through the porous matrix, and to feed a power supply for the electrode's reactions, may also have impact in the total variable costs of the overall ED process ( $\sim 7\%$ ).

As expected, the higher the current intensity used in the ED treatment, the higher the electrical energy requirements for the same amount of circulated charge. In the experiments presented, those carried out at 50 mA during 2 h required almost half of the electrical energy to produce the electrolysis reactions than those carried out at 100 mA during 1 h. On the other hand, higher applied currents obtain better removal efficiencies, provided that there are no phase-transfer kinetic limitations, such as dissolution or desorption processes.

In general, one of the main advantages of the ED treatment applied to liquid matrices compared to ED treatments applied solid porous matrices is that the energy requirements for the electrolysis reactions are considerably smaller, due to the higher conductivity of the matrices. Thus, in solid porous matrices, the ED treatment would reach higher voltage gradients due to the lower conductivity and will require long-lasting treatments. The ED treatments presented show requirements of electrical power for the electrolysis in the range of 1–5 W. However, ED treatments carried out for the mine tailings suspension required additional energy for the stirring system at the sample central cell compartment. A 10 W stirrer system was used, meaning that the electrical energy required for the stirring system could be up to ten-fold compared to the energy required for the electrolysis reactions. For the purpose of energy optimization in ED treatments applied to suspensions, the reduction of stirring costs is critical. In this sense, PEMFC could be an important factor in ED energy savings by reducing the operation costs by powering a low-energy stirring system.

To evaluate the possibility of reducing energy requirements from the ED treatments by the *in-operando* production of electricity from  $H_2$  gas formed at the cathode, a PEMFC was connected directly to the exhaust pipe of the cathode compartment in experiments 7–9, corresponding to the same matrices under ED treatment at 100 mA during 1 h.

The initial open circuit voltage of the PEMFC was, in all cases, near 1.4 V, and it decreased and stabilized at a value of  $\sim 1 \text{ V}$  (Fig. 7), as expected for a single PEMFC [32]. To obtain higher voltages, a stack of FCs connected in series could be used. Comparing the voltage generated by PEMFC in the different cases, there are no statistically significant differences ( $p < 0.05$ ) (see Table C at supplementary data). The data supported the statement that the production of electricity by a PEMFC is independent of environmental matrices used in the ED treatments presented, despite the fluctuation observed for the case of effluent.

The data presented in this study indicates that the gas produced at the cathode has a purity between 72.4% and 99.3%. Therefore, in a field scale ED treatment, the produced  $H_2$  could also be stored and sold for transportation or other industrial sectors. The production costs of  $H_2$  via electrolysis vary around 8–11 €/kg, which is higher than that obtained via steam methane reforming using natural gas or biogas [36,37]. The  $H_2$  produced during ED treatments, that until now has been an unexploited byproduct, may be an alternative source of  $H_2$  for transportation or energy storage.

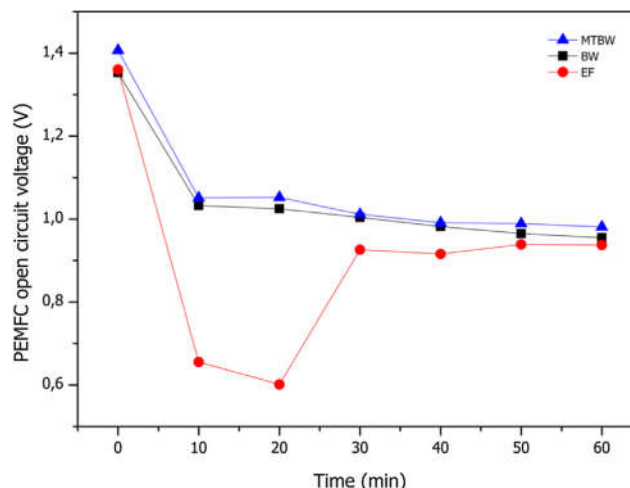


Fig. 7. Proton-exchange membrane fuel cell (PEMFC) generated open circuit voltage during the electrochemical experiments at 100 mA. BW-Briny Water; EF-Effluent; MT-Mine Tailings.

## 5. Conclusions

In this study it is proved the possibility to produce  $H_2$  with average purities between 73% and 98% from electrochemical treatments and used to generate electrical energy with a proton-exchange membrane fuel cell. This estimation was performed according to the  $H_2$  formed at the cathode electrolysis reaction, which can reduce the energy costs associated to the electrochemical treatments, as well as any other remediation treatment based on electrochemically-induced transport.

The efficiency of chemical to electrical energy conversion at the fuel cell would depend on the quality of the  $H_2$  gas produced. Thus, specific studies on possible competitive cathode reactions are needed depending on the system. However, in the matrices tested in this study,  $H_2$  gas was produced in all cases. This suggests that  $H_2$  purity seems to be more affected by external factors (experimental errors, nitrate reduction to  $NO_2$  or temperature increase) than the matrices composition. Flowing the produced  $H_2$  gas through a single proton-exchange membrane fuel cell, resulted in a stable open circuit voltage ( $\sim 1 \text{ V}$ ), that demonstrated the potential to recover energy from the  $H_2$  byproduct, that otherwise would be released to the atmosphere and lost.

This research shows there are new possibilities for energy saving and  $H_2$  production for different purposes in electrochemical treatment, leading to an increase in the sustainability and applicability of the electro-remediation, decontamination or degradation contaminant processes.

## Acknowledgments

This work has received fundings from the European Union's Horizon 2020 research and innovation programme under Grant Agreement No. 776811, under the Marie Skłodowska-Curie grant agreement No. 778045, and from Portuguese funds from FCT/MCTES through grants UID/AMB/04085/2019 and PTDC/FIS-NAN/0909/2014. C. Magro and J. Almeida acknowledge Fundação para a Ciência e a Tecnologia for their PhD fellowships SFRH/BD/114674/2016 and PD\BD\135170\2017, respectively. The authors acknowledge Carla Rodrigues and Nuno Costa from REQUIMTE for the ICP and IC analysis, and Ricardo Chagas from LAQV- REQUIMTE.

## Appendix A. Supplementary material

Supplementary data to this article can be found online at <https://doi.org/10.1016/j.apenergy.2019.113839>.

## References

- [1] Hart PS, Feldman L. Would it be better to not talk about climate change? The impact of climate change and air pollution frames on support for regulating power plant emissions. *J Environ Psychol* 2018;1–33. <https://doi.org/10.1016/j.jenvp.2018.08.013>.
- [2] Pei P, Jia X, Xu H, Li P, Wu Z, Li Y, et al. The recovery mechanism of proton exchange membrane fuel cell in micro-current operation. *Appl Energy* 2018;226:1–9. <https://doi.org/10.1016/j.apenergy.2018.05.100>.
- [3] Majlan EH, Rohendi D, Daud WRW, Husaini T, Haque MA. Electrode for proton exchange membrane fuel cells: a review. *Renew Sustain Energy Rev* 2018;89:117–34. <https://doi.org/10.1016/j.rser.2018.03.007>.
- [4] Abdalla AM, Hossain S, Nisfindy OB, Azad AT, Dawood M, Azad AK. Hydrogen production, storage, transportation and key challenges with applications: a review. *Energy Convers Manag* 2018;165:602–27. <https://doi.org/10.1016/j.enconman.2018.03.088>.
- [5] Nikolaidis P, Poullikkas A. A comparative overview of hydrogen production processes. *Renew Sustain Energy Rev* 2017;67:597–611. <https://doi.org/10.1016/j.rser.2016.09.044>.
- [6] Baykara SZ. Hydrogen: A brief overview on its sources, production and environmental impact. *Int J Hydrogen Energy* 2018;43:10605–14. <https://doi.org/10.1016/j.ijhydene.2018.02.022>.
- [7] Alshawabkeh AN. Electrokinetic soil remediation: challenges and opportunities. *Sep Sci Technol* 2009;44:2171–87. <https://doi.org/10.1080/01496390902976681>.
- [8] Ribeiro AB, Mateus EP, Couto N, editors. Electrokinetic across disciplines and continents. New strategies for sustainable development. Springer International Publishing; 2016, 427p, 10.1007/978-3-319-20179-5.
- [9] Gomes HI, Dias-Ferreira C, Ribeiro AB. Overview of in situ and ex situ remediation technologies for PCB-contaminated soils and sediments and obstacles for full-scale application. *Sci Total Environ* 2013;445–446:237–60. <https://doi.org/10.1016/j.scitotenv.2012.11.098>.
- [10] Yukselen-Aksoy Y, Reddy KR. Effect of soil composition on electrokinetically enhanced persulfate oxidation of polychlorobiphenyls. *Electrochim Acta* 2012;86:164–9. <https://doi.org/10.1007/s12520-016-0397-x>.
- [11] Ferreira C, Jensen P, Ottosen L, Ribeiro A. Removal of selected heavy metals from MSW fly ash by the electro-dialytic process. *Eng Geol* 2005;77:339–47. <https://doi.org/10.1016/j.enggeo.2004.07.024>.
- [12] Kirkelund GM, Magro C, Guedes P, Jensen PE, Ribeiro AB, Ottosen LM. Electro-dialytic removal of heavy metals and chloride from municipal solid waste incineration fly ash and air pollution control residue in suspension – test of a new two compartment experimental cell. *Electrochim Acta* 2015;181:73–81. <https://doi.org/10.1016/j.electacta.2015.03.192>.
- [13] Ebbens B, Ottosen LM, Jensen PE. Electro-dialytic treatment of municipal wastewater and sludge for the removal of heavy metals and recovery of phosphorus. *Electrochim Acta* 2015;181:90–9. <https://doi.org/10.1016/j.electacta.2015.04.097>.
- [14] Lacasa E, Cotillas S, Saez C, Lobato J, Cañizares P, Rodrigo MA. Environmental applications of electrochemical technology. What is needed to enable full-scale applications? *Curr Opin Electrochem* 2019;16:149–56. <https://doi.org/10.1016/j.coelec.2019.07.002>.
- [15] Villen-Guzman M, Gomez-Lahoz C, Garcia-Herruzo F, Vereda-Alonso C, Paz-Garcia JM, Rodriguez-Maroto JM. Specific energy requirements in electrokinetic remediation. *Transp Porous Media* 2018;121:585–95. <https://doi.org/10.1007/s11242-017-0965-2>.
- [16] Kone J-P, Zhang X, Yan Y, Hu G, Ahmadi G. CFD modeling and simulation of PEM fuel cell using OpenFOAM. *Energy Procedia* 2018;145:64–9. <https://doi.org/10.1016/j.egypro.2018.04.011>.
- [17] Staffell I, Green R, Kendall K. Cost targets for domestic fuel cell CHP. *J Power Sources* 2008;181:339–49. <https://doi.org/10.1016/j.jpowsour.2007.11.068>.
- [18] Ahmadi MH, Mohammadi A, Pourfayaz F, Mehrpooya M, Bidi M, Valero A, et al. Thermodynamic analysis and optimization of a waste heat recovery system for proton exchange membrane fuel cell using transcritical carbon dioxide cycle and cold energy of liquefied natural gas. *J Nat Gas Sci Eng* 2016;34:428–38. <https://doi.org/10.1016/j.jngse.2016.07.014>.
- [19] Cameselle C, Gouveia S. Electrokinetic remediation for the removal of organic contaminants in soils. *Curr Opin Electrochem* 2018;11:41–7. <https://doi.org/10.1016/j.coelec.2018.07.005>.
- [20] Ribeiro AB, Rodríguez-Maroto JM. Electroremediation of heavy metal-contaminated soils. Processes and applications. Cap. 18. In: Prasad MNV, Sajwan KS, Naidu R, editors. Trace Elements in the environment: biogeochemistry, biotechnology and bioremediation, Taylor & Francis, Florida, USA: CRC Press; 2006, p. 341–68.
- [21] Magro CC, Guedes PR, Kirkelund GM, Jensen PE, Ottosen LM, Ribeiro AB. Incorporation of different fly ashes from MSWI as substitute for cement in mortar: an overview of the suitability of electro-dialytic pre-treatment. In: Ribeiro AB, Mateus EP, Couto N, editors. Electrokinetic across disciplines and continents. New strategies for sustainable development. Springer International Publishing; 2016, p. 225–47. 10.1007/978-3-319-20179-5\_12.
- [22] Guedes P, Mateus EP, Couto N, Rodríguez Y, Ribeiro AB. Electrokinetic remediation of six emerging organic contaminants from soil. *Chemosphere* 2014;117:124–31. <https://doi.org/10.1016/j.chemosphere.2014.06.017>.
- [23] Guedes P, Couto N, Ottosen LM, Ribeiro AB. Phosphorus recovery from sewage sludge ash through an electro-dialytic process. *Waste Manag* 2014;34:886–92. <https://doi.org/10.1016/j.wasman.2014.02.021>.
- [24] Villen-Guzman M, Paz-Garcia JM, Rodriguez-Maroto JM, Gomez-Lahoz C, Garcia-Herruzo F. Acid enhanced electrokinetic remediation of a contaminated soil using constant current density: Strong vs. weak acid. *Sep Sci Technol* 2014;49:1461–8. <https://doi.org/10.1080/01496395.2014.898306>.
- [25] Paz-García JM, Johannesson B, Ottosen LM, Alshawabkeh AN, Ribeiro AB, Rodríguez-Maroto JM. Modeling of electrokinetic desalination of bricks. *Electrochim Acta* 2012;86:213–22. <https://doi.org/10.1016/j.electacta.2012.05.132>.
- [26] Hansen HK, Rojo A, Ottosen LM. Electro-dialytic remediation of copper mine tailings. *Procedia Eng* 2012;44:2053–5. <https://doi.org/10.1016/j.proeng.2012.09.042>.
- [27] Pedersen KB, Jensen PE, Ottosen LM, Barlinthaug J. Influence of electrode placement for mobilising and removing metals during electro-dialytic remediation of metals from shooting range soil. *Chemosphere* 2018;210:683–91. <https://doi.org/10.1016/j.chemosphere.2018.07.063>.
- [28] Lefebvre G, García R, Arragonés M, Moya M, Monge Q, Maund N. Report on balance between demand and supply of refractory metals in the EU. MSP-REFRAM 2016;D1(3):40.
- [29] Ávila PF, Da Silva EF, Salgueiro AR, Farinha JA. Geochemistry and mineralogy of mill tailings impoundments from the panasqueira mine (Portugal): Implications for the surrounding environment. *Mine Water Environ* 2008;27:210–24. <https://doi.org/10.1007/s10230-008-0046-4>.
- [30] Ribeiro AB, Mexia JT. A dynamic model for the electrokinetic removal of copper from a polluted soil. *J Hazard Mater* 1997;56:257–71. [https://doi.org/10.1016/S0304-3894\(97\)00060-5](https://doi.org/10.1016/S0304-3894(97)00060-5).
- [31] Yuan S, Gou N, Alshawabkeh AN, Gu AZ. Efficient degradation of contaminants of emerging concerns by a new electro-Fenton process with Ti/MMO cathode. *Chemosphere* 2013;93:2796–804. <https://doi.org/10.1016/j.chemosphere.2013.09.051>.
- [32] Joshua OS, Ejura GJ, Essien VE, Olokungbemi IB, Oluwaseun AY, Okon EP. Fuel cell types and factors affecting them. *Int J Sci Eng Res* 2014; 2:11–4, ISSN (Online): 2347-3878.
- [33] Magro C, Paz-garcia JM, Ottosen LM, Mateus EP, Ribeiro AB. Sustainability of construction materials: Electro-dialytic technology as a tool for mortars production. *J Hazard Mater* 2019;363:421–7. <https://doi.org/10.1016/j.jhazmat.2018.10.010>.
- [34] Zhang Z, Ottosen LM, Wu T, Jensen PE. Electro-remediation of tailings from a multi-metal sulphide mine: comparing removal efficiencies of Pb, Zn, Cu and Cd. *Chem Ecol* 2019;35:54–68. <https://doi.org/10.1080/02757540.2018.1529173>.
- [35] Tuvíč T, Pašti I, Mentus S. Tungsten electrochemistry in alkaline solutions—Anodic dissolution and oxygen reduction reaction. *Russ J Phys Chem A* 2011;85:2399–405. <https://doi.org/10.1134/S0036024411130322>.
- [36] How Middlehurst T. much does a hydrogen car cost to run? *Evening Stand* 2017.
- [37] Baxley P, Verdugo-Peralta C, Weiss W. Rollout strategy topic team report: California 2010 Hydrogen highway network; 2005.

## Glossary

- ED: Electro-dialytic  
 GC-TCD: Gas Chromatography with Thermal Conductivity Detector  
 IC: Ion Chromatography  
 ICP-OES: Inductively Coupled Plasma with Optical Emission Spectrometry  
 PEMFC: Proton-exchange membrane fuel cell

## Paper

*“Sustainability of construction materials: electro-dialytic technology as a tool for mortars production”*

*C Magro, JM Paz-Garcia, LM Ottosen, EP Mateus & AB Ribeiro*

*Published in: Journal of Hazardous Materials, 2019*







Contents lists available at ScienceDirect

## Journal of Hazardous Materials

journal homepage: [www.elsevier.com/locate/jhazmat](http://www.elsevier.com/locate/jhazmat)

## Sustainability of construction materials: Electrodialytic technology as a tool for mortars production

C. Magro<sup>a,b,\*</sup>, J.M. Paz-Garcia<sup>c</sup>, L.M. Ottosen<sup>b</sup>, E.P. Mateus<sup>a</sup>, A.B. Ribeiro<sup>a,\*</sup><sup>a</sup> CENSE, Departamento de Ciências e Engenharia do Ambiente, Faculdade de Ciências e Tecnologia, Universidade Nova de Lisboa, Caparica, 2829-516, Portugal<sup>b</sup> Department of Civil Engineering, Technical University of Denmark, Lyngby, Denmark<sup>c</sup> Department of Chemical Engineering, University of Malaga, Malaga, Spain

## ARTICLE INFO

## Keywords:

Electrodialytic technology  
Mortars production  
Secondary water resources  
Circular economy

## ABSTRACT

The reduction of tap water consumption in all activity sectors, including the building industry, is crucial to the sustainability of water resources. Effluents from wastewater treatment plants have the potential to replace freshwater in the construction sector but they contain a critical mixture of impurities, which hampers their use in mortars production. In this work, the viability of using effluent as an alternative to potable water for the production of mortars, after electrodialytic treatment, was assessed. Electrodialytic technology (ED-T) is a proven technique for decontamination of porous and aqueous matrices.

ED-T experiments were conducted with 500 mL of effluent for 6, 12 and 24 h, with a current intensity of 25 mA. The results showed that after ED-T 6 h, the removal efficiencies of critical components were above 85% of their initial concentrations. Mortar properties such as setting time, workability, flexural strength, compressive strength and morphology were obtained for 100% effluent and tap water/effluent mixtures (50:50) with and without ED-T pre-treatment. The mortars with the ED-T treated effluent showed similar initial setting times and workability, higher flexural and compressive strength compared to the mortars reference.

## 1. Introduction

The world's freshwater resources are in short supply, as economic activities, population growth, climate change, and the lack of appropriated resources management have caused a significant increase of water use. The United Nations' Sustainable Development Goals stated in 2015 that: water scarcity affects more than 40% of the global population and is estimated to rise [1]. Currently, water scarcity affects an estimated 1.9 billion people and 2.1 billion people live with drinking water services not safely managed [2]. The critical point of water scarcity has led scientists to look for new and efficient ways to make the most out of nontraditional sources, including sea water, brackish water and wastewater. To match the demand of "zero-waste" system, it is essential to find solutions that minimize the consumption of freshwater.

Concrete is the second most consumed material in the world after water, being directly related to the use of freshwater [3]. Water use for the concrete industry represents 9% of all industry withdrawals and 1.7% of all global water consumption [4]. In a concrete mix, the water-cement ratio is around 0.45 to 0.60. In other words, more than 17 billion m<sup>3</sup> of freshwater are used in the production of concrete per year

[4]. Nowadays, freshwater is the only type of water that fulfils the industrial standards, for quality and safety demands. In fact, if polluted water was used, the quality of the concrete would be significantly lower, leading to structural failures that would represent 5%–9.4% of the total costs in concrete production [5].

Various sources of non-freshwater have already been tested as alternatives to freshwater in concrete mixtures, such as (a) processed wastewater sludge [6], (b) polyvinyl acetate resin wastewater [7], (c) car washing wastewater [8], (d) untreated/treated textile effluent [9] and (e) domestic wastewater before chlorination [10]. Noruzman et al. [11] proved that the use of non-freshwater in the concrete mix can provide a proper mix design and acceptable standards regarding tolerable limits. However, due to the composition specifications and to different types of impurities that can exist in each type of water, it is difficult to draw a sound conclusion. Thus, some improvements in past studies need to be addressed in order to take water reuse into consideration: (1) expected degree of human contact, (2) concentration of microbiological and chemicals and, (3) which pre-treatments are necessary [12].

The electrodialytic technology (ED-T) consists on the application of

\* Corresponding authors at: CENSE, Departamento de Ciências e Engenharia do Ambiente, Faculdade de Ciências e Tecnologia, Universidade Nova de Lisboa, Caparica, 2829-516, Portugal.

E-mail addresses: [c.magro@campus.fct.unl.pt](mailto:c.magro@campus.fct.unl.pt) (C. Magro), [abr@fct.unl.pt](mailto:abr@fct.unl.pt) (A.B. Ribeiro).

<https://doi.org/10.1016/j.jhazmat.2018.10.010>

Received 3 October 2017; Received in revised form 22 September 2018; Accepted 3 October 2018

Available online 04 October 2018

0304-3894/ © 2018 Elsevier B.V. All rights reserved.

a low level current density, either direct current or alternate current, of a few mA/cm and a low potential gradient of V/cm, between suitably located electrodes [13]. In the ED-T, ion-exchange membranes are used to separate the matrix to be treated from the electrode compartments. An anion-exchange membrane (AEM) is used at the anode end and a cation-exchange membrane (CEM) at the cathode end. This set-up allows selective separation of anions and cations from the matrix. Cationic species move towards the cathode through the CEM, that hinders the transport of anions and anions move towards the anode through the AEM, that only partially hinders the transport of protons, as it does not work as a perfect rectifier. The ED-T has proved to be efficient for the removal of organic or/and inorganic contaminants, such as heavy metals and salts [14], in decreasing organic matter and fats [15] and in the inactivation of microorganisms in fresh sewage sludge from wastewater treatment plant (WWTP) [16].

Therefore, the present study aims to investigate the use of effluent from an urban WWTP secondary treatment, after electro-dialytic process in mortars' production. The physical and functional mortar properties were performed and compared with the industry main standards.

## 2. Materials and methods

### 2.1. Materials

Tap water was collected at the Technical University of Denmark, Lyngby, Denmark. The effluent was sampled after the secondary clarifier at Mølleåværket A/S WWTP in Lyngby, Denmark. The plant uses the BioDenitro method in the aeration tanks and no tertiary treatment [17]. The plant treats 8–12 million m<sup>3</sup> of wastewater on a yearly basis, corresponding to a 115 000 population equivalent.

The cement used for mortar preparation was the Ordinary Portland Cement (OPC) and the sand was the CEN standard sand.

### 2.2. Tap water and effluent characterization

All experiments were carried out in triplicate.

The pH in the effluent and tap water were measured with a Radiometer pH-electrode and conductivity in a Radiometer Analytic.

Total concentrations of Ca, K, Mg, Ni, P, S, Si and Zn were determined by Inductively Coupled Plasma with Optical Emission Spectrometry (ICP-OES), and Cl<sup>-</sup>, NO<sub>3</sub><sup>-</sup> and SO<sub>4</sub><sup>2-</sup> by Ion Chromatography (IC).

The regulatory parameters for effluent discharge in water bodies – namely biological oxygen demand (BOD<sub>5</sub>), chemical oxygen demand (COD), NH<sub>4</sub><sup>+</sup>, NO<sub>2</sub> and N<sub>total</sub> – were determined by Spectrophotometer DR2800 kits, and total suspended solids (TSS) by gravimetric analysis.

### 2.3. Electrodialytic experiments

Three different electro-dialytic experiments ED-T were carried out, in triplicate, according to the conditions presented in Table 1.

The ED-T cell used (Fig. 1) was a 3 compartment conventional one [18], made of plastic (RIAS, Acryl XT). The internal diameter was 8 cm and the central compartment length was 10 cm. The 2 electrode compartments were separated from the central one by ion exchange membranes, an AEM AR204SZRA, MKIII, Blank and a CEM CR67, MKIII,

**Table 1**  
Electrodialytic experimental conditions.

Experiment	Code	Effluent treated (mL)	Duration (h)	Current intensity (mA)
1	ED-T 6 h	500	6	25
2	ED-T 12 h		12	
3	ED-T 24 h		24	

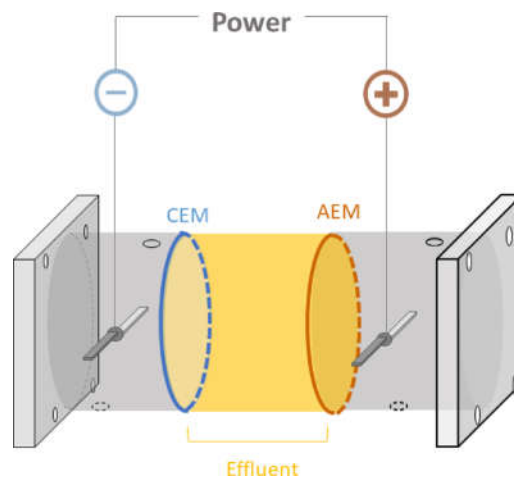


**Fig. 1.** Electrodialytic 3 compartments cell with  $\phi = 8$  cm, central compartment  $L = 10$  cm and electrolyte compartment  $L = 5$  cm. CEM – cation exchange membrane; AEM – anion exchange membrane.

Blank, both from Ionics. The electrodes were platinum coated titanium wire ( $\phi = 3$  mm) by Grønvold & Karnov A/S. A power supply (Hewlett Packard E3612 A) was used, maintaining a constant current of 25 mA.

The effluent (500 mL) was placed on the central cell compartment. Both anolyte and catholyte compartments were set with 500 mL of 0.01 M NaNO<sub>3</sub> adjusted to pH 2 with HNO<sub>3</sub>, and recirculated by using “Pan World” magnetic pumps (Plastomec Magnet Pump model P05).

Control experiments for each treatment, without applied current, were also carried out.

pH and conductivity in the electrolytes and in the central compartment were measured twice ( $T_0$  and  $T_{6,12,24h}$ ) per treatment.

At the end of the ED-T experiments, the effluent in the central compartment was analyzed by ICP-OES and IC (as in Section 2.2). Membranes were soaked in 1 M HNO<sub>3</sub> and the electrodes in 5 M HNO<sub>3</sub>, overnight, being their aqueous phases collected and analyzed for Ca, K, Mg, Ni, P, S, Si and Zn by ICP-OES, as well as the electrolytes.

### 2.4. Mortars bars: physical and functional tests

After ED-T, the treated effluent was used to prepare mortars according to EN 196-7 [19]. The mixture consisted of 225 mL water (tap water or effluent), 450 g of OPC and 1350 g of CEN standard sand, with 0.5 water/binder ratio and a sand/cement ratio of 3%. Mortar samples were performed using tap water, ED-T pre-treated effluent and mixtures of 50% each. The tested mortar samples consisted of horizontal prismatic specimens (160 × 40 × 40 mm) made in triplicates. The mortar bars were defined as:

- Reference (100% tap water)
- Raw (effluent without pre-treatment; 50% or 100%)
- ED-T (effluent with ED-T pre-treatment during 24 h, 12 h, 6 h; 50% or 100%)

Mortars demolding was carried out after 24 h and the samples were cured horizontally in a tap water bath for 7, 14 or 28 days at 20–21 °C.

The following tests were carried out on the mortar specimens in accordance with:

- Setting time (min) - Standard ASTM C 191 [20] performed by a Vicat Needle. The period of penetration tests was performed by allowing a 1 mm Vicat needle to settle into this paste. The Vicat initial setting time was the time elapsed between the initial contact of raw materials and the time when penetration was measured to be 25 mm or less. The Vicat final setting time was the end point to be the first

penetration measure that does not mark the specimen surface with a complete circular impression.

- Workability - Standard EN-1015-3 [21] using a flow table test, where vertical difference between the top of the mold and the displaced original center of the top surface of the specimen was measured as the slump value.
- Flexural strength at 28-day - Standard EN 196-1 [22] with third point loading (two steel supporting rollers of  $\text{Ø } 10.0 \pm 0.5$  mm and a third steel loading roller of the same diameter placed centrally between the other two) at a loading rate of 0.2 kN/s, performed by Instron 6022 10 kN;
- Compressive strength at 7, 14 and 28 days - Standard EN 196-1C [22] by a Toni machine using a loading rate of 2.5 kN/s (t-test was performed to find statistical differences, 95% of confidence level)
- Morphology at 28 days with 100% of replacement by raw and ED-T effluent - performed by scanning electron microscope (SEM). No sample pre-treatment was performed. Acceleration voltage of the SEM was 20–25 kV with large field detector, in low vacuum with a magnification of 800x.

### 3. Results and discussion

#### 3.1. Characterization of tap water and effluent before and after electro-dialytic treatment

##### 3.1.1. Initial characterization

Table 2 presents the characteristics of water samples under study: Tap water and effluent. The data shows that almost all raw effluent components were higher than those found in tap water. The exception was for Ca, Mg, Si, Zn average concentrations, nevertheless within the BS EN 1008 (2002) requirements [23].

Chemical impurities in water are active players in the reactions between water and cement and, being prone to interfere with the setting and hardening of cement and consequently with the development of strength and durability of concrete [24].

Comparing the chloride content in the raw effluent and in tap water (207.3 vs 63.0 mg/L, Table 2), and according to BS EN 1008 (2002)

[23] requirements (to pre-stressed concrete or grout propose, chloride shall not exceed the level of 500 mg/L;  $\text{Cl}_2$  residual  $\leq 1$  mg/L), both are under the standard, but not under NP 423  $\leq 50$  mg/L [25]. The lower the chloride concentration the better, as a high  $\text{Cl}^-$  content will increase the potential for corrosion in reinforced concrete. Also, sulfate (65.7 vs 31.7 mg/L; BS EN 1008  $\leq 2000$  mg/L; NP 413  $\leq 30$  mg/L [26]) together with macro elements, can lead to the formation of complexes, increasing the cracking formation.

The value of COD, was higher in the raw effluent (comparing with the other experiments), and presented a large variability between samples (69% RSD). This parameter plays an important role in water and cement reaction, promoting a negative effect in the control of the cement paste of mortars (delays in setting time) [27]. Moreover, when handling effluents, their pathogen content is also relevant due to safety reasons and material acceptance for further uses.

Thereby, the ED-T proposed as a pre-treatment with the potential for the removal of unwanted parameters was studied.

##### 3.1.2. ED-T experiments

The conductivity decreased with time, from 1.3 mS/cm to 0.1  $\mu\text{S}/\text{cm}$  in about 12 h (Table 2), which is a consequence of the desalination of the effluent, leading to increase system resistivity (expressed by the cell voltage). In the ED-T experiments the final voltage achieved 35.9, 74.2 and 74.1 V, for respectively 6, 12 and 24 h. In the case of the experiments with 12 and 24 h, the voltage increased up to the limit of the power supply and, thus, the current decreased below the established 25 mA, down to almost open-circuit conditions.

The final pH of the ED-T effluent was 4–5 (Table 2), inside the range of the standard BS EN 1008 (2002)  $\geq 4$ –8 [23].

##### 3.1.3. Removal rates

The ED-T treatment reduced the concentration of all ions, elements and parameters in the effluent in all experiments (Table 2).

The data shows that the transport in the bench reactor is fast achieving, in a few hours, the necessary removal of ions to prevent the side effects on the mortar properties (Table 2). Anions removal at the end of the ED-T experiments ranged between 85–99.7%. The results

**Table 2**  
Characterization of the tap water and effluent before and after 24, 12 and 6 h of ED-T.

	Tap Water	Effluent			
		Raw	ED-T 24 h	ED-T 12 h	ED-T 6 h
pH	7.7 $\pm$ 0.1	7.9 $\pm$ 0.3	4.0 $\pm$ 0.3	4.0 $\pm$ 0.5	5.0 $\pm$ 0.3
Conductivity ( $\mu\text{S}/\text{cm}$ )	755.5 $\pm$ 23.3	1304.5 $\pm$ 109.6	0.1 $\pm$ 0.02	0.1 $\pm$ 0.01	0.2 $\pm$ 0.01
Parameters (mg/L)					
TSS	–	< 4	<i>n.d.</i>	<i>n.d.</i>	<i>n.d.</i>
BOD <sub>5</sub>	–	3.55 $\pm$ 0.05	3.1 $\pm$ 0.0	5.1 $\pm$ 0.4	4.1 $\pm$ 0.4
COD	–	403.5 $\pm$ 279.3	226	230 $\pm$ 4.2	221 $\pm$ 8.5
N <sub>total</sub>	–	7	2	6	1
NO <sub>2</sub>	–	0.11 $\pm$ 0.00	0.02 $\pm$ 0.00	0.02 $\pm$ 0.00	0.02 $\pm$ 0.00
NH <sub>4</sub> <sup>+</sup>	–	0.16 $\pm$ 0.01	0.08 $\pm$ 0.01	0.07 $\pm$ 0.01	0.09 $\pm$ 0.01
P <sub>total</sub>	–	0.63 $\pm$ 0.42	<i>n.d.</i>	<i>n.d.</i>	<i>n.d.</i>
Elements (mg/L)					
Ca	105.3 $\pm$ 12.1	99.7 $\pm$ 13.3	0.3 $\pm$ 0.0	0.3 $\pm$ 0.1	5.9 $\pm$ 3.6
K	4.9 $\pm$ 0.7	24.2 $\pm$ 0.7	0.5 $\pm$ 0.2	0.3 $\pm$ 0.2	1.2 $\pm$ 0.4
Mg	20.3 $\pm$ 0.7	15.7 $\pm$ 0.9	0.05 $\pm$ 0.01	0.04 $\pm$ 0.01	1.2 $\pm$ 0.7
Na	35.6 $\pm$ 4.2	118.7 $\pm$ 0.7	0.5 $\pm$ 0.1	1.5 $\pm$ 1.8	10.2 $\pm$ 8.3
S	11.1 $\pm$ 3.3	20.6 $\pm$ 1.9	0.2 $\pm$ 0.1	0.2 $\pm$ 0.1	3.0 $\pm$ 1.1
Ni	0.005 $\pm$ 0.000	0.06 $\pm$ 0.02	0.004 $\pm$ 0.005	0.003 $\pm$ 0.004	0.004 $\pm$ 0.004
Si	9.3 $\pm$ 0.7	8.4 $\pm$ 0.4	5.8 $\pm$ 0.6	6.6 $\pm$ 0.2	7.5 $\pm$ 0.6
Zn	0.8 $\pm$ 0.6	0.05 $\pm$ 0.02	$\pm$ 0.01	0.01 $\pm$ 0.01	0.02 $\pm$ 0.02
Anions (mg/L)					
Cl <sup>-</sup>	63.0 $\pm$ 2.2	207.3 $\pm$ 3.9	2.0 $\pm$ 0.2	2.1 $\pm$ 0.8	23.1 $\pm$ 10.5
NO <sub>3</sub> <sup>-</sup>	2.0 $\pm$ 2.8	13.5 $\pm$ 3.2	8.3 $\pm$ 3.8	9.1 $\pm$ 15.7	11.9 $\pm$ 19.4
SO <sub>4</sub> <sup>2-</sup>	31.7 $\pm$ 2.2	65.7 $\pm$ 2.3	0.4 $\pm$ 0.1	0.2 $\pm$ 0.3	9.9 $\pm$ 3.9

\*n.d. – not detected.

showed (Table 2) that an optimal removal of the ions was achieved in approx. 6 h, indicating that there is no need of expending more energy as in ED-T 12 h or 24 h. The anions removal is an important variable due to its weak interaction with cement, for example, on the mortars final compressive strength.

The removal of the elements quantified by ICP analysis was in the range of 50–97.8%.

The parameters TSS and COD, that interfere with the cement paste final properties, were also reduced after ED-T (COD removal rates: ED-T 24 h 44%; ED-T 12 h 43%; ED-T 6 h 45%) complying with the requirements of standard NP 1414 (COD  $\leq$  500 mg/L) [27]. The effluent values of BOD<sub>5</sub> before and after ED-T experiments were in accordance with USEPA limit of BOD<sub>5</sub>  $\leq$  30 mg/L [28]. Furthermore, Guedes et al. 2016 [29] reported the inactivation of biological activity in similar environmental matrices using ED-T, thus is expected the same phenomena in the present work.

The qualitative and quantitative analysis of ED-T treated effluent shows that its overall composition after 6 h of treatment matches the standards and can supply a product with less risk components, such as corrosion, than the used conventional tap water.

Assuming a linear behavior of the voltage in time, for the ED-T 6 h experiment at 25 mA, the treatment required approximately 4.05 kWh/m<sup>3</sup> of pre-treated effluent. With an average energy price in Denmark of 0.30 € per kWh (in Europe is  $\sim$  0.2 € per kWh), the estimated cost related to the energy consumption is 1.215 €/m<sup>3</sup> of pre-treated effluent. The electricity energy cost can be significantly reduced by an optimization study on the duration of the ED-T pre-treatment based on the material's mechanical properties.

The results suggest that the operational time, and therefore the energy costs, could be reduced by using less concentrated electrolytes in the electrode compartments. The low pH found in the effluent at the end of the experiments suggests that protons are entering the central compartment via permeation through the non-ideal AEM or by diffusion from the cathode compartment. Optimizing the electrolyte concentrations for the process will increase the selectivity and improve the energy efficiency.

Nevertheless, for optimization purposes, a variability in the effluent characteristics is expected to occur as they are influenced by daily factors such as weather conditions, influent composition or operational conditions at the biological reactor, and must be taken into account.

### 3.2. Mortars bars: physical and functional quality parameters

#### 3.2.1. Effects on cement paste – setting time and workability

Setting time and workability are important properties of materials. Setting time is defined as a specified time required for concrete or mortar to change from liquid state (initial setting time) to a solid state (final setting time), where the surface becomes sufficiently rigid to withstand a definite amount of pressure. Workability can be divided into three different categories (low, medium and high), describing the ability to mix, place, consolidate and finish with minimal loss of homogeneity a mortar preparation. Workability is a property that directly impacts strength, quality, appearance, and the cost of labor operations. Setting time and workability are influenced by pH, dissolved organic matter, COD and salts. The aim of the tests was to understand if the moderately low pH after the ED-T would affect those two parameters.

Table 3 presents the initial and final setting time, workability category and slump values tests according to pH of the aqueous matrices used. Standards BS EN 1008 (2002) [23] and ASTM C94 [30] recommend that the water used for concrete production should have a pH  $\geq$  4–8, since a lower pH can promote the dissolution of cement in the mortar mix. The final pH obtained in all effluents was in accordance to the values referred in the two standards (pH between 8–4).

Setting time can be divided into initial setting time and final setting time based on the degree of rigidity. Comparing the different mixtures,

**Table 3**

Setting times and slump values using: tap water (reference), raw effluent (50 and 100% replacement) and effluent with ED-T treatment (50% and 100% replacement).

	Mix	Initial Setting time (min)	Final Setting time (min)	Workability (mm)	Slump (mm)
pH 7.7	Reference (tap water)	140	290	High 100 – 150	101 $\pm$ 2
pH 7 - 8	Raw 50%	160	340		117 $\pm$ 2
	Raw 100%	160	420		129 $\pm$ 3
pH 4 - 5	ED-T 50%	150	400		131 $\pm$ 2
	ED-T 100%	140	420		134 $\pm$ 9

with reference tap water, there was a delay on the initial setting time of 20 min, when the mix was performed with 100% or 50% raw effluent and 10 min when performed with 50% ED-T treated effluent (Table 3). Using 100% ED-T treated effluent no measurable difference was observed comparing to the reference mortar. The final setting time increased when raw and ED-T effluent is incorporated, having a reference time difference of 50–130 min.

Delay in setting times is related to pH, temperature, humidity, sugars and dissolved organic matter (constituent of COD) presented on raw effluent. Sugars adsorb on the surface of the cement grains and thus might delay the cement hydration. The obtained results are in line with other studies [31,32]. Dissolved salts also influence the setting time process [31]. The ammonia in the raw effluent has been reported to cause bleeding action (flow of water to the top of the concrete due to osmotic pressure) [33]. In the current study, applying ED-T as a pre-treatment decreased approximately 60% the NH<sub>4</sub><sup>+</sup> concentration. This will eliminate the possible bleeding action and turn the paste similar with the reference's setting time. According to BS EN 1008 the initial time shall not be less than 1 h from the reference mortar (experiments achieved a range of difference 0–20 min) and the final setting time should not exceed 12 h (experiments between 4.8 and 7 h).

Workability tests were conducted as described in Section 2.4, where vertical difference between the top of the mold and the displaced original center on the specimen top surface was measured as the slump value. The use of effluent, either with or without ED-T treatment, increased the slump: 16–33 mm differences (Table 3). The cement paste produced with reference water was considered, according to EN 1015-3 [21], as a high workability mortar. The experiments using mixed effluents resulted in a high workability category cement paste as well [21]. High workability paste can be used in inaccessible locations, large flat areas, underwater applications and pumping concrete over long distances (BS EN 206) [34]. This similarity in the paste prepared with effluent, can present a positive enhancement in the mortars production, since it can be an alternative to the use of superplasticizer to stabilize and manipulate the paste [10,35,8].

#### 3.2.2. Effects on mortar properties – flexural strength, compressive strength and morphology

Flexural strength of concrete is a key mechanical property, which represents the ability of a beam or slab to resist failure in bending. The load, extension and flexural strength (also known as modulus of rupture, or bend strength, or transverse rupture strength) results were determined for three 40  $\times$  40  $\times$  160 mm prisms specimens. These specimens were casted and tested after 28 days of curing, as showed in Fig. 2.

Comparing with the reference, flexural strength results showed ED-T 12 h experiment effluent replacement as the highest strength (data in line with the similar morphology as Fig. 4a and d). Consequently, the same experiment had the highest load, where the most similar to the reference were ED-T 6 h and 24 h with 50% of tap water replacement. Comparing the 100% of replacement (Fig. 2b), the highest flexural

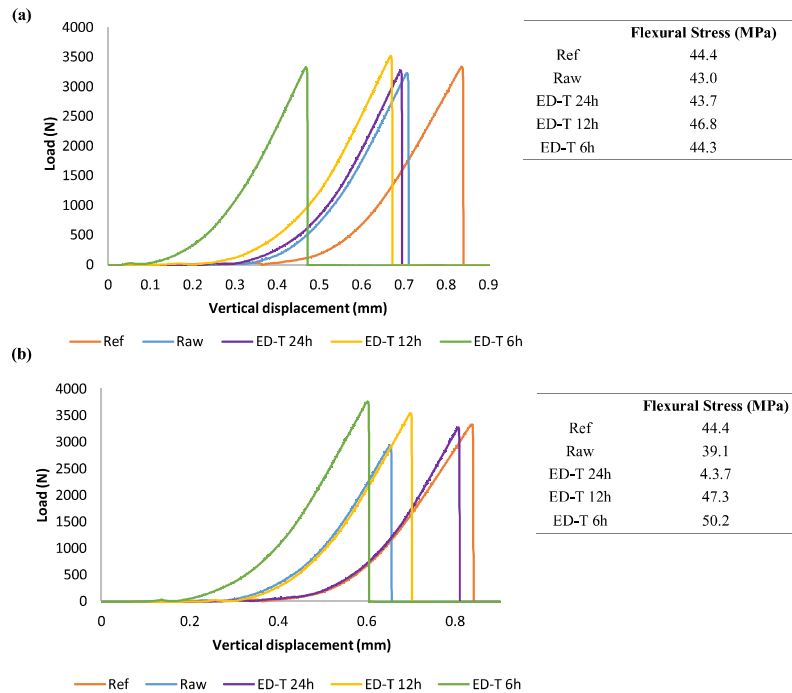


Fig. 2. Load, vertical displacement and flexural stress values of mortar at 28 days of curing age for tap water (reference), (a) raw effluent and effluent after ED-T treatment with 50% of replacement and (b) raw effluent and effluent after ED-T treatment with 100% of replacement.

stress was obtained after ED-T 6h treated effluent, followed by ED-T 12h. Regarding the extension - deflection of the material - for all the mortars made with untreated or treated effluent, after the application of the load, the moment of failure occurred earlier comparing to the reference. In this way, the largest extension for the reference mortar indicates that the strengthening was more required in this experiment than in the ED-T or raw effluent experiments.

Fig. 3 presents the compressive strength of mortars produced with tap water, 50% and 100% of raw effluent and treated effluents (ED-T 6, 12 and 24 h) with 7, 14 and 28 days of curing age. The increase of material strength is related with mortar age. The higher the strength value, less deformable is the material.

The strength variations addressed between the reference (7,14 and 28 days) and the other mortar experiments (7, 14 and 28 days) are within BS EN 1008 [23] (Fig. 3), which refers that the average

compressive strength shall be at least 90% of the average compressive strength of corresponding specimens prepared with tap water.

Comparing 7 days cured specimens, with 100% of raw effluent and 50% of ED-T 12h treated effluent, with the reference mortar, a trend in increased mortar strength was observed, c.a. 5 and 11% of gain;  $\sigma = 0.2$  and 1.4, respectively). Still, this was only statistical relevant when the 50% of effluent treated in ED-T for 12h was used ( $p < 0.05$ ). The same trend for increased strength was also observed for the specimens after 28 days of curing, ED-T 12h effluent either with 50% or 100% replacement and ED-T 6h effluent with 50% of replacement (55.9, 56.8, 58.6 MPa;  $\sigma = 1.3, 2.1$  and 0.8, respectively), although without statistical relevance at 95% confidence level. This highest “early” strength could be a result of changes in effluent chemical properties during ED treatment, that highly influences mortar physico-chemical parameters. This might be due to the decreased COD in the effluent after

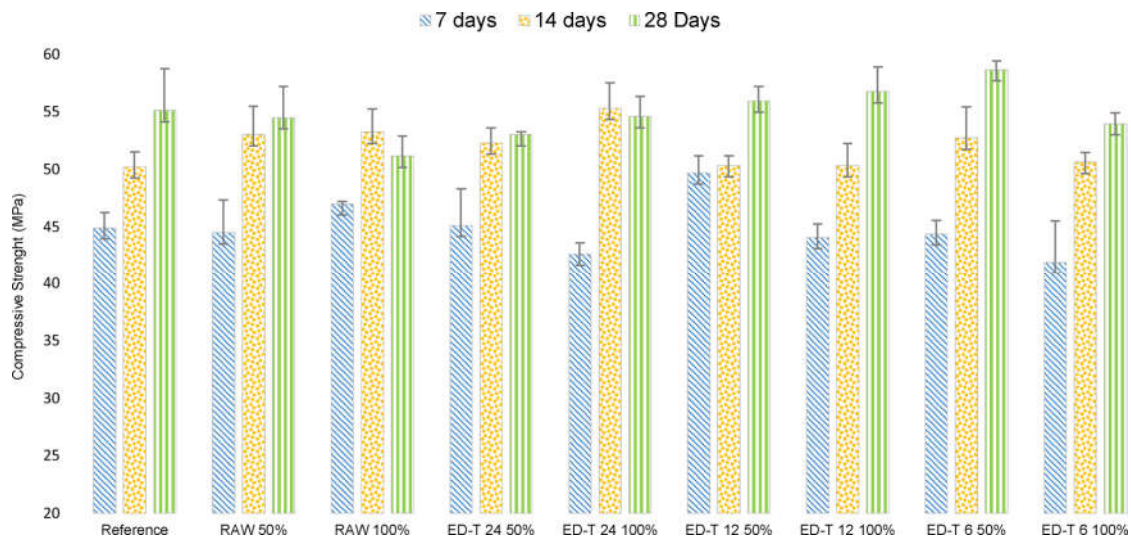
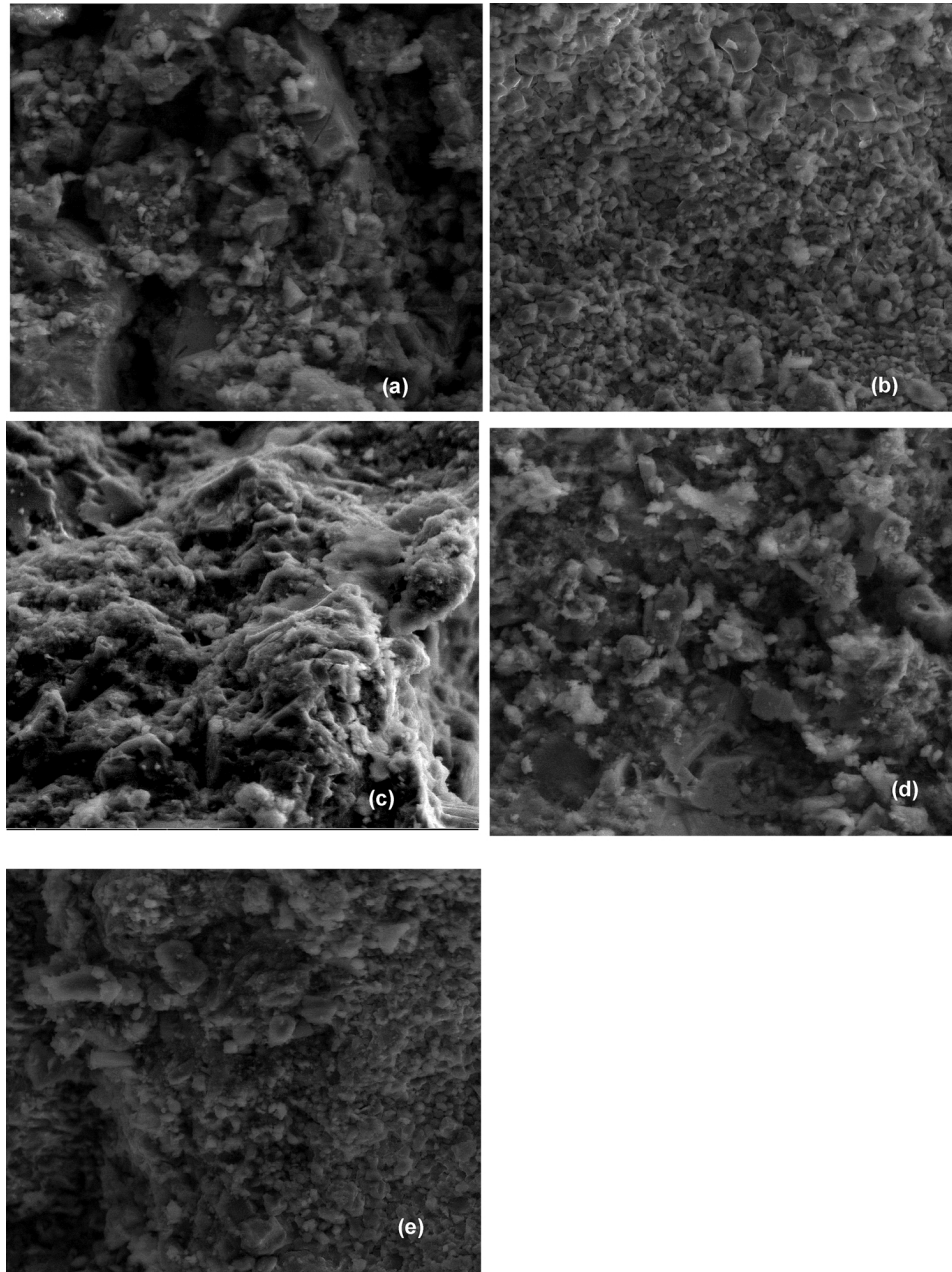


Fig. 3. Compressive strength of age 7, 14 and 28 days using: tap water (reference), raw effluent (50 and 100% replacement) and effluent with ED-T treatment (6, 12 and 24 h - 50% and 100% replacement).



**Fig. 4.** Images of SEM: (a) reference mortar, (b) 100% of replacement with raw effluent, (c) 100% of replacement with ED-T 24 h effluent, (d) 100% of replacement with ED-T 12 h effluent, (e) 100% of replacement with ED-T 6 h effluent; magnification: 800x.

electrochemical treatment (Table 2), a parameter that is known to decrease material strength [36]. After the ED-T pre-treatment, a COD removal was achieved in the three ED-T experiments (43–45%; Table 2).

### 3.2.3. Morphology SEM

Scanning electron microscope was used to visualize the dimensional morphology of the prepared mortar samples to compare visual characteristics, such as formation of different crystals, void spaces and crack formation, in relation to the reference (using tap water Fig. 4a). Fig. 4 showed that the most significant difference was obtained when the tap water was replaced by 100% of raw effluent. It was also possible to observe the new formation of subhedral to anhedral crystals, more pronounced in Fig. 4b) and e). The bed matrix became denser and with less void spaces compared to the reference. In the case of ED-T 6, 12 and 24 h (Fig. 4e, d and c), mortar specimens' structures between aggregate

are structurally intact. This observation corroborates the higher strength in compressive tests in ED-T specimens, as less interatomic spacing requires higher stresses for unwanted cracks to occur, being, therefore, a positive outcome [37]. In all mortar specimens' micro cracks effect were not observed.

## 4. Conclusion

Concerned with water scarcity around the world, the aim of the present study was to explore alternatives for freshwater use in the building industry. Herein, the feasibility of using ED-T as a pre-treatment in mortar preparation was investigated, to remove effluent contaminants such as Ca, Zn, Cl<sup>-</sup>, SO<sub>4</sub><sup>2-</sup> and COD that influence properties of the mortars' material. Based on the experimental conditions observed the following main conclusions are drawn:

- 1 The electro-dialytic pre-treatment achieved a high removal of critical elements and a decrease in the effluent discharged parameters that affect materials' quality and durability.
- 2 Workability that affect the mortar were moderate and tolerable. The workability increased in all the mortars compared to the reference. These results can avoid further use of superplasticizer. Compressive tests had an increase on resistance in specimens prepared with ED-T effluent, comparing with the reference and raw effluent. SEM showed changes in the morphology, where the replacement with raw effluent seems to show no space between pours, causing a possible problem. However, even if the void spaces are inferior with ED-T 12 h and ED-T 6 h, they are still tolerable and had a positive impact in flexural and compressive strength.
- 3 In some specimens, even if the raw effluent showed the potential to replace water in construction materials, the authors are concerned about the pathogens and other impurities that affect the material final quality, durability and safety. Hence, the ED-T can be a way to make effluents non-hazardous contributing for a large scale use.

Further studies are needed on the long-term durability performance and micro-biological activity of mortars mixed with urban effluent treated with ED-T, as well as on the process optimization.

#### Acknowledgments

C. Magro acknowledges Fundação para a Ciência e a Tecnologia for her PhD fellowship (SFRH/BD/114674/2016). Paz-García acknowledges the financial support from the “Plan Propio de Investigación y Transferencia de la Universidad de Málaga”, code: PPIT.UMA.B1.2017/20 and PPIT.UMA.B5.2018/17, and the “Ministerio de Educación, Cultura y Deporte - Subprograma Estatal de movilidad, y Plan Estatal de Investigación Científica y Técnica y de Investigación 2013–2016”, code: CAS17/00196. This work has received funding from the European Union's Horizon 2020 research and innovation programme under the Marie Skłodowska-Curie grant agreement No. 778045, and from FCT/MEC through grant UID/AMB/04085/2013.

#### References

- [1] United Nations General Assembly, Transforming our world: The 2030 agenda for sustainable development, [http://www.un.org/ga/search/view\\_doc.asp?symbol=A/RES/70/1&Lang=E](http://www.un.org/ga/search/view_doc.asp?symbol=A/RES/70/1&Lang=E). (2015) 1–5. doi:10.1007/s13398-014-0173-7.2.
- [2] WWAP (United Nations World Water Assessment Programme)/UN-Water, The United Nations World Water Development Report 2018: Nature-Based Solutions for Water, Paris (2018).
- [3] M.-S. Low, Material Flow Analysis of Concrete in the United States, Massachusetts Institute of Technology, MA, US, 2005, p. 189 M.Sc. Thesis in Building Technology.
- [4] S.A. Miller, A. Horvath, P.J.M. Monteiro, Impacts of booming concrete production on water resources worldwide, *Nat. Sustain.* 1 (2018) 69–76, <https://doi.org/10.1038/s41893-017-0009-5>.
- [5] P.E. Josephson, Y. Hammarlund, The causes and costs of defects in construction: a study of seven building projects, *Autom. Constr.* 8 (1999) 681–687, [https://doi.org/10.1016/S0926-5805\(98\)00114-9](https://doi.org/10.1016/S0926-5805(98)00114-9).
- [6] C. Barrera-Díaz, G. Martínez-Barrera, O. Gencel, L.A. Bernal-Martínez, W. Brostow, Processed wastewater sludge for improvement of mechanical properties of concretes, *J. Hazard. Mater.* 192 (2011) 108–115, <https://doi.org/10.1016/j.jhazmat.2011.04.103>.
- [7] Z.Z. Ismail, E.A. Al-Hashmi, Assessing the recycling potential of industrial wastewater to replace fresh water in concrete mixes: application of polyvinyl acetate resin wastewater, *J. Clean. Prod.* 19 (2011) 197–203, <https://doi.org/10.1016/j.jclepro.2010.09.011>.
- [8] K.S. Al-Jabri, A.H. Al-Saidy, R. Taha, A.J. Al-Kemyani, Effect of using wastewater on the properties of high strength concrete, *Procedia. Eng.* 14 (2011) 370–376, <https://doi.org/10.1016/j.proeng.2011.07.046>.
- [9] S.B.M. Kanitha, P. Ramya, V. Revathi, Potential utilisation of untreated/treated textile effluent in concrete, *Int. J. Res. Eng. Technol.* 3 (2014) 518–522, <https://doi.org/10.15623/ijret.2014.0319093>.
- [10] G. Asadollahfardi, M. Delnavaz, V. Rashnoie, N. Ghonabadi, Use of treated domestic wastewater before chlorination to produce and cure concrete, *Constr. Build. Mater.* 105 (2016) 253–261, <https://doi.org/10.1016/j.conbuildmat.2015.12.039>.
- [11] A.H. Noruzman, B. Muhammad, M. Ismail, Z. Abdul-Majid, Characteristics of treated effluents and their potential applications for producing concrete, *J. Environ. Manage.* 110 (2012) 27–32, <https://doi.org/10.1016/j.jenvman.2012.05.019>.
- [12] M. Silva, T.R. Naik, Sustainable use of resources – recycling of sewage treatment plant water in concrete, in: J. Zachar, P. Claisse, T.R. Naik, E. Ganjian (Eds.), *Second Int. Conf. Sustain. Constr. Mater. Technol.* 2010, pp. 1–10 INC.
- [13] Y.B. Acar, A.N. Alshawabkeh, Principles of electrokinetic remediation, *Environ. Sci. Technol.* 27 (1993) 2638–2647, <https://doi.org/10.1021/es00049a002>.
- [14] G.M. Kirkelund, C. Magro, P. Guedes, P.E. Jensen, A.B. Ribeiro, L.M. Ottosen, Electro-dialytic removal of heavy metals and chloride from municipal solid waste incineration fly ash and air pollution control residue in suspension - test of a new two compartment experimental cell, *Electrochim. Acta* 181 (2015) 73–81, <https://doi.org/10.1016/j.electacta.2015.03.192>.
- [15] B. Ebbens, L.M. Ottosen, P.E. Jensen, Electro-dialytic treatment of municipal wastewater and sludge for the removal of heavy metals and recovery of phosphorus, *Electrochim. Acta* 181 (2015) 90–99, <https://doi.org/10.1016/j.electacta.2015.04.097>.
- [16] P. Guedes, C. Magro, N. Couto, A. Mosca, E.P. Mateus, A.B. Ribeiro, Potential of the electro-dialytic process for emerging organic contaminants remediation and phosphorus separation from sewage sludge, *Electrochim. Acta* 181 (2015) 109–117, <https://doi.org/10.1016/j.electacta.2015.03.167>.
- [17] Lyngby-Taarbæk Kommune - Økonomiudvalget, (2014), pp. 1–90 <https://lyngbytaarbaek.plan.ramboll.dk/view.html?planid=08541641-0f8e-45b1-87fd-82022c7840e>.
- [18] A.B. Ribeiro, J.T. Mexia, A dynamic model for the electrokinetic removal of copper from a polluted soil, *J. Hazard. Mater.* 56 (1997) 257–271, [https://doi.org/10.1016/S0304-3894\(97\)00060-5](https://doi.org/10.1016/S0304-3894(97)00060-5).
- [19] BS EN 196-7:2007 - Methods of Testing Cement. Methods of Taking and Preparing Samples of Cement, British Standards Institution, 2008.
- [20] ASTM C191-18, Standard Test Methods for Time of Setting of Hydraulic Cement by Vicat Needle, West Conshohocken, PA, (2018), <https://doi.org/10.1520/C0191-18>.
- [21] BS EN 1015-3:1999 - Methods of Test for Mortar for Masonry Part 3: Determination of Consistency of Fresh Mortar (by Flow Table), British Standards Institution, 1999.
- [22] BS EN-196-3:2016 - Methods of Testing Cement. Determination of Setting Times and Soundness, British Standards Institution, 2016.
- [23] BS EN 1008:2002 - Mixing Water for Concrete. Specification for Sampling, Testing and Assessing the Suitability of Water, Including Water Recovered From Processes in the Concrete Industry, As Mixing Water for Concrete, British Standards Institution, 2002.
- [24] P. Tiwari, R. Chandak, R.K. Yadav, Effect of salt water on compressive strength of concrete, *Int. J. Eng. Res. Appl.* 4 (2014) 38–42 ISSN 2248-9622 [https://ijera.com/papers/Vol4\\_issue4/Version%205/H044053842.pdf](https://ijera.com/papers/Vol4_issue4/Version%205/H044053842.pdf).
- [25] NP 423:1966, Água. Determinação do teor de cloretos, IGPAI (in Portuguese), Lisboa, 1966.
- [26] NP 413:1966, Água. Determinação do teor de sulfatos, IGPAI (in Portuguese), Lisboa, 1966.
- [27] NP 1414:1977, Determinação do consumo químico de oxigénio de águas de amassadura e de águas em contacto com betões. Processo do dicromato de potássio, IGPAI (in Portuguese), Lisboa, 1977.
- [28] Environmental Protection Agency (EPA), Guidelines for Water Reuse Technical Issues in Planning Water Reuse Systems, Washington (DC) (2004).
- [29] P. Guedes, E.P. Mateus, J. Almeida, A.R. Ferreira, N. Couto, A.B. Ribeiro, Electro-dialytic treatment of sewage sludge: current intensity influence on phosphorus recovery and organic contaminants removal, *Chem. Eng. J.* 306 (2016) 1058–1066, <https://doi.org/10.1016/j.cej.2016.08.040>.
- [30] ASTM C94/C94M-17A - Standard Specification for Ready-mixed Concrete, (2017), <https://doi.org/10.1520/C0094M-17A> West Conshohocken, PA.
- [31] O.S. Lee, M.R. Salim, M. Ismail, M.D.I. Ali, Reusing treated effluent in concrete technology, *J. Teknol.* 34 (2001) 1–10, <https://doi.org/10.11113/jt.v34.648>.
- [32] I. Al-Ghusain, M.J. Terro, Use of treated wastewater for concrete mixing in Kuwait, *Kuwait J. Sci. Eng.* 30 (2003) 213–228.
- [33] A.M. Neville, Properties of Concrete, Pearson Education Limited, England, 2011, <https://doi.org/10.4135/9781412975704.n88>.
- [34] BS EN 206-1:2000 Concrete - Part 1: Specification, Performance, Production and Conformity, British Standards Institution, 2001.
- [35] P.C. Aitcin, Cements of yesterday and today - concrete of tomorrow, *Cem. Concr. Res.* 30 (2000) 1349–1359, [https://doi.org/10.1016/S0008-8846\(00\)00365-3](https://doi.org/10.1016/S0008-8846(00)00365-3).
- [36] K. Sarkor, T.M. Miretu, B. Bhattacharjee, Curing of concrete with wastewater and curing compounds: effect on strength and water absorption, *Indian Concr. J.* 88 (2014) 87–93.
- [37] B. Muhammad, M. Ismail, M.A.R. Bhutta, Z. Abdul-Majid, Influence of non-hydrocarbon substances on the compressive strength of natural rubber latex-modified concrete, *Constr. Build. Mater.* 27 (2012) 241–246, <https://doi.org/10.1016/j.conbuildmat.2011.07.054>.





## Provisional Patent Application

*“Electrodialytic reactor and process for the treatment of contaminated aqueous matrices”*

*Inventors: C Magro, AB Ribeiro, EP Mateus P Guedes*

*Registration number: 115384*



**ABSTRACT**

*"ELECTRODIALYTIC REACTOR AND PROCESS FOR THE TREATMENT OF  
CONTAMINATED AQUEOUS MATRICES"*

The present application relates to an electro dialytic reactor suitable for the treatment of contaminated aqueous matrices by removing macro and micro elements. The present application also relates to a process for the removal of said elements from the contaminated aqueous matrices. The reactor described herein is a three compartment apparatus and takes advantage of electrodes and separators to remove positively charged compounds from the matrix in a first step and elements with negative charge in a second step, assessing also differences in the pH. Enhancements in the reactor configuration lead to an improvement of the final characteristics of the aqueous matrix and increase its value for further use. Additionally, it is possible to couple a fuel cell to the reactor in order to recover and use the hydrogen produced and transform it to energy to power the reactor or stored and sold.

Registration number: 115384

Priority data: 21 March 2019



## Market assessment

*C Magro, AB Ribeiro & EP Mateus*

*Business plan for 2 Resource potential solution, in: Hitech program, NOVA SBE, March-July, 2018*



## EXECUTIVE SUMMARY

2Resource is an electro-dialytic reactor that convert treated wastewater into water that can be reused in several applications, with a main focus on the production of concrete, an industry that represents 1.7% of all global water consumption. The solution will reduce the fresh water consumption on concrete production, replacing 100% of the fresh water by treated wastewater. Climate change, rapidly growing populations and increased urbanization are some of the factors that have a high impact on water consumption around the globe. Focusing on the concept of circular economy, 2Resource aims to have a direct contribution to solve water problems namely in water scarce regions (Middle east) or with high water pollution (Asia). In these regions, concrete batch plants oftentimes have no other choice than to use reclaimed or low quality water in a concrete mix. This can result in low quality concrete, hence in construction defects, structural failure leading to safety and insurance problems. 2Resource has lower capital expenditures and lower operation costs, including maintenance and energy consumption, no chemicals are used during the entire process, electrodes are not destroyed during the process and does not produce hazardous by-products. Also, 2Resource has the flexibility on the customizable reactor that will fit for the client's needs. After the cleaning process, the water characteristics are ideal (e.g. salt content) to be reused in the production of concrete, ensuring highest material quality. 2Resource consists of an interdisciplinary team with a mix of members with more than 20 years of electro-based technology technologies and project management, together with the energy and knowledge of PhD students all with a remarkable passion for climate innovation and entrepreneurship. After completing the registration priority data in the patent process, 2Resource will need 3 years until the go to market with the final product and the breakeven will be reached before the end of the second year in the market. Total funding is estimated to be around €1,9 million.

### *Our vision*

*Providing an eco-friendly, efficient and effective wastewater treatment for a wide range of industries through an electro-based reactor technology.*

### *Our mission*

*Providing wastewater as a safe renewable resource for citizens, industries and companies contributing to sustainable water use.*





# Chapter

*“Sensors potential to monitoring electroremediation systems: emerging organic contaminants in wastewater”*

*C Magro, EP Mateus, M Raposo & AB Ribeiro*

*Under preparation, 2019*



## **Sensors potential to monitoring electroremediation systems: emerging organic contaminants in wastewater**

C. Magro<sup>1</sup>, EP. Mateus<sup>1</sup>, M. Raposo<sup>2</sup> & AB. Ribeiro<sup>1</sup>

<sup>1</sup>CENSE, Department of Sciences and Environmental Engineering, NOVA School of Science and Technology, NOVA University Lisbon, Caparica Campus, 2829-516 Caparica, Portugal

<sup>2</sup>CEFITEC, Department of Physics, NOVA School of Science and Technology, NOVA University Lisbon, Caparica Campus, 2829-516 Caparica, Portugal

### **Abstract**

Chromatography conventional techniques are the gold standards to detect pollutants in environmental matrices. Those methods are known to be highly selective, when compared to modern alternatives, such as sensors. Nevertheless, sensors have shown advantages in sample's manipulation and preparation, accelerating contamination's cloud responses in a cost-effective way. Thus, sensors are now attractive to the market, being sustainable and highly sensitive to organic molecules, with the nano-material choice as the key point for success. Not only the methods for detection are under the spotlight, but also the new removal technologies. The combination between sensors and removal treatments can provide powerful tools for the future of environmental monitoring. However, there is a lack of information when a multi-analyte analysis is the ultimate goal. This chapter will discuss the drawbacks, challenges and advantages on having electronic tongues coupled with electrokinetic processes, to access the detection on emerging organic contaminants in wastewater.

**Keywords:** *sensors; electronic tongue; nano-materials; electrokinetic process; environmental monitoring*



# Chapter

*“Self-hydrogen recovery in electro-based technologies applied to environmental contaminated matrices”*

*C Magro, J Almeida, JM Paz-Garcia, EP Mateus & AB Ribeiro*

*Under preparation, 2019*



## **Self-hydrogen recovery in electro-based technologies applied to environmental contaminated matrices**

C. Magro<sup>1</sup>, J. Almeida<sup>1</sup>, JM. Paz-Garcia<sup>2</sup>, EP. Mateus<sup>1</sup> & AB. Ribeiro<sup>1</sup>

<sup>1</sup>CENSE, Department of Sciences and Environmental Engineering, NOVA School of Science and Technology, NOVA University Lisbon, Caparica Campus, 2829-516 Caparica, Portugal

<sup>2</sup>Department of Chemical Engineering, Faculty of Sciences, University of Malaga, Teatinos Campus, 29010 Málaga, Spain

### **Abstract**

Electro-based technologies consist on the application of a low-level electrical current to produce electrolysis reactions and consequent electrochemically-induced transport of contaminants. Although the in-depth research on pollutants removal efficiencies carried out in the past two decades, the technology readiness level is still far to leverage its introduction in the market. In an electro-dialytic reactor, the self-hydrogen recovery from the electrolytic production at the cathode compartment is now raising awareness to innovative strategies, mitigating electroremediation drawbacks. Hydrogen production during the electro-dialytic treatment of three different matrices: briny water; wastewater; and mine residues suspensions, was recently reviewed with positive achievements. The improvement of the removal and recovery ratio of substances was studied by the combination of solid and liquid matrices. Also, hydrogen purity and energy savings within the process were accessed.

**Keywords:** *Technology transfer, scale-up potential market, electroremediation, wastewater, mine residues, hydrogen, energy.*





## Conference Paper

*“Detection and adsorption of Triclosan on sensors based on PAH/PVS thin-films”*

*J Pereira-da-Silva, PM Zagalo, C Magro, I Pinto, PA Ribeiro & M Raposo*

*Published in: Proceedings IEEE, 2018*



# Detection and adsorption of Triclosan on sensors based on PAH/PVS thin-films

J. Pereira-da-Silva<sup>(1)</sup>, P. M. Zagalo<sup>(1)</sup>, C. Magro<sup>(2)</sup>, I. Pinto<sup>(3)(4)</sup>, P. A. Ribeiro<sup>(1)</sup>, M. Raposo<sup>(1)</sup>

(1) CEFITEC, Departamento de Física, (2) CENSE, Departamento de Ambiente, (3) Centro de Matemática e Aplicações, Faculdade de Ciências e Tecnologia, Universidade Nova de Lisboa, 2829-516 Caparica, Portugal,

(4) Instituto Superior de Engenharia de Lisboa

{jvp.silva, p.zagalo, c.magro}@campus.fct.unl.pt, ipintoadm.isel.pt, {mfr, pfr}@fct.unl.pt

**Abstract**—Given the vital role of water in life it is paramount to thrive and succeed in areas that look to clean and prevent further contamination in water bodies. Triclosan (TCS) is present in most of our day-to-day products and if left unchecked it can lead to long-term significant problems due to its many inauspicious effects in both human and animal health. Thus arose the need to develop sensors to detect and possibly remove TCS for aqueous solutions. This work was rooted on this premise and sensors based on LbL polyelectrolyte thin-films were developed, such as poly(allylamine hydrochloride) (PAH) and poly(vinylsulfonic acid, sodium salt) (PVS), namely (PAH/PVS)<sub>10</sub> and (PAH/PVS)/PAH<sub>10</sub>. The goal of this work was to analyze the amount of TCS adsorbed onto reused (PAH/PVS)<sub>10</sub> and (PAH/PVS)/PAH<sub>10</sub> LbL thin-films when immersed in TCS aqueous solutions with decreasing pH. It was demonstrated that sensors with an outer layer of PAH led to a significantly better TCS molecules adsorption (removal). Additionally, sensors composed of (PAH/PVS)<sub>10</sub> presented higher sensibility in discriminating TCS solutions with concentrations between 10<sup>-5</sup> M and 10<sup>-8</sup> M, using impedance spectroscopy.

**Index Terms**—Triclosan, adsorption, pH, impedance spectroscopy, thin-film, PAH, PVS

## I. INTRODUCTION

Triclosan (TCS) is present in many pharmaceuticals and personal care products (PPCP) such as toothpastes, soaps and first-aid products [1]. TCS presents a significant drawback given that it has high toxicity levels. Recent works have demonstrated that it can cause alarming effects due to the ability to impair biological responses directly related with thyroid hormone homeostasis and estrogen effects or even the ability to block certain processes that can lead to bacterial resistance, thus resulting in an urgent need to detect and quantify TCS [2, and references therein]. The presence of TCS in the environment has been growing at an accelerated rate inevitably culminating in its deposition in groundwaters, surface waters and soils [3, 4]. Additionally, TCS has been detected in blood, human breast milk and there is evidence that day-to-day products containing TCS promote its accumulation in the human body [2, and references therein].

Recent studies have been well succeeded in using sensors composed of layer-by-layer (LbL) thin-films of polyelectrolytes to detected TCS in water matrices, working as an effective electronic tongue. One of these has used thin-films of (PAH/PAZO)<sub>n</sub> (poly (allylamine hydrochloride) (PAH) and poly[1-[4-(3-carboxy-4-hydroxyphenylazo) ben-

zene sulfonamido]-1,2ethanediy], sodium salt] (PAZO)), where  $n$  represents the number of bilayers [5]. Additionally, it has been demonstrated that TCS adsorbed amount per unit of area on thin-films of (PAH/PAZO)<sub>n</sub> is optimized using the positive charged polyelectrolyte PAH as the outer layer at pH 6.5 [2]. The adsorption is affected by the solution pH and the degree of ionization of the last polyelectrolyte of the LbL film [2]. Therefore, the pKa value of TCS is important for the adsorption of the molecule. TCS ( $pK_a = 7.9$ ) is an ionizable organic chemical that at a typical environmental pH ( $pH \approx 8$ ) exhibits both non-dissociated and dissociated species, which can be estimated through the equations 1 and 2 [2]:

$$f_A^N = (1 + 10^{pH - pK_a})^{-1} \quad (1)$$

$$f_I^N = (1 + 10^{pK_a - pH})^{-1} \quad (2)$$

Noteworthy, as the pH increases the TCS solubility also increases [6].

The goal of this work is to analyze the adsorption behavior of TCS with a constant concentration onto reused (PAH/PVS)<sub>10</sub> and (PAH/PVS)<sub>10</sub>/PAH LbL thin-films when immersing in solutions with decreasing pH. Additionally, the impedance spectroscopy technique was used to assess the sensitivity of an array of interdigitated electrodes (IEs) coated with (PAH/PVS)<sub>10</sub> for TCS detection in aqueous solutions within the 10<sup>-15</sup> M to 10<sup>-5</sup> M concentrations range.

## II. MATERIALS AND METHODS

### A. Chemicals and samples preparation

TCS and the polyelectrolytes were acquired from *Sigma-Aldrich*. A stock solution was attained by dissolving 2.895 mg of TCS into 10 mL of pure methanol and stored at 4°C.

The sample solutions for all adsorption tests were prepared by diluting the stock solution in ultra-pure water supplied by a Milli-Q system from Millipore (resistivity of 18 MΩ cm), to achieve a solution of TCS with 10<sup>-4</sup> M of concentration and containing 1% methanol. The solutions' pH were adjusted adding drops of aqueous solutions of 0.10 M sodium hydroxide (NaOH) and hydrochloric acid 37% to the TCS solutions. The pH of the final solutions was measured using a Digital pH Meter ProLab 1000.

Regarding the impedance spectroscopy, the TCS solutions were prepared by diluting the stock solution in Milli-Q ultra-pure water, in order to attain concentrations ranging from  $10^{-5}$  M to  $10^{-15}$  M, in increments of  $10^{-1}$  M and containing 1% methanol.

The thin-films of PAH/PVS were produced using the layer-by-layer technique [5]. The solutions of PAH and PVS were prepared with a concentration of  $10^{-2}$  M through the dissolution of the compounds in Milli-Q ultra-pure water.

### B. Adsorption experiments

The ultraviolet–visible (UV-Vis) absorbance spectra of each LbL film was measured, before and after 45 minutes of adsorption, using a UV 2101 PC Scanning Spectrophotometer. After that, the absorbance of the adsorbed TCS on each thin-film was determined from the difference between both spectra.

Two different LbL thin-films were produced:  $(\text{PAH/PVS})_{10}$  and  $(\text{PAH/PVS})_{10}/\text{PAH}$ . Each of them was immersed in several solutions with decreasing pH. The LbL thin-film composed of  $(\text{PAH/PVS})_{10}$  was immersed in solutions with pH of 2.48, 3.7, 5.68, 6.94, 8.08 and 9.79 and the  $(\text{PAH/PVS})_{10}/\text{PAH}$  LbL thin-film was immersed in solutions with pH of 3.7, 5.68, 6.94, 8.08 and 9.79. The absorbances at 232 nm and 280 nm were plotted and compared between each thin-film, because these are the two main UV-Vis absorption bands of TCS [2].

### C. Impedance Spectroscopy (IS) experiments

Sensors based on  $(\text{PAH/PVS})_{10}$  LbL thin-films deposited on glass supports with inter-digitated gold electrodes were used to detect TCS in aqueous solutions with increasing concentrations, ranging from  $10^{-15}$  M to  $10^{-5}$  M. A solution of 0 M was also used as a reference and all measurements were performed at room temperature of  $25^\circ\text{C}$ . The sensors were immersed in the TCS solutions following an increasing order of concentrations, from 0 M up to  $10^{-5}$  M. The applied AC voltage was 1 V in a frequency range from 1 Hz up to 1 MHz, using electrical resistance, electrical reactance, electrical capacitance and loss tangent as transducing variables at fixed frequencies. This set of data was attained with a SI 1260 impedance/gain-phase analyzer(Solartron).

### D. Statistical Analysis

An exploratory analysis of the data was carried out initially, followed by a data modeling phase. In order to analyze the effect of using the PAH or PVS as the outer on TCS adsorption and consequent UV-vis absorbance, the Student t-test was used for each wavelength, 232 nm and 280 nm. Regarding the impedance spectroscopy study, principal component analysis (PCA) was used as a multivariate method to reduce the size of data and to obtain a new space of orthogonal components in which different concentration patterns can be identified. The bilateral statistical tests were considered significant when the respective p values were lower than the significance level of 0.05. Statistical analysis was performed using the SPSS program Statistics® version 22.0. (IBM Corp. Released 2013. IBM SPSS Statistics for Windows, Version 22.0. Armonk, NY: IBM Corp.).

## III. Results

### A. Adsorption experiment

Figures 1 A and 1 B present respectively the absorbances at 232 nm and 280 nm of reused sensors based on  $(\text{PAH/PVS})_{10}$  and  $(\text{PAH/PVS})_{10}/\text{PAH}$  LbL films after immersion in  $10^{-4}$  M TCS solutions with decreasing pH of 9.79, 8.08, 6.94, 5.68, 3.7 and 2.48. These absorbances were calculated by subtracting the UV-Vis spectrum after immersion from the initial UV-Vis spectrum of each thin-film.

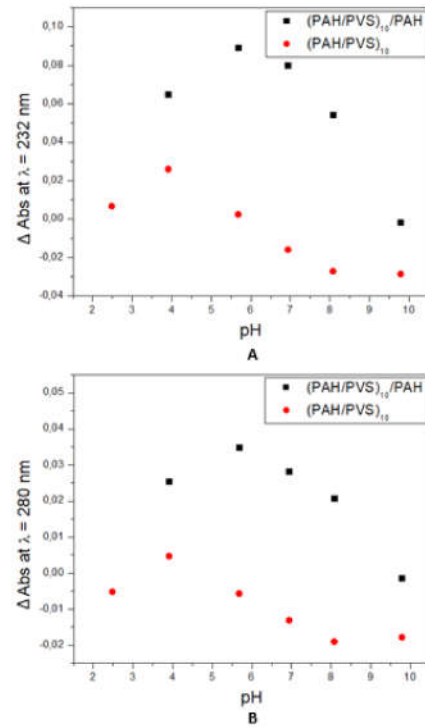


Fig. 1. Absorbances of TCS in the  $(\text{PAH/PVS})_{10}$  and  $(\text{PAH/PVS})_{10}/\text{PAH}$  thin-films vs pH (A) at 232 nm (B) at 280 nm

In Figures 1 A and 1 B it is possible to observe that after the first immersion at pH 9.79, desorption phenomena of the polyelectrolytes PAH/PVS occurred. The  $(\text{PAH/PVS})_{10}$  and  $(\text{PAH/PVS})_{10}/\text{PAH}$  thin-films revealed a similar adsorption behaviour of TCS. As pH decreased absorbances tended to increase both at 232 nm and at 280 nm. The highest absorbances were observed at pH 5.68 for  $(\text{PAH/PVS})_{10}/\text{PAH}$  thin-film and 3.7 for  $(\text{PAH/PVS})_{10}$  thin-film. After that, at more acidic pH the adsorption of TCS tended to decrease at both wavelengths. The  $(\text{PAH/PVS})_{10}/\text{PAH}$  thin-film presented significantly higher absorbances values at all analyzed pH comparing with  $(\text{PAH/PVS})_{10}$  thin-film ( $p < 0.007$ ) in both, 232 nm and 280 nm.

### B. Impedance spectroscopy experiment

Figure 2 shows the dependence of electrical resistance as a function of the frequency.

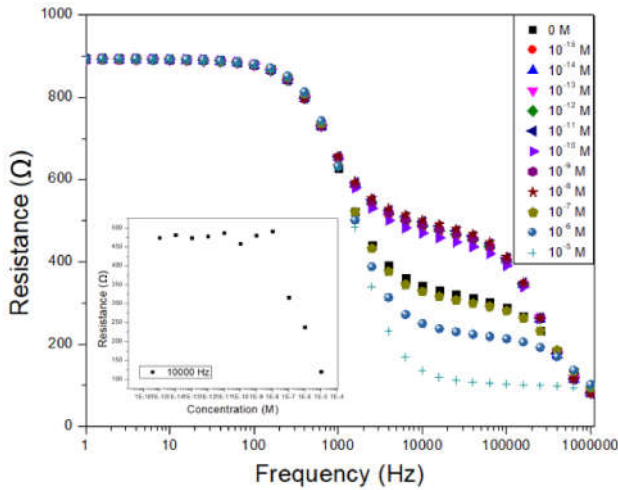


Fig. 2. Resistance spectra of (PAH/PVS)<sub>10</sub> sensor when immersed in TCS solutions at different frequencies

The figure 2 shows that this sensor is capable of discriminating the different concentrations namely between 1000 Hz and 25000 Hz regarding the electrical resistance spectrum. In order to better analyze this particular behaviour, the frequency at 10000 Hz was chosen and the graph of electrical resistance was plotted in the inset of figure 2 as functions of concentration.

Through the analysis of the electrical resistance at 10000 Hz, it is possible to observe that as the concentration increases, the resistance tends to decrease, namely after  $10^{-8}$  M. On the other hand, the capacitance displays an inverse behaviour given that as concentration increases, this electrical parameter tends to increase at 10000 Hz. The PCA methodology (Figure 3) was implemented in order to analyze the impedance spectra at all frequencies.

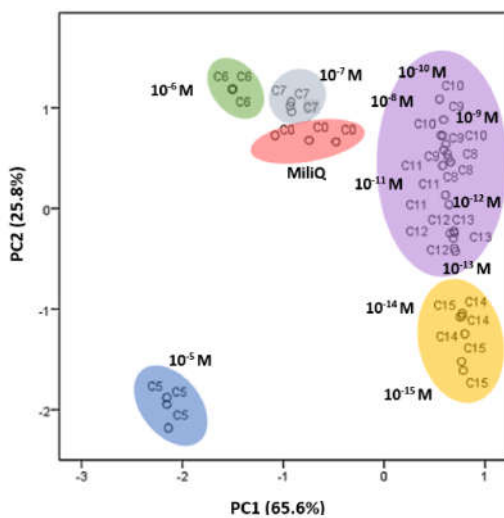


Fig. 3. PCA plot of TCS concentrations ( $10^{-5}$  M to  $10^{-15}$  M).

It is possible to observe that the TCS concentrations between  $10^{-5}$  M and  $10^{-8}$  M is well discriminated. However, above this range, it is not possible to clearly sort out the rest of TCS concentrations.

#### IV. DISCUSSION

##### A. Successive immersions of PAH/PVS thin-films in TCS solutions with decreasing pH

Figures 1 A and B show the adsorption behaviour of TCS on (PAH/PVS)<sub>10</sub> and (PAH/PVS)<sub>10</sub>/PAH thin-films, respectively. It is possible to observe that the desorption phenomena of (PAH/PVS)<sub>10</sub> thin-film are significant at higher pH. It has been demonstrated that the electrostatic assembly of LbL PAH/PVS thin-films result in poor stability, especially in alkaline solutions [7].

Recent studies demonstrated that the adsorption of TCS onto thin-films composed of polyelectrolytes, is affected by the pH of TCS solution [2, and references therein]. The pH affected both the degree of ionization of the last polyelectrolyte in the LbL thin-film and the dissociation of TCS [2, 8]. Using the equations 1 and 2 it was possible to calculate the dissociation fraction of TCS. It begins to dissociate at pH 6.14 and is completely converted into its anionic state at pH 10.14. Figures 1 A and B show that the adsorption capability of TCS on both thin-films is lower at alkaline pH. Regarding (PAH/PVS)<sub>10</sub>/PAH thin-film, this can be explained by the lower amount of positive charges on PAH layer at alkaline pH ( $pH > pKa$ ) [2, 8]. Thus, the electrostatic attraction between PAH polyelectrolyte and the deprotonated TCS weakens as the degree of ionization of PAH decreases [2, 8]. Additionally, the hydrogen bonds between the nitrogen of PAH and the phenolic group of TCS, tend also to diminish given that the anionic TCS can not provide hydroxyl hydrogen atoms [9]. Regarding (PAH/PVS)<sub>10</sub> thin-film, the amount of negative charges of PVS polyelectrolyte is higher at alkaline pH, consequently the electrostatic repulsion overlap the attractive forces [2, and references therein].

As the pH of TCS solutions decreased the adsorption on both LbL thin-films increased. At pH 8.08 and 6.94, the electrostatic attraction between the anionic TCS species and PAH tended to increase given that the PAH surface becomes positively charged. At this range of pH the adsorption of TCS onto (PAH/PVS)<sub>10</sub>/PAH thin-film was higher than (PAH/PVS)<sub>10</sub> thin-film. The adsorption capability of TCS tends to increase on both LbL thin-films at  $\lambda = 232$  nm and  $\lambda = 280$  nm, namely below pH 6.14 ( $pH < pKa$ ) [2, and references therein]. At acidic pH, TCS is nearly non-dissociated, hence an improved adsorption capacity was observed due to the increase of attractive interactions on the PAH layer (H-bond formation and hydrophobic interaction) [2, and references therein]. In addition, since protonated TCS molecules are more hydrophobic than the deprotonated anions, increased adsorption is likely to occur on the PAH and PVS layers at lower pH [10, 11]. It is important to note that the highest absorbances of TCS onto (PAH/PVS)<sub>10</sub>/PAH and (PAH/PVS)<sub>10</sub> both at 232 nm and 280 nm were at pH 5.68

and 3.7, respectively. The highest absorbance on (PAH/PVS)<sub>10</sub> thin-film was observed at a lower pH. This is probably related to the fact that the sulfonic group of PVS has a low pKa and consequently the negative charges tend to increase with pH [12]. Hence, the electrostatic repulsion between PVS and TCS are predominant at  $pH > 3.7$ .

#### B. Impedance spectroscopy experiment

For the impedance spectroscopy experiment, only the (PAH/PVS)<sub>10</sub> thin-film sensor was assessed given that there is less adsorption of TCS than with the (PAH/PVS)<sub>10</sub>/PAH thin-film sensor. Thus, it is possible to deduce that (PAH/PVS)<sub>10</sub> sensor is more easily reused.

The analysis of the electrical resistance spectrum in the inset of figure 2 reveals that at 10000 Hz as the concentration increased, the resistance decreased, namely between  $10^{-5}$  M and  $10^{-8}$  M of TCS concentration. This could be explained by the gradual increasing of TCS anions in solution. For current to flow, ions must be present in solution to carry the charge from one electrode to another. Increasing the number of ions in solution will increase the amount of charge that can be carried between electrodes and will increase the conductivity. The PCA graph depicted in Figure 3 supports the claim that (PAH/PVS)<sub>10</sub> thin-film sensor has an acceptable sensitivity in discriminating the concentrations between  $10^{-5}$  M and  $10^{-8}$  M of the TCS solutions. However, below this range of concentrations, it is not possible to sort out lower concentrations, meaning that the (PAH/PVS)<sub>10</sub> sensor presents a threshold for TCS detection.

#### CONCLUSIONS

It has been demonstrated that TCS adsorbed significantly more on (PAH/PVS)<sub>10</sub>/PAH than on (PAH/PVS)<sub>10</sub>. This phenomenon was affected by the solution pH and the degree of ionization of the last polyelectrolyte of the thin-film. The highest absorbances of TCS onto (PAH/PVS)<sub>10</sub>/PAH and (PAH/PVS)<sub>10</sub> were at pH 5.68 and 3.7, respectively. Additionally, the detection of TCS through impedance spectroscopy yielded acceptable results for (PAH/PVS)<sub>10</sub> sensors. This sensor showed detection sensitivity for concentrations between  $10^{-5}$  M and  $10^{-8}$  M. Thus, the (PAH/PAZO)<sub>10</sub>/PAH thin-film is better for the adsorption and possible removal of TCS from solutions. On the other hand, (PAH/PVS)<sub>10</sub> thin-films are the best option for the production of reusable sensors.

#### ACKNOWLEDGMENT

The authors acknowledge the financial support from FEDER, through Programa Operacional Factores de Competitividade—COMPETE and Fundação para a Ciência e a Tecnologia—FCT, by the project PTDC/FIS-NAN/0909/2014 and for the Portuguese research Grant No. PEst-OE/FIS/UI0068/2011 and UID/FIS/00068/2013. J. Pereira-da-Silva and P.M. Zagalo acknowledge their fellowships PD/BD/142768/2018, PD/BD/142767/2018 from RABBIT Doctoral Programme, respectively. C. Magro acknowledges Fundação para a Ciência e a Tecnologia for her PhD fellowship SFRH/BD/114674/2016.

#### REFERENCES

- [1] R. D. Jones, H. B. Jampani, J. L. Newman, and A. S. Lee, "Triclosan: A review of effectiveness and safety in health care settings," *American Journal of Infection Control*, vol. 28, no. 2, pp. 184–196, 2000.
- [2] J. Pereira-da-Silva, P. M. Zagalo, G. Magalhães-Mota, P. A. Ribeiro, and M. Raposo, "Adsorption of Triclosan on sensors based on PAH/PAZO thin-films: the effect of pH," *Lecture Notes in Bioinformatics, Conference paper, accepted*, 2018.
- [3] L. W. B. Olaniyan, N. Mkwetshana, and A. I. Okoh, "Triclosan in water, implications for human and environmental health," *SpringerPlus*, vol. 5, no. 1, p. 1639, 2016.
- [4] M. O. Mendez, E. M. Valdez, E. M. Martinez, M. Saucedo, and B. A. Wilson, "Fate of Triclosan in Irrigated Soil: Degradation in Soil and Translocation into Onion and Tomato," *Journal of Environment Quality*, vol. 45, no. 3, p. 1029, 2016.
- [5] I. Marques, G. Magalhães-Mota, F. Pires, S. Sérgio, P. A. Ribeiro, and M. Raposo, "Detection of traces of triclosan in water," *Applied Surface Science*, vol. 421, pp. 142–147, 2017.
- [6] J. Wu, C. Hu, C. Li, Z. Cai, and D. Hu, "Determination of 2,8-dichlorodibenzo-p-dioxin in toothpaste and mouth-wash consumer products using GC-MS," *Environmental Science and Pollution Research*, vol. 22, no. 23, pp. 18927–18932, 2015.
- [7] F. Ji, Y. Zhang, Y. Geng, Y. Zong, and L. Wang, "Fabrication of covalently linked PAH/PVS layer-by-layer assembled multilayers via a post-photochemical cross-linking strategy," *Chemical Research in Chinese Universities*, vol. 32, no. 3, pp. 493–498, 2016.
- [8] Q. Ferreira, P. J. Gomes, P. A. Ribeiro, N. C. Jones, S. V. Hoffmann, N. J. Mason, O. N. Oliveira, and M. Raposo, "Determination of degree of ionization of poly(allylamine hydrochloride) (PAH) and poly[1-[4-(3-carboxy-4-hydroxyphenylazo)benzene sulfonamido]-1,2-ethanediyl, sodium salt] (PAZO) in layer-by-layer films using vacuum photoabsorption spectroscopy," *Langmuir*, vol. 29, no. 1, pp. 448–455, 2013.
- [9] C. Lei, Y. Y. Hu, and M. Z. He, "Adsorption characteristics of triclosan from aqueous solution onto cetylpyridinium bromide (CPB) modified zeolites," *Chemical Engineering Journal*, vol. 219, pp. 361–370, 2013.
- [10] Y. Tong, B. K. Mayer, and P. J. McNamara, "Triclosan adsorption using wastewater biosolids-derived biochar," *Environmental Science: Water Research and Technology*, vol. 2, no. 4, pp. 761–768, 2016.
- [11] L. M. G. Abegão, J. Ribeiro, P. A. Ribeiro, and M. Raposo, "Nano-molar deltamethrin sensor based on electrical impedance of PAH/PAZO layer-by-layer sensing films," *Sensors*, vol. 13, no. 8, pp. 10167–10176, 2013.
- [12] D. H. Ripin and D. A. Evans, "pKa's of Nitrogen Acids," *Heterocycles*, vol. 462, no. 2067, pp. 1–6, 2005.

## Conference Paper

*“Detection of Triclosan in tuned solutions by pH and ionic strength using PAH/PAZO thin films”*

*PM Zagalo, C Magro, J Pereira-da-Silva, B Bouchikhi, N el Bari, PA Ribeiro & M Raposo*

*Published in: Sensors Proceedings I3S, 2019*





# Detection of Triclosan in Tuned Solutions by pH and Ionic Strength Using PAH/PAZO Thin Films <sup>†</sup>

Paulo M. Zagalo <sup>1,\*</sup>, Cátia Magro <sup>2,\*</sup>, João Pereira-da-Silva <sup>1</sup>, Benachir Bouchikhi <sup>3</sup>, Nezha El Bari <sup>4</sup>, Paulo António Ribeiro <sup>1</sup> and Maria Raposo <sup>1</sup>

<sup>1</sup> CEFITEC, Departamento de Física, Faculdade de Ciências e Tecnologia, Universidade Nova de Lisboa, 2829-516 Caparica, Portugal

<sup>2</sup> CENSE, Departamento de Ciências e Engenharia do Ambiente, Faculdade de Ciências e Tecnologia, Universidade Nova de Lisboa, 2829-516 Caparica, Portugal

<sup>3</sup> Sensor Electronic and Instrumentation Group, Physics Department, Faculty of Sciences, Moulay Ismaïl University, Meknes 50003, Morocco

<sup>4</sup> Sensor Biotechnology Agroalimentary and Biomedical Analysis Group, Biology Department, Faculty of Sciences, Moulay Ismaïl University, Meknes 50003, Morocco

\* Correspondence: p.zagalo@campus.fct.unl.pt (P.M.Z.); c.magro@campus.fct.unl.pt (C.M.)

<sup>†</sup> Presented at 7th International Symposium on Sensor Science, Napoli, Italy, 9–11 May 2019.

Published: 15 July 2019

**Abstract:** The electronic tongue concept based on layer-by-layer (LbL) films can be used to the detection in water of triclosan (TCS), a pernicious molecule used in personal care products and widely released in the environment. In this work, we analyzed the adsorption of TCS on poly(allylaminehydrochloride) (PAH) and poly[1-[4-(3-carboxy-4hydroxyphenylazo) benzenesulfonamido]-1,2-ethanediyl, sodium salt] (PAZO) layers of PAH/PAZO LbL films. We demonstrate that the adsorbed amount is strongly dependent of pH, the efficiency of adsorption of TCS on PAH layer is higher, and, when PAZO is the outmost layer, the electrical parameters can discriminate the ionic strength on solutions of TCS.

**Keywords:** triclosan; LbL; sensor; impedance spectroscopy; adsorption

## 1. Introduction

Water is an essential and indispensable good to human health and nature's wellbeing, and therefore it is of the utmost importance to preserve and maintain its quality and cleanliness. That is why the detection and monitorization of triclosan in water bodies, such as rivers, groundwater, as well as soils, remains as a paramount necessity due to it being present in a multitude of day-to-day products (dubbed PPCPs—pharmaceuticals and personal care products) and displaying fairly high levels of toxicity [1–5]. Therefore, and also related to the non-regulation of this compound, there is a growing concern about the presence and impact of PPCPs, as well as the need for reliable and effective water monitoring using sensors capable of detecting the target molecules in complex media [6]. One of the main challenges in sensors' monitoring is the ensure analyte effective detection in environmental complex matrices that contain countless spurious molecules (potential interfering compounds), as well as microscopic life. These molecules, such as salts or even fluctuations of pH can jeopardize the analysis of a target molecule.

The purpose of this study was to assess the sensitivity of a sensor based on the electronic tongue concept [7] composed by an array of thin films prepared by layer-by-layer (LbL) technique [6]. In the present case, LbL films of poly(allylamine hydrochloride) (PAH) and poly[1-[4-(3-carboxy-4hydroxyphenylazo) benzene sulfonamido]-1,2-ethanediyl, sodium salt] (PAZO) (PAH/PAZO) were prepared onto quartz supports or gold interdigitated electrode deposited on glass (DropSens) by

alternated adsorbed layers using  $10^{-2}$  M aqueous solutions of these polyelectrolytes. In the present case, thin-films with 10 bilayers of PAH/PAZO ((PAH/PAZO)<sub>10</sub> and (PAH/PAZO)<sub>10</sub>/PAH) were prepared. The amount of TCS adsorbed on these films was measured by ultraviolet-visible (UV-vis) spectroscopy using a UV 2101 PC Scanning Spectrophotometer while the characterization of electrical measurements when these films are immersed in  $10^{-5}$  M aqueous solutions of TCS prepared with different salt concentrations was done using a Solartron 1260 Impedance Analyzer (frequency range of [1–1M] Hz, AC voltage of 25 mV).

## 2. Results

Figure 1a,b presents the absorbances at 232 nm and 280 nm of reused sensors based on (PAH/PAZO)<sub>10</sub> and (PAH/PAZO)<sub>10</sub>/PAH LbL films after immersion in  $10^{-4}$  M TCS solutions with decreasing pH of 9.04, 8.04, 7.0, 6.13, 4.68, 3.70 and 2.30. These absorbances were calculated by subtracting the UV-Vis spectrum after immersion from the initial one of each thin film.

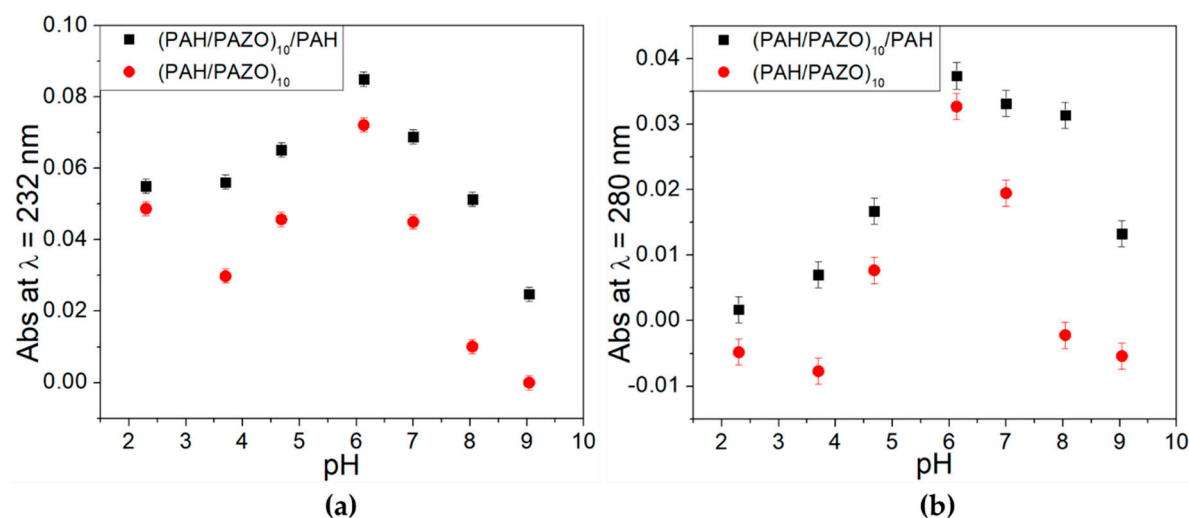


**Figure 1.** Absorbance of TCS at: (a) 232 nm and (b) 280 nm in the LbL thin films vs. pH.

From data presented in Figure 1 it is possible to observe that the adsorbed amounts of TCS, proportional to measured absorbances, are higher for all pHs when the TCS is adsorbed on (PAH/PAZO)<sub>10</sub>/PAH films. Despite presenting different values of absorbances, the adsorption behaviour of TCS in both thin films is similar confirming that we are analyzing the same adsorbed amount. Starting at alkaline pH, as pH decreases the absorbances tend to increase until pH 6.13. Then, as pH decreases the absorbances tend to decrease. However, at the lowest pH of 2.30, the (PAH/PAZO)<sub>10</sub> presents a slight increment of absorbances. At acidic pH (lower than 6.13), the absorbance tends to decrease due to desorption phenomena, particularly of PAH/PAZO thin-films. Adsorption studies of PAZO onto PAH/PAZO LbL films revealed that the electrostatic forces, governing the interactions between PAH and PAZO layers, are strongly dependent on solutions pH [8]. It has been reported that the adsorbed amount of PAZO decreases as the pH of PAH aqueous solutions become more acidic, namely at pH 4 [9]. It is also important to note that at pH 2.30, the absorbance of (PAH/PAZO)<sub>10</sub> thin film revealed a slight increment. This fact is justified by a shift in the absorption bands of PAZO at acidic pH [10]. In fact, we also measured the spectra of  $10^{-4}$  M PAZO solutions at pH 2.5 and pH 6, data not shown here, and an increase of absorbance, namely at 232 nm, was observed as well as a shift on the PAZO peak position which proves that the increase of absorbance at pH 2.30 is not related to adsorption of TCS.

The pH and ionic strength of the TCS solutions can also influence the electrical properties measured when these films are immersed in these solutions, namely, the ionic strength affects the impedance spectra at higher frequencies. In order to conduct this study, seven solutions were

prepared, each with different concentrations of NaCl: 0 M,  $10^{-3}$  M,  $10^{-2.5}$  M,  $10^{-2}$  M,  $10^{-1.5}$  M,  $10^{-1}$  M and 0.5 M. Figure 2a,b illustrate the principle components analysis (PCA) [11] of this study.

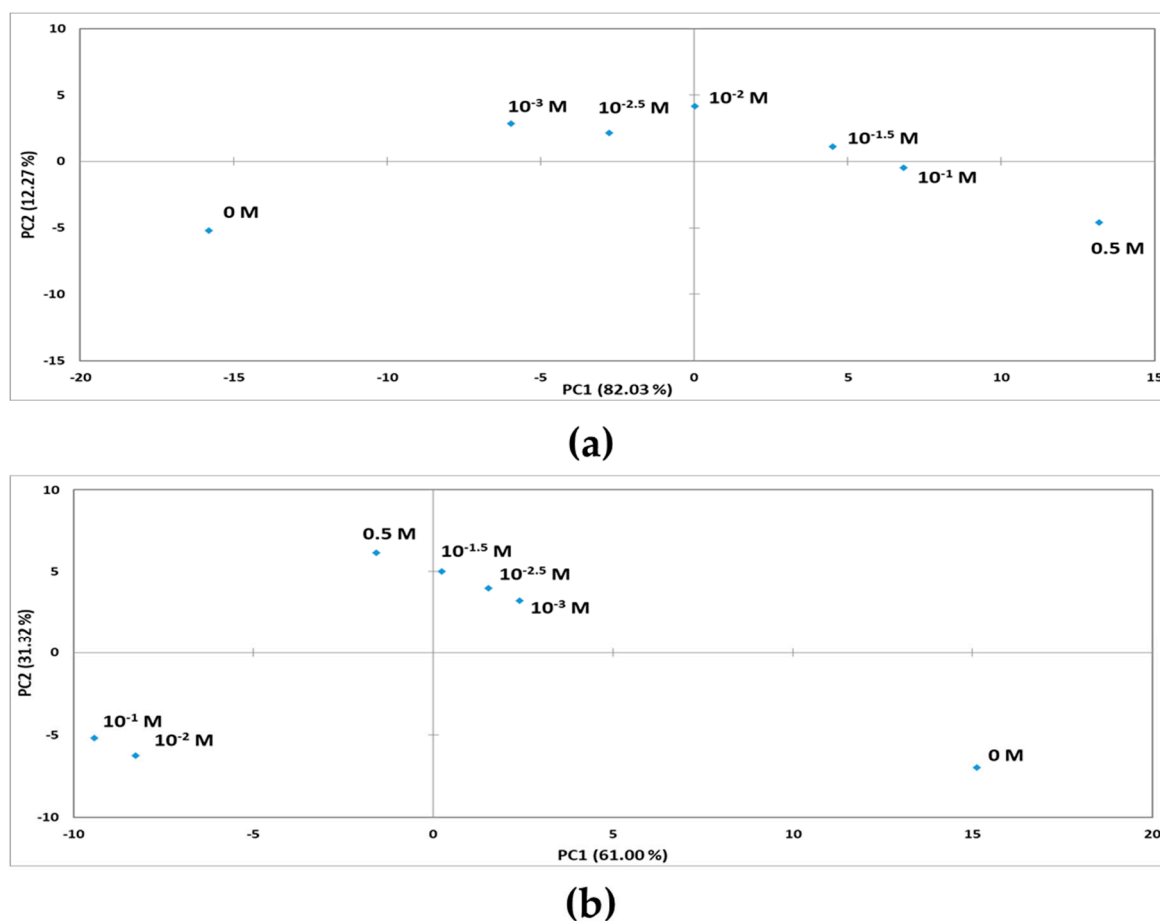


**Figure 2.** PCA plot of: (a) (PAH/PAZO)<sub>10</sub> and (b) (PAH/PAZO)<sub>10</sub>/PAH thin films immersed in TCS aqueous solutions with different NaCl concentrations (0 M to 0.5 M).

The obtained PCA plots, Figure 2a,b, demonstrate that the impedance spectra data obtained with both type of films allow the distinction between different salt concentrations. However, the one obtained with (PAH/PAZO)<sub>10</sub> LbL films has succeeded in distinguishing of the NaCl concentration, displaying a sequential-like pattern. For example, considering the obtained values of PC1, if one plots its values versus NaCl concentration, a function is obtained.

### 3. Conclusions

This study allowed to conclude that TCS adsorbs on both (PAH/PAZO)<sub>10</sub> and (PAH/PAZO)<sub>10</sub>/PAH LbL films but there is an adsorption increase of TCS when the outmost layer is positive. We also verified that the adsorbed amount of TCS increases when the pH decreases attaining a maximum and followed by a decrease as pH also decreases. We proved that this last decrease is not related to the decrease of TCS on the surface but to the change of PAZO spectra for lower pH. We also demonstrated that although pH and ionic strength have a strong influence in the impedance spectra of these films when immersed in solutions, one can find patterns that allow to distinguish between different ionic strengths. Interestingly, when we consider (PAH/PAZO)<sub>10</sub> films one can attain a pattern in which the values of PC1 follow a function when plotted versus the salt concentration. Finally, it should be referred that the characterization of adsorption variables are fundamental in the choice of the adequate LbL films that can be used in the development of electronic tongue to detect, in the present case, TCS.

**Author Contributions:** Conceptualization, P.M.Z.; methodology, P.M.Z.; software, P.M.Z., C.M. and J.P.-d.-S.; validation, P.M.Z., C.M. and J.P.-d.-S.; formal analysis, P.M.Z.; investigation, P.M.Z.; resources, M.R.; data curation, P.M.Z., C.M. and J.P.-d.-S.; writing—original draft preparation, P.M.Z.; writing—review and editing, P.M.Z.; visualization, P.M.Z.; supervision, P.A.R. and M.R.; project administration, P.A.R. and M.R.; funding acquisition, N.E.B., B.B., P.A.R. and M.R.

**Funding:** This research was funded by Fundação para a Ciência e a Tecnologia through projects UID/AMB/04085/2013, PTDC/FIS-NAN/0909/2014 and a Portugal-Morocco bilateral project.

**Acknowledgments:** P.M. Zagalo and J. Pereira-da-Silva acknowledge their fellowships PD/BD/142768/2018, PD/BD/142767/2018 from RABBIT Doctoral Programme, respectively. C Magro acknowledges Fundação para a Ciência e a Tecnologia for her PhD fellowship SFRH/BD/114674/2016.

**Conflicts of Interest:** The authors declare no conflict of interest. The funders had no role in the design of the study; in the collection, analyses, or interpretation of data; in the writing of the manuscript, or in the decision to publish the results.

## References

1. Adolfsson-Erici, M.; Pettersson, M.; Parkkonen, J.; Sturve, J. Triclosan, a commonly used bactericide found in human milk and in the aquatic environment in Sweden. *Chemosphere* **2002**, *46*, 1485–1489.
2. Roberts, J.; Kumar, A.; Du, J.; Hepplewhite, C.; Ellis, D.J.; Christy, A.G.; Beavis, S.G. Pharmaceuticals and personal care products (PPCPs) in Australia's largest inland sewage treatment plant, and its contribution to a major Australian river during high and low flow. *Sci. Total Environ.* **2016**, *541*, 1625–1637.
3. Yueh, M.-F.; Tukey, R.H. Triclosan: A Widespread Environmental Toxicant with Many Biological Effects. *Annu. Rev. Pharmacol. Toxicol.* **2016**, *56*, 251–272.
4. Mendez, M.O.; Valdez, E.M.; Martinez, E.M.; Saucedo, M.; Wilson, B.A. Fate of Triclosan in Irrigated Soil: Degradation in Soil and Translocation into Onion and Tomato. *J. Environ. Qual.* **2016**, *45*, 1029.
5. Olaniyan, L.W.B.; Mkwetshana, N.; Okoh, A.I. Triclosan in water, implications for human and environmental health. *SpringerPlus* **2016**, *5*, 1485.
6. Marques, I.; Magalhães-Mota, G.; Pires, F.; Sério, S.; Ribeiro, P.A.; Raposo, M. Detection of traces of triclosan in water. *Appl. Surf. Sci.* **2017**, *421*, 142–147.
7. Magro, C.; Mateus, E.P.; Raposo, M.; Ribeiro, A. B. Overview of electronic tongue sensing in environmental aqueous matrices: Potential for monitoring emerging organic contaminants. *Environ. Rev.* **2018**, *27*, 202–214.
8. Raposo, M.; Ferreira, Q.; Timóteo, A.R.M.; Ribeiro, P.A.; Rego, A.M.B.D. Contribution of counterions and degree of ionization for birefringence creation and relaxation kinetics parameters of PAH/PAZO films. *J. Appl. Phys.* **2015**, *118*, 114504.
9. Ferreira, Q.; Ribeiro, P.A.; Oliveira, O.N.; Raposo, M. Long-Term Stability at High Temperatures for Birefringence in PAZO/PAH Layer-by-Layer Films. *ACS Appl. Mater. Interfaces* **2012**, *4*, 1470–1477.
10. Ferreira, Q.; Gomes, P. J.; Ribeiro, P. A.; Jones, N. C.; Hoffmann, S. V.; Mason, N. J.; Oliveira, O. N.; Raposo, M. Determination of degree of ionization of poly(allylamine hydrochloride) (PAH) and poly[1-[4-(3-carboxy-4 hydroxyphenylazo)benzene sulfonamido]-1,2-ethanediyl, sodium salt] (PAZO) in layer-by-layer films using vacuum photoabsorption spectroscopy. *Langmuir* **2013**, *29*, 448–455.
11. Shlens, J. A Tutorial on Principal Component Analysis. 2014. Available online: <https://arxiv.org/pdf/1404.1100.pdf> (accessed on 12 September 2018).



© 2019 by the authors. Licensee MDPI, Basel, Switzerland. This article is an open access article distributed under the terms and conditions of the Creative Commons Attribution (CC BY) license (<http://creativecommons.org/licenses/by/4.0/>).

## Conference Paper

*“Triclosan Detection in Aqueous Environmental Matrices by Thin-Films Sensors”*

*C Magro, PM Zagalo, J Pereira-da-Silva, EP Mateus, AB Ribeiro, PA Ribeiro & M Raposo*

*Published in: Sensors Proceedings I3S, 2019*



# Triclosan Detection in Aqueous Environmental Matrices by Thin-Films Sensors <sup>†</sup>

Cátia Costa Magro <sup>1,\*</sup>, Paulo Morgado Zagalo <sup>2</sup>, João Pereira-da-Silva <sup>2</sup>, Eduardo Pires Mateus <sup>1</sup>, Alexandra Branco Ribeiro <sup>1</sup>, Paulo António Ribeiro <sup>2</sup> and Maria Fátima Raposo <sup>2</sup>

<sup>1</sup> CENSE, Departamento de Ciências e Engenharia do Ambiente, Faculdade de Ciências e Tecnologia, Universidade Nova de Lisboa, Caparica 2829-516, Portugal

<sup>2</sup> CEFITEC, Departamento de Física, Faculdade de Ciências e Tecnologia, Universidade Nova de Lisboa, Caparica 2829-516, Portugal

\* Correspondence: c.magro@campus.fct.unl.pt

<sup>†</sup> Presented at the 7th International Symposium on Sensor Science, Napoli, Italy, 9–11 May 2019.

Published: 15 July 2019

**Abstract:** Triclosan (TCS), a bacteriostatic detected in water bodies, have inauspicious effects in human and biota. Consequently, there is a critical need of monitoring these type of compounds in aqueous matrices. In this sense, sensors, based on polyethyleneimine and polysodium 4-styrenesulfonate layer-by-layer thin-films adsorbed on supports with gold interdigitated electrodes deposited, were developed. The aim was analyze the sensitivity of discrimination of TCS ( $10^{-15}$  M to  $10^{-5}$  M) in deionized water, Luso<sup>®</sup> and in an effluent, by measuring the impedance spectra. LbL films can distinguish TCS concentrations in EF, while in LW was achieved an acceptable sensibility when interdigitated electrodes without films were used.

**Keywords:** triclosan monitoring; thin-films interdigitated sensors; impedance spectroscopy

## 1. Introduction

Water management is one of the most serious economic, political, social and ecological issues that mankind faces today. A major challenge is to keep water resources clean and safe, taking into account that the mixture of potential contaminants is continuously changing in a dynamic society. Over the last decade, beyond the legacy contaminants, (e.g., “priority” pollutants and industrial intermediates) that display persistence in the environment, new classes of environmental emerging organic contaminants, mainly composed of products used in a large scale in everyday life, are being detected and reported worldwide and accumulating in water, soil and biota [1]. Among them Pharmaceuticals and Personal Care Products, a group that includes numerous chemical classes, is under increased concern due to its continuous detection in water compartments and permanent introduction into environment across the world [2]. Triclosan (TCS) is a bacteriostatic used in household items such as toothpaste or soaps. TCS has raised health concerns that include allergy risk, antimicrobial resistance, developmental toxicity, and endocrine disruption [3–8]. The actual non-regulation demands the urgency of having reliable tools that will allow the real time monitoring of these emergent compounds [9–11].

The aim of the present work was explore the potential of electronic tongue concept [12,13] using thin-films sensors based on polyethyleneimine (PEI) and poly(sodium 4-styrenesulfonate) (PSS)—to detect TCS spiked aqueous solutions: deionized water (DW), Luso<sup>®</sup> Portuguese mineral water (LW) and an effluent from a wastewater treatment plant (EF), with different concentrations ( $10^{-15}$  M to  $10^{-5}$  M). The PEI/PSS thin-films with 5 bilayers [PEI/PSS]<sub>5</sub>, with  $10^{-2}$  M monomeric concentrations, were prepared by the layer-by-layer (LbL) technique onto solid supports with deposited gold electrodes sensors as described in [14]. The detection of TCS was achieved by measuring the

impedance spectra of thin-films when immersed in the TCS aqueous solutions. The impedance spectra were measured, using a Solartron 1260 Impedance Analyzer, in the frequency range of 1 Hz to 1 MHz applying an AC voltage of 25 mV.

## 2. Results

The impedance spectra of [PEI/PSS]<sub>5</sub> LbL films adsorbed on glass supports with interdigitated electrodes when immersed in TCS solutions prepared with different waters were measured. For comparison, the impedance spectra of glass support with interdigitated electrodes were also measured in the same conditions. Some examples of the obtained results are presented here. Figure 1a1,c1 show the resistance spectra of [PEI/PSS]<sub>5</sub> LbL film immersed in TCS solutions prepared with DW and EF, respectively. While Figure 1b1 shows the loss tangent spectra of interdigitated electrodes without LbL films immersed in TCS solutions prepared with LW. The dependence of electrical resistance and loss tangent as a function of the frequency for the [PEI/PSS]<sub>5</sub> combination was the better for DW and EF, contrary to LW where the best solution was the use of interdigitated electrodes without deposited thin-films. It seems that for more complex media, as LW or EF, the sensor is capable of discriminating TCS concentrations at high frequencies (LW [38,000 to 100,000 Hz]; EF [1000 to 10,000 Hz]), contrarily to DW [100 to 250 Hz]. From the measured spectra data, resistance and/or loss tangent at fixed frequencies were prepared. Figure 1a2,b2,c2 shows the resistance at 250 Hz, loss tangent at ~64 kHz and resistance at ~4 kHz plotted as a function of TCS concentration of the solutions prepared with DW, LW and EF, respectively. In the case of Figure 1a2, there is no clear tendency behavior, only a slight increment on the resistance between 10<sup>-15</sup> M to 10<sup>-13</sup> M, but still poor sensibility for the target molecule. Moreover, to LW the loss tangent tends to decrease with the increase of the TCS concentration, opposite to EF that increase the resistance with the increase of the TCS concentrations.

The adsorption of TCS onto polyelectrolytes thin-films, is affected by the pH of TCS solution [15]. The pH affected both the degree of ionization of the last polyelectrolyte in the LbL thin-film and the dissociation of TCS [16]. DW, LW and EF pH: 8.00, 5.80, 8.26. The acidic pH in the LW, contributed to the slight desorption of the film. The desorption results, not shown here, were obtained measuring the ultraviolet-visible spectra of the films before and after immersion in the TCS solutions in an UV-VIS 2101 PC Scanning spectrophotometer. Hence, as previous observed, the best sensor to this water was gold interdigitated electrodes without deposited thin-films. Also, in more complex media, as EF matrix, [higher conductivity] the high amount of molecules promotes a higher fixed of the thin-films into the solid supports, having therefore less propensity to desorption or adsorption phenomena.



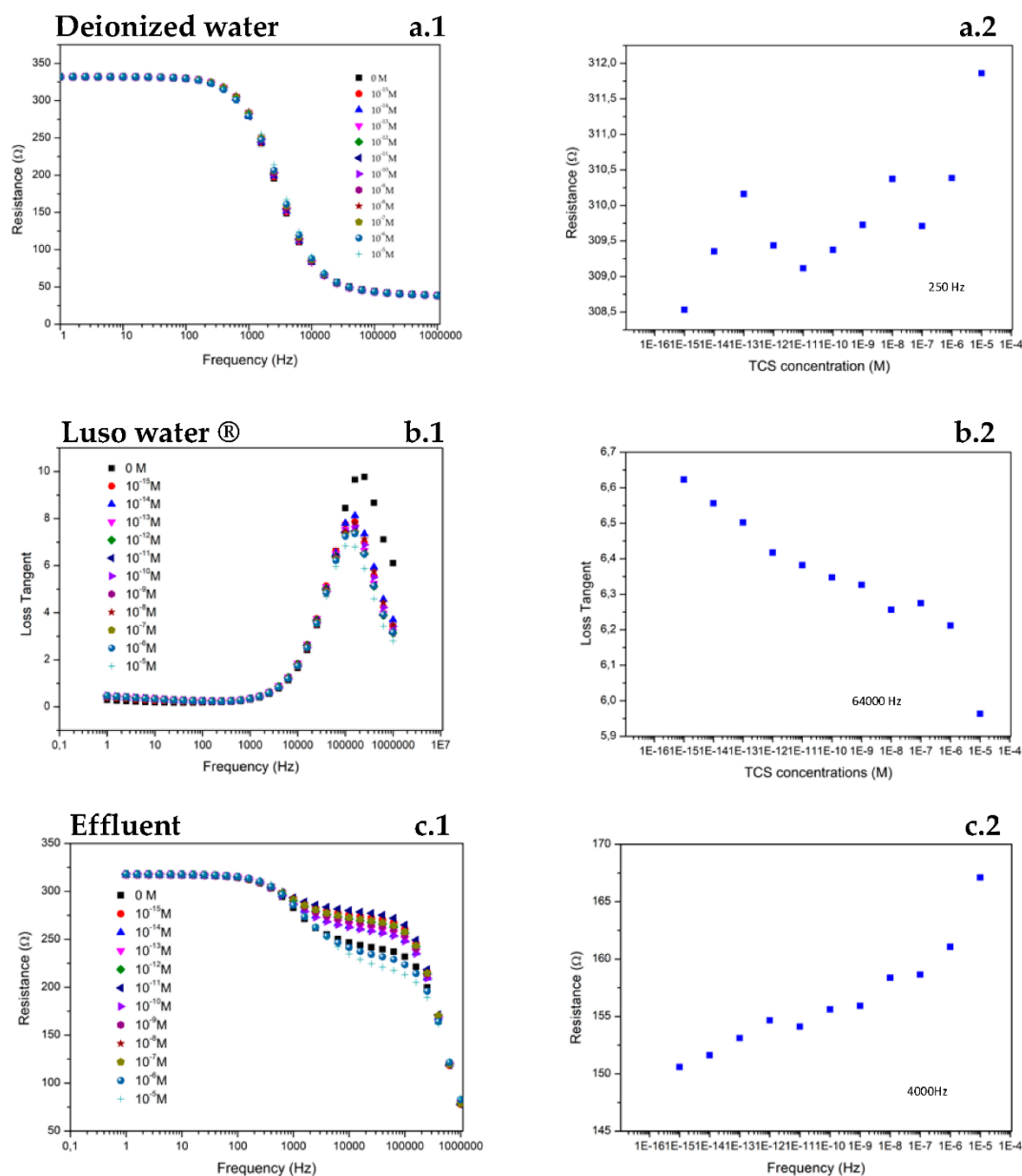


**Figure 1.** (a1) Resistance spectra of [PEI/PSS]<sub>5</sub> LbL film immersed in TCS solutions prepared with DW and (a2) Resistance at 250 Hz vs. TCS solutions prepared with DW; (b1) loss tangent spectra of interdigitated electrodes without LbL films immersed in TCS solutions prepared with LW and (b2) Loss tangent at 64 kHz vs. TCS solutions prepared with LW; (c1) Resistance spectra of [PEI/PSS]<sub>5</sub> LbL film immersed in TCS solutions prepared with EF and (c2) Resistance at 4000 Hz vs. TCS solutions prepared with EF.

### 3. Conclusions

The detection of TCS through impedance spectroscopy yielded acceptable results for [PEI/PSS]<sub>5</sub> in EF and interdigitated sensor with films in LW. To EF there was not observed desorption of the molecules of the films neither adsorption of TCS, confirming the sensor capability to detected TCS target molecule.

**Author Contributions:** Conceptualization, C.C.M.; methodology, C.C.M.; software, C.C.M., P.M.Z. and J.P.-d.-S.; validation, C.C.M., P.M.Z. and J.P.-d.-S.; formal analysis, C.C.M.; investigation, C.C.M.; resources, A.B.R. and M.F.R.; data curation, C.C.M., P.M.Z. and J.P.-d.-S.; writing—original draft preparation, C.C.M.;

writing—review and editing, C.C.M.; visualization, C.C.M.; supervision, E.P.M., A.B.R. and M.F.R.; project administration, A.B.R. and M.F.R.; funding acquisition, E.P.M., A.B.R., P.A.R. and M.F.R.

**Funding:** This research was funded by Fundação para a Ciência e Tecnologia through projects UID/AMB/04085/2013, UID/FIS/00068/2013, PTDC/FIS-NAN/0909/2014 and FCT-CNRST Transnational Cooperation (FCT-UNL, Portugal and Meknes University, Morocco).

**Acknowledgments:** C Magro acknowledges Fundação para a Ciência e a Tecnologia for her PhD fellowship SFRH/BD/114674/2016. J Pereira-da-Silva and PM Zagalo acknowledge their fellowships PD/BD/142768/2018, PD/BD/142767/2018 from RABBIT Doctoral Programme, respectively.

**Conflicts of Interest:** The authors declare no conflict of interest. The funders had no role in the design of the study; in the collection, analyses, or interpretation of data; in the writing of the manuscript, or in the decision to publish the results.

## References

1. Daughton, C.G.; Ternes, T.A. Pharmaceuticals and personal care products in the environment: Agents of subtle change? *Environ. Health Perspect.* **1999**, *107*, 907–938.
2. Chalew, E.A.; Halden, R.U. Environmental exposure of aquatic and terrestrial biota to triclosan and triclocarban. *J. Am. Water Resour. Assoc.* **2009**, *45*, 4–13.
3. Fang, J.; Stingley, R.L.; Beland, F.A.; Harrouk, W.; Lumpkins, D.L.; Howard, P. Occurrence, Efficacy, Metabolism, and Toxicity of Triclosan. *J. Environ. Sci. Health Part C* **2010**, *28*, 147–171.
4. Sabaliunas, D.; Webb, S.F.; Hauk, A.; Jacob, M.; Eckhoff, W.S. Environmental fate of Triclosan in the River Aire Basin, UK. *Water Res.* **2003**, *37*, 3145–3154.
5. Skarha, J.; Mínguez-alarcón, L.; Williams, P.L.; Korevaar, T.I.M.; de Poortere, R.A.; Broeren, M.A.C.; Ford, J.B.; Eliot, M.; Hauser, R.; Braun, J.M. Cross-sectional associations between urinary triclosan and serum thyroid function biomarker concentrations in women. *Environ. Int.* **2019**, *122*, 256–262.
6. Ma, X.; Wan, Y.; Wu, M.; Xu, Y.; Xu, Q.; He, Z.; Xia, W. Occurrence of benzophenones, parabens and triclosan in the Yangtze River of China, and the implications for human exposure. *Chemosphere* **2018**, *213*, 517–525.
7. Juric, A.; Singh, K.; Hu, X.F.; Chan, H.M. Exposure to triclosan among the Canadian population: Results of the Canadian Health Measures Survey (2009–2013). *Environ. Int.* **2019**, *123*, 29–38.
8. Lehutso, R.F.; Daso, A.P.; Okonkwo, J.O. Occurrence and environmental levels of triclosan and triclocarban in selected wastewater treatment plants in Gauteng Province, South Africa. *Emerg. Contam.* **2017**, *3*, 107–114.
9. Wu, T.; Li, T.; Liu, Z.; Guo, Y.; Dong, C. Talanta Electrochemical sensor for sensitive detection of triclosan based on graphene / palladium nanoparticles hybrids. *Talanta* **2017**, *164*, 556–562.
10. Liu, Y.; Song, Q.J.; Wang, L. Development and characterization of an amperometric sensor for triclosan detection based on electropolymerized molecularly imprinted polymer. *Microchem. J.* **2009**, *91*, 222–226.
11. Zheng, J.; Zhang, M.; Ling, Y.; Xu, J.; Hu, S.; Hayat, T.; Alharbi, N.S.; Yang, F. Fabrication of one dimensional CNTs/Fe<sub>3</sub>O<sub>4</sub>@PPy/Pd magnetic composites for the accumulation and electrochemical detection of triclosan. *J. Electroanal. Chem.* **2018**, *818*, 97–105.
12. Magro, C.; Mateus, E.; Raposo, M.; Ribeiro, A.B. Overview of electronic tongue sensing in environmental aqueous matrices: Potential for monitoring emerging organic contaminants. *Environ. Rev.* **2018**, *27*, 202–214.
13. Marques, I.; Magalhães-Mota, G.; Pires, F.; Sério, S.; Ribeiro, P.A.; Raposo, M. Detection of traces of triclosan in water. *Appl. Surf. Sci.* **2017**, *421*, 142–147.
14. Abegão, L.; Ribeiro, J.; Ribeiro, P.; Raposo, M. Nano-Molar Deltamethrin Sensor Based on Electrical Impedance of PAH/PAZO Layer-by-Layer Sensing Films. *Sensors* **2013**, *13*, 10167–10176.

15. da Silva, J.P.; Zagalo, P.M.; Magalhães-Mota, G.; Ribeiro, P.A.; Raposo, M. Adsorption of Triclosan on sensors based on PAH/PAZO thin-films: the effect of pH. In Proceedings of 15th International Conference on Computational Intelligence methods for Bioinformatics and Biostatistics, Caparica, Portugal, 6–8 September 2018; pp. 1–48.
16. Ferreira, Q.; Gomes, P.J.; Ribeiro, P.A.; Jones, N.C.; Hoffmann, S.V.; Mason, N.J.; Oliveira, O.N., Jr.; Raposo, M. Determination of Degree of Ionization of Poly(allylamine hydrochloride) (PAH) and Poly[1-[4-(3-carboxy-4 hydroxyphenylazo)benzene sulfonamido]-1,2-ethanediyl, sodium salt] (PAZO) in Layer-by-Layer Films using Vacuum Photoabsorption Spectroscopy. *Langmuir* **2013**, *29*, 448–455.



© 2019 by the authors. Licensee MDPI, Basel, Switzerland. This article is an open access article distributed under the terms and conditions of the Creative Commons Attribution (CC BY) license (<http://creativecommons.org/licenses/by/4.0/>).



## Conference Contribution

*“Triclosan detection in aqueous environmental matrices by thin-films sensors”*

*C Magro, PM Zagalo, J Pereira-da-Silva, EP Mateus, AB Ribeiro, PA Ribeiro & M Raposo*

*Oral presented in: 7th International Symposium on Sensor Science, Naples, Italy, May 9-11,  
2019*



# Triclosan Detection in Aqueous Environmental Matrices by Thin-Films Sensors <sup>†</sup>

Cátia Costa Magro <sup>1\*</sup>, Paulo Morgado Zagalo <sup>2</sup>, João Pereira-da-Silva <sup>2</sup>, Eduardo Pires Mateus <sup>1</sup>, Alexandra Branco Ribeiro <sup>1</sup>; Paulo António Ribeiro <sup>2</sup> and Maria Fátima Raposo <sup>2</sup>

<sup>1</sup> CENSE, Departamento de Ciências e Engenharia do Ambiente, Faculdade de Ciências e Tecnologia, Universidade Nova de Lisboa, Caparica 2829-516, Portugal; [epm@fct.unl.pt](mailto:epm@fct.unl.pt) (E.P.M.); [abr@fct.unl.pt](mailto:abr@fct.unl.pt) (A.B.R.)

<sup>2</sup> CEFITEC, Departamento de Física, Faculdade de Ciências e Tecnologia, Universidade Nova de Lisboa, Caparica 2829-516, Portugal; [p.zagalo@campus.fct.unl.pt](mailto:p.zagalo@campus.fct.unl.pt) (P.M.Z.); [joaosilva473@gmail.com](mailto:joaosilva473@gmail.com) (J.P.-d.-S.); [pfr@fct.unl.pt](mailto:pfr@fct.unl.pt) (P.A.R.); [mfr@fct.unl.pt](mailto:mfr@fct.unl.pt) (M.F.R.)

\* Correspondence: [c.magro@campus.fct.unl.pt](mailto:c.magro@campus.fct.unl.pt)

<sup>†</sup> Presented at the 7th International Symposium on Sensor Science, Napoli, Italy, 9–11 May 2019.

**Abstract:** The widespread use of pharmaceuticals and personal care products (PPCPs) over the years has resulted in the contamination of aquatic environments. Triclosan (TCS) is a bacteriostatic used in household items, such as toothpaste or soaps. TCS has raised health concerns that include antimicrobial resistance and endocrine disruption both to humans and biota. The actual non-regulation demands the urgency of having reliable tools that can allow the real time monitoring of these emergent compounds.

The aim of the present work was to explore the potential of using thin-films sensors based on poly(allylamine hydrochloride (PAH), graphene oxide (GO), polyethyleneimine (PEI) and polysodium 4-styrenesulfonate (PSS) - to detect different TCS concentrations (10<sup>-15</sup>M to 10<sup>-5</sup>M). Deionized water, Luso® a Portuguese mineral water and an effluent from a wastewater treatment plant, were used to prepare the TCS solutions which were characterized by impedance spectroscopy (1Hz to 1MHz, electrical resistance, electrical capacitance and loss tangent as the transducing variables at fixed frequencies, AC voltage of 25 mV) using a Solartron 1260 Impedance Analyzer.

The obtained data was analyzed by Principal Component Analysis. The results demonstrated discrimination of TCS concentrations in effluent wastewater for combination of [PEI/PSS]5 or [PEI/PSS]20. Additionally, in order to understand the thin-film behavior (desorption and/or adsorption) in the different waters and, consequently, different pHs (3, 6 and ≈ 8), the thin films were characterized with a UV-VIS 2101 PC Scanning spectrophotometer. These stability studies verified that thin-films molecules do not desorb or adsorb in the TCS solutions at pH ≈ 8

**Keywords:** triclosan monitoring; thin-films interdigitated sensors; impedance spectroscopy





## Conference Contribution

*“Electrodialytic technology as effluent treatment for reuse in construction materials”*

*C Magro, LM Ottosen, EP Mateus & AB Ribeiro*

*Oral presented in: 5th International Conference on Sustainable Solid Waste Management,  
Athens, Greece, June 21–24, 2017*



## **Electrodialytic technology as effluent treatment for reuse in construction materials**

*Cátia Magro<sup>1</sup>, Lisbeth Ottosen<sup>2</sup>, Eduardo P. Mateus<sup>1</sup>, Alexandra B. Ribeiro<sup>1\*</sup>*

<sup>1</sup>CENSE, Departamento de Ciências e Engenharia do Ambiente, Faculdade de Ciências e Tecnologia, Universidade Nova de Lisboa, Caparica 2829-516, Portugal

<sup>2</sup>Department of Civil Engineering, Technical University of Denmark, Lyngby, Denmark

Keywords: effluent, electrodialytic process, construction materials

\*presenting author email: [abr@fct.unl.pt](mailto:abr@fct.unl.pt)

Nowadays, keeping water resources clean and safe is one of the biggest challenges in water management systems. Water crisis is increasing due to the population growth, improvement of lifestyle, climate changes and also because of the lack of appropriate water resource management. Therefore, it is crucial to reduce tap water consumption in all activity sectors, including the high volume in building industry. In this industry potable water is usually used since it is recommended by most specifications and its chemical composition is known and well regulated. However, in order to create a balance between the resource and the demand, other alternatives are needed to re-cycle non-fresh water and promote the “zero-waste circular economy”.

Effluents from wastewater treatment plants have a potential to replace water in construction sector due to their characteristics. On the other hand, effluents may contain a complex mixture of anthropogenic and natural compounds that are not removed by conventional treatments and, consequently, different types of impurities are present, making difficult to draw a sound conclusion concerning their utilization in concrete mixtures.

To handle with these barriers, a clean water technology before the reuse is required. Electrodialytic (ED) process is a remediation technique applied to contaminated matrices. The main principle is that when a low level direct current is applied between a pair of electrodes, the generated electric field induces transport processes and physicochemical changes in the applied matrix. These changes lead to species transport by coupled mechanisms, acting as the “cleaning agent”, by which the contaminants move out of the matrix towards one of the electrode compartments. The ED process has proved to be efficient for the removal of organic or/and inorganic contaminants, such as heavy metals and salts.

In this work the viability to use ED treated effluent in construction materials (e.g. mortars) as an alternative to tap water was assessed, thus promoting water management.

The ED process was optimized to remove or immobilize the heavy metals and salts from effluents collected from different wastewater treatment plants. Effluents were characterized before and after the ED process. The treated effluent was then used in the production of mortars. Characterization of cement was performed by X-ray diffraction, SEM-EDX and laser diffraction to understand the influence in the replacement of tap water by ED treated effluent. Materials tests were conducted (e.g. permeability, workability, compressive strength) as well as environmental safety tests (e.g. concentration levels and leaching of heavy metals and salts).

### **Acknowledgments**

Financial support was provided by projects PTDC/FIS-NAN/0909/2014 - Development of Nanostructures for Detection of Triclosan Traces on Aquatic Environments, UID/AMB/04085/2013 and by ERASMUS+ programme.



## Conference Contribution

*“Development of target methods for triclosan monitorization in effluents at trace levels using gas chromatography-triple quadrupole mass spectrometry and electronic tongues”*

*C Magro, D Mendes, F Freitas, MG Silva, AB Ribeiro & EP Mateus*

*Poster presented in: 11th Encontro Nacional de Cromatografia, Costa de Caparica, Portugal,  
December 9–11, 2019*



# Gas chromatographic analysis of underivatized triclosan is an old problem.

**Sensors** can be complementary tools when speed and lower-cost routine responses are required.



Development of target methods for triclosan monitorization in effluents at trace levels using gas chromatography-triple quadrupole mass spectrometry and electronic tongues

• Cátia Magro<sup>1</sup>, Davide Mendes<sup>2</sup>, Flávia Freitas<sup>2</sup>, Marco Gomes da Silva<sup>2</sup>, Alexandra B. Ribeiro<sup>1</sup> & Eduardo P. Mateus<sup>1</sup>

**INTRODUCTION** Triclosan is a bacteriostatic used in household items that has been raising health concerns, due to the promotion of antimicrobial resistance and endocrine effects both to humans and biota. Triclosan is being released to the environment by wastewater treatment plants processing at sub-ppb effluent concentrations, demanding therefore new tools for its continuous supervising and monitoring in complex matrices. Gas chromatography-triple quadrupole mass spectrometry (GC/MS/MS) is one of the most employed method for emerging organic contaminants (EOCs) detection, due to its selectivity and sensitivity. On the other hand, also sensors devices are under the spotlight when fast and non-complex monitoring tools are needed.

## METHODOLOGY

### GC/MS/MS - Optimized parameters

Gas Chromatography - Triple Quadrupole MS Systems - EVOQ Bruker	
Instrument	Gas Chromatography - Triple Quadrupole MS Systems - EVOQ Bruker
Column	DB-5 30 m, 0.25 mm i.d., 0.25 µm film (d <sub>i</sub> )
Running	
Initial Temperature	40 °C for 1 min
Heating Ramp	10 °C/min
Final Temperature	300 °C for 3 min
Carrier Gas	helium
Constant Flow	1 mL/min
Injector	250 °C, 1 min splitless
Interface	290 °C
Source	260 °C
MRM	TCS (288>218, 288>155)
Collision gas pressure	2.4
Collision energy	20eV

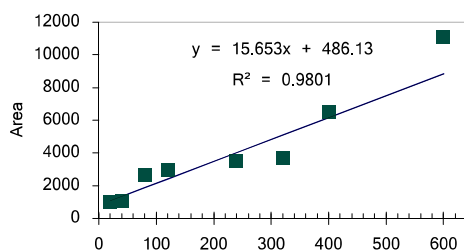


### Sensors build-up

Layer-by-layer films [poly(ethyleneimine)/ poly(sodium 4-styrene sulfonate)]<sub>n</sub>, prepared onto gold interdigitated electrodes, using electrical impedance spectroscopy as means of transduction.

## RESULTS

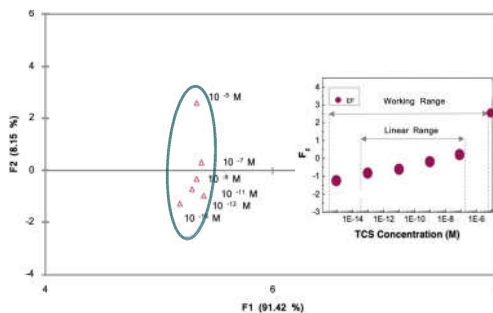
GC/MS/MS - monitoring triclosan at ng/L in effluent



Triclosan detected in effluent real samples

I	II	III	IV	V	VI
127.8	106.6	472.4	623.6	519.9	458.4

Sensor (PEI/PSS)<sub>5</sub> - monitoring triclosan at pg/L in effluent

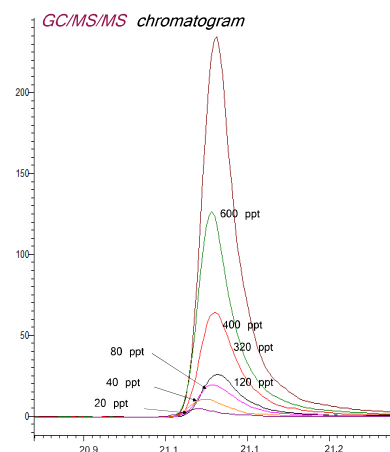
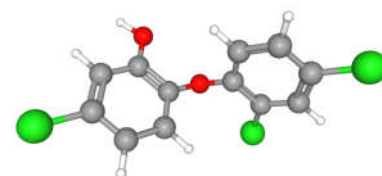


Linear range: 10<sup>-13</sup>M to 10<sup>-7</sup>M (30µg/L to 30 pg/L)

$$y = 0.4225x - 0.6537$$

$$R^2 = 0.9642$$

## EXTRA INFORMATION



## CONCLUSIONS

GC/MS/MS

Detection limit = 132 ppt & Quantification limit = 395 ppt

• Standard methods should be adjusted "case-by-case"

Sensors

• Sensitivity = 0.19±0.02 & resolution = 0.13 pM (quantification and detection limit of 0.2 & 0.1 pg/L, respectively)

## Acknowledgments

- ✓ PTDC/FIS-NAN/0909/2014
- ✓ CENSE - UID/AMB/04085/2013
- ✓ Fundação para a Ciência e a Tecnologia for C.Magro PhD fellowship, SFRH/BD/114674/2016



Scan me to download the full team information





## Conference Contribution

*“Innovating from Science: 2Resource – Recovering water, creating Resources to build”*

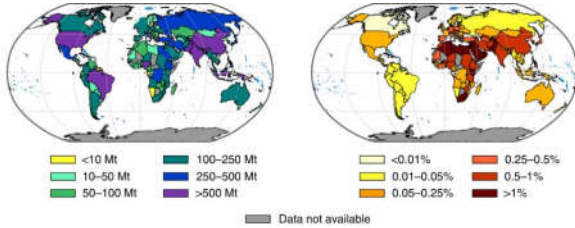
*C Magro, EP Mateus & AB Ribeiro*

*Poster presented in: HiTech Closing Session, July 3, 2018*



# The Problem

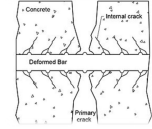
x 2050 scenario in **water stress** from **concrete production**



70% of the global population will be living in cities

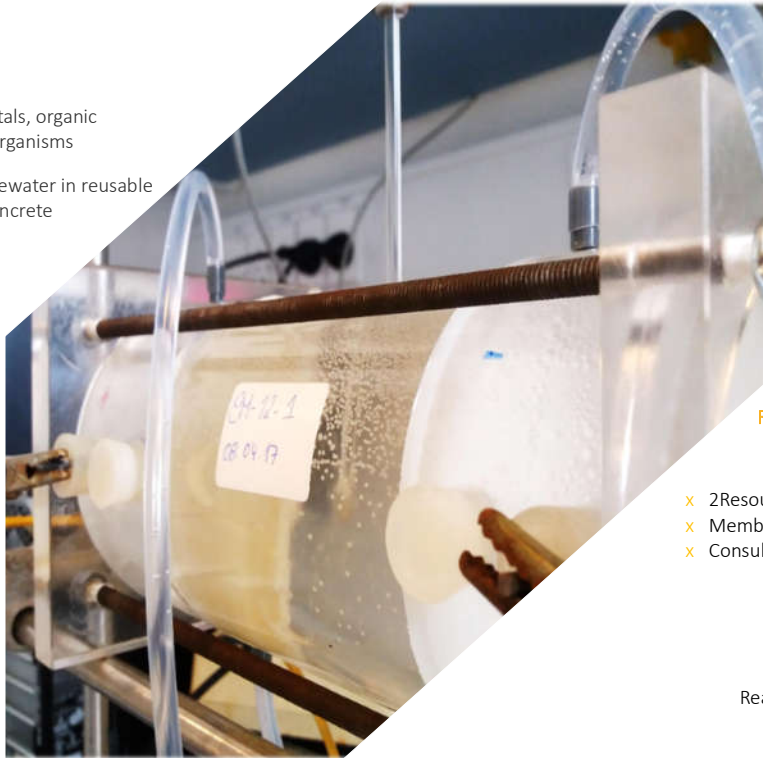


- x Increasing use of concrete concurrent with **increasing urbanization** and industrialization, finding demand exceeding **population growth**
- x Water use for the concrete industry is 9% of all industry withdrawals and **1.7% of all global water consumption**
- x Concrete production is responsible for consuming **1.7 Billion m<sup>3</sup> of fresh water**
- x Concrete production needs regulated water that fulfils industry standards – to achieve high quality materials – if polluted water is used – structural failures will happen



## Solution

- Remove salts, heavy metals, organic contaminants & micro-organisms
- Transforms treated wastewater in reusable water for high quality concrete



## Main benefits

- Avoid problems of contaminating concrete
- Fine-tune treated wastewater e.g. manipulation of pH
- Fulfilling the regulatory standards

## Competitors

### Direct

*Fresh & untreated water*

- High capital expenditure
- Lower operational costs
- Avoid structural failure
- Manipulation of the water characteristics

### Indirect

*Water solution technologies*

- Lower capital expenditure
- Lower operational costs
- No need of chemicals
- By-products reuse

## Business model

### Revenue model

- x 2Resource reactor
- x Membranes
- x Consulting & maintenance

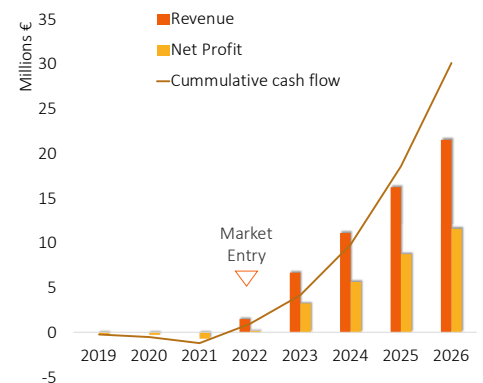
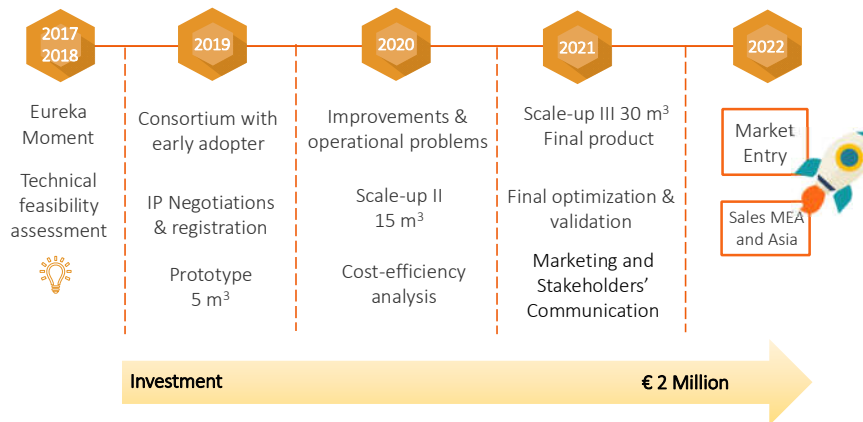
### Key partners

- x Construction industry
- x Manufacturing
- x Water distributors



Reactor's delivery & assembling : Outsourcing

## Roadmap & Financial Projection



## Our team\*



Cátia Magro

PhD student



Alexandra Ribeiro

Associate Professor



Eduardo Mateus

Senior Researcher



Eric Schiltz

Management student

## Market needs

"Reuse of wastewater in construction materials and agriculture, will have strict regulations - starting on 2020. We will see a war of water solution technologies, because a pre-treatment will be required before reuse."

Workshop in Reuse of wastewater in Portugal (May 2018)

"In areas where we don't know the water sources and its characteristics, the material's quality is compromised. Meaning losing money, time and resources"

Pedro Pinto Lopes, Grupo Casais (April 2018)



## Conference Contribution

*“Prospective energy savings in electro-based technologies – PEM fuel”*

*C Magro, J Almeida, JM Paz-Garcia, EP Mateus & AB Ribeiro*

*Poster presented in: 6th International Conference on Sustainable Solid Waste Management,  
Naxos, Greece, June 13-16, 2018*





# PROSPECTIVE ENERGY SAVINGS IN ELECTRO-BASED TECHNOLOGIES – PEM FUEL CELL

C. Magro<sup>1\*</sup>, J. Almeida<sup>1</sup>, JM. Paz-García<sup>2</sup>, EP. Matos<sup>1</sup> & AB. Ribeiro<sup>1</sup>

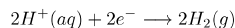
<sup>1</sup>CENSE, Departamento de Ciências e Engenharia do Ambiente, Faculdade de Ciências e Tecnologia, Universidade NOVA de Lisboa

<sup>2</sup>Department of Chemical Engineering, Faculty of Sciences, University of Malaga

\*c.magro@campus.fct.unl.pt

## INTRODUCTION

Electrodialytic technology (ED-T) is a clean-up process with feasible applications in environmental aqueous matrices. This process is based on the application of an electric current density of mA/cm<sup>2</sup> to the cross-sectional area of a matrix between pairs of electrodes. Water oxidation and reduction reactions are dominant, involving the generation of hydrogen gas:



Thus, collecting the hydrogen (H<sub>2</sub>) produced, there is a potential to increase ED-T cost-effectiveness, either using a proton exchange membrane fuel cell (PEM-FC), that converts the chemical energy into power needs or by selling H<sub>2</sub> for other applications.

## METHODOLOGY

### H<sub>2</sub> production in an ED-T laboratory scale – Figure 1

3 compartments cell → L= 15 cm & Ø = 8 cm

Electrodes MMO/Ti (from Permaskand) → L= 5 cm & Ø = 0.3 cm

**CEM** Cation exchange membrane & **AEM** Anion exchange membrane (from Ionics)

Electrolyte → 250 mL NaNO<sub>3</sub> 10<sup>-2</sup> M

### Matrices tested

**SW** Salty Water → 250 mL tap water + 0.2 g NaCl

**EE** Secondary Effluent (from a WWTP, 760,000 equivalent inhabitants, Lisbon, PT) → 250 mL

### H<sub>2</sub> energy conversion

Mini PEM Fuel cell (from Fuelcell store) → (w × h × d) 32 mm×32 mm×10 mm \*max power output → appx. 0.6 V

### Conditions tested

DC current → 100 or 50 mA & Duration → 1 and 2 h

### Parameters monitored

Voltage, pH, conductivity, H<sub>2</sub> volume (mL), % of H<sub>2</sub> purity by Gas Chromatography Thermal Conductivity Detector (GC-TCD)

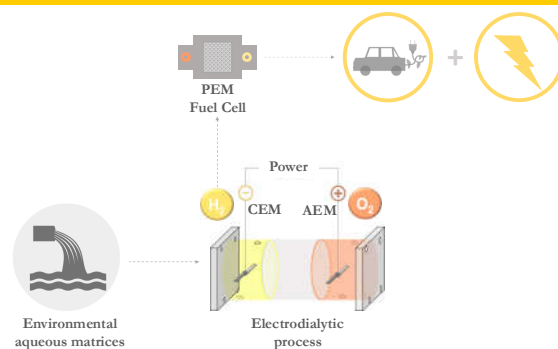


Figure 1. Graphical ideation scheme

## RESULTS & DISCUSSION

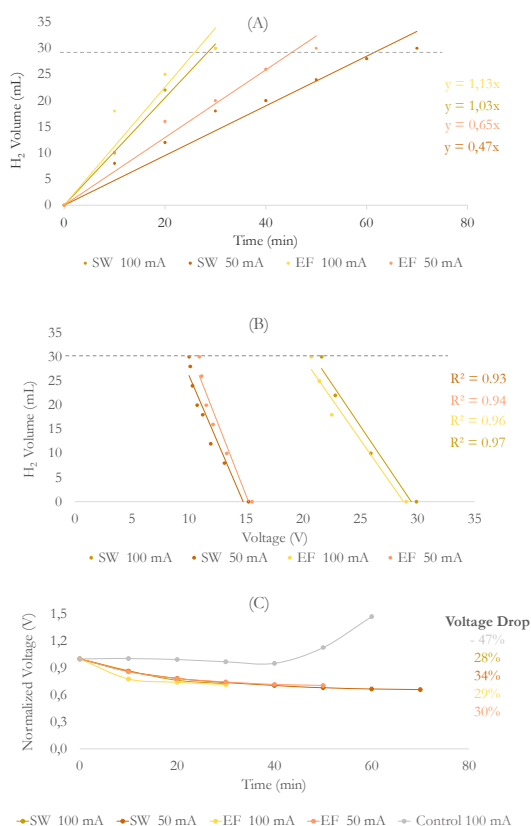


Figure 2. (A) H<sub>2</sub> volume variation, (B) Relation between H<sub>2</sub> volume production and voltage & (C) Normalized voltage

----- Measurement volume limit

- GC-TCD: H<sub>2</sub> produced by ED-T ≈ 95% purity
- ED-T final parameters: SW 50 mA (pH 6.5, 1.4 mS/cm) & 100 mA (pH 3.2, 0.9 mS/cm); EF 50 mA (pH 6.4, 1.2 mS/cm) & 100 mA (pH 3.3, 1.3 mS/cm)
- Time to reach 30 mL of H<sub>2</sub> (full volume capacity): SW 50 mA - 70 min; SW 100 mA - 30 min; EF 50 mA - 50 min; EF 100 mA - 30 min
- ED-T:** The flow rate production for H<sub>2</sub> is directly related to current intensity and matrix (Figure 2A)
- A strong relation between voltage and H<sub>2</sub> volume is supported by data shown in Figure 2B (R<sup>2</sup> ≥ 0.93)
- The voltage in conventional ED-T systems (Control: O<sub>2</sub> and H<sub>2</sub> are released to the atmosphere, recirculation/agitation), shows a different behavior comparing to the ED-T-PEM-FC systems (H<sub>2</sub> gas is collected-isolated reactor). The voltage increased in the Control while in ED-T-PEM-FC systems a dropped voltage was observed (Figure 2C). The second behavior may happen due to the activated polarization:
  - Overpotential → more pressure → increased particle's collisions → increasing the velocity of the H<sub>2</sub> reaction generation
- 100 mA of current intensity means more energy consumption and costs in both matrices (Figure 3)

### PEM-FC – Energy potential generation

- To decrease the energy consumption of the ED-T 100 mA and take advantage of the H<sub>2</sub> produced during the treatment, a PEM-FC was connected to the ED-T gas collector for H<sub>2</sub> power conversion
- Considering PEM-FC maximum output voltage (appx. 0.6 V): 1) SW produced 0.1 V in 100 min (until the average voltage in 3h of ED-T); 2) EF produced 0.8 V in 50 min (until the average voltage in 3h of ED-T)
- Comparing SW with EF, the latest showed 3.5% more efficiency in the potential measured, meaning higher savings/year in a full scale reactor (Figure 4) - more ions in the effluent matrix (data supported by Ion Chromatography). Also, the voltage was more stable during the complete ED-T process
- The efficiency of the PEM-FC is directly proportional to the PEM area (10 cm<sup>2</sup>). Extrapolating PEM area to 300 cm<sup>2</sup>, PEM-FC would cover the total power needs of a complete ED-T treatment (≤ 3h)

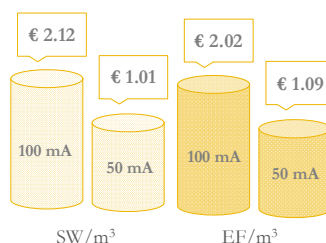


Figure 3. ED-T energy consumption

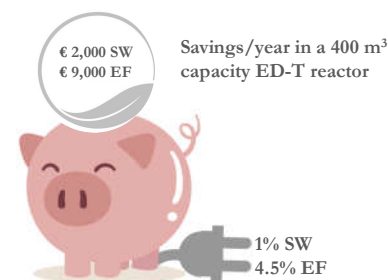


Figure 4. ED-T energy savings with PEM-FC

## CONCLUSIONS

This study suggests new possibilities for energy savings in ED-T and H<sub>2</sub> production for different purposes.

## ACKNOWLEDGMENTS

Project “Development of Nanostructures for Detection of Triclosan Traces on Aquatic Environments” (PTDC/FIS-NAN/0909/2014). CENSE-which is financed by national funds from FCT/MEC (UID/AMB/04085/2013). C. Magro and J. Almeida acknowledges Fundação para a Ciência e a Tecnologia for their PhD fellowships: SFRH/BD/114674/2016 & PD\BD\135170\2017.





## Conference Contribution

*“Optimization of an analytical method for the determination of underivatized triclosan and related compounds by gas chromatography-triple quadrupole mass spectrometry”*

*C Magro, D Mendes, M Silva AB Ribeiro & EP Mateus*

*Poster presented in: 10th Encontro Nacional de Cromatografia, Bragança, Portugal,  
December 4–6, 2017*



# OPTIMIZATION OF AN ANALYTICAL METHOD FOR THE DETERMINATION OF UNDERIVATIZED TRICLOSAN AND RELATED COMPOUNDS BY GAS CHROMATOGRAPHY-TRIPLE QUADRUPOLE MASS SPECTROMETRY

Cátia Magro<sup>1</sup>, Davide Mendes<sup>1,2</sup>, Marco Silva<sup>2</sup>, Alexandra Ribeiro<sup>1</sup> and Eduardo Mateus<sup>1</sup>

<sup>1</sup>CENSE, Departamento de Ciências e Engenharia do Ambiente, Faculdade de Ciências e Tecnologia, Universidade Nova de Lisboa, Caparica, Portugal

<sup>2</sup>LAQV, REQUIMTE, Departamento de Química, Faculdade de Ciências e Tecnologia, Universidade Nova de Lisboa, Caparica, Portugal

## INTRODUCTION

Triclosan (TCS) a antimicrobial agent and galaxolide (HHCB) a synthetic musk, are personal care products (PCPs) widely used on a daily basis. Methyl-triclosan (M-TCS) is a metabolite of TCS more lipophilic and environmentally persistent. These PCPs are released to the environment by WWTP processing at sub-ppb effluent concentrations, presenting endocrine disrupting activities. The continuous detection of PCPs have led to debate on its safety, effectiveness and regulation usage, that comply with the needs of monitoring environmental friendly techniques. Thus, an effective and non-use of derivatization method for determination of the target PCPs was developed.

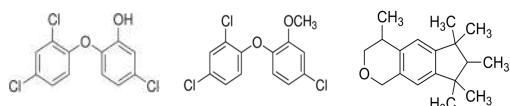


Figure 1. TCS, M-TCS and HHCB molecular structure

## FINAL CONDITIONS

**Initial Temperature:** 40 °C for 1 min  
**Heating Ramp:** 10 °C/min  
**Final Temperature:** 300 °C for 3 min  
**Carrier Gas:** helium  
**Constant Flow:** 1 mL/min  
**Injector:** 250 °C, 1 min splitless  
**Interface:** 290 °C  
**Source:** 260 °C  
**Column:** DB-5 30 m, 0,25 mm i.d., 0,25 µm film (df)  
**MRM - TCS** (288>218>155);  
**M-TCS** (302>189>252);  
**GLX** (243>128>155)  
**Collision gas pressure:** 2.4  
**Collision energy:** TCS (20eV); M-TCS (35eV);  
**GLX** (40eV)

## INITIAL AND FINAL PEAK SHAPE

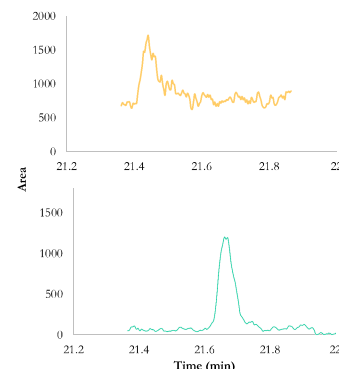


Figure 2. TCS initial and final peak shape

## INJECTION SYSTEM

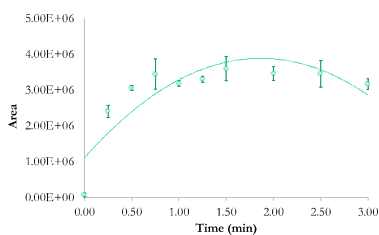


Figure 3. Split time optimization

## GC/MS

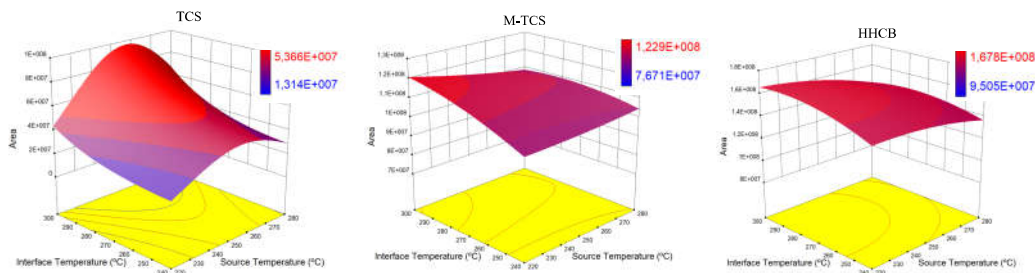


Figure 4. Interface and source temperature (injector: 250°C)

## GC/QQQ

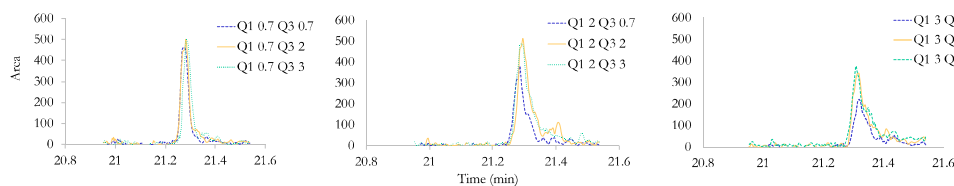


Figure 5. Resolutions Q1 and Q3: TCS peak shape

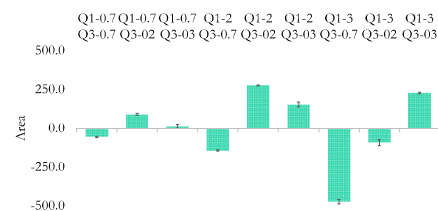


Figure 6. Resolutions Q1 and Q3: TCS areas offset

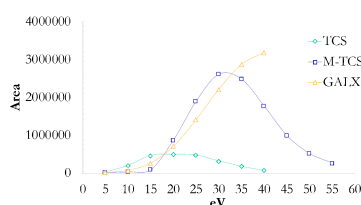


Figure 7. Energy collisions (CID: 2.4 mTorr)

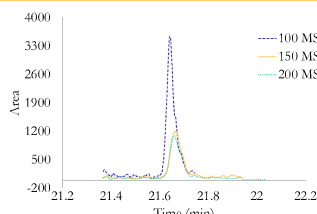


Figure 8. Dwell time: TCS peak shape

Table 1. Method linearity, limit of detection (LOD) and limit of quantification (LOQ)

TCS	M-TCS	GLX
$y = 3.905x + 1070$	$y = 10.50x + 146$	$y = 7.10x + 1420$
$R^2 = 0.975$	$R^2 = 0.999$	$R^2 = 0.995$
LOD: 161 ppt LOQ: 483 ppt	LOD: 25 ppt LOQ: 76 ppt	LOD: 76 ppt LOQ: 279 ppt

## CONCLUSION

This method will allow the fast and efficient environmental monitoring of PCPs in aqueous matrices.

## ACKNOWLEDGMENTS

Project "Development of Nanostructures for Detection of Triclosan Traces on Aquatic Environments" (PTDC/FIS-NAN/0909/2014). CENSE-which is financed by national funds from FCT/MEC (UID/AMB/04085/2013). C. Magro acknowledges Fundação para a Ciência e a Tecnologia for her PhD fellowship (SFRH/BD/114674/2016).



## Conference Contribution

*“Assessment of emergent contaminants removal from wastewater by electrokinetics”*

*C Magro, EP Mateus & AB Ribeiro*

*Poster presented in: 15th International Symposium on Electrokinetic Remediation,  
Montreal, Canada, August 6- 8, 2017*



# Assessment of emergent contaminants removal from wastewater by electrokinetics

Cátia Magro, Eduardo Mateus and Alexandra Ribeiro<sup>1</sup>

<sup>(1)</sup> CENSE, Departamento de Ciências e Engenharia do Ambiente, Faculdade de Ciências e Tecnologia, Universidade Nova de Lisboa, Caparica, Portugal

## Introduction and Aim

Pharmaceutical and personal care products (PPCPs) are environmental emerging organic contaminants (EOCs). PPCPs reached wastewater treatment plants (WWTP) where they are not completely removed by conventional treatments. PPCPs are therefore detected in the effluent discharged and receiving water bodies. Triclosan (TCS) is an antibacterial agent that is widely used in soaps and first-aid products. This compound is under concern due to its characteristics - stable and lipophilic - has been widely found in sediments, fish and human milk. Methyl-Triclosan (M-TCS) is a metabolite of TCS more lipophilic and environmentally persistent. The repeated exposure to chlorine in water treatment facilities can chlorinate TCS. 2,4-dichlorophenol (2,4-DCP) and 2,4,6-trichlorophenol (2,4,6-TCP) are TCS by-products formatted by photochemical degradation. 2,4-DCP may be fatal if large amounts are absorbed by the body and 2,4,6-dichlorophenol (2,4,6-TCP) is an endocrine disruptor. Electrokinetic technology (EK-T) can be a reliable option to improve the WWTP ECs removal rates.

The EK-T design was carried out aiming the possible future implementation in a WWTP removal stage. The TCS and its by-products behavior in EK-T was studied.

## Wastewater characteristics

- ✓ **Matrix source:** Effluent collected at the output of the secondary settling tank at Q<sup>ta</sup> do Conde (Setúbal, Portugal)

Table 1 – Effluent characterization

pH	(μS/cm)		(mg/L)							
	Conductivity	TSS	BOD <sub>5</sub>	COD	N <sub>T</sub>	P <sub>T</sub>	NH <sub>4</sub>	Cl <sup>-</sup>	NO <sub>3</sub> <sup>-</sup>	SO <sub>4</sub> <sup>2-</sup>
7.97 ± 0.15	790 ± 0.1	28	17	72	20	4	15	104	30675	33

## Methodology

### Electrokinetic experiments

- EK process was conducted in a laboratory scale cell (Figure 1)
- Cell dimensions: L = 10 cm, internal diameter = 8 cm; working electrodes = platinized titanium bars from Bergsøe, with a Ø = 3 mm and L = 10 cm;
- Experiments were conducted for 4 hours at a constant current of 25 mA
- Five experiments were carried [ Individual: TCS; M-TCS; 2,4-DCP; 2,4,6-TCP and Mix ]
- Containers (not completely closed), with 200 mL of effluent spiked with 400 μg L<sup>-1</sup> TCS and its by-products
- ✓ Replicates n = 2
- ✓ Blank with and without Azide (microorganisms' inhibitor)

### TCS and by-products analysis

- Extraction: Solid phase extraction (200 mg, 6 cc Oasis HLB cartridges from Waters)
- Analysis: high-performance liquid chromatography-diode array detector (scan from 200 to 800 nm)

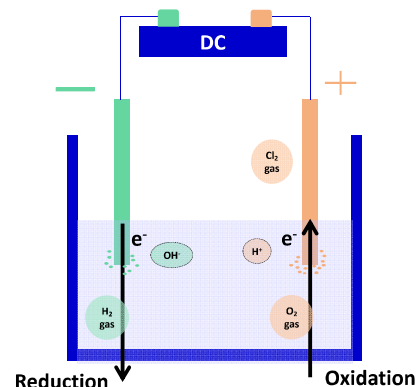
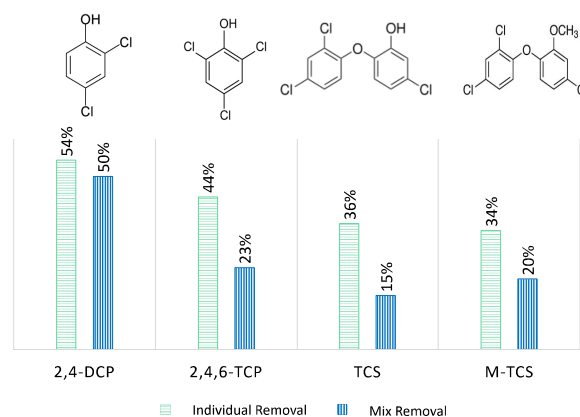


Figure 1. Schematic view of the EK set-up

## Results

### When 25 mA were applied during 4h:

- pH increased (8 to 9.4) and the conductivity decreased (800 to 600 μS cm<sup>-1</sup>)
- pH effluent > pKa EOCs (pKa > 6) => EOCs in ionized form
- Between 15 to 50 % of the EOC were degraded in the Mix solution
- Between 34% to 54% of the EOC were degraded in the Individual solution
- The comparison of the removal rates (mix vs individual) suggested a competition between compounds in the mix .
- The HPLC-DAD analysis did not detected new chromatographic peaks that can be associated to degradation compounds of the EOCs under study.



## Conclusions

- EOCs under studies presented slightly different behaviors during EK-T
- The results here presented are of valuable starting point for the electro-remediation knowledge of TCS, M-TCS, 2,4-DCP, 2,4,6-TCP and similar compounds using the EK-T

## Acknowledges

Financial support was provided by project "Development of Nanostructures for Detection of Triclosan Traces on Aquatic Environments" (PTDC/FIS NAN/0909/2014) and CENSE-Center for Environmental and Sustainability Research which is financed by national funds from FCT/MEC (UID/AMB/04085/2013). C.Magro acknowledges Fundação para a Ciência e a Tecnologia for her PhD fellowship (SFRH/BD/114674/2016).

